Wave propagation in fluid saturated granular media

Slade, R. E.

Award date:
1995

Awarding institution:
University of Bath

H

Wave Propagation in Fluid Saturated Granular Media

submitted by

R. E. Slade

for the degree of Ph.D

of the

University of Bath

1995

ProQuest LLC
789 East Eisenhower Parkway
P.O. Box 1346
Ann Arbor, MI 48106-1346

Summary

The term 'granular media' is used to describe a variety of differing materials in a wide range of circumstances. Many mathematical models describing granular media are available, each appropriate to the particular application envisaged. A large proportion of these models attempt to relate macroscopic properties to microscopic quantities. Examples of the macroscopic quantities of interest are the effective elastic moduli, wave speeds and energy dissipation. Microscopic properties include the elastic moduli of the grain material, the grain sizes, the interaction between grains and the internal geometry of the medium.

The particular type of model studied in this thesis is one in which the grains are made up of discrete particles of solid matrix tightly packed together to form the granular medium. Many authors have studied the sphere as perhaps the simplest grain shape and chapter 1 includes a description of the random sphere packing model of Walton [67]. Chapter 2 makes a correction to this model required when the packing is under uniaxial compression.

The form of intergranular contact is very important in such models. One of the aims of this work is to include a frictional contact law in the random sphere packing model, and in chapter 3 the required contact problem for two identical elastic spheres with a finite non-zero coefficient of friction between them is solved. The results of this frictional contact problem are used in chapter 4 to model waves propagating through a cubic packing of spheres. Obviously, a cubic packing is a highly simplified geometry for a model of a granular material and in chapter 5 we introduce an averaging scheme which allows us to consider frictional contacts within random packings. The addition of a saturating fluid is briefly discussed.

The final two chapters attempt to model a granular material made up of aligned spheroidal grains instead of spheres. Although the equations are much more complex, it is still possible to write down expressions for the effective elastic moduli in terms of averaging integrals which may then be evaluated numerically.

Acknowledgments

In no particular order, I would like to thank the following people for the following reasons: My parents for their support through university and beyond; My wife Ruth for marrying me halfway through the project; Dr Keith Walton of the School of Mathematical Sciences at the University of Bath for being a helpful and understanding supervisor throughout the three years, and for always finding time to answer my questions; Most of my fellow officemates for their good humour and friendship.

The work contained in chapters 6 and 7 was undertaken as part of a three month industrial placement (July–Oct 1994) in the Seismics Department of Schlumberger Cambridge Research, as recommended in the SERC studentship handbook paragraph 12.6. I would like to thank Dr John Hudson of the Department of Applied Mathematics and Theoretical Physics, University of Cambridge and Dr Brian Hornby of Schlumberger Cambridge Research for their help and guidance during this placement.

I also acknowledge the financial support of the former Science and Engineering Research Council (SERC).

Contents

List of Figures

Chapter 1

Introduction

1.1 Overview of Thesis

In recent years much progress has been made in the study of granular materials. Although the subject can hardly be described as new, novel applications are constantly arising in fields as diverse as civil engineering, the pharmaceutical industry and petrochemical prospecting. Two major international and inter-disciplinary conferences, 'Powders and Grains', have been held in Clermont-Ferrand, France in 1989 [4] and at Aston University in 1993 [57], both of which were devoted to advances in the field of particulate systems. These conferences demonstrate the rapid growth of knowledge in the field and the large number of known and potential applications.

This thesis is concerned with modelling granular media as an ensemble of particles or grains and predicting the overall behaviour from known microstructural properties. Examples of the properties we aim to predict are the effective elastic moduli, the attenuation properties of sound within the medium and the speed of propagation of elastic waves. Typical microstructural features affecting these overall properties are particle shape, elastic properties of the individual grains, packing density and the form of intergranular contact. Two chapters are devoted to the study of the contact between solid particles. Chapter 3 examines the contact of two elastic spheres, extending the work of Walton [66] and Mindlin and Deresiewicz [45] to consider the most general oblique-oblique contact problem with a finite non-zero value of the coefficient of friction. In chapter 6 we change the particle geometry from spheres to oblate spheroidal particles. Many authors, such as Mindlin [44], Vermeulen and Johnson [61] and Sackfield and

Hills [49], have considered contact of non-spherical bodies; the work in chapter 6 is an extension of the more general oblique-oblique loading considered by Walton [66] for spheres. Explicit results are derived for the problem of contacting aligned spheroids.

The solutions of the two contact problems described above are used in chapters 4,5 and 7. The results of the sphere contact problem with friction are used in chapter 4 to model a cubic packing of spheres under uniaxial compression. Expressions for the average stresses under this strain are derived and the dynamic wave speeds are calculated for further incremental displacements. A random packing of spheres is considered in chapter 5. The contact laws of chapter 3 are used to extend the work of Walton [67], which previously treated only the case of zero friction or infinite friction, to a packing in which friction is finite and non-zero. The elastic wave speeds are derived and the effective elastic moduli are determined; in particular we examine the case of an initial uniaxial compression since it is shown that friction plays an important role under this loading.

The contact laws of chapter 6 are used in chapter 7 to model a random packing of aligned oblate spheroidal particles. The basic approach is similar to that seen in Walton [67]. However, due to the loss of many of the spherical symmetries, the equations and the effective properties of the medium are shown to be radically different.

Chapter 2 contains work relating to a correction of the random packing paper by Walton [67]. One specific case of initial loading, a uniaxial compression, was found to cause problems with the equilibrium of individual spheres. The solution should include rotations of each sphere thereby ensuring rotational equilibrium.

1.2 Contact Problems

In this section we present some results which will be of use in later chapters concerning the problems of contact of elastic bodies. First of all we consider the loading of a semi-infinite elastically isotropic half-space and give expressions for the resulting displacements. These displacements are later required for the solution of certain contact problems using the Hertz theory of elastic contact [30], described in section (1.2.4).

The displacements are then calculated for the particular case of a circular region with

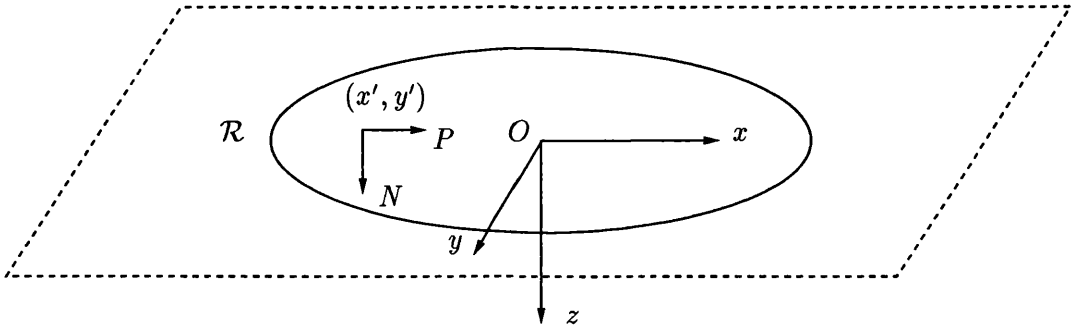

Figure 1-1: *The half-space $z > 0$ and region $\mathcal{R}$*

parabolic distributions of pressure which, as we will see later, are required for the solution of the Hertzian contact of two elastic spheres.

1.2.1 Surface Displacements

Consider the set of rectangular Cartesian axes $Oxyz$ with the z-axis directed downwards as shown in figure 1-1. The elastic half-space is shown as the region $z > 0$ bounded by the plane $z = 0$. Normal and tangential tractions are applied to the closed region $\mathcal{R}$ contained within the plane $z = 0$. Exterior to $\mathcal{R}$ both normal and tangential tractions are zero, thus establishing the problem in elasticity as one in which the tractions are specified over the whole boundary $z = 0$. We use the well known potential functions of Boussinesq and Cerutti to obtain expressions for the displacements occurring on the surface of the half-space.

Since the solution may only be determined to within an arbitrary rigid body displacement, we also require that the displacement tends to zero as the distance from the origin tends to infinity.

The Potential Functions of Boussinesq and Cerutti

The surface displacements due to concentrated normal and tangential point forces acting on the surface $z = 0$ may be determined using the potential functions of Boussinesq [7] and Cerutti [15]. A number of authors present the derivation of the potentials, see for example Love [42], Mal and Singh [43] and Westergaard [71]. Here we list the results of

Walton [66] for point forces of the form

$$N\delta(x-x')\delta(y-y') \tag{1.1}$$

acting normally (the z-direction) and

$$P\delta(x-x')\delta(y-y') \tag{1.2}$$

acting tangentially (x-direction), where $\delta(\cdot)$ is the Dirac delta function. These concentrated forces act at the point (x', y'), as shown in figure 1-1, and are of magnitudes N and P respectively. The surface displacements due purely to the normal force (1.1) are, in the $x-$, $y-$ and z-directions respectively,

$$\begin{aligned} u(x,y) &= -\frac{(B-C)NX}{2S^2} \\ v(x,y) &= -\frac{(B-C)NY}{2S^2} \\ w(x,y) &= \frac{BN}{S} \end{aligned} \tag{1.3}$$

and similarly, those due to the tangential force(1.2) are

$$\begin{aligned} u(x,y) &= \left(\frac{B}{S}+\frac{CX^2}{S^3}\right)P \\ v(x,y) &= \frac{CPXY}{S^3} \\ w(x,y) &= \frac{(B-C)PX}{2S^2} \end{aligned} \tag{1.4}$$

where we have defined local Cartesian coordinates $O'XY$ with origin (x', y') as

$$X = x - x' \quad \text{and} \quad Y = y - y'. \tag{1.5}$$

The quantity S is defined as

$$S^2 = X^2 + Y^2 \tag{1.6}$$

and the elastic constants B and C are given in terms of the Lamé moduli λ and μ by

$$B = \frac{1}{4\pi}\left(\frac{1}{\mu} + \frac{1}{\lambda+\mu}\right) \quad \text{and} \quad C = \frac{1}{4\pi}\left(\frac{1}{\mu} - \frac{1}{\lambda+\mu}\right). \tag{1.7}$$

These constants are also included in the table of isotropic elastic constants found in appendix E.

Distributed Normal and Tangential Tractions

We now consider a general distribution of traction: $N(x,y)$ in the normal direction and $P(x,y)$, $Q(x,y)$ acting in the tangential x- and y- directions respectively. These forces may be considered as a continuous distribution of point forces acting over some region $\mathcal{R}$ and are defined to be zero outside $\mathcal{R}$. Integrating the displacements (1.3) and (1.4) due to the point forces over the loaded region, we obtain

$$\begin{aligned}
u(x,y) &= \int_{\mathcal{R}} \left\{ \frac{BP(x',y')}{S} + C\left[\frac{X^2P(x',y') + XYQ(x',y')}{S^3}\right] \right. \\
&\qquad \left. - \frac{(B-C)XN(x',y')}{2S^2} \right\} \mathrm{d}x'\mathrm{d}y' \\
v(x,y) &= \int_{\mathcal{R}} \left\{ \frac{BQ(x',y')}{S} + C\left[\frac{XYP(x',y') + Y^2Q(x',y')}{S^3}\right] \right. \\
&\qquad \left. - \frac{(B-C)YN(x',y')}{2S^2} \right\} \mathrm{d}x'\mathrm{d}y' \\
w(x,y) &= \int_{\mathcal{R}} \left\{ \frac{(B-C)\left[XP(x',y') + YQ(x',y')\right]}{2S^2} + \frac{BN(x',y')}{S} \right\} \mathrm{d}x'\mathrm{d}y'.
\end{aligned} \tag{1.8}$$

For certain types of problems, the force distributions $P(x,y)$, $Q(x,y)$ and $N(x,y)$ will satisfy a number of symmetries which may be made use of. Walton [66] states that, for the distributions arising during the contact of two elastic spheres the centres of which move in the plane $y = 0$ only, the following symmetries must be satisfied:

1. P and N are symmetric and Q is antisymmetric in both x and y;

2. u and w are symmetric and v is antisymmetric in y.

With these properties in mind, the following definitions are made

$$\begin{aligned}
u_s(x,y) &= \frac{1}{2}\{u(x,y) + u(-x,y)\}, \quad u_a(x,y) = \frac{1}{2}\{u(x,y) - u(-x,y)\}, \\
v_s(x,y) &= \frac{1}{2}\{v(x,y) + v(-x,y)\}, \quad v_a(x,y) = \frac{1}{2}\{v(x,y) - v(-x,y)\},
\end{aligned}$$

$$w_s(x,y) = \frac{1}{2}\{w(x,y)+w(-x,y)\}, \quad w_a(x,y) = \frac{1}{2}\{w(x,y)-w(-x,y)\} \quad (1.9)$$

which splits the surface displacements $u(x,y)$, $v(x,y)$ and $w(x,y)$ into symmetric (subscript s) and antisymmetric (subscript a) parts with respect to the coordinate x. By substituting the above definitions into the integrals (1.8) and making use of the above symmetries, the displacements are given as

$$\begin{aligned} u_a(x,y) &= -\frac{1}{2}(B-C)\int_{\mathcal{R}} \frac{XN(x',y')}{S^2}\,\mathrm{d}x'\,\mathrm{d}y' \\ v_s(x,y) &= -\frac{1}{2}(B-C)\int_{\mathcal{R}} \frac{YN(x',y')}{S^2}\,\mathrm{d}x'\,\mathrm{d}y' \\ w_s(x,y) &= B\int_{\mathcal{R}} \frac{N(x',y')}{S}\,\mathrm{d}x'\,\mathrm{d}y' \end{aligned} \quad (1.10)$$

and

$$\begin{aligned} u_s(x,y) &= \int_{\mathcal{R}} \left\{ \frac{BP(x',y')}{S} + \frac{C\,[X^2P(x',y')+XYQ(x',y')]}{S^3} \right\} \mathrm{d}x'\,\mathrm{d}y' \\ v_a(x,y) &= \int_{\mathcal{R}} \left\{ \frac{BQ(x',y')}{S} + \frac{C\,[XYP(x',y')+Y^2Q(x',y')]}{S^3} \right\} \mathrm{d}x'\,\mathrm{d}y' \\ w_a(x,y) &= \frac{1}{2}(B-C)\int_{\mathcal{R}} \frac{[XP(x',y')+YQ(x',y')]}{S^2}\,\mathrm{d}x'\,\mathrm{d}y' \end{aligned} \quad (1.11)$$

which are uncoupled in the sense that the integrals (1.10) contain only the effects of normal forces and the integrals (1.11) contain only the effects of tangential forces. Later in this chapter we will make use of a similar decoupling by considering the relative and absolute displacements.

1.2.2 Pressure Applied to a Circular Region

Hertz Pressure Distribution

Consider a normal force distribution of the form

$$N(r) = \begin{cases} N_0(a^2-r^2)^{1/2} & ,0 \le r \le a \\ 0 & ,r > a \end{cases} \quad (1.12)$$

where (r,θ) is a system of plane-polar coordinates in the xy-plane sharing the common

origin O as defined in section (1.2.1). The region $\mathcal{R}$ is a circle of radius a centred on O and N_0 is a constant. This is the Hertz distribution which will be of use in section (1.2.4) and the displacements on the region $\mathcal{R}$ are obtained from the integrals (1.10) as

$$\begin{aligned} u_a(x,y) &= -\frac{\pi N_0}{3}(B-C)x\left\{\frac{a^3-(a^2-r^2)^{3/2}}{r^2}\right\} \\ v_s(x,y) &= -\frac{\pi N_0}{3}(B-C)y\left\{\frac{a^3-(a^2-r^2)^{3/2}}{r^2}\right\} \\ w_s(x,y) &= \frac{\pi^2 N_0}{4}B(2a^2-r^2). \end{aligned} \tag{1.13}$$

Similarly, for a distribution in the x-direction of the form

$$P(r) = \begin{cases} K(a^2-r^2)^{1/2} & ,0 \le r \le a \\ 0 & ,r > a \end{cases} \tag{1.14}$$

where K is a constant and the distribution in the y-direction $Q(x,y)$ is zero, the resulting displacements are found from the integrals (1.11) as

$$\begin{aligned} u_s(x,y) &= \frac{\pi^2}{4}(2B+C)Ka^2 - \frac{\pi^2}{16}K\left\{(4B+C)x^2+(4B+3C)y^2\right\} \\ v_a(x,y) &= \frac{\pi^2}{8}KCxy \\ w_a(x,y) &= \frac{\pi}{3}K(B-C)x\left\{\frac{a^3-(a^2-r^2)^{3/2}}{r^2}\right\}. \end{aligned} \tag{1.15}$$

Further details on the calculation of these displacements, interior or exterior to the region $\mathcal{R}$, may be obtained from Johnson [35] page 56.

Punch Type Pressure Distribution

When a flat frictionless punch, having a circular cross-section of radius a, is pushed normally into an elastic half-space, the type of normal pressure arising is

$$N(r) = \begin{cases} N_0(a^2-r^2)^{-1/2} & ,0 \le r \le a \\ 0 & ,r > a \end{cases} \tag{1.16}$$

which causes uniform displacements over the contact region, in this case a circle of radius a. The normal displacements, on $r \leq a$ only, may be obtained from equations (1.10) and (1.11) as

$$\begin{aligned} w_s(x,y) &= \pi^2 B N_0 \\ w_a(x,y) &= 0. \end{aligned} \tag{1.17}$$

We will also make use of a tangential distribution of the same form, namely

$$P(r) = \begin{cases} K(a^2 - r^2)^{-1/2} & ,0 \leq r \leq a \\ 0 & ,r > a \end{cases} \tag{1.18}$$

in the x-direction, the tangential force in the y-direction being zero. This type of tangential distribution does not occur in the normal punch problem but will be useful later on in section (1.2.5). The required displacements due to this distribution (1.18) are, on $r \leq a$ only,

$$\begin{aligned} u_s(x,y) &= \frac{\pi^2(2B+C)}{2} K \\ v_a(x,y) &= 0. \end{aligned} \tag{1.19}$$

Johnson [35] page 71, discusses the punch problem and the derivation of the surface displacements in greater detail.

1.2.3 The Geometry of Bodies in Contact

Before examining Hertz theory for two contacting spheres, it is necessary to consider the geometry of non-conforming bodies of general profile. Non-conforming refers to bodies which curve outwardly from each other in all directions, and consequently will touch initially at a single point. Contact of conforming bodies which touch along a line or a large area of surface is considered by Johnson [35] page 114.

Hertz theory requires that the surface of each body may be represented satisfactorily as a second order expansion about some fixed point or origin. The point of first contact of

the two bodies defines an origin of a rectangular Cartesian coordinate system in which the xy-plane is the common tangent plane and the z-axis is directed along the common normal into the lower solid. Johnson [35] gives the profile of the lower surface as

$$z_1 = \frac{1}{2R_1'}x_1^2 + \frac{1}{2R_1''}y_1^2 \tag{1.20}$$

where R_1' and R_1'' are the principal radii of curvature of the surface at the origin and the x_1- and y_1-axes are chosen such that any terms in $x_1 y_1$ vanish. Similarly, for the upper surface

$$z_2 = -\left(\frac{1}{2R_2'}x_2^2 + \frac{1}{2R_2''}y_2^2\right). \tag{1.21}$$

The separation between the two surfaces is given by $h = z_1 - z_2$ and so relative to a common set of axes x and y

$$h = \alpha x^2 + \beta y^2 + \gamma xy \tag{1.22}$$

where α, β and γ are constants depending on the four radii in equations (1.20) and (1.21). Choosing axes such that γ becomes zero we obtain

$$h = \alpha x^2 + \beta y^2 = \frac{1}{R'}x^2 + \frac{1}{R''}y^2 \tag{1.23}$$

where R' and R'' are the principal relative radii of curvature. If the x_1- and x_2-axes are inclined to each other at an angle θ then it can be shown that

$$\begin{aligned}
\alpha + \beta &= \frac{1}{2}\left(\frac{1}{R'} + \frac{1}{R''}\right) = \frac{1}{2}\left(\frac{1}{R_1'} + \frac{1}{R_1''} + \frac{1}{R_2'} + \frac{1}{R_2''}\right) \\
|\alpha - \beta| &= \frac{1}{2}\left\{\left(\frac{1}{R_1'} - \frac{1}{R_1''}\right)^2 + \left(\frac{1}{R_2'} - \frac{1}{R_2''}\right)^2 \right. \\
&\qquad \left. + 2\left(\frac{1}{R_1'} - \frac{1}{R_1''}\right)\left(\frac{1}{R_2'} - \frac{1}{R_2''}\right)\cos 2\theta\right\}^{1/2}
\end{aligned} \tag{1.24}$$

from which the solutions for α and β may be determined. For later convenience we introduce an equivalent radius defined by

$$R_e = (R'R'')^{1/2} = \frac{1}{2}(\alpha\beta)^{-1/2}. \tag{1.25}$$

As an example of the above geometry, consider a pair of identical circular cylinders of radius R with their axes inclined at 45°. The radius parameters in this case are $R_1' = R_2' = R$; $R_1'' = R_2'' = \infty$, and the angle is $\theta = \pi/4$. The equations (1.24) give values for α and β of

$$\alpha = \frac{1 - 1/\sqrt{2}}{2R} \quad \text{and} \quad \beta = \frac{1 + 1/\sqrt{2}}{2R} \tag{1.26}$$

and the effective radius is

$$R_e = \frac{1}{2}(\alpha\beta)^{-1/2} = R\sqrt{2}. \tag{1.27}$$

For equal spheres of radius R we have $R_1' = R_2' = R_1'' = R_2'' = R$ and $\theta = 0$ giving values for α and β of

$$\alpha = \frac{1}{R} \quad \text{and} \quad \beta = \frac{1}{R}. \tag{1.28}$$

The equations (1.24) are useful in chapter 6 when considering the contact of bodies of a general profile. Also in chapter 6, the constants α and β are determined explicitly for two identical oblate spheroidal bodies having aligned axes.

Figure 1-2 shows the two elastic bodies deforming in the vicinity of the point of first contact O due to the application of a normal pressure. A contact area is formed which is assumed to be small in comparison with the sizes of the bodies. Points distant from the contact region approach each other by an amount $\delta_1 + \delta_2$. The surface displacements are denoted by $w^{(1)}$ for the lower body and $w^{(2)}$ for the upper body. Thus we may write

$$w^{(1)} + w^{(2)} + h = \delta_1 + \delta_2 \tag{1.29}$$

for points on the contact area, where $h(x, y)$ is the initial separation of the surfaces given by equation (1.23), and at points outside the contact area the displacements must satisfy

$$w^{(1)} + w^{(2)} + h > \delta_1 + \delta_2. \tag{1.30}$$

In terms of the constants α and β from equation (1.23), these conditions of contact may be written as

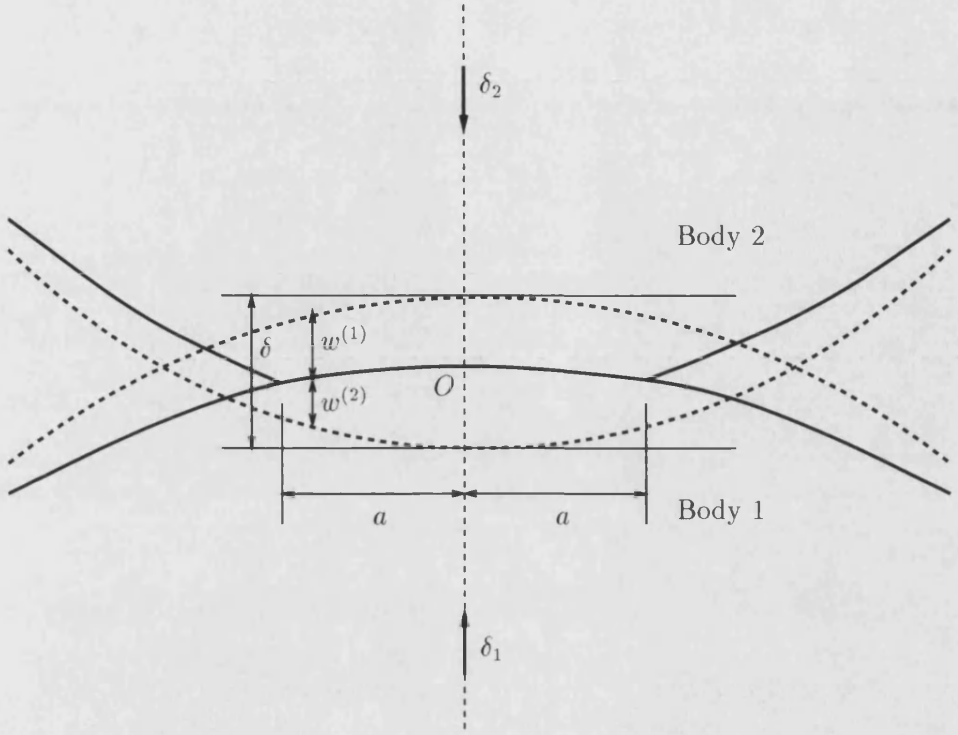

Figure 1-2: *Cross-section of two contacting bodies*

$$w^{(1)} + w^{(2)} = \delta - \alpha x^2 - \beta y^2 \tag{1.31}$$

on the contact area, where $\delta = \delta_1 + \delta_2$, and outside the contact area the displacements must satisfy

$$w^{(1)} + w^{(2)} > \delta - \alpha x^2 - \beta y^2. \tag{1.32}$$

1.2.4 Hertz Theory of Elastic Contact

The first satisfactory treatment of the contact of non-conforming elastically isotropic bodies was given by Hertz [30] in 1882. The profiles of the two bodies is shown in figure 1-2. Initially, the two bodies are assumed to be in contact at a single point O, until there is an application of a loading pressure (perpendicular to the common tangent plane of the two bodies) which causes a deformation in the neighbourhood of the point of first contact. Thus a finite contact area is formed and, assuming the two bodies have identical elastic properties, the tractions acting on it are purely normal. When the elastic properties of the two bodies differ, tangential or shear tractions occur which

may give rise to slip between the two surfaces.

For the purposes of this thesis, when considering specific contact problems (spheres and spheroids for example) the bodies will be assumed isotropic with equal elastic moduli. Johnson [35] page 90, considers contacting solids with differing elastic moduli and Willis [72] examines the effects of anisotropy within the bodies.

A number of assumptions are made by Hertz theory and are listed by Johnson [35] page 91, as:

1. The surfaces are smooth, continuous and non-conforming;
2. The strains are small;
3. Each solid may be approximated by an elastic half-space;
4. The surfaces are frictionless.

These assumptions are necessary to ensure that the surfaces in the region of the contact area approximate to a plane and that the strains are small enough to be within the scope of linear elasticity. By approximating the bodies as half-spaces the boundary conditions are greatly simplified and use can be made of the extensive theory available for half-space problems, such as the results seen in sections (1.2.1) and (1.2.2).

The problem in elasticity is now reduced to the determination of the normal pressure distributions acting on the contact area which will produce normal displacements of the form given by (1.31) and satisfy the condition (1.32) outside the contact area.

We take as an example of the application of Hertz theory the normal compression of two identical elastic spheres. By symmetry about the central axis of the two spheres, the shape of the contact area is circular and has radius a. The radius of the spheres is R and, as we have already seen, the system (1.24) gives values for α and β as

$$\alpha = \frac{1}{R} \quad \text{and} \quad \beta = \frac{1}{R}. \tag{1.33}$$

Since the spheres are identical and have equal elastic moduli, we may write $w_0 = \delta_1 = \delta_2$ so that $2w_0 = \delta_1 + \delta_2$ where w_0 is the relative compression of each sphere. Also the surface displacements may be written as $w^{(1)} + w^{(2)} = 2w_s(x, y)$ where $w_s(x, y)$ is given

by equation (1.13) and $w_a(x,y) = 0$. Then the condition of contact (1.31) on the contact area is

$$2w_s(x,y) = 2w_0 - \frac{x^2}{R} - \frac{y^2}{R}. \tag{1.34}$$

The problem in elasticity is to determine the distribution of pressure $N(x,y)$ on $r \leq a$ which gives rise to displacements of the above form. One such distribution is that given by equation (1.12) as

$$N(x,y) = N_0(a^2 - r^2)^{1/2} \tag{1.35}$$

with normal displacements

$$w_s(x,y) = \frac{\pi^2 N_0}{4} B(2a^2 - r^2) \quad \text{and} \quad w_a(x,y) = 0. \tag{1.36}$$

Substituting into equation (1.34) we obtain

$$\frac{\pi^2 N_0}{2} B(2a^2 - r^2) = 2w_0 - \frac{r^2}{R} \tag{1.37}$$

and matching the constant terms and the coefficients of r^2, we solve for N_0 and w_0 as

$$N_0 = \frac{2}{\pi^2 RB} \quad \text{and} \quad a^2 = Rw_0. \tag{1.38}$$

Thus the normal force distribution (1.12) is given by

$$N_0(r) = \frac{2}{\pi^2 RB}(a^2 - r^2)^{1/2} \tag{1.39}$$

and the Hertzian contact area radius is given by

$$a^2 = Rw_0. \tag{1.40}$$

1.2.5 Hertz Loading with a Tangential Component

As stated earlier, according to Hertz theory, tangential tractions do not occur when bodies having the same elastic moduli are compressed normally. When the bodies are displaced tangentially as well as normally, tangential tractions arise on the contact area. Mindlin [44] considered a loading in which a tangential force is imposed on the existing

normal compressive force. Considerations of symmetry showed that the distribution of normal traction is not affected by the application of the tangential load as long as the two bodies have identical elastic properties. It was also shown that if no slip occurred (infinite friction) the tangential displacement was a rigid body displacement. The solution to such a boundary value problem, for the special case of spheres, was shown to be of the form (1.18); the tangential traction being proportional to $(a^2-r^2)^{-1/2}$.

Walton [66] also considered tangential loading of the Hertz problem but examined the more general oblique problem in which the normal and tangential displacements occur simultaneously from zero. By decoupling the problem into normal and tangential systems, as was seen for the half-space problem in section (1.2.1), the normal and tangential problems were solved to obtain a distribution of traction (P, Q, N) on the contact area. Using the notation of section (1.2.1), the force exerted on the lower sphere by the upper sphere is

$$\begin{aligned} P(r) &= -\frac{4u_0}{\pi^2 R(2B+C)w_0}(a_0^2 - r^2)^{1/2} \\ Q(r) &= -\frac{4v_0}{\pi^2 R(2B+C)w_0}(a_0^2 - r^2)^{1/2} \\ N(r) &= \frac{2}{\pi^2 RB}(a_0^2 - r^2)^{1/2} \end{aligned} \tag{1.41}$$

where $(u_0, v_0, -w_0)$ is the displacement of the centre of the lower sphere relative to the origin O, and the radius of the contact area is a_0. The solution to this problem may also be obtained from the results of Mindlin and Deresiewicz [45] by taking the initial normal compression to be zero. The addition of an incremental displacement $(\delta u_0, \delta v_0, -\delta w_0)$ on the above initial state is considered in Walton [67]. The cases of $\delta w_0 > 0$ (compression) and $\delta w_0 < 0$ (unloading) are solved—the incremental displacement is assumed small enough that separation of the spheres does not occur. The distribution of normal traction in both cases is

$$N + \delta N = \frac{2}{\pi^2 RB}(a^2 - r^2)^{1/2} \tag{1.42}$$

where the initial contact area radius a_0 has been replaced by the new radius for the incremental problem a (denoted b in reference [67]). An infinite value of the coefficient of friction ensures that there is no relative displacement between the contact areas.

Considering first the case when $\delta w_0 < 0$, the form of tangential tractions arising are

$$\begin{aligned} P + \delta P &= K_1(a^2 - r^2)^{1/2} + K_2(a^2 - r^2)^{-1/2} \\ Q + \delta Q &= L_1(a^2 - r^2)^{1/2} + L_2(a^2 - r^2)^{-1/2} \end{aligned} \tag{1.43}$$

the K_2 and L_2 terms being the punch-type pressure of Mindlin [44] and section (1.2.2). Walton [67] gives no details of the calculation of the constants K_1, K_2, L_1 and L_2 and since chapter 3 solves problems of this nature, the method is given here: To decouple the problem into normal and tangential systems, similar to those seen in section (1.2.1), we define relative and absolute displacements by

$$\begin{aligned} u_r(x,y) &= \frac{1}{2}\{u_+(x,y) - u_-(x,y)\} \\ u_a(x,y) &= \frac{1}{2}\{u_+(x,y) + u_-(x,y)\} \end{aligned} \tag{1.44}$$

with similar definitions for v_r, v_a, w_r and w_a. The displacements $u_+(x,y)$ are in the z-direction on the surface of the half space $z > 0$ due to the distribution (P, Q, N), and the displacements $u_-(x,y)$ are in the z-direction on the surface of the half space $z > 0$ due to the distribution $(-P, -Q, -N)$. The decoupling of the displacement integrals (1.8) and the interpretations of the relative and absolute displacements are discussed in chapter 3. The displacements $u_r(x,y)$ and $v_r(x,y)$ on the contact area at the end of the initial compression are calculated in chapter 3 as

$$\begin{aligned} u_r(x,y) &= u_0 + \frac{\pi^2}{4}(2B + C)K_0 a_0^2 \\ &\quad - \frac{\pi^2}{16}K_0\{(4B + C)x^2 + (4B + 3C)y^2\} + \frac{\pi^2}{8}L_0 C x y \\ v_r(x,y) &= v_0 + \frac{\pi^2}{4}(2B + C)L_0 a_0^2 \\ &\quad - \frac{\pi^2}{16}L_0\{(4B + 3C)x^2 + (4B + C)y^2\} + \frac{\pi^2}{8}K_0 C x y. \end{aligned} \tag{1.45}$$

Recall that the half-space problem which gave rise to the displacements (1.15) requires that the displacements be zero at infinity. However, for the contact problem we require that the displacement at infinity (for the lower sphere) be $(u_0, v_0, -w_0)$ and this is

included in the expressions above.

The constant K_0 is the force constants for the distributions (1.41) and is given by

$$K_0 = -\frac{4u_0}{\pi^2 R(2B+C)w_0}. \tag{1.46}$$

The displacements due to the distribution (1.43) are, from equations (1.15) and (1.19),

$$\begin{aligned} u_r(x,y) &= u_0 + \delta u_0 + \frac{\pi^2}{4}(2B+C)K_1 a_0^2 + \frac{\pi^2}{2}(2B+C)K_2 \\ &\quad - \frac{\pi^2}{16}K_1\left\{(4B+C)x^2 + (4B+3C)y^2\right\} + \frac{\pi^2}{8}L_1 Cxy \\ v_r(x,y) &= v_0 + \delta v_0 + \frac{\pi^2}{4}(2B+C)L_1 a_0^2 + \frac{\pi^2}{2}(2B+C)L_2 \\ &\quad - \frac{\pi^2}{16}L_1\left\{(4B+3C)x^2 + (4B+C)y^2\right\} + \frac{\pi^2}{8}K_1 Cxy. \end{aligned} \tag{1.47}$$

The no-slip condition (no relative displacement of the surfaces) requires that this displacement matches that at the end of the initial displacement. Matching the constant terms and the coefficients of x^2 and y^2 we obtain equations for K_1 and K_2 as

$$\begin{aligned} K_1 &= K_0 \\ u_0 + \frac{\pi^2}{4}(2B+C)K_0 a_0^2 &= u_0 + \delta u_0 + \frac{\pi^2}{4}(2B+C)K_1 a^2 + \frac{\pi^2}{2}(2B+C)K_2 \end{aligned} \tag{1.48}$$

and equations for L_1 and L_2 as

$$\begin{aligned} L_1 &= L_0 \\ v_0 + \frac{\pi^2}{4}(2B+C)L_0 a_0^2 &= v_0 + \delta u_0 + \frac{\pi^2}{4}(2B+C)L_1 a^2 + \frac{\pi^2}{2}(2B+C)L_2. \end{aligned} \tag{1.49}$$

Solving for K_1, K_2, L_1 and L_2 the distribution obtained is

$$\begin{aligned} P + \delta P &= \frac{2}{\pi^2 R(2B+C)w_0}\left\{2u_0(a^2-r^2)^{1/2} + (a_0^2 u_1 - a^2 u_0)(a^2-r^2)^{-1/2}\right\} \\ Q + \delta Q &= \frac{2}{\pi^2 R(2B+C)w_0}\left\{2v_0(a^2-r^2)^{1/2} + (a_0^2 v_1 - a^2 v_0)(a^2-r^2)^{-1/2}\right\} \end{aligned} \tag{1.50}$$

where $u_1 = u_0 + \delta u_0$ and $v_1 = v_0 + \delta v_0$.

When $\delta w_0 > 0$ new contact area is being formed. The no-slip condition may be applied on the original contact area and a similar condition must apply on any new contact surfaces formed. This boundary condition plus an energy flux argument presented in Walton [66] is enough to make the solution unique. The tangential tractions are

$$\begin{aligned} P + \delta P &= K_1(a^2 - r^2)^{1/2} + K_2(a_0^2 - r^2)^{1/2} \\ Q + \delta Q &= L_1(a^2 - r^2)^{1/2} + L_2(a_0^2 - r^2)^{1/2}. \end{aligned} \tag{1.51}$$

Calculating the displacements due to this distribution using equation (1.15) and matching terms in the same way as before, results in the distributions

$$\begin{aligned} P + \delta P &= \frac{4}{\pi^2 R^2 (2B + C) w_0 \delta w_0} \Big\{ (a^2 u_0 - a_0^2 u_0)(a_0^2 - r^2)^{1/2} \\ &\qquad + (u_1 - u_0) a_0^2 (a^2 - r^2)^{1/2} \Big\} \\ Q + \delta Q &= \frac{4}{\pi^2 R^2 (2B + C) w_0 \delta w_0} \Big\{ (a^2 v_0 - a_0^2 v_0)(a_0^2 - r^2)^{1/2} \\ &\qquad + (v_1 - v_0) a_0^2 (a^2 - r^2)^{1/2} \Big\}. \end{aligned} \tag{1.52}$$

1.2.6 Frictional Contact

The first scientific study of friction was carried out by Guillaume Admontons (1663–1705) and in 1699 he published a paper in which he rediscovered two forgotten laws of friction, originally derived by Leonardo da Vinci (1452–1519). The first law states that for rigid bodies in sliding contact over some plane region the tangential force P is proportional to the normal force N. The constant of proportionality is known as the coefficient of friction, denoted f, and so this law may be written as

$$P = fN. \tag{1.53}$$

When sliding does not occur, that is there is no relative displacement between the two surfaces, it is required that

$$P \leq fN. \tag{1.54}$$

Admontons' second law simply states that the coefficient of friction is independent of the size of the bodies. In addition to these two laws, we also require that the direction of relative slip (u_r, v_r) opposes the direction of the force causing it; this condition will be significant when examining the oscillating forces of section (1.2.9) and chapter 3.

Admontons recognised that the surfaces he worked with were not smooth and attributed friction to the work done in overcoming surface irregularities. The effects of surface roughness were studied by Charles Augustus Coulomb (1736–1806) in his book 'Theory of Simple Machines', published in 1781. Coulomb also published papers [18] on laws similar to that derived by Admontons. For a historical account of the work of Admontons, Coulomb and others who studied friction, see Bowden and Tabor [9].

Although widely accepted, Admontons' law does not apply to contact between all materials. For example, Tüzün and Walton [60] use a modified friction law in which the coefficient of friction depends on the normal load and the area of contact

$$P = \tau_0 A + \alpha N \tag{1.55}$$

where A is the interfacial contact area, τ_0 is the interfacial shear strength and α is a pressure coefficient. Laws of this form are often exhibited by highly polished metal surfaces (Bowden and Tabor [8]) and glass spheres, Winkler [74]. The above law is often used to describe the frictional properties of powders and powder flows. Kendall [37] examines the inadequacy of Coulomb's law for fine powders and explains the increase in friction for smaller particles using the JKR theory of adhesive contact, Johnson, Kendall and Roberts [36].

However, Tüzün and Walton [60] also state that particles with rough surfaces show no such load dependence (see Briscoe, Pope and Adams [11], Tüzün, Pope and Adams [59] and figure 1 of [60]). Therefore, for the purposes of this thesis, Admontons' law will be adequate. Several authors have examined the frictional Hertz contact problem using Admontons' law, including Raoof and Hobbs [47] and Bryant and Keer [12]. Both of these references considered the frictional contact of geometrically and elastically identical curved bodies with an elliptical contact area. Here we will examine the frictional Hertz contact problem for two identical elastic spheres.

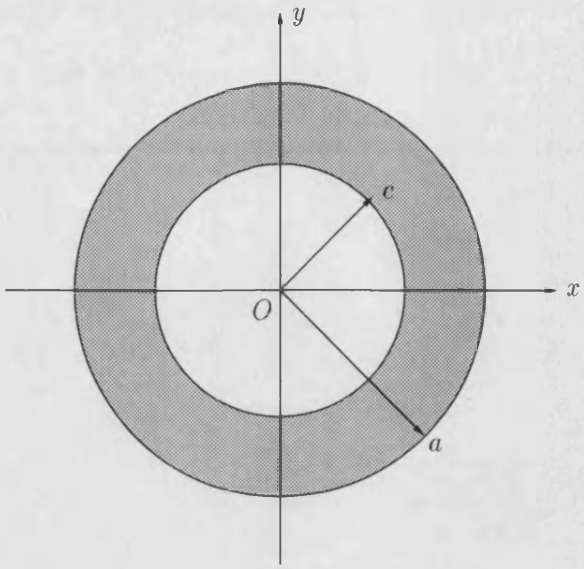

Figure 1-3: *The annulus of slip* $c \leq r \leq a$

1.2.7 Loading with Partial Slip

Cattaneo [14] and Mindlin [44] independently studied the tangential loading of two elastic bodies, initially compressed by a Hertzian normal pressure, with a finite non-zero value of the coefficient of friction between the contact surfaces. By first assuming that no slip occurs on the contact area, as was seen in section (1.2.5), solutions of the form (1.18) were obtained. These solutions are physically unrealistic due to the square-root singularity occurring at the edge of contact. Because the tangential traction is unbounded as r approaches a, the application of Admontons' law (1.54) requires that slip must occur at some point on the contact area. Mindlin's solution was to assume that an annulus of slip progressed from $r = a$ to some value $r = c$. Within this annulus the slip condition (1.53) is satisfied, and on the inner circle $r < c$, the condition (1.54) must be true with no slip between the two surfaces. The required distribution of traction is given as equations (98) and (99) of Mindlin [44], which in the notation of this section is

$$P(r) = \begin{cases} \dfrac{3f\overline{N}}{2\pi a^2}\left(1-\dfrac{r^2}{a^2}\right)^{1/2} - \dfrac{3f\overline{N}c}{2\pi a^3}\left(1-\dfrac{r^2}{c^2}\right)^{1/2} & , \ r \leq c \\ \dfrac{3f\overline{N}}{2\pi a^2}\left(1-\dfrac{r^2}{a^2}\right)^{1/2} & , \ c \leq r \leq a \end{cases} \tag{1.56}$$

the normal force being

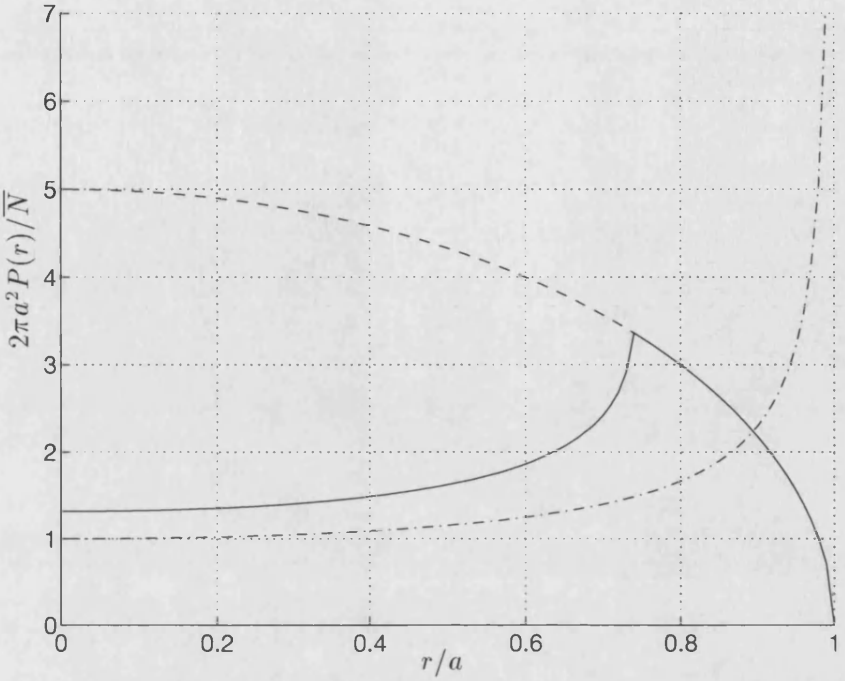

Figure 1-4: *The tangential force distribution* $P(r)$

$$N(r) = \frac{3\overline{N}}{2\pi a^2}\left(1 - \frac{r^2}{a^2}\right)^{1/2} \tag{1.57}$$

where $\overline{N}$ is the total applied normal force. The radius of slip c is calculated by balancing the total force due to the distribution above with the applied tangential force $\overline{P}$ to obtain

$$c = a\left(1 - \frac{\overline{P}}{f\overline{N}}\right)^{1/3} \tag{1.58}$$

and the annulus $c \leq r \leq a$ is shown in figure 1-3. Figure 1-4 plots the tangential force distribution (1.56) for r/a from 0 to 1 with a value of $\overline{P}/f\overline{N} = 0.6$ (solid line). The dashed line is the function $fN(r)$ where $N(r)$ is the normal force given by equation (1.57), and the dash-dotted line is the no-slip solution with a square-root singularity at $r = a$.

It is well known that the slip solution described above is only an approximate solution to the elastic boundary value problem. Within the slip annulus $c \leq r \leq a$, although the tangential force distribution is in the x-direction at any given point the direction of slip

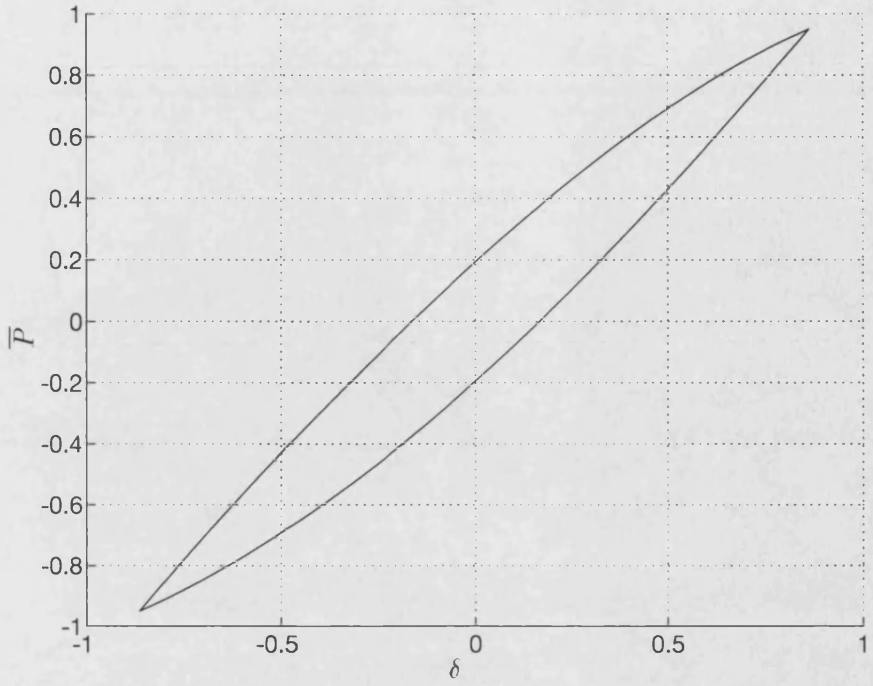

Figure 1-5: *The tangential force-displacement relationship* $\delta(\overline{P})$

is found to be slightly offset from the direction of the x-axis. Therefore the condition that the slip must be in the direction of the frictional traction is not precisely satisfied. However, Johnson [35] page 219, has calculated the deviation of the slip in the x- and y-directions, denoted s_x ands_y respectively, and has shown that the ratio of s_y to s_x is of the order $\nu/(2-\nu) \approx 0.09$, where ν is Poisson's ratio. The the inclination of the slip to the x-axis will not be more than a few degrees and consequently the approximation of tangential traction acting everywhere parallel to the x-axis is a good one.

1.2.8 Unloading with Counterslip

Section 2 of a paper by Mindlin and Deresiewicz [45] considers the problem of loading with slip, as seen in the previous section, followed by an equal and opposite unloading. Again the spheres are held together with an initial Hertzian compression of magnitude $\overline{N}$ which remains constant throughout. The distribution of tangential traction at the end of the initial loading is

$$P(r) = \begin{cases} \frac{3f\overline{N}}{2\pi a^3}\left[(a^2-r^2)^{1/2}-(c^2-r^2)^{1/2}\right] & , \ r \le c \\ \frac{3f\overline{N}}{2\pi a^3}(a^2-r^2)^{1/2} & , \ c \le r \le a \end{cases} \tag{1.59}$$

where the radius of slip has reached its fixed minimum value of

$$c = a\left(1-\frac{\overline{P}^*}{f\overline{N}}\right)^{1/3} \tag{1.60}$$

$\overline{P}^*$ being the maximum value of the applied tangential load, $0 < \overline{P}^* < f\overline{N}$. Unloading starts from $\overline{P} = \overline{P}^*$ and progresses to $\overline{P} = -\overline{P}^*$. Prevention of slip would again result in the infinite tractions (1.18) and so a radius of counterslip b is assumed to progress from $r = a$ to $r = b$. The resulting tangential tractions are

$$P(r) = \begin{cases} -\frac{3f\overline{N}}{2\pi a^3}\left[(a^2-r^2)^{1/2}-2(b^2-r^2)^{1/2}+(c^2-r^2)^{1/2}\right] & , \ r \le c \\ -\frac{3f\overline{N}}{2\pi a^3}\left[(a^2-r^2)^{1/2}-2(b^2-r^2)^{1/2}\right] & , \ c \le r \le b \\ -\frac{3f\overline{N}}{2\pi a^3}(a^2-r^2)^{1/2} & , \ b \le r \le a. \end{cases} \tag{1.61}$$

The radius b is found in the same way as before to be

$$b = a\left(1-\frac{\overline{P}^*-\overline{P}}{2f\overline{N}}\right)^{1/3}. \tag{1.62}$$

Clearly we must have $c \le b \le a$. At $\overline{P} = 0$ the displacements calculated in [45] show that a permanent displacement or 'set' has occurred. When the tangential load is fully reversed at $\overline{P} = -\overline{P}^*$ then $b = c$ and the initial slip has been fully reversed.

1.2.9 Oscillating Forces

The tangential distribution (1.56) demonstrates that the determination of the tractions on the contact area depend not only on the initial state, but also on the entire history of loading. In section 5 of Mindlin and Deresiewicz [45] the tangential force is oscillated between $-\overline{P}^*$ and $\overline{P}^*$. The result is that radii of slip and counterslip oscillate between $r = a$ and $r = c$. The displacement of the centre of the top sphere is shown to follow a

hysteresis path of the form

$$\delta_i = -\delta_d(-\overline{P}) = -\frac{3(2-\nu)f\overline{N}}{16\mu a}\left[2\left(1-\frac{\overline{P}^* + \overline{P}}{2f\overline{N}}\right)^{2/3} - \left(1-\frac{\overline{P}^*}{f\overline{N}}\right)^{2/3} - 1\right] \quad (1.63)$$

where δ_i denotes the displacement on the increasing cycle and δ_d denotes the displacement on the decreasing cycle. The elastic constants ν and μ are Poisson's ratio and the shear modulus respectively. This tangential force-displacement relationship is plotted in figure 1-5.

Oblique loading imposed on the initial normal compression is considered in subsequent sections of Mindlin and Deresiewic [45]; the normal and tangential forces are varied simultaneously. Many different cases are considered such as combinations of $\overline{N}$ increasing or decreasing and $\overline{P}$ increasing or decreasing from either $\overline{P} = \pm\overline{P}^*$ or from any point on an unloading curve. These results are then used to derive the tangential tractions due to oscillating oblique forces. After a number of loading and unloading phases, stable cycles are established with a repeating pattern of slip or stick. These stable cycles are found to depend on the conditions $d\overline{P}/d\overline{N} \leq f$ or $d\overline{P}/d\overline{N} \geq f$. When $d\overline{P}/d\overline{N} \geq f$ a stable cycle of slip is established in which energy is dissipated, and when $d\overline{P}/d\overline{N} \leq f$ a cycle in which no slip occurs (the surfaces stick together) is established.

The results of Mindlin and Deresiewicz [45] have been analysed experimentally by Johnson [34]. A steel ball is pressed normally onto a hard steel plate and oscillating oblique forces are cycled 10,000 times at varying angles of obliqueness. Damage due to surface fretting occurs in the form of an annulus; photographs are reproduced as figure 5 of [34] and also on page 228 of Johnson [35]. Experimental agreement of the expected energy losses due to slip (past the critical angle of friction) and the observed radii of slip are described by Johnson as 'surprisingly close'.

1.3 Granular Media

The elastic properties of granular media are of interest in a wide variety of research fields ranging from powder compaction in the pharmaceutical industry to the study of soil mechanics in civil engineering. Applications of the theory of granular media include rock mechanics, wave propagation within ocean sediments and geophysical exploration

for petroleum. Many theories and models are available to predict the elastic properties of granular media depending on the type of media to be modelled and the application required. Wang and Nur [70] summarise and discuss a number of such theories under the chapter headings:

1. Effective medium theories;
2. Wave propagation theories;
3. Contact theories;
4. Anisotropy.

Our interests lie with the first three categories and mainly in the third: contact theories. Here we will say a few words about effective medium and wave propagation theories before concentrating on a description of contact models and how the results obtained in section (1.2) may be bought together to form a model of certain types of granular media.

Effective Medium Theories

Effective medium theories are mainly applied to composite materials consisting of two or more phases with different elastic properties. The simplest types of effective medium theories are those in which the properties of each phase are averaged with a weighting proportional to the volume fraction of each phase, for example Wood [75]. Other theories, such as those of Voigt [62] and Reuss [48], provide upper and lower bounds respectively for the effective elastic moduli of such a composite medium. Hashin and Shtrikman [29] used a variational principle to provide closer upper and lower bounds for an isotropic two-phase composite than the sometimes impractical values given by the Voigt and Reuss models. The values calculated by Hashin and Shtrikman give the least upper bound and highest lower bound and therefore will be much closer to the true values of the effective elastic moduli.

Wave Propagation and Self-Consistent Theories

Wave propagation theories generally consider the dynamic propagation of waves through a granular or porous medium. Often the medium is saturated with fluid such as in

Biot [5] and [6] and Walton and Digby [69]. These models predict the speeds of propagation of elastic waves through the medium accounting for both the solid matrix and fluid properties and the relative motion between them.

The self-consistent method of Hill [31] may be used to estimate the elastic properties of multi-phase materials. Briefly, the method draws on the known solution to the problem of a loaded elastic medium containing an isolated ellipsoidal inclusion. For self-consistency, the properties of an appropriately chosen medium are assigned to the matrix material and similarly for the inclusion. Thus the effective elastic moduli of the entire medium may be estimated from the solution of this inclusion problem giving the well known 'self-consistent approximation' or SCA.

Contact Theories

Granular media modelled using contact theories are the main subject of this thesis. The major application is in the study of materials made of packings of distinct grains, sandstones and ocean sediments for example. The interactions of individual grains are described either by Hertz theory [30], in which only normal pressure between grains is applied, or by contact described by Mindlin [44], seen in section (1.2.5), in which the grains are compressed normally and then sheared tangentially or obliquely.

Perhaps the most natural grain shape to consider is that of the sphere. Early sphere packing models such as those of Duffy [25], Deresiewicz [21] and Walton [63], considered regular geometries such as the simple cubic packing or close-packed hexagonal packing. Chapter 4 of this thesis considers a cubic packing of elastic spheres under a uniaxial compression with a finite non-zero value of the coefficient of friction between each sphere. Brant [10] considered a random packing of spheres but only derived the effective bulk modulus. Digby [22] also considered a random packing model in which the spheres were bonded together.

The random packing model we summarise in the next section is that of Walton [67] which predicts the effective elastic moduli of the packing. The model considers the special cases of zero friction and infinite friction, that is the spheres are either perfectly smooth or infinitely rough. Chapter 5 extends these results to the intermediate case in which there is a finite non-zero value of the coefficient of friction.

1.3.1 The Effective Elastic Moduli of a Random Packing of Spheres

The calculation of the effective elastic moduli of a random packing of spheres is considered in a paper by Walton [67]. Chapters 5 and 7 use methods derived in this paper and so in this section we present the main results and techniques used.

The spheres within the packing are identical in that they are of the same size and have the same elastic moduli. The sphere material is homogeneous and elastically isotropic. The packing is random in the sense that the distribution of contact points is uniform over the surface of each sphere. Initially, each sphere is in point contact with several of its neighbours. In order to create contact areas between adjacent spheres and to ensure that no inter-granular separation occurs, the boundary of the medium is subjected to an initial confining strain. For simplicity, we assume that no new contacts are formed although Endres [26] examines the effects of contact generation in this model. The effective elastic moduli are calculated relative to this initial state by imposing a further incremental deformation which is assumed to be much smaller than the initial deformation. The relationship between the incremental stress and strain is determined and hence the effective moduli are obtained.

Results of the Contact Problem

The contact problem considered is one in which the spheres are compressed obliquely (corresponding to the initial compression) as seen in Walton [66] and section (1.2.5), followed by an oblique incremental compression as described above. In the initial deformation the centre of the lower sphere is displaced by an amount $(u_0, v_0, -w_0)$ and the centre of the upper sphere is displaced by an amount $(-u_0, -v_0, w_0)$. Similarly, in the incremental phase the centres of the lower and upper sphere centres are displaced by amounts $(\delta u_0, \delta v_0, -\delta w_0)$ and $(-\delta u_0, -\delta v_0, \delta w_0)$ respectively. The results of this two stage compression are considered for an infinite value of the coefficient of friction. The total forces acting on the contact area at the end of the initial state are

$$\overline{P_0} = -\frac{8u_0(Rw_0)^{1/2}}{3\pi(2B+C)}, \quad \overline{Q_0} = -\frac{8v_0(Rw_0)^{1/2}}{3\pi(2B+C)}, \quad \overline{N_0} = \frac{4R^{1/2}w_0^{3/2}}{3\pi B} \tag{1.64}$$

which are obtained by integrating the distributions (1.41) over the contact area. During the incremental phase, the total incremental forces when $\delta w_0 < 0$ are listed as

$$\begin{aligned}
\overline{\delta P} &= -\frac{4}{3\pi R(2B+C)w_0}\{3a_0^2 a\delta u_0 - (a_0-a)^2(2a_0+a)u_0\} \\
\overline{\delta Q} &= -\frac{4}{3\pi R(2B+C)w_0}\{3a_0^2 a\delta v_0 - (a_0-a)^2(2a_0+a)v_0\} \\
\overline{\delta N} &= \frac{4(a^3-a_0^3)}{3\pi RB}
\end{aligned} \tag{1.65}$$

which may be obtained by integrating the distributions (1.42) and (1.43) over the contact area, and when $\delta w_0 > 0$ they are

$$\overline{\delta P} = -\frac{8(a^3-a_0^3)\delta u_0}{3\pi R(2B+C)\delta w_0}, \quad \overline{\delta Q} = -\frac{8(a^3-a_0^3)\delta v_0}{3\pi R(2B+C)\delta w_0} \tag{1.66}$$

and

$$\overline{\delta N} = \frac{4(a^3-a_0^3)}{3\pi RB} \tag{1.67}$$

which are found by integrating the distributions (1.42) and (1.51) over the contact area. The notation of Walton [67] has been changed slightly to be consistent with chapter 3: the initial radius is denoted a_0 and the radius during the incremental phase is denoted a. The Hertz relationships in this case are

$$a_0^2 = Rw_0 \quad \text{and} \quad a^2 = R(w_0+\delta w_0). \tag{1.68}$$

The radius of the sphere is R and the moduli B and C are given in terms of the Lamé moduli λ and μ by equation (1.7).

When the incremental displacements are infinitesimal, the forces (1.65) and (1.66) both reduce to the same form

$$\overline{\delta P} = -\frac{4(Rw_0)^{1/2}\delta u_0}{\pi(2B+C)}, \quad \overline{\delta Q} = -\frac{4(Rw_0)^{1/2}\delta v_0}{\pi(2B+C)}, \quad \overline{\delta N} = \frac{2(Rw_0)^{1/2}\delta w_0}{\pi B}. \tag{1.69}$$

The analogous results for perfectly smooth spheres are also listed as equations (2.15) and (2.16) of Walton [67]

$$\overline{P} = \overline{Q} = 0, \quad \overline{N} = \frac{4R^{1/2}w_0^{3/2}}{3\pi B} \tag{1.70}$$

and

$$\overline{\delta P} = \overline{\delta Q} = 0, \quad \overline{\delta N} = \frac{2(Rw_0)^{1/2}\delta w_0}{\pi B}. \tag{1.71}$$

The Initial Deformed State

Considering the packing as a whole, we assume that it occupies a large volume and contains many spheres. Relative to some fixed origin the n-th sphere has its centre at position vector $\mathbf{X}^{(n)}$ and is initially in point contact with several of its neighbours. In attaining the initial deformed state, the boundary of the packing is subjected to a displacement $\mathbf{u}$ which is given in Walton [67] as

$$u_i = e_{ij}x_j \tag{1.72}$$

where e_{ij} is a constant symmetric tensor relative to fixed axes. For a continuous medium e_{ij} would be the average strain within the medium and this is the interpretation retained for the granular case. The centre of the n-th sphere undergoes a displacement of $\mathbf{u}^{(n)}$. Here sphere rotations are neglected, however in chapter 2 we show that they are significant in one of the initial states considered in Walton [67]. For now we take rotations to be zero and consider a second sphere m, in contact with the n-th sphere, undergoing displacement $\mathbf{u}^{(m)}$ from its initial position $\mathbf{X}^{(m)}$. By symmetry, the position vector of the initial contact point is

$$\mathbf{x}_c = \frac{1}{2}(\mathbf{X}^{(n)} + \mathbf{X}^{(m)}) \tag{1.73}$$

and this undergoes a displacement of

$$\frac{1}{2}(\mathbf{u}^{(n)} + \mathbf{u}^{(m)}). \tag{1.74}$$

Thus relative to this point, the displacements of the sphere centres are

$$\frac{1}{2}(\mathbf{u}^{(n)} - \mathbf{u}^{(m)}) \quad \text{and} \quad \frac{1}{2}(\mathbf{u}^{(m)} - \mathbf{u}^{(n)}) \tag{1.75}$$

respectively for spheres n and m. The unit vector along the line joining the centres of these two spheres is defined as

$$\mathbf{I}^{(nm)} = \frac{\mathbf{X}^{(n)} - \mathbf{X}^{(m)}}{2R}. \tag{1.76}$$

During this initial compression contact areas are forming between spheres initially in point contact. Each sphere will be in contact with several of its neighbours and displacements and forces caused by one contact will affect the others. For Hertzian contact theory to apply we need to consider each contact area in isolation. The Hertzian assumptions require that the contact area is small in comparison with the sphere radius allowing each sphere to be approximated by an elastic half-space in the region of the contact area. Walton [63] examined these assumptions for the case of purely normal compression and showed that surface displacements are negligible except in some small neighbourhood of the contact area. It is reasonable to assume that this will also be the case when tangential tractions are present and therefore the effects of one contact area on the others are neglected.

It is now possible to apply the results of the Hertz-type contact problems of section (1.2.5). The normal component of the relative displacement of the sphere m may be identified as

$$w_0 = \frac{1}{2}(\mathbf{u}^{(m)} - \mathbf{u}^{(n)}) \cdot \mathbf{I}^{(nm)} \tag{1.77}$$

and is in the direction $\mathbf{I}^{(nm)}$. The shear displacement is the remainder of the relative displacement (1.75) and is written as

$$\frac{1}{2}(\mathbf{u}^{(m)} - \mathbf{u}^{(n)}) - w_0\mathbf{I}^{(nm)}. \tag{1.78}$$

Combining the above with the total normal and tangential forces (1.64), the total vector force exerted by sphere m on sphere n across the contact area may be written as

$$\begin{aligned}\mathbf{F}^{(nm)} = \frac{(2R)^{1/2}}{3\pi B(2B+C)} \Big\{ & 2B\left[(\mathbf{u}^{(m)} - \mathbf{u}^{(n)}) \cdot \mathbf{I}^{(nm)}\right]^{1/2} (\mathbf{u}^{(m)} - \mathbf{u}^{(n)}) \\ & + C\left[(\mathbf{u}^{(m)} - \mathbf{u}^{(n)}) \cdot \mathbf{I}^{(nm)}\right]^{3/2} \mathbf{I}^{(nm)} \Big\}. \end{aligned} \tag{1.79}$$

The Averaging Scheme

In order to relate the average stress to the average strain, we define the average of quantities such as the Cauchy stress σ_{ij} within the medium as

$$\langle \sigma_{ij} \rangle = \frac{1}{V} \int_{\text{spheres}} \sigma_{ij} \, \mathrm{d}V = \frac{1}{V} \sum_n \int_{V_n} \sigma_{ij}^{(n)} \, \mathrm{d}V \tag{1.80}$$

where V is the volume of the entire medium (not just the spheres), V_n is the volume of an individual sphere, $\sigma_{ij}^{(n)}$ is the Cauchy stress within a sphere and the summation is taken over all spheres within V. For the n-th sphere it is easily shown that

$$\int_{V_n} \sigma_{ij}^{(n)} \, \mathrm{d}V = \frac{1}{2} \int_{S_n} (x_i' t_j^{(n)} + x_j' t_i^{(n)}) \, \mathrm{d}S \tag{1.81}$$

where $\mathbf{x}' = \mathbf{x} - \mathbf{X}^{(n)}$ is the position vector of a material point on the sphere relative to its centre, S_n denotes the surface of V_n and $\mathbf{t}^{(n)}$ is the traction vector acting on S_n. Since the contact area is small we may approximate $\mathbf{x}'$ over the contact area as

$$\mathbf{x}' = \frac{1}{2}(\mathbf{X}^{(m)} - \mathbf{X}^{(n)}). \tag{1.82}$$

The integral of the traction over the contact area is given by $\mathbf{F}^{(nm)}$. The surface S_n is traction free everywhere except where spheres are in contact, meaning that equation (1.81) may be written as

$$\int_{V_n} \sigma_{ij}^{(n)} \, \mathrm{d}V = \frac{1}{2} \sum_m \left\{ \frac{1}{2}(X_i^{(m)} - X_i^{(n)}) F_j^{(nm)} + \frac{1}{2}(X_j^{(m)} - X_j^{(n)}) F_i^{(nm)} \right\} \tag{1.83}$$

in which the summation in m is over all spheres in contact with the n-th sphere. Substituting this into equation (1.80) we obtain the expression for the average stress within the medium as

$$\langle \sigma_{ij} \rangle = -\frac{R}{V} \sum_{\text{contacts}} \left\{ I_i^{(nm)} F_j^{(nm)} + I_j^{(nm)} F_i^{(nm)} \right\}. \tag{1.84}$$

The summation is taken over all contacts between all spheres and since each contact appears twice in the summation over n and m, the factor of $1/2$ does not appear. By assuming a packing dense enough that the summations may be written as averages, we obtain

$$\langle \sigma_{ij} \rangle = -\frac{RnN}{2V} \{ \langle I_i F_j \rangle + \langle I_j F_i \rangle \} \tag{1.85}$$

where n is the average number of contacts per sphere (sometimes known as the coordination number), and N is the total number of spheres within V.

Thus the average stress within the medium is given by the expression (1.85) in terms of the geometrical properties of the packing and the force between two spheres. Similar expressions have also been used by Christoffersen [17] and Cambou [13].

The Average Initial Stress

Calculating the average stress in the initial state involves substituting the force $\mathbf{F}^{(nm)}$ into the expression (1.85). To achieve this it is necessary to make assumptions about the form of the relative displacement (1.75). Batchelor and O'Brien [2] considered thermal and electrical conduction in a medium with a large number of spherical inclusions. In this case it was assumed that the displacements of the centres of the spheres were consistent with the applied uniform strain. Digby [22] made the same assumption and in our case this may be written as

$$u_i^{(n)} = e_{ij} X_j^{(n)} \tag{1.86}$$

which is commonly known as the uniform strain assumption. The above is clearly consistent with equation (1.72) but, in general, it is not true for individual spheres. However, we would expect the displacements to be, on average, of the form (1.86) and so this is a reasonably good approximation to make. Then substituting (1.86) into (1.75) we obtain

$$\frac{1}{2}(u_i^{(m)} - u_i^{(n)}) = \frac{1}{2} e_{ij}(X_j^{(m)} - X_j^{(n)}) = -R e_{ij} I_j^{(nm)} \tag{1.87}$$

The average stress is now obtained by substituting the above and the force (1.79) into the expression (1.85) to obtain

$$\langle \sigma_{ij} \rangle = \frac{\phi n}{\pi^2 B(2B+C)} \left\{ B \left\langle (-e_{pq} I_p I_q)^{1/2} (e_{ik} I_k I_j + e_{jk} I_k I_i) \right\rangle - C \left\langle (-e_{pq} I_p I_q)^{3/2} I_i I_j \right\rangle \right\} \tag{1.88}$$

where ϕ is the volume fraction given by

$$\phi = \frac{N V_n}{V} = \frac{4\pi R^3 N}{3V}, \tag{1.89}$$

N being the total number of spheres contained within V.

Thus the average stress is obtained in terms of the applied strain and statistical properties such as n and ϕ. For a discussion of the measurement of these quantities and the statistical properties of random packings in general, see Scott [53] and Bernal and Mason [3].

Two cases of practical interest were considered in Walton [67] for which the averages of equation (1.88) may be evaluated analytically. The first of these cases is a hydrostatic compression which may be written as

$$e_{ij} = e\delta_{ij} \tag{1.90}$$

where $e < 0$ for compression. Equation (1.88) simplifies to

$$\langle \sigma_{ij} \rangle = -\frac{\phi n(-e)^{3/2}}{3\pi^2 B}\delta_{ij}. \tag{1.91}$$

The second case considered is that of a uniaxial compression in the z-direction given by

$$e_{ij} = e_3\delta_{i3}\delta_{j3} \tag{1.92}$$

where $e_3 < 0$ for a compression. The following stresses are obtained

$$(\langle \sigma_{ij} \rangle) = \mathrm{diag}(\langle \sigma_1 \rangle, \langle \sigma_1 \rangle, \langle \sigma_3 \rangle) \tag{1.93}$$

where

$$\langle \sigma_1 \rangle = -\frac{\phi nC(-e_3)^{3/2}}{24\pi^2 B(2B+C)} \quad \text{and} \quad \langle \sigma_3 \rangle = -\frac{\phi n(3B+C)(-e_3)^{3/2}}{6\pi^2 B(2B+C)}. \tag{1.94}$$

The Incremental Problem

The medium is now subjected to a further incremental deformation. In analogy with equation (1.72), the boundary of the medium is subjected to an incremental displacement $\delta\mathbf{u}$ which is also consistent with a uniform strain δe_{ij} of the form

$$\delta u_i = \delta e_{ij} x_j. \tag{1.95}$$

An analogous method to that seen in the previous section may be used to show that the average incremental stress is given by

$$\langle \delta\sigma_{ij} \rangle = -\frac{R}{V} \sum_{\text{contacts}} \left\{ I_i^{(nm)} \delta F_j^{(nm)} + I_j^{(nm)} \delta F_i^{(nm)} \right\}. \tag{1.96}$$

Following the methods seen in the previous section for deriving the force (1.79), but making use of the linearised incremental forces (1.69), the incremental force vector $\delta\mathbf{F}^{(nm)}$ is calculated as

$$\begin{aligned} \delta\mathbf{F}^{(nm)} &= \frac{(2R)^{1/2}\left[(\mathbf{u}^{(m)} - \mathbf{u}^{(n)}) \cdot \mathbf{I}^{(nm)}\right]^{1/2}}{2\pi B(2B+C)} \{\, 2B(\delta\mathbf{u}^{(m)} - \delta\mathbf{u}^{(n)}) \\ &\qquad + C\left[(\delta\mathbf{u}^{(m)} - \delta\mathbf{u}^{(n)}) \cdot \mathbf{I}^{(nm)}\right]\mathbf{I}^{(nm)} \,\}. \end{aligned} \tag{1.97}$$

Again, the uniform strain assumption is used and so, in analogy with equation (1.86),

$$\delta u_i^{(n)} = \delta e_{ij} X_j^{(n)} \tag{1.98}$$

which is consistent with equation (1.95). Thus the average incremental stress is obtained in the same way as equation (1.88) was derived as

$$\begin{aligned} \langle \delta\sigma_{ij} \rangle &= \frac{3n\phi}{2\pi^2 B(2B+C)} \Big\{ B \left\langle (-e_{pq} I_p I_q)^{1/2} (\delta e_{ik} I_k I_j + \delta e_{jk} I_k I_i) \right\rangle \\ &\qquad + C \left\langle (-e_{pq} I_p I_q)^{1/2} I_i I_j I_k I_l \right\rangle \delta e_{kl} \Big\} \end{aligned} \tag{1.99}$$

and this relates the average incremental stress to the average incremental strain. Since the effective elastic moduli C^*_{ijkl} are defined through the relationship

$$\langle \delta\sigma_{ij} \rangle = C^*_{ijkl} \langle \delta e_{kl} \rangle \tag{1.100}$$

we obtain, from equation (1.99),

$$\begin{aligned} C^*_{ijkl} &= \frac{3n\phi}{4\pi^2 B(2B+C)} \Big\{ B \left\langle (-e_{pq} I_p I_q)^{1/2} I_j I_k \right\rangle \delta_{il} + B \left\langle (-e_{pq} I_p I_q)^{1/2} I_i I_k \right\rangle \delta_{jl} \\ &\qquad + B \left\langle (-e_{pq} I_p I_q)^{1/2} I_j I_l \right\rangle \delta_{ik} + B \left\langle (-e_{pq} I_p I_q)^{1/2} I_i I_l \right\rangle \delta_{jk} \\ &\qquad + 2C \left\langle (-e_{pq} I_p I_q)^{1/2} I_i I_j I_k I_l \right\rangle \Big\} \end{aligned} \tag{1.101}$$

where the symmetric part in indices k and l has been taken. Note that all the required

symmetries are present. The elastic moduli are seen to depend strongly on the initial strain and the medium is, in general, anisotropic. Since it is difficult to say more without specifying the initial strain e_{ij}, the two special cases presented earlier are considered. For the hydrostatic compression (1.90) the moduli are given by

$$C^*_{ijkl} = \frac{3n\phi(-e)^{1/2}}{4\pi^2 B(2B+C)}\{B\langle I_i I_k\rangle \delta_{il} + B\langle I_i I_k\rangle \delta_{jl} + B\langle I_i I_l\rangle \delta_{ik} + B\langle I_i I_l\rangle \delta_{jk} + 2C\langle I_i I_j I_k I_l\rangle\}. \quad (1.102)$$

The averaged quantities in the above expression are easily evaluated (see chapter 5 and appendix B) to give the effective Lamé moduli

$$\lambda^* = \frac{n\phi C(-e)^{1/2}}{10\pi^2 B(2B+C)} \quad \text{and} \quad \mu^* = \frac{n\phi(5B+C)(-e)^{1/2}}{10\pi^2 B(2B+C)} \quad (1.103)$$

and so in this case the medium is statistically isotropic.

In the second case of an initial uniaxial compression (1.92), the moduli (1.101) reduce to

$$C^*_{ijkl} = \frac{3n\phi(-e_3)^{1/2}}{4\pi^2 B(2B+C)}\{B\langle |I_3| I_j I_k\rangle \delta_{il} + B\langle |I_3| I_i I_k\rangle \delta_{jl} + B\langle |I_3| I_j I_l\rangle \delta_{ik} + B\langle |I_3| I_i I_l\rangle \delta_{jk} + 2C\langle |I_3| I_i I_j I_k I_l\rangle\}. \quad (1.104)$$

Averages of the type appearing in the above expression are evaluated in appendix B and in this case the only non-zero moduli are

$$\begin{aligned} C^*_{1111} &= 3(\alpha+2\beta), \quad C^*_{1122} = \alpha - 2\beta, \quad C^*_{1133} = 2C^*_{1122}, \\ C^*_{3333} &= 8(\alpha+\beta), \quad C^*_{1313} = 2\alpha + 5\beta \end{aligned} \quad (1.105)$$

in which

$$\alpha = \frac{\phi n(-e_3)^{1/2}}{32\pi^2 B} \quad \text{and} \quad \beta = \frac{\phi n(-e_3)^{1/2}}{32\pi^2(2B+C)}. \quad (1.106)$$

Thus in the case of an initial uniaxial compression the resulting medium is statistically transversely isotropic with the five elastic constants required to describe such a medium given by equation (1.105).

Note that the modulus C^*_{1313} listed here is different to that quoted in equation (4.14) of Walton [67], which gives the incorrect value of

$$C^*_{1313} = \alpha + 7\beta. \tag{1.107}$$

Furthermore, although the modulus C^*_{1313} given in equation (1.105) has been calculated correctly using equation (1.101) and the averages of appendix B, its value is still incorrect and in chapter 2 it is shown that individual sphere rotations need to be included in the calculation.

All of the results presented here apply when friction is infinite requiring that there be no slip between contacting spheres. Results are also derived in Walton [67] for the case of zero friction in which the spheres slide freely over each other. A finite non-zero value of the coefficient of friction for the simplified case of an initial uniaxial compression followed by an incremental uniaxial compression was considered in Slade and Walton [55]. The problem for the general form of an incremental strain with finite friction is examined in chapter 5.

Chapter 2

Sphere Rotations Within Random Packings

2.1 Introduction

One assumption of Walton [67] is that, although individual spheres may rotate, the average rotations within the packing as a whole are zero and that the individual sphere rotations are negligible. However, for this assumption to be valid, certain symmetries must exist in the way the packing is deformed initially. In this chapter we examine which of the specific initial loadings considered in Walton [67] has the required symmetries, and we derive modified equations for general strains which do not have these symmetries.

The main results of Walton [67] were summarised in section (1.3.1). The spheres are assumed to be elastically identical, of equal radii and composed of a homogeneous, isotropic material. Equation (1.84) gives the average stress within the packing, at the end of the initial confining compression, as

$$\langle \sigma_{ij} \rangle = -\frac{R}{V} \sum_{\text{contacts}} \left\{ I_i^{(nm)} F_j^{(nm)} + I_j^{(nm)} F_i^{(nm)} \right\} \tag{2.1}$$

where R is the sphere radius, V is the volume of the entire packing, $\mathbf{I}^{(nm)}$ is the unit vector in the direction of the line joining the n-th and the m-th sphere centres and $\mathbf{F}^{(nm)}$ is the force at the m-th contact of the n-th sphere.

Equation (2.1) may also be written in terms of the averaging scheme $\langle \cdot \rangle$, defined in

section (1.3.1) by equation (1.80), replacing the summation over the contacts within the total packing volume V:

$$\langle \sigma_{ij} \rangle = -\frac{RnN}{2V} \{ \langle I_i F_j \rangle + \langle I_j F_i \rangle \} . \tag{2.2}$$

The coordination number n is the average number of contacts per sphere and N is the total number of spheres within V. The quantity $\langle I_i F_j \rangle$ is required to be symmetric if there is to be no resultant torque on individual spheres. This being the case, we may write the above as

$$\langle \sigma_{ij} \rangle = -\frac{RnN}{V} \langle I_i F_j \rangle . \tag{2.3}$$

The incremental strain, which is now imposed on this initial state, gives rise to an average incremental stress denoted $\langle \delta\sigma_{ij} \rangle$. Equation (1.96) gives the incremental version of the expression (2.1):

$$\langle \delta\sigma_{ij} \rangle = -\frac{R}{V} \sum_{\text{contacts}} \left\{ I_i^{(nm)} \delta F_j^{(nm)} + I_j^{(nm)} \delta F_i^{(nm)} \right\} \tag{2.4}$$

and, in the same way as before, this may be written in terms of averages as

$$\langle \delta\sigma_{ij} \rangle = -\frac{RnN}{V} \langle I_i \delta F_j \rangle \tag{2.5}$$

where $\delta\mathbf{F}^{(nm)}$ is the incremental force on the contact area. However, when the quantity $\langle I_i \delta F_j \rangle$ is calculated (given the form of the initial strain) using the incremental force given by equation (2.5), the result is found to be generally non-symmetric in i and j. Since the stress should always be symmetric we conclude that the force used must be incorrect. Furthermore, since a non-symmetric stress would imply that the average moment $\langle \mathbf{I} \wedge \delta\mathbf{F} \rangle$ within the medium is non-zero, individual spheres must suffer rotations to reach equilibrium.

When the term $\langle I_i F_j \rangle$ or $\langle I_i \delta F_j \rangle$ is calculated without considering rotations, if it is symmetric this confirms that the rotations are zero and $\langle \sigma_{ij} \rangle$ or $\langle \delta\sigma_{ij} \rangle$ may be calculated using equations (2.3) or (2.5) respectively. Otherwise, rotations occur and must be included in the expression for $\mathbf{F}^{(nm)}$ or $\delta\mathbf{F}^{(nm)}$. Here we will show that rotations are not required when calculating the stress in the initial state but that they are significant in the incremental problem to ensure equilibrium of moments.

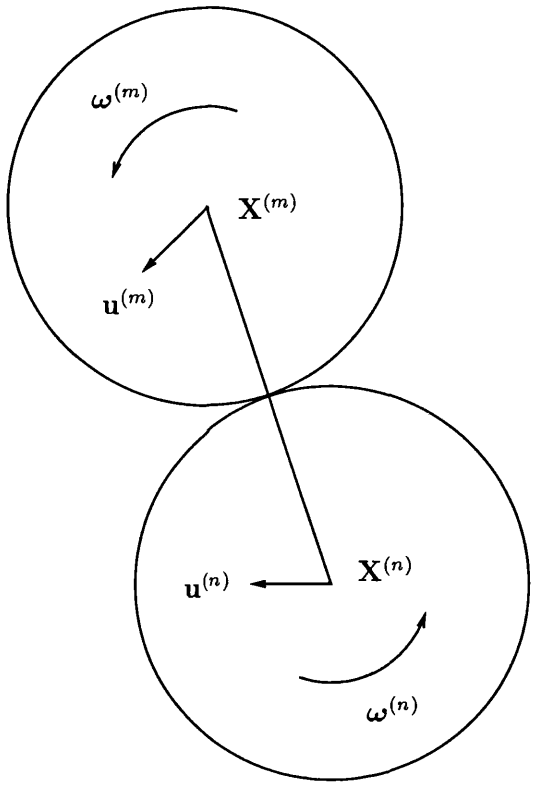

Figure 2-1: *Initial deformation with rotations*

2.2 The Initial State

Figure 2-1 shows the n-th sphere in contact with the m-th sphere. Using the notation of section (1.3.1), the centre of sphere n is initially at $\mathbf{X}^{(n)}$ and undergoes displacement $\mathbf{u}^{(n)}$. The rotation of sphere n is denoted by $\omega^{(n)}$ about an axis through its centre.

In section (1.3.1) and Walton [67], two cases of practical interest were considered for the initial confining strain: a hydrostatic compression and a uniaxial compression. Here we show that, for both of these cases, the term $\langle I_i F_j \rangle$ is symmetric without the need to consider rotations.

Equation (3.6) of Walton [67] gives the force without rotations as

$$F_i^{(nm)} = -\frac{4R^2}{3\pi B(2B+C)}\Big\{2B(-e_{pq}I_p^{(nm)}I_q^{(nm)})^{1/2}e_{ik}I_k^{(nm)} - C(-e_{pq}I_p^{(nm)}I_q^{(nm)})^{3/2}I_i^{(nm)}\Big\} \qquad (2.6)$$

from which we may calculate the averaged quantity

$$\langle I_i F_j \rangle = \frac{4R^2}{3\pi B(2B+C)} \left\{ 2B \left\langle (-e_{pq} I_p I_q)^{1/2} e_{jk} I_k I_i \right\rangle - C \left\langle (-e_{pq} I_p I_q)^{3/2} I_i I_j \right\rangle \right\} \quad (2.7)$$

where B and C are elastic moduli defined in terms of the Lamé moduli λ and μ by equation (1.7). We now consider the specific cases of confining strain mentioned above.

2.2.1 Initial Hydrostatic Compression

The hydrostatic compression is described in section (1.3.1) and may be written as

$$e_{ij} = e\delta_{ij} \quad (2.8)$$

where $e < 0$ for compression. Substituting into equation (2.7), we calculate the quantity

$$\langle I_i F_j \rangle = \frac{4R^2(-e)^{3/2}}{3\pi B} \langle I_i I_j \rangle \quad (2.9)$$

which is obviously symmetric in i and j. Thus the average stress under an initial hydrostatic strain is found by using the above in equation (2.3) as

$$\langle \sigma_{ij} \rangle = -\frac{\phi n(-e)^{3/2}}{\pi^2 B} \langle I_i I_j \rangle \quad (2.10)$$

where ϕ is the solid volume fraction, given in terms of N and V through the relationship

$$\phi = \frac{4\pi R^3 N}{3V}. \quad (2.11)$$

Therefore, the stress under the initial hydrostatic strain is given by equation (2.10) and is symmetric in indices i and j. This symmetry can also be explained using geometric arguments since, under a hydrostatic loading, the forces attempting to rotate a given sphere clockwise would be exactly balanced by those turning it anticlockwise.

2.2.2 Initial Uniaxial Compression

The uniaxial compression in the z-direction, as described in section (1.3.1), is given by

$$e_{ij} = e_3 \delta_{i3} \delta_{j3} \quad (2.12)$$

where $e_3 < 0$. Again, by substituting into equation (2.3) we obtain

$$\langle I_i F_j \rangle = -\frac{4R^3 nN(-e_3)^{3/2}}{3\pi VB(2B+C)} \left\{ 2B \langle |I_3| I_3 I_i \rangle \delta_{j3} + C \langle |I_3|^3 I_i I_j \rangle \right\}. \tag{2.13}$$

The second term within the brackets can be seen to be symmetric in i and j. The term $\langle |I_3| I_3 I_i \rangle$ may be evaluated explicitly using the results of appendix B. When $i = 1$ or $i = 2$ we have

$$\langle |I_3| I_3 I_1 \rangle = \langle |I_3| I_3 I_2 \rangle = \frac{1}{4\pi} \int_0^{2\pi} \mathrm{d}\phi \int_0^{\pi} \mathrm{d}\theta \, |\cos\theta| \cos\phi \sin^2\theta \cos\theta = 0 \tag{2.14}$$

and when $i = 3$, we obtain

$$\langle |I_3| I_3^2 \rangle = \frac{1}{4\pi} \int_0^{2\pi} \mathrm{d}\phi \int_0^{\pi} \mathrm{d}\theta \, |\cos\theta| \cos^2\theta \sin\theta = \frac{1}{4}. \tag{2.15}$$

We may write this term as

$$\langle |I_3| I_3 I_i \rangle \delta_{j3} = \langle |I_3| I_3^2 \rangle \delta_{i3} \delta_{j3} \tag{2.16}$$

which is symmetric in i and j, hence ensuring that (2.13) is symmetric in i and j. The average stress under an initial uniaxial strain is now given by

$$\langle \sigma_{ij} \rangle = -\frac{\phi n(-e)^{3/2}}{\pi^2 B(2B+C)} \left\{ 2B \langle |I_3| I_3^2 \rangle \delta_{i3} \delta_{j3} + C \langle |I_3|^3 I_i I_j \rangle \right\}. \tag{2.17}$$

2.3 The Incremental Problem

In the previous section we showed that, for the two cases considered, the rotations were zero. Here we consider the incremental problem and show that rotations are significant when the initial state is the uniaxial compression, but that only one of the five moduli given in equation (1.105) is affected.

The position vector of the contact point is $(\mathbf{X}^{(n)} + \mathbf{X}^{(m)})/2$, and relative to this point the incremental displacement of the centre of sphere m may be written as

$$\frac{1}{2}(\delta\mathbf{u}^{(m)} - \delta\mathbf{u}^{(n)}) + \frac{1}{2}(\delta\boldsymbol{\omega}^{(m)} + \delta\boldsymbol{\omega}^{(n)}) \wedge R\mathbf{I}^{(nm)}. \tag{2.18}$$

The normal component of the relative displacement of the upper sphere, denoted δw_0, is given by

$$\delta w_0 = \left\{ \frac{1}{2}(\delta \mathbf{u}^{(m)} - \delta \mathbf{u}^{(n)}) + \frac{1}{2}(\delta \boldsymbol{\omega}^{(m)} + \delta \boldsymbol{\omega}^{(n)}) \wedge R\mathbf{I}^{(nm)} \right\} \cdot \mathbf{I}^{(nm)}. \quad (2.19)$$

Noting that the term containing the vector cross product must be zero, the above expression reduces to

$$\delta w_0 = \frac{1}{2}(\delta \mathbf{u}^{(m)} - \delta \mathbf{u}^{(n)}) \cdot \mathbf{I}^{(nm)} \quad (2.20)$$

which is the magnitude of the displacement in the normal direction $\mathbf{I}^{(nm)}$. The shear displacement, which is the displacement in the plane to which $\mathbf{I}^{(nm)}$ is perpendicular, is the remainder of the relative displacement, that is

$$\frac{1}{2}(\delta \mathbf{u}^{(m)} - \delta \mathbf{u}^{(n)}) + \frac{1}{2}(\delta \boldsymbol{\omega}^{(m)} + \delta \boldsymbol{\omega}^{(n)}) \wedge R\mathbf{I}^{(nm)} - \delta w_0 \mathbf{I}^{(nm)}. \quad (2.21)$$

The incremental force vector is formed from the normal and shear displacements (2.20) and (2.21) respectively, and the incremental tangential and normal forces, as given in equations (1.69). The incremental vector force is found to be

$$\begin{aligned} \delta \mathbf{F}^{(nm)} = & \frac{(2R)^{1/2}\left[(\mathbf{u}^{(m)} - \mathbf{u}^{(n)}) \cdot \mathbf{I}^{(nm)}\right]^{1/2}}{2\pi B(2B + C)} \{\, 2B(\delta \mathbf{u}^{(m)} - \delta \mathbf{u}^{(n)}) \\ & + 2B(\delta \boldsymbol{\omega}^{(m)} + \delta \boldsymbol{\omega}^{(n)}) \wedge R\mathbf{I}^{(nm)} + C\left[(\delta \mathbf{u}^{(m)} - \delta \mathbf{u}^{(n)}) \cdot \mathbf{I}^{(nm)}\right] \mathbf{I}^{(nm)} \,\} \end{aligned} \quad (2.22)$$

which can be seen to be equation (1.97) with an extra term due to the rotation of the spheres. Making the assumption used in Walton [67] that the displacement of the centre of each sphere is consistent with the applied uniform field, we arrive at the approximations, also seen in section (1.3.1), that

$$u_i^{(n)} = e_{ij} X_j^{(n)} \quad \text{and} \quad \delta u_i^{(n)} = \delta e_{ij} X_j^{(n)}. \quad (2.23)$$

As discussed in section (1.3.1), individual spheres will not follow the above displacements precisely, but it is a reasonable approximation to assume that the overall displacements will be of these forms (2.23). A similar assumption may be made about the form of the rotations: we assume that they are equal for each sphere, that is

$$\delta\omega^{(n)} = \delta\omega^{(m)} = \delta\omega \tag{2.24}$$

where individual spheres will rotate by this amount in the average sense only. Substituting equations (2.23) and (2.24) into (2.22) and using the definition of the unit normal vector

$$\mathbf{I}^{(nm)} = \frac{\mathbf{X}^{(n)} - \mathbf{X}^{(m)}}{2R}, \tag{2.25}$$

the incremental force may be written in the form

$$\delta F_i^{(nm)} = \frac{-2R^2(-e_{pq}I_pI_q)^{1/2}}{\pi B(2B+C)}\{C\delta e_{kl}I_kI_lI_i + 2B\delta e_{il}I_l - 2B\epsilon_{ikl}\delta\omega_kI_l\} \tag{2.26}$$

where each vector component I_i should bear the superscripts (nm) which has been omitted for brevity.

2.3.1 Conditions of Equilibrium

For equilibrium of the n-th sphere we require that the sum of all the incremental forces be zero and also that the sum of the moments be zero, that is

$$\sum_m \mathbf{I}^{(nm)} \wedge \delta\mathbf{F}^{(nm)} = \mathbf{0} \tag{2.27}$$

$$\sum_m \delta\mathbf{F}^{(nm)} = \mathbf{0}. \tag{2.28}$$

Substituting the incremental force (2.26) into equation (2.27) we obtain the condition for equilibrium of moments as

$$\sum_m 2B(-e_{pq}I_pI_q)^{1/2}(\delta_{ik} - I_iI_k)\delta\omega_k = \sum_m \left[C\epsilon_{irs}(-e_{pq}I_pI_q)^{1/2}I_sI_rI_kI_l + 2B\epsilon_{irk}(-e_{pq}I_pI_q)^{1/2}I_rI_l\right]\delta e_{kl}. \tag{2.29}$$

where the summations are over all spheres m in contact with the n-th sphere and the superscript (nm) has again been omitted. The first term in the right-hand sum is zero

since it is the sum over the indices r and s of a symmetric tensor mutilplied by an anti-symmetric tensor. The condition reduces to

$$\sum_m (-e_{pq}I_pI_q)^{1/2}(\delta_{ik} - I_iI_k)\delta\omega_k = \sum_m \epsilon_{irk}(-e_{pq}I_pI_q)^{1/2}I_rI_l\delta e_{kl} \tag{2.30}$$

or, by summing also over each sphere n and assuming a packing dense enough that the summation over m and n may be written in terms of averages, the condition becomes

$$\left\langle (-e_{pq}I_pI_q)^{1/2}(\delta_{ik} - I_iI_k)\right\rangle \langle\delta\omega_k\rangle = \epsilon_{irk}\left\langle (-e_{pq}I_pI_q)^{1/2}I_rI_l\right\rangle \langle\delta e_{kl}\rangle\,. \tag{2.31}$$

The rotation vector $\delta\omega$ may now be determined, from the above, in terms of the given incremental strain δe_{ij}.

The condition for linear equilibrium of the incremental forces (2.28) becomes

$$\left\langle (-e_{pq}I_pI_q)^{1/2}\left\{CI_kI_lI_i + B\delta_{ik}I_l\right\}\delta e_{kl}\right\rangle - 2B\epsilon_{ikl}\left\langle (-e_{pq}I_pI_q)^{1/2}I_l\delta\omega_k\right\rangle = 0 \tag{2.32}$$

and in section (2.4.1) we will show that this condition is satisfied for an initial uniaxial compression.

2.3.2 The Incremental Stress

Having determined the rotation vector for any initial strain field, the incremental force is given by equation (2.26) and contains a term involving $\delta\omega$. Substituting the incremental force (2.26) into (2.5) we obtain

$$\begin{aligned}\langle\delta\sigma_{ij}\rangle \;=\; & \frac{3n\phi}{2\pi^2B(2B+C)}\Big\{C\left\langle (-e_{pq}I_pI_q)^{1/2}I_iI_jI_kI_l\right\rangle \delta e_{kl} \\ & + 2B\left\langle (-e_{pq}I_pI_q)^{1/2}I_lI_i\right\rangle \delta e_{jl} - 2B\epsilon_{jkl}\left\langle (-e_{pq}I_pI_q)^{1/2}I_iI_l\right\rangle \delta\omega_k\Big\}\end{aligned} \tag{2.33}$$

from which the effective moduli may be determined. Equation (2.31) may be used to find the required rotations in terms of the incremental strain. Walton [67] considered two confining strains of practical interest: a hydrostatic compression and a uniaxial compression. Here we consider only the uniaxial case since equation (3.16) of Walton [67]

and equation (2.8) show that rotations play no part in the hydrostatic case.

2.4 Initial Uniaxial Compression

The initial uniaxial strain may be described by

$$e_{ij} = e_3 \delta_{i3} \delta_{j3} \tag{2.34}$$

where $e_3 < 0$ for compression. Substituting into (2.26), the incremental force becomes

$$\delta F_i^{(nm)} = \frac{-R^2(-e_3)^{1/2}|I_3^{(nm)}|}{\pi B(2B+C)} \left\{ 4B\delta e_{ip} I_p^{(nm)} + 2C\delta e_{pq} I_p^{(nm)} I_q^{(nm)} I_i^{(nm)} - 4B\epsilon_{ipq}\delta\omega_p I_q^{(nm)} \right\} \tag{2.35}$$

and the incremental stress (2.33) is given by

$$\langle \delta\sigma_{ij} \rangle = \frac{3n\phi(-e_3)^{1/2}}{2\pi^2 B(2B+C)} \left\{ \left[B \langle |I_3| I_i I_l \rangle \delta_{jk} + B \langle |I_3| I_i I_k \rangle \delta_{jl} + C \langle |I_3| I_i I_j I_k I_l \rangle \right] \langle \delta e_{kl} \rangle - 2B\epsilon_{jpq} \langle |I_3| I_q I_i \rangle \delta\omega_p \right\}. \tag{2.36}$$

2.4.1 Conditions of Equilibrium

The rotation vector $\delta\omega$ may be found from equation (2.31) which, under the strain field (2.34), becomes

$$\left\{ \langle |I_3| I_i I_k \rangle - \delta_{ik} \langle |I_3| \rangle \right\} \delta\omega_k = \epsilon_{iks} \langle |I_3| I_s I_l \rangle \langle \delta e_{kl} \rangle . \tag{2.37}$$

We may evaluate directly the term

$$\langle |I_3| \rangle = \frac{1}{4\pi} \int_0^{2\pi} \mathrm{d}\phi \int_0^{\pi} \mathrm{d}\theta \, |\cos\theta| \sin\theta = \frac{1}{2} \tag{2.38}$$

and notice that terms of the form $\langle |I_3| I_i I_j \rangle$ are zero unless $i = j$, giving

$$\langle |I_3| I_i I_j \rangle = \begin{cases} 0 & , \ i \neq j \\ 1/8 & , \ i = j = 1 \ \text{ or } \ i = j = 2 \\ 1/4 & , \ i = j = 3. \end{cases} \tag{2.39}$$

Putting $i = 1, 2, 3$ in turn, we obtain the incremental rotation vector in terms of the incremental strain field as

$$\delta\omega_1 = -\frac{1}{3}\delta e_{23}, \quad \delta\omega_2 = \frac{1}{3}\delta e_{13}, \quad \delta\omega_3 = 0. \tag{2.40}$$

Finally, we return to the condition (2.32) which in this case becomes

$$\{C\langle|I_3|I_kI_lI_i\rangle + B\langle|I_3|I_l\rangle\delta_{ik}\}\langle\delta e_{kl}\rangle - 2B\epsilon_{ikl}\langle|I_3|I_l\rangle\delta\omega_k = 0. \tag{2.41}$$

The terms $\langle|I_3|I_kI_lI_i\rangle$ and $\langle|I_3|I_l\rangle$ must be zero by symmetry, and so the condition holds.

2.4.2 The Effective Elastic Moduli

Now that the incremental rotation is known, the incremental stress and the effective elastic moduli for this initial state may be calculated. Comparing equation (2.36) for the incremental stress with its equivalent in Walton [67], it can be seen that there is an extra term, contained within the brackets, given by

$$\epsilon_{jpq}\langle I_iI_q|I_3|\rangle\delta\omega_p. \tag{2.42}$$

For this term to be non-zero the indices j, p and q must be distinct, otherwise the permutation tensor will be zero. In particular, we must have $j \neq q$. As already seen in equation (2.39), for the averaged quantity to be non-zero we must have $i = q$ and so, taking these two requirements together, we must have $i \neq j$. Therefore, whenever $i = j$ the extra term is zero and the result obtained is identical to that obtained in Walton [67]. However, when $i \neq j$ the extra term will affect the result; but, as will be shown, only one of the five independent elastic moduli is altered. The effective elastic moduli C^*_{ijkl} are defined through the relationship

$$\langle\delta\sigma_{ij}\rangle = C^*_{ijkl}\langle\delta e_{kl}\rangle. \tag{2.43}$$

Taking $i = j = 1$ in equation (2.36) we obtain

$$\langle\delta\sigma_{11}\rangle = \frac{3n\phi(-e_3)^{1/2}}{2\pi^2B(2B+C)}\{B\langle|I_3|I_1I_l\rangle\delta_{1k} + B\langle|I_3|I_1I_k\rangle\delta_{1l} + C\langle I_1^2I_kI_l|I_3|\rangle\}\langle\delta e_{kl}\rangle \tag{2.44}$$

from which we may evaluate the moduli

$$\begin{aligned} C^*_{1111} &= \frac{3n\phi(-e_3)^{1/2}(4B+C)}{32\pi^2 B(2B+C)} \\ C^*_{1122} &= \frac{n\phi(-e_3)^{1/2}C}{32\pi^2 B(2B+C)} \\ C^*_{1133} &= \frac{n\phi(-e_3)^{1/2}C}{16\pi^2 B(2B+C)}. \end{aligned} \tag{2.45}$$

Similarly, when $i = j = 3$,

$$\langle \delta\sigma_{33} \rangle = \frac{3n\phi(-e_3)^{1/2}}{2\pi^2 B(2B+C)} \left\{ B \left\langle |I_3|I_3 I_l\rangle \delta_{3k} + B \left\langle |I_3|I_3 I_k\right\rangle \delta_{3l} + C \left\langle I_3^2 I_k I_l |I_3|\right\rangle \right\} \langle \delta e_{kl} \rangle \tag{2.46}$$

from which

$$C^*_{3333} = \frac{n\phi(-e_3)^{1/2}(3B+C)}{4\pi^2 B(2B+C)}. \tag{2.47}$$

The extra rotation term is non-zero when $i = 1$ and $j = 3$ in which case the average incremental stress is given by

$$\begin{aligned} \langle \delta\sigma_{13} \rangle = \frac{3n\phi(-e_3)^{1/2}}{2\pi^2 B(2B+C)} \{ & [B \left\langle |I_3|I_1 I_l\right\rangle \delta_{3k} + B \left\langle |I_3|I_1 I_k\right\rangle \delta_{3l} + C \left\langle I_1 I_3 I_k I_l |I_3|\right\rangle] \langle \delta e_{kl} \rangle \\ & - 2B\epsilon_{3pq}\delta\omega_p \left\langle |I_3|I_1 I_q\right\rangle \}. \end{aligned} \tag{2.48}$$

The extra term may be evaluated using (2.39) and (2.40) as

$$\epsilon_{3pq}\delta\omega_p \left\langle |I_3|I_1 I_q\right\rangle = -\delta\omega_2/8 = -\delta e_{31}/24 \tag{2.49}$$

and so the required modulus may be calculated from (2.48) as

$$C^*_{1313} = \frac{n\phi(-e_3)^{1/2}(4B+C)}{16\pi^2 B(2B+C)}. \tag{2.50}$$

The five independent effective elastic moduli required to describe such a transversely isotropic medium can be written as

$$\begin{aligned} C^*_{11} = C^*_{1111} &= 3(\alpha + 2\beta) \\ C^*_{12} = C^*_{1122} &= \alpha - 2\beta \\ C^*_{13} = C^*_{1133} = C^*_{2233} &= 2(\alpha - 2\beta) \\ C^*_{33} = C^*_{3333} &= 8(\alpha + \beta) \\ C^*_{44} = C^*_{1313} = C^*_{2323} &= 2(\alpha + 2\beta) \end{aligned} \tag{2.51}$$

in which α and β are defined, as in Walton [67], by

$$\alpha = \frac{\phi n(-e_3)^{1/2}}{32\pi^2 B} \quad \text{and} \quad \beta = \frac{\phi n(-e_3)^{1/2}}{32\pi^2(2B+C)}. \tag{2.52}$$

For completeness, we calculate the remaining non-zero modulus defined as

$$C^*_{66} = C^*_{1212} = \frac{n\phi(-e_3)^{1/2}(6B+C)}{32\pi^2 B(2B+C)} \tag{2.53}$$

which, for a transversely isotropic medium, can be expressed in terms of the other elastic constants (see Mal and Singh [43]) as

$$C^*_{66} = \frac{C^*_{11} - C^*_{12}}{2}. \tag{2.54}$$

Therefore, there are five independent elastic moduli given by equation (2.51).

Chapter 3

The Oblique Contact of Two Elastic Spheres with Friction

3.1 Introduction

When considering deformations of sphere packings, a fundamental problem which arises is that of the compression of two of the component spheres. In general, the relative displacement of adjacent spheres will not be along the line joining the two centres but will be inclined at an angle to this centre line. Therefore, the contact problem is one of oblique compression in which the centres of the two spheres are displaced both vertically and horizontally simultaneously. In particular, when an elastic wave propagates through the packing, the relative displacement is oscillatory and therefore the spheres are alternately loaded and unloaded.

This chapter considers the oblique compression of two identical elastic spheres with a finite non-zero value of the coefficient of friction between them. The spheres are of equal sizes and are made of a homogeneous and elastically isotropic material. Initially the two spheres are in contact at a single point. The deformation proceeds in two stages: in the initial stage, the spheres are pushed together, obliquely, by equal amounts in opposite directions. The effect of this deformation is to create a finite contact area in the region of the initial contact point. Walton [66] considered this problem of oblique compression and showed that the resulting contact area was circular and described by the Hertz theory of elastic contact. Secondly, an oblique incremental deformation is considered

and the effects of the initial deformation on the solution of the incremental problem are examined. The initial deformation corresponds to the initial compression of the packing, as described in section (1.3.1), and the incremental displacement corresponds to the deformation caused by an elastic wave propagating through the medium.

The method of solution follows that seen in section (1.2.5) where we considered the oblique sphere contact problem with an infinite value of the coefficient of friction; the no-slip displacement boundary condition was applied over the entire contact area. In the finite friction case however, this condition may only be applied over the part of the contact area which suffers no slip, and on the remainder of the contact region we must apply the slip conditions discussed in section (1.2.6). A number of different cases arise which are distinguished by the angle of compression and the coefficient of friction. The incremental displacement is oscillated along a straight line path; some cases result in an annulus of slip in which relative displacement of points on the contact area occurs, thereby establishing a cycle of slip. Otherwise, there is no relative displacement of points on the contact area resulting in a cycle in which the surfaces adhere or stick together. These stable cycles are established over several phases of oscillation, as was seen in Mindlin and Deresiewicz [45] and Johnson [34]. The work in this chapter differs significantly to that of Mindlin and Deresiewicz since the initial compression is oblique rather than normal, and the influence of this initial compression appears in the incremental deformation.

After the stable cycles have been established, the total forces acting on the contact area at any stage in each cycle are calculated. Finally, these forces are linearised when the incremental deformation is much smaller than the initial deformation, and the linearised cycles are found to be equal within a constant displacement.

3.2 Surface Displacements

Before proceeding further, we list some useful results concerning the surface displacements arising from both normal and tangential Hertz pressure distributions acting on an infinite elastic half-space. Consider a set of rectangular Cartesian axes $Oxyz$ with the z-axis directed downwards. The half-space is defined as the region $z > 0$ (as shown in figure 3-1) and the force distributions act normally and tangentially on the xy-plane. We also define a system of plane polar coordinates (r, θ) in the xy-plane sharing the

common origin O. For force distributions of the form

$$N(x,y) = \begin{cases} N_0(a^2 - r^2)^{1/2} & , \ 0 \leq r \leq a \\ 0 & , \ r > a \end{cases} \tag{3.1}$$

acting normally (in the z-direction), and

$$P(x,y) = \begin{cases} K(a^2 - r^2)^{1/2} & , \ 0 \leq r \leq a \\ 0 & , \ r > a \end{cases} \tag{3.2}$$

acting tangentially (in the x-direction), where N_0 and K are force constants and a is the contact area radius, the displacements (u, v, w) are given in terms of the integrals (1.8) as

$$\begin{aligned} u(x,y) &= u_0 + \int_{\mathcal{R}} \left\{ \frac{BP(x',y')}{S} + C\left[\frac{X^2P(x',y') + XYQ(x',y')}{S^3}\right] \right. \\ &\qquad \left. - \frac{(B-C)XN(x',y')}{2S^2} \right\} \mathrm{d}x'\mathrm{d}y' \\ v(x,y) &= v_0 + \int_{\mathcal{R}} \left\{ \frac{BQ(x',y')}{S} + C\left[\frac{XYP(x',y') + Y^2Q(x',y')}{S^3}\right] \right. \\ &\qquad \left. - \frac{(B-C)YN(x',y')}{2S^2} \right\} \mathrm{d}x'\mathrm{d}y' \\ w(x,y) &= -w_0 + \int_{\mathcal{R}} \left\{ \frac{(B-C)\left[XP(x',y') + YQ(x',y')\right]}{2S^2} + \frac{BN(x',y')}{S} \right\} \mathrm{d}x'\mathrm{d}y' \end{aligned} \tag{3.3}$$

where the displacement of the sphere centre has been added to ensure that the displacement is correct at infinity. Walton [66] made use of the symmetries of the problem to decouple the integrals into normal and tangential systems. In this chapter it is more convenient to consider the relative and absolute displacements defined as

$$\begin{aligned} w_r(x,y) &= \frac{1}{2}\{w_+(x,y) - w_-(x,y)\} \\ w_a(x,y) &= \frac{1}{2}\{w_+(x,y) + w_-(x,y)\} \end{aligned} \tag{3.4}$$

where $w_+(x,y)$ is the displacement in the z-direction on the surface of the half-space

$z > 0$ due to the distribution (P, Q, N) and $w_-(x, y)$ is the displacement on the surface of the half-space $z < 0$ due to the distribution $(-P, -Q, -N)$ i.e. the problem is rotated through 180°.

Similar definitions may be made for the tangential displacements $u(x, y)$ and $v(x, y)$ to form functions $u_r(x, y)$, $u_a(x, y)$, $v_r(x, y)$ and $v_a(x, y)$. By substituting these functions into the integrals (3.3), we obtain the systems

$$\begin{aligned} u_r(x,y) &= u_0 + \int_{\mathcal{R}} \left\{ \frac{BP(x',y')}{S} + \frac{C\left[X^2 P(x',y') + XYQ(x',y')\right]}{S^3} \right\} \mathrm{d}x'\,\mathrm{d}y' \\ v_r(x,y) &= v_0 + \int_{\mathcal{R}} \left\{ \frac{BQ(x',y')}{S} + \frac{C\left[XYP(x',y') + Y^2 Q(x',y')\right]}{S^3} \right\} \mathrm{d}x'\,\mathrm{d}y' \\ w_a(x,y) &= \frac{1}{2}(B-C) \int_{\mathcal{R}} \frac{\left[XP(x',y') + YQ(x',y')\right]}{S^2}\,\mathrm{d}x'\,\mathrm{d}y' \end{aligned} \tag{3.5}$$

and

$$\begin{aligned} u_a(x,y) &= -\frac{1}{2}(B-C) \int_{\mathcal{R}} \frac{XN(x',y')}{S^2}\,\mathrm{d}x'\,\mathrm{d}y' \\ v_a(x,y) &= -\frac{1}{2}(B-C) \int_{\mathcal{R}} \frac{YN(x',y')}{S^2}\,\mathrm{d}x'\,\mathrm{d}y' \\ w_r(x,y) &= -w_0 + B \int_{\mathcal{R}} \frac{N(x',y')}{S}\,\mathrm{d}x'\,\mathrm{d}y' \end{aligned} \tag{3.6}$$

which are decoupled in the sense that equation (3.6) contains only the effects of normal forces and equation (3.5) contains only the effects of tangential forces. The splitting of the displacements in this way may be interpreted as follows: at a point where the two surfaces are adhered together there can be no further relative slip between them and therefore we must have

$$u_r(x,y) = 0,\ v_r(x,y) = 0,\ w_r(x,y) = 0 \tag{3.7}$$

at any point where the surfaces were initially stuck together. The function $w_a(x, y)$ on the contact area gives the warping of the contact surface and is an odd function of x.

3.2.1 Displacements Inside the Loaded Region, $r \leq a$

The displacements inside the loaded region ($r \leq a$) due to the distributions (3.1) and (3.2) may be calculated by evaluating the integrals (3.6) and (3.5) to obtain

$$\begin{aligned} u_r(x,y) &= u_0 + \frac{\pi^2}{4}(2B+C)Ka^2 - \frac{\pi^2}{16}K\left\{(4B+C)x^2 + (4B+3C)y^2\right\} \\ v_r(x,y) &= \frac{\pi^2}{8}KCxy \\ w_a(x,y) &= \frac{\pi K}{3}(B-C)x\left\{\frac{a^3-(a^2-r^2)^{3/2}}{r^2}\right\} \end{aligned} \tag{3.8}$$

and

$$\begin{aligned} u_a(x,y) &= -\frac{\pi N_0}{3}(B-C)x\left\{\frac{a^3-(a^2-r^2)^{3/2}}{r^2}\right\} \\ v_a(x,y) &= -\frac{\pi N_0}{3}(B-C)y\left\{\frac{a^3-(a^2-r^2)^{3/2}}{r^2}\right\} \\ w_r(x,y) &= -w_0 - \frac{r^2}{2R}. \end{aligned} \tag{3.9}$$

Note that for the half-space problem the displacement at infinity was required to be zero, but for the case of contacting spheres the displacement at infinity is $(u_0, 0, -w_0)$.

3.2.2 Displacements Outside the Loaded Region, $r > a$

Outside the loaded region the displacements are again given by the integrals (3.6) and (3.5) although the range of integration is different. Evaluation of the integrals for the force distributions (3.1) and (3.2) give the relative external displacements u_r and v_r as

$$\begin{aligned} u_r(x,y) &= u_0 + \frac{\pi}{8}K\left\{4(2B+C)a^2 - (4B+C)x^2 - (4B+3C)y^2\right\}\sin^{-1}(a/r) \\ &\quad + \frac{\pi}{8}Ka(r^2-a^2)^{1/2}\left\{4B + \frac{C}{r^2}\left[x^2+3y^2+2a^2\left(\frac{x^2-y^2}{r^2}\right)\right]\right\} \\ v_r(x,y) &= \frac{\pi}{4}K\frac{Cxy}{r^4}\left\{r^4\sin^{-1}(a/r) + a(2a^2-r^2)(r^2-a^2)^{1/2}\right\}. \end{aligned} \tag{3.10}$$

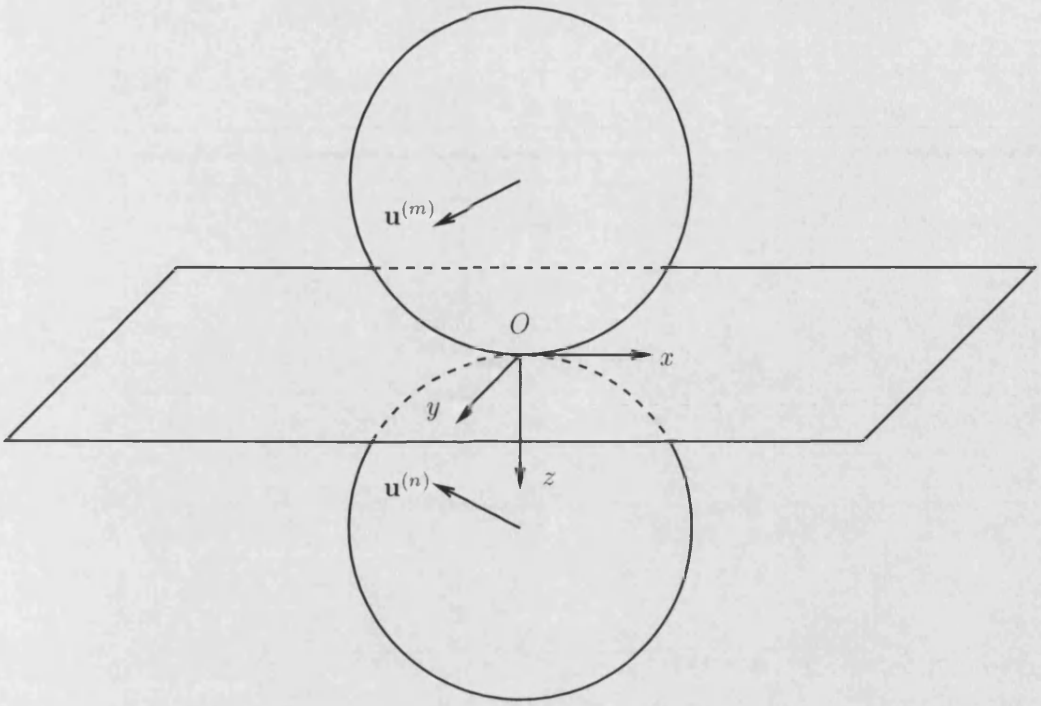

Figure 3-1: *The initial undeformed configuration*

3.3 The Initial Deformation

The spheres are shown in their initial undeformed configuration in figure 3-1. Their point of first contact O defines the origin of a rectangular Cartesian system of coordinates having the xy-axes lying in the common tangent plane and the z-axis being directed into the lower sphere along the line of centres. Each sphere has radius R and the top and bottom centres are displaced obliquely by amounts $(-u_0, 0, w_0)$ and $(u_0, 0, -w_0)$ respectively, relative to the point of first contact, causing them to deform in the vicinity of the origin and form a contact area. Whether or not the two contact surfaces displace relative to each other depends on the coefficient of friction and the angle of compression. We begin by assuming that no slip occurs between the two spheres and subsequently derive conditions under which slip must occur.

3.3.1 The No Sliding Solution

Walton [66] considered a similar problem and showed that the problem has a unique solution, namely that of Hertzian compression. The Hertz contact area is shown to be circular and of radius a_0 with a normal force distribution of the form

$$N_0(r) = \frac{2}{\pi^2 RB}(a_0^2 - r^2)^{1/2} \tag{3.11}$$

where r is the radius in plane polar coordinates (r, θ) and B is an elastic modulus defined in terms of the Lamé moduli by equation (1.7). We will later make use of the similar elastic modulus C also defined in equation (1.7). The contact area radius is given by the Hertz relationship

$$a_0^2 = Rw_0. \tag{3.12}$$

Tangentially, we assume a force distribution of the form

$$P_0(r) = K_0(a_0^2 - r^2)^{1/2} \tag{3.13}$$

in the x-direction only. The force constant K_0 is determined by considering the displacements given by the integrals (3.6) and (3.5). Substituting the distribution (3.13) into equation (3.5) we obtain tangential displacements

$$\begin{aligned} u_r(x,y) &= u_0 + \frac{\pi^2}{4}(2B+C)K_0 a_0^2 - \frac{\pi^2}{16}K_0\{(4B+C)x^2 + (4B+3C)y^2\} \\ v_r(x,y) &= \frac{\pi^2}{8}K_0 Cxy. \end{aligned} \tag{3.14}$$

By applying the condition that no relative displacement occurs between the two surfaces, we require that $u_r(0,0) = 0$ and $v_r(0,0) = 0$ in the above equations. Solving for the constant K_0 we find that

$$K_0 = -\frac{4u_0}{\pi^2 R(2B+C)w_0} \tag{3.15}$$

giving the tangential force distribution (3.13) as

$$P_0(r) = -\frac{4u_0}{\pi^2 R(2B+C)w_0}(a_0^2 - r^2)^{1/2}. \tag{3.16}$$

When a finite non-zero value for the coefficient of friction exists between the two spheres, Admontons' law (1.53) states that the magnitude of the tangential force can never exceed the coefficient of friction multiplied by the normal force at any point on the contact area. This condition may be written as

$$|P_0| \leq fN_0, \tag{3.17}$$

where f is the coefficient of friction, and is satisfied when

$$\left|\frac{u_0}{w_0}\right| \leq \left(\frac{2B+C}{2B}\right) f \quad \text{or} \quad \tan\theta_0 \leq \tan\theta_c \tag{3.18}$$

where the angle of compression is defined as

$$\tan\theta_0 = \frac{u_0}{w_0} \tag{3.19}$$

and the angle of friction θ_c is defined as

$$\tan\theta_c = \left(\frac{2B+C}{2B}\right) f \tag{3.20}$$

being the critical value for which equality holds in the inequality (3.18). If the magnitude of the calculated tangential forces violates the condition (3.18) at any point, then slip will occur with the tangential force being equal to the coefficient of friction times the normal force at that point. The above condition can be seen to be independent of position on the contact area, meaning that if slip does occur it is in the form of sliding, that is slip over the entire contact area.

We now consider the problem when the condition (3.18) is violated and sliding occurs.

3.3.2 The Sliding Solution

Sliding will occur for any values of u_0, v_0 and w_0 satisfying

$$\left|\frac{u_0}{w_0}\right| > \left(\frac{2B+C}{2B}\right) f \quad \text{or} \quad \tan\theta_0 > \tan\theta_c. \tag{3.21}$$

During sliding, the magnitude of the tangential force must equal the coefficient of friction times the normal force which gives rise to the equation

$$|K_0| = \frac{2f}{\pi^2 RB} \tag{3.22}$$

Secondly, to satisfy the laws of friction discussed in section (1.2.6), and to complete the specification of the boundary conditions on the contact area, we require that the direction of sliding opposes the tangential force. In this case we see that K_0 must be

negative and thus we obtain

$$K_0 = -\frac{2f}{\pi^2 RB} \tag{3.23}$$

giving the required tangential force distribution as

$$P_0(r) = -\frac{2f}{\pi^2 RB}(a_0^2 - r^2)^{1/2} \tag{3.24}$$

and the normal distribution for this sliding solution remains unchanged as

$$N_0(r) = \frac{2}{\pi^2 RB}(a_0^2 - r^2)^{1/2}. \tag{3.25}$$

The tangential displacements at the end of this initial stage are given by

$$\begin{aligned} u_r(x,y) &= u_0 + \frac{\pi^2}{4}(2B+C)K_0 a_0^2 - \frac{\pi^2}{16}K_0\{(4B+C)x^2 + (4B+3C)y^2\} \\ v_r(x,y) &= \frac{\pi^2 K_0}{8}Cxy. \end{aligned} \tag{3.26}$$

We conclude that two solutions may occur in attaining the initial state depending on the condition (3.18). When (3.18) is satisfied the solution which arises is that for which there is no relative displacement between the two spheres ie. a 'stick solution' given by equation (3.16). Conversely, when the condition (3.18) is violated, the magnitude of the tangential force must be equal to the coefficient of friction times the normal force and the 'sliding solution' (3.24) is obtained. The stick and sliding regions are shown in figure 3-4 separated by the dashed line through the origin. The normal component of the solution is given by the distribution (3.11) in each case.

3.4 The Incremental Deformation

Any subsequent state will depend strongly on whether sliding occurred or not in attaining the initial state. The cases of sliding originally and no sliding originally must now be considered separately when imposing a further incremental deformation $(\delta u_0, 0, -\delta w_0)$ on the initial state. The angle of compression in the incremental state is defined as

$$\tan\theta = \frac{\delta u_0}{\delta w_0}. \tag{3.27}$$

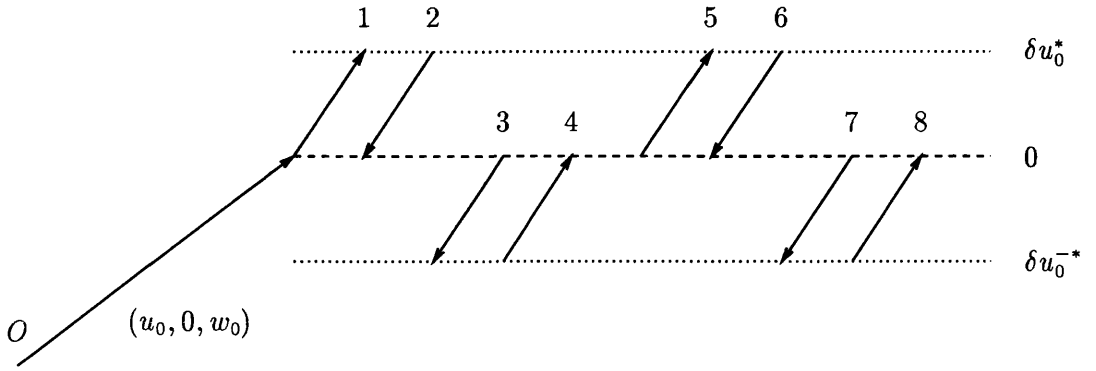

Figure 3-2: *Path of sphere centres during the incremental loading cycle*

A similar problem was considered by Walton [66] but friction was treated by assuming either a zero or infinite value of the coefficient of friction. The problem of finite friction to be considered here is considerably more complex due to both the influence of the initial state and the number of possibilities arising from stick or slip. The incremental problem consists of a sequence of loadings and unloadings, the stages of which are shown in figure 3-2. Eventually, after a number of loading and unloading cycles, a repeating stable cycle is established.

We begin by considering the incremental problem imposed on the initial state in which no sliding occurred. In the same way as before, we assume at first that no further slip occurs and then derive conditions under which the no-slip condition (3.18) will be violated.

3.4.1 No Sliding Originally, No Further Slip - $\theta_0 \leq \theta_c$ and $\theta \leq \theta_c$

Assuming that no further slip occurs, the form of normal force distribution remains that of Hertzian compression given by

$$N + \delta N = \frac{2}{\pi^2 RB}(a^2 - r^2)^{1/2} \tag{3.28}$$

in which a is the varying contact area radius as opposed to the now fixed initial radius a_0. The new radius now increases or decreases depending on the increments δw_0 through the Hertz relationship

$$a^2 = R(w_0 + \delta w_0). \tag{3.29}$$

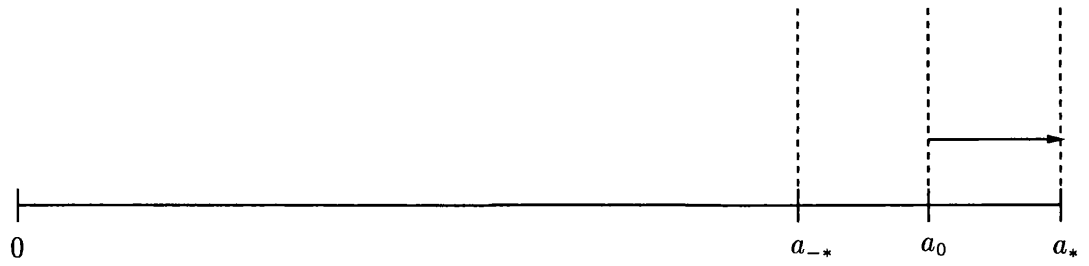

Figure 3-3: *Phase 1 : Loading with no further slip*

Phase 1 : Loading with no further slip

Phase 1 consists of a loading from $\delta u_0 = 0$ to a maximum value of $\delta u_0 = \delta u_0^*$. The contact radius progresses from its initial value of a_0 to a maximum value of a_* as shown in figure 3-3. The appropriate form of tangential force distribution is postulated to be, in the x-direction,

$$P + \delta P = \begin{cases} K_1(a^2 - r^2)^{1/2} + K_2(a_0^2 - r^2)^{1/2} & , \ 0 \leq r \leq a_0 \\ K_1(a^2 - r^2)^{1/2} & , \ a_0 \leq r \leq a \end{cases} \tag{3.30}$$

and since the increment is purely in the x-direction, the force distribution in the y-direction remains as $Q + \delta Q = 0$.

We now determine the force constants K_1 and K_2 by considering the displacements over the contact area. Tangentially, the displacements due to the distribution (3.30) may be found from equation (3.8) and are calculated as

$$\begin{aligned} u_r(x,y) &= u_0 + \delta u_0 + \frac{\pi^2}{4}(2B + C)\left\{K_1 a^2 + K_2 a_0^2\right\} \\ &\quad - \frac{\pi^2}{16}(K_1 + K_2)\left\{(4B + C)x^2 + (4B + 3C)y^2\right\} \\ v_r(x,y) &= \frac{\pi^2}{8}(K_1 + K_2)Cxy. \end{aligned} \tag{3.31}$$

Applying the no-slip condition on $0 \leq r \leq a$ we match terms of the above with the displacements at the end of the initial loading (3.14) to obtain

$$\begin{aligned} K_1 + K_2 &= \frac{-4u_0}{\pi^2 R(2B+C)w_0} \\ u_0 + \frac{\pi^2}{4}(2B+C)K_0 a_0^2 &= u_0 + \delta u_0 + \frac{\pi^2}{4}(2B+C)\left\{K_1 a_0^2 + K_2 a^2\right\}. \end{aligned} \tag{3.32}$$

Solving the above for K_1 and K_2 we obtain

$$\begin{aligned} K_1 &= -\frac{4}{\pi^2 R(2B+C)}\frac{\delta u_0}{\delta w_0} \\ K_2 &= \frac{4}{\pi^2 R(2B+C)}\left(\frac{\delta u_0}{\delta w_0} - \frac{u_0}{w_0}\right) \end{aligned} \tag{3.33}$$

which determines the force distribution (3.30).

The condition for slip considered in section (3.4.1) states that no slip will occur at any point on the contact area satisfying

$$|P + \delta P| \leq f(N + \delta N). \tag{3.34}$$

Equivalently, by substituting the distribution (3.30) into the above, we obtain

$$\left|\frac{\delta u_0}{\delta w_0}\right| \leq \left(\frac{2B+C}{2B}\right) f \quad \text{or} \quad \tan\theta \leq \tan\theta_c \tag{3.35}$$

where

$$\tan\theta = \frac{\delta u_0}{\delta w_0} \tag{3.36}$$

and θ is the angle of compression for the incremental problem. The critical angle of friction θ_c is the value of θ for which equality occurs in equation (3.35).

Thus there are two possible solutions in the incremental solution with no initial sliding: Firstly, when (3.35) is satisfied there exists a stick solution, given by (3.33) in which the spheres suffer no relative displacement and secondly, when (3.35) is violated, there exists a solution in which a degree of slip must take place somewhere on the contact area. We continue here with the stick solution and examine the slip solution in section (3.4.2). These two cases are illustrated in figure 3-4, the letters SLP and STK denoting the slip and stick regions respectively.

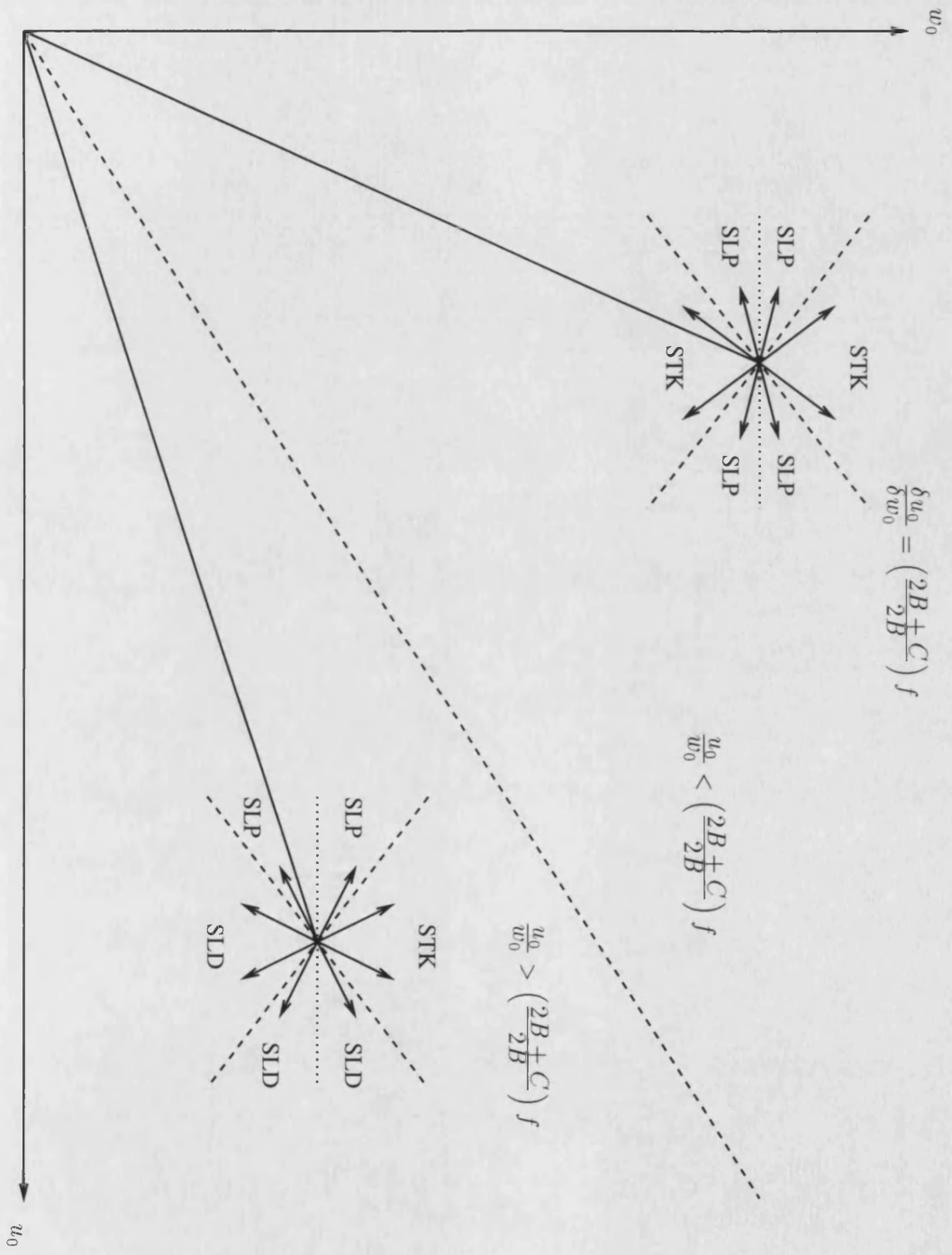

Figure 3-4: *Path of sphere centres for initial and incremental displacements*

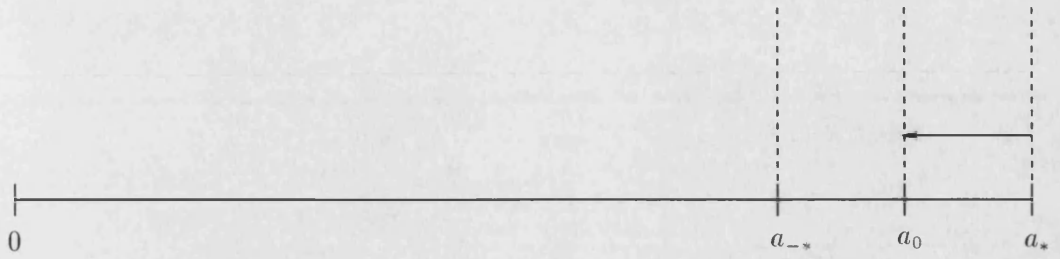

Figure 3-5: *Phase 2 : Unloading with no further slip*

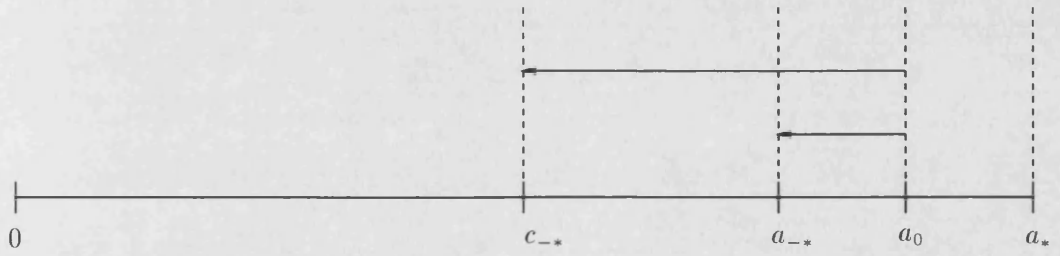

Figure 3-6: *Phase 3 : Unloading with partial slip*

Phase 2 : Unloading, reversal of phase 1

During phase 2, the displacement is unloaded from its maximum value of $\delta u_0 = \delta u_0^*$ to $\delta u_0 = 0$. The contact radius decreases from a_* to a_0 as shown in figure 3-5. Since no slip occurred during the loading phase, we may take the same solution during unloading, that is the displacement is simply reversed along the phase 1 path. Thus at the end of phase 2 the force distributions are precisely those at the end of the initial stage (3.16), as if the loading and unloading had never occurred.

Phase 3 : Unloading with slip

Phase 3 covers the further unloading from $\delta u_0 = 0$ to $\delta u_0 = \delta u_0^{-*}$. The contact radius decreases throughout this phase, as shown in figure 3-6, and so terms of the form $(a_0^2 - r^2)^{1/2}$ cannot be considered because a is always less than or equal to a_0 meaning that the force distribution at $r = a$ would be non-zero. Instead it is necessary to consider a slip solution of the form

$$P+\delta P=\begin{cases} K_1(a^2-r^2)^{1/2}+K_2(c^2-r^2)^{1/2} & ,\ 0\le r<c \\ K_1(a^2-r^2)^{1/2} & ,\ c\le r\le a \end{cases} \tag{3.37}$$

where $r=c$ is the boundary separating the central region of stick $0\le r\le c$ and the slip annulus $c\le r\le a$.

Since this section is concerned with establishing a no-slip stable cycle and because this particular slip phase will not occur during the stable cycle, we leave the details of the solution until section (3.4.2) and simply list the force constants as

$$\begin{aligned} K_1 &= \frac{2f}{\pi^2 RB} \\ K_2 &= -\frac{2f}{\pi^2 RB}-\frac{4u_0}{\pi^2 R(2B+C)w_0}. \end{aligned} \tag{3.38}$$

The radius of slip is given by

$$\frac{c^2}{a^2} = 1+\frac{\delta u_0+\left(\frac{2B+C}{2B}\right)f\delta w_0}{u_0+\left(\frac{2B+C}{2B}\right)fw_0}. \tag{3.39}$$

The minimum value of this radius is denoted c_{-*} occurring when $\delta u_0=\delta u_0^{-*}$ and may be calculated as

$$\frac{c_{-*}^2}{a^2} = 1-\frac{\delta u_0^*+\left(\frac{2B+C}{2B}\right)f\delta w_0^*}{u_0+\left(\frac{2B+C}{2B}\right)fw_0}. \tag{3.40}$$

The corresponding final displacements on $0\le r\le c_{-*}$ are calculated as

$$\begin{aligned} u_r^{-*}(x,y) &= u_0+\delta u_0^{-*}+\frac{\pi^2}{4}(2B+C)\left\{K_1a_{-*}^2+K_2c_{-*}^2\right\} \\ &\quad -\frac{\pi^2}{16}(K_1+K_2)\left\{(4B+C)x^2+(4B+3C)y^2\right\} \\ v_r^{-*}(x,y) &= \frac{\pi^2}{8}(K_1+K_2)Cxy. \end{aligned} \tag{3.41}$$

Phases 4 and 5 : Reloading without slip

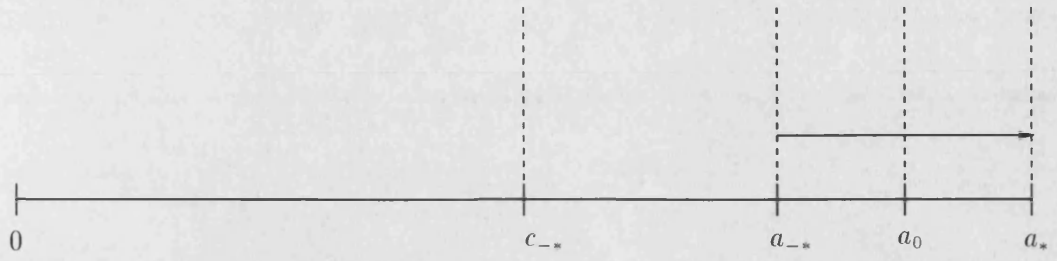

Figure 3-7: *Phases 4 and 5 : Loading with no further slip*

Phases 4 and 5 consist of the reloading from $\delta u_0 = \delta u_0^{-*}$ to $\delta u_0 = \delta u_0^*$ and may be considered together. The contact radius is shown in figure 3-7 progressing from a_{-*} to a_*. The no-slip solution has a force distribution of the form

$$P + \delta P = \begin{cases} K_1(a^2 - r^2)^{1/2} + K_2(c_{-*}^2 - r^2)^{1/2} + K_3(a_{-*}^2 - r^2)^{1/2} & , \ 0 \le r \le c_{-*} \\ K_1(a^2 - r^2)^{1/2} + K_3(a_{-*}^2 - r^2)^{1/2} & , \ c_{-*} \le r \le a_{-*} \\ K_1(a^2 - r^2)^{1/2} & , \ a_{-*} \le r \le a. \end{cases} \tag{3.42}$$

The displacements on the central stick region $0 \le r \le c_{-*}$ due to this distribution are

$$\begin{aligned} u_r(x,y) &= u_0 + \delta u_0 + \frac{\pi^2}{4}(2B + C)\left\{K_1 a^2 + K_2 c_{-*}^2 + K_3 a_{-*}^2\right\} \\ &\quad - \frac{\pi^2}{16}(K_1 + K_2 + K_3)\left\{(4B + C)x^2 + (4B + 3C)y^2\right\} \\ v_r(x,y) &= \frac{\pi^2}{8}(K_1 + K_2 + K_3)Cxy. \end{aligned} \tag{3.43}$$

We apply the no-slip condition (3.35) over the contact area by matching terms of the above displacements with the displacements at the end of phase 3 (3.41) to obtain

$$K_1 + K_2 + K_3 = \frac{-4u_0}{\pi^2 R(2B + C)w_0} \tag{3.44}$$

and

$$u_0 + \delta u_0 + \frac{\pi^2}{4}(2B + C)\left\{K_1 a^2 + K_2 c_{-*}^2 + K_3 a_{-*}^2\right\} = u_0 + \delta u_0^{-*} + \frac{\pi^2}{4}(2B + C)\left\{K_1' a_{-*}^2 + K_2' c_{-*}^2\right\}. \quad (3.45)$$

The constants K_1' and K_2' are the values of the constants during phase 3 given by equation (3.38). By matching the displacements on the annulus $c_{-*} \leq r \leq a_{-*}$ we obtain the extra equation

$$K_2 = K_2'. \quad (3.46)$$

Details of the calculation of these external displacements and the matching of the terms on the annulus are left until section (3.4.2) which considers the solution of the problem with an evolving slip annulus as opposed to the static case seen here.

Solving the above equations for K_1, K_2 and K_3 we obtain

$$\begin{aligned} K_1 &= -\frac{4}{\pi^2 R(2B + C)}\left(\frac{\delta u_0 + \delta u_0^*}{\delta w_0 + \delta w_0^*}\right) \\ K_2 &= -\frac{2f}{\pi^2 RB} - \frac{4u_0}{\pi^2 R(2B + C)w_0} \\ K_3 &= \frac{4}{\pi^2 R(2B + C)}\left(\frac{\delta u_0 + \delta u_0^*}{\delta w_0 + \delta w_0^*}\right) + \frac{2f}{\pi^2 RB} \end{aligned} \quad (3.47)$$

Note that, since the centres of the two spheres are assumed to be displaced in a straight line, we may write the gradients as

$$\frac{\delta u_0}{\delta w_0} = \frac{\delta u_0^*}{\delta w_0^*} = \frac{\delta u_0^{-*}}{\delta w_0^{-*}} = \frac{\delta u_0 + \delta u_0^*}{\delta w_0 + \delta w_0^*}. \quad (3.48)$$

Since no slip has occurred during phases 4 and 5, any subsequent loading or unloading will follow the solution (3.47). Thus the stable cycle is established in which the displacement oscillates from $\delta u_0 = \delta u_0^{-*}$ to $\delta u_0 = \delta u_0^*$ and back again with force distribution (3.42).

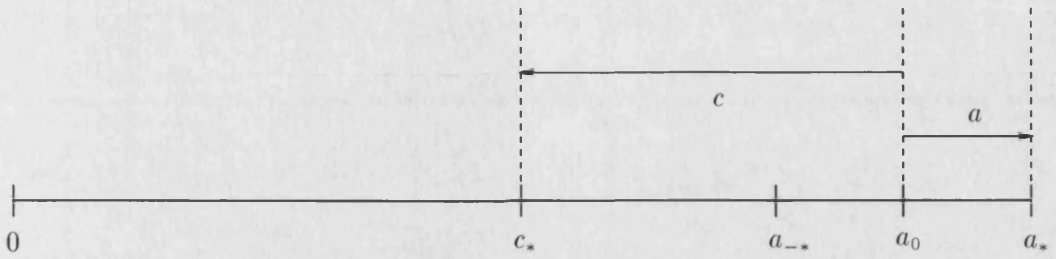

Figure 3-8: *Phase 1 : Loading with partial slip*

3.4.2 No Sliding Originally, Further Slip - $\theta_0 \leq \theta_c$ and $\theta > \theta_c$

Continuing the loading for no original sliding, we now consider the case when condition (3.35) is violated, that is $\theta > \theta_c$ and slip must occur somewhere on the contact area. The normal force remains unchanged from section (3.4.1) as

$$N + \delta N = \frac{2}{\pi^2 RB}(a^2 - r^2)^{1/2}. \tag{3.49}$$

Phase 1 : Loading with slip annulus

During this loading from $\delta u_0 = 0$ to $\delta u_0 = \delta u_0^*$, the contact area radius increases from a_0 to its maximum value of a_*. A radius of slip c is assumed to progress from a_0 to its final value of c_* as shown in figure 3-8. The appropriate tangential force distribution is

$$P + \delta P = \begin{cases} K_1(a^2 - r^2)^{1/2} + K_2(c^2 - r^2)^{1/2} & , \ 0 \leq r \leq c \\ K_1(a^2 - r^2)^{1/2} & , \ c \leq r \leq a. \end{cases} \tag{3.50}$$

Since slip is occurring in the annulus $c \leq r \leq a$ we apply the slip condition

$$|P + \delta P| = f(N + \delta N) \tag{3.51}$$

within this region giving K_1 as

$$K_1 = -\frac{2f}{\pi^2 RB} \tag{3.52}$$

where in this case, the sign is taken to be negative so that the tangential force opposes the direction of slip. Note that the solution obtained in this manner does not precisely satisfy the condition that the slip opposes the force causing it, but the deviation is very

small as discussed in section (1.2.7).

In the region $0 \leq r \leq c$ we apply the no-slip condition of no relative displacement between the two surfaces. The displacements due to the distribution (3.50) are

$$\begin{aligned} u_r(x,y) &= u_0 + \delta u_0 + \frac{\pi^2}{4}(2B+C)\left\{K_1 a^2 + K_2 c^2\right\} - \\ &\quad \frac{\pi^2}{16}(K_1+K_2)\left\{(4B+C)x^2 + (4B+3C)y^2\right\} \\ v_r(x,y) &= \frac{\pi^2}{8}(K_1+K_2)Cxy. \end{aligned} \tag{3.53}$$

Equating coefficients with the displacement at the end of the initial loading (3.16), we obtain the equations

$$K_1 + K_2 = K_0 = -\frac{4u_0}{\pi^2 R(2B+C)w_0} \tag{3.54}$$

and

$$u_0 + \frac{\pi^2}{4}(2B+C)K_0 a_0^2 = u_0 + \delta u_0 + \frac{\pi^2}{4}(2B+C)\left\{K_1 a^2 + K_2 c^2\right\}. \tag{3.55}$$

Substituting the value K_1 (3.52) we obtain, from equation (3.54),

$$K_2 = \frac{2f}{\pi^2 RB} - \frac{4u_0}{\pi^2 R(2B+C)w_0}. \tag{3.56}$$

The values of K_1 and K_2 substituted into the equation (3.55) gives the radius of slip as

$$\frac{c^2}{a_0^2} = 1 + \frac{\delta u_0 - \left(\frac{2B+C}{2B}\right) f\delta w_0}{u_0 - \left(\frac{2B+C}{2B}\right) f w_0}. \tag{3.57}$$

Thus within the circle $0 \leq r \leq c$ there is no relative displacement of the two surfaces and we have a 'stick' region. Within the annulus $c \leq r \leq a$ there occurs a region in which the tangential force equals the coefficient of friction times the normal force and slip is occurring.

When the displacement increment reaches its maximum value of $\delta u_0 = \delta u_0^*$, the radius of slip is at its minimum value denoted

$$\frac{c_*^2}{a_0^2} = 1 + \frac{\delta u_0^* - \left(\frac{2B+C}{2B}\right) f\delta w_0^*}{u_0 - \left(\frac{2B+C}{2B}\right) f w_0}. \tag{3.58}$$

The final displacement on the stick region $0 \leq r \leq c_*$ at the end of phase 1 is given by

$$\begin{aligned} u_r^*(x,y) &= u_0 + \delta u_0^* + \frac{\pi^2}{4}(2B+C)\left\{K_1 a_*^2 + K_2 c_*^2\right\} \\ &\quad - \frac{\pi^2}{16}(K_1+K_2)\left\{(4B+C)x^2 + (4B+3C)y^2\right\} \\ v_r^*(x,y) &= \frac{\pi^2}{8}(K_1+K_2)Cxy. \end{aligned} \tag{3.59}$$

To calculate the displacement on the annulus $c_* \leq r \leq a_*$ we must sum the displacements within the loaded circle $r \leq a_*$ due to the $K_1(a_*^2 - r^2)^{1/2}$ term, calculated from equation (3.8), and the displacements due to the $K_2(c_*^2 - r^2)^{1/2}$ term outside the loaded region, calculated from equation (3.10), to obtain

$$\begin{aligned} u_r^*(x,y) &= u_0 + \delta u_0^* + \frac{\pi^2}{4}(2B+C)K_1 a_*^2 - \frac{\pi^2}{16}K_1\left\{(4B+C)x^2 + (4B+3C)y^2\right\} \\ &\quad + \frac{\pi}{8}K_2\left\{4(2B+C)c_*^2 - (4B+C)x^2 - (4B+3C)y^2\right\}\sin^{-1}(c_*/r) \\ &\quad + \frac{\pi}{8}K_2 c_*(r^2 - c_*^2)^{1/2}\left\{4B + \frac{C}{r^2}\left[x^2 + 3y^2 + 2c_*^2\left(\frac{x^2-y^2}{r^2}\right)\right]\right\} \\ v_r(x,y) &= \frac{\pi^2}{8}K_1 Cxy + \frac{\pi}{4}K_2\frac{Cxy}{r^4}\left\{r^4\sin^{-1}(c_*/r) + c_*(2c_*^2 - r^2)(r^2 - c_*^2)^{1/2}\right\}. \end{aligned} \tag{3.60}$$

Phase 2 : Unloading with counterslip

During the unloading of phase 2, the contact radius reduces from a_* to a_0 and a radius of counterslip, that is slip in the opposite sense encountered in phase 1, progresses from a_* to b_0. Figure 3-9 shows the radius of counterslip during phase 2. The normal distribution is again given by (3.11) and the tangential distribution is of the form

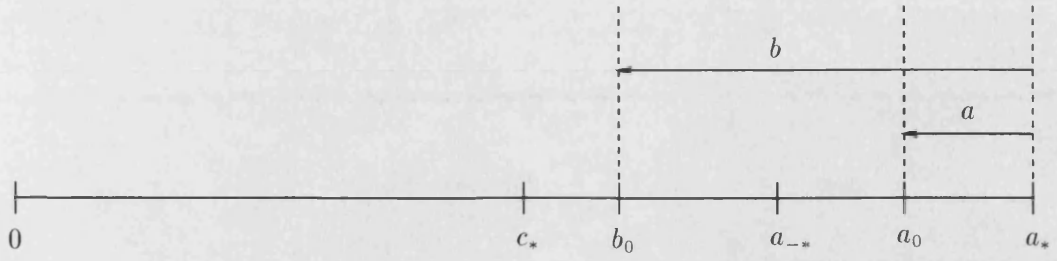

Figure 3-9: *Phase 2 : Unloading with counterslip*

$$P+\delta P=\begin{cases} K_1(a^2-r^2)^{1/2}+K_2(c_*^2-r^2)^{1/2}+K_3(b^2-r^2)^{1/2} & ,\ 0\le r\le c_* \\ K_1(a^2-r^2)^{1/2}+K_3(b^2-r^2)^{1/2} & ,\ c_*\le r\le b \\ K_1(a^2-r^2)^{1/2} & ,\ b\le r\le a. \end{cases} \tag{3.61}$$

Again, slip only occurs on an annulus, in this case $b \le r \le a$ shown in figure 3-10, and therefore the value of K_1 which satisfies the condition (1.53) and opposes the direction of slip is

$$K_1 = \frac{2f}{\pi^2 RB}. \tag{3.62}$$

The displacement on the inner circle $0 \le r \le c_*$ is given by

$$\begin{aligned} u_r(x,y) &= u_0+\delta u_0+\frac{\pi^2}{4}(2B+C)\left\{K_1a^2+K_2c_*^2+K_3b^2\right\} \\ &\quad -\frac{\pi^2}{16}(K_1+K_2+K_3)\left\{(4B+C)x^2+(4B+3C)y^2\right\} \\ v_r(x,y) &= \frac{\pi^2}{8}(K_1+K_2+K_3)Cxy. \end{aligned} \tag{3.63}$$

Matching terms of the above with the displacements at the end of phase 1 (3.53), we obtain

$$K_1+K_2+K_3 = K_1'+K_2', \tag{3.64}$$

where K_1' and K_2' are the values of these constants during phase 1, given by equa-

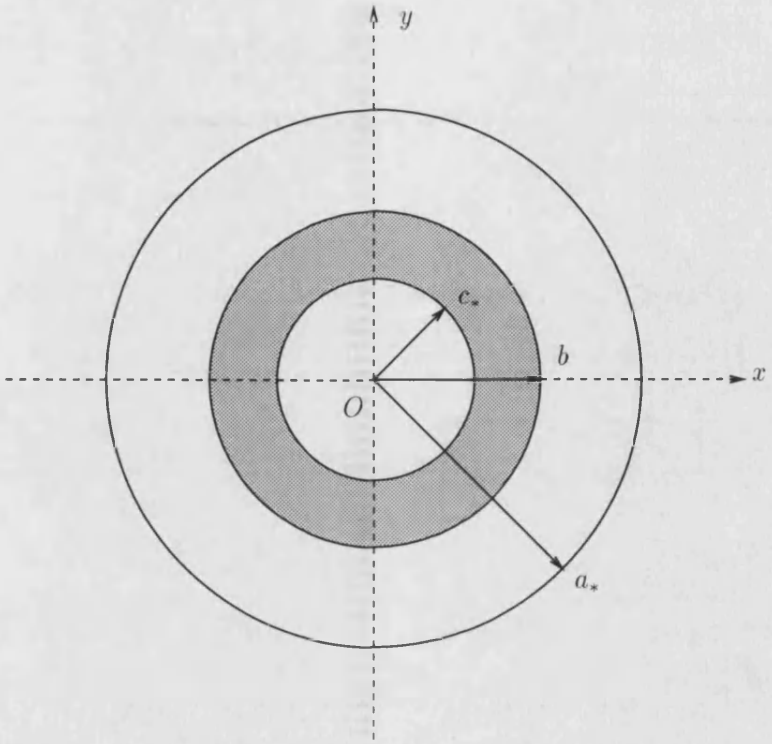

Figure 3-10: *The annulus* $c_* \leq r \leq b$

tions (3.52) and (3.56), and the constant terms equate to

$$u_0 + \delta u_0 + \frac{\pi^2}{4}(2B + C)\left\{K_1 a^2 + K_2 c_*^2 + K_3 b^2\right\} = u_0 + \delta u_0^* + \frac{\pi^2}{4}(2B + C)\left\{K_1' a_*^2 + K_2' c_*^2\right\}. \qquad (3.65)$$

On the annulus $c_* \leq r \leq b$, the displacement due to the distribution (3.61) is made up of contributions from each of the three terms. The two terms K_1 and K_3 contribute displacements inside the loaded circle $r \leq b$ of the form given by equation (3.8). The remaining term K_2 contributes displacements external to the loaded region of the form of equation (3.10). Thus the total displacements are

$$\begin{aligned} u_r(x,y) = {} & u_0 + \delta u_0 + \frac{\pi^2}{4}(2B + C)\left\{K_1 a^2 + K_3 b^2\right\} \\ & - \frac{\pi^2}{16}(K_1 + K_3)\left\{(4B + C)x^2 + (4B + 3C)y^2\right\} \\ & + \frac{\pi}{8}K_2\left\{4(2B + C)c_*^2 - (4B + C)x^2 - (4B + 3C)y^2\right\} \sin^{-1}(c_*/r) \end{aligned}$$

$$+\frac{\pi}{8}K_2c_*(r^2-c_*^2)^{1/2}\left\{4B+\frac{C}{r^2}\left[x^2+3y^2+2c_*^2\left(\frac{x^2-y^2}{r^2}\right)\right]\right\}$$

$$\begin{aligned} v_r(x,y) &= \frac{\pi^2}{8}(K_1+K_3)Cxy \\ &\quad +\frac{\pi}{4}K_2\frac{Cxy}{r^4}\left\{r^4\sin^{-1}(c_*/r)+c_*(2c_*^2-r^2)(r^2-c_*^2)^{1/2}\right\}. \end{aligned} \tag{3.66}$$

Equating coefficients of the above with the displacements at the end of phase 1, we obtain the system of equations

$$\begin{aligned} K_2 &= K_2' \\ K_1+K_3 &= K_1' \\ u_0+\delta u_0+\frac{\pi^2}{4}\{K_1a^2+K_3b^2\} &= u_0+\delta u_0^*+\frac{\pi^2}{4}(2B+C)K_1'a_*^2. \end{aligned} \tag{3.67}$$

Thus we have five equations for the remaining unknowns K_2, K_3 and b. However, by substituting $K_2 = K_2'$ into equations (3.64) and (3.65), we see that they are equivalent to two of the equations in (3.67) leaving only three equations for the three unknowns. Using the value K_1 from (3.62) and solving the above system, we obtain the solution as

$$\begin{aligned} K_1 &= \frac{2f}{\pi^2RB} \\ K_2 &= \frac{2f}{\pi^2RB}-\frac{4u_0}{\pi^2R(2B+C)w_0} \\ K_3 &= -\frac{4f}{\pi^2RB}. \end{aligned} \tag{3.68}$$

From these values and equation (3.67), the radius of counterslip is found to be

$$\frac{b^2}{a_0^2}=1+\frac{\delta w_0+\delta w_0^*}{2w_0}+\frac{B}{(2B+C)fw_0}(\delta u_0-\delta u_0^*). \tag{3.69}$$

At the end of phase 2, the values of δu_0 and δw_0 are zero, meaning that the above counterslip has reached a value b_0 of

$$\frac{b_0^2}{a_0^2}=1+\frac{\delta w_0^*}{2w_0}-\frac{B\delta u_0^*}{(2B+C)fw_0}. \tag{3.70}$$

Comparing the above with equation (3.58) we see that

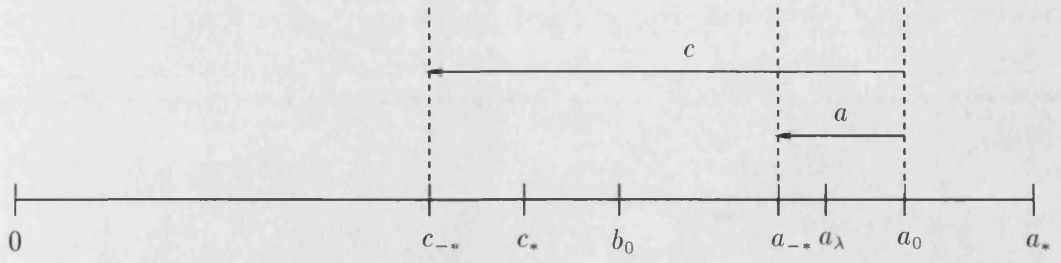

Figure 3-11: *Phase 3 : Unloading with counterslip*

$$\frac{b_0^2}{a_0^2} > \frac{c_*^2}{a_0^2} \tag{3.71}$$

showing that the radius of counterslip does not relieve all of the phase 1 slip before the end of this phase.

Phase 3 : Unloading with counterslip

During phase 3 the contact area reduces from a_0 to a_{-*}, as shown in figure 3-11. The radius of counterslip started during phase 2 continues from b_0 and it is necessary to determine whether or not this counterslip reaches the radius c_* before the end of this phase. To do this, we continue the tangential force distribution

$$P + \delta P = \begin{cases} K_1(a^2 - r^2)^{1/2} + K_2(c_*^2 - r^2)^{1/2} + K_3(b^2 - r^2)^{1/2} & , \ 0 \le r < c_* \\ K_1(a^2 - r^2)^{1/2} + K_3(b^2 - r^2)^{1/2} & , \ c_* \le r \le b \\ K_1(a^2 - r^2)^{1/2} & , \ b \le r \le a \end{cases} \tag{3.72}$$

with constants

$$\begin{aligned} K_1 &= \frac{2f}{\pi^2 RB} \\ K_2 &= \frac{2f}{\pi^2 RB} - \frac{4u_0}{\pi^2 R(2B + C)w_0} \\ K_3 &= -\frac{4f}{\pi^2 RB} \end{aligned} \tag{3.73}$$

and the radius of counterslip continues from b_0 as

$$\frac{b^2}{a_0^2} = 1 + \frac{\delta w_0 + \delta w_0^*}{2w_0} + \frac{B}{(2B+C)fw_0}(\delta u_0 - \delta u_0^*). \tag{3.74}$$

Equating the above equation for b_0^2/a_0^2 with the equation for c_*^2/a_0^2 (3.58), we calculate that b will pass c_* for values of u_0 and w_0 satisfying

$$\frac{u_0 + (\frac{2B+C}{2B})\, fw_0}{u_0 - (\frac{2B+C}{2B})\, fw_0} = \frac{\delta u_0 + (\frac{2B+C}{2B})\, f\delta w_0}{\delta u_0^* - (\frac{2B+C}{2B})\, f\delta w_0^*}. \tag{3.75}$$

The contact radius at which this occurs is denoted a_λ as shown in figure 3-11. Here we will consider only the case in which b passes c_* since the case when b does not reach c_* is very similar and the eventual linearised cycles, derived in section (3.6), are the same to within a constant displacement.

Substituting $b = c_*$ into equation (3.72), we obtain the distribution

$$P_0 + \delta P = \begin{cases} K_1(a_\lambda^2 - r^2)^{1/2} + (K_2 + K_3)(c_*^2 - r^2)^{1/2} & , \ 0 \le r \le c_* \\ K_1(a_\lambda^2 - r^2)^{1/2} & , \ c_* \le r \le a_\lambda \end{cases} \tag{3.76}$$

where

$$\begin{aligned} K_1 &= \frac{2f}{\pi^2 RB} \\ K_2 + K_3 &= -\frac{2f}{\pi^2 RB} - \frac{4u_0}{\pi^2 R(2B+C)w_0}. \end{aligned} \tag{3.77}$$

At this point, the slip of phase 1 has been totally relieved by the counterslip and so the radius c_* will play no further part. Continuing the unloading, the slip continues from c_* and progresses to c_{-*} with force distribution

$$P + \delta P = \begin{cases} K_1(a^2 - r^2)^{1/2} + K_2(c^2 - r^2)^{1/2} & , \ 0 \le r \le c \\ K_1(a^2 - r^2)^{1/2} & , \ c \le r \le a. \end{cases} \tag{3.78}$$

The slip condition requires a value for K_1 of

$$K_1 = \frac{2f}{\pi^2 RB}. \tag{3.79}$$

By matching the displacements with those at the end of phase 2 we obtain

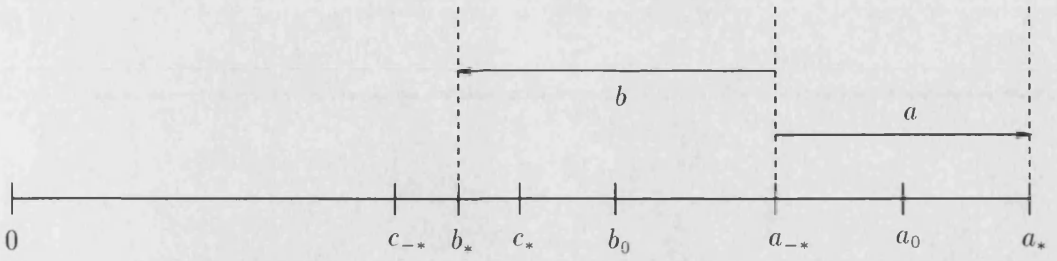

Figure 3-12: *Phases 4 and 5 : Re-loading with slip*

$$K_2 = -\frac{2f}{\pi^2 RB} - \frac{4u_0}{\pi^2 R(2B+C)w_0} \tag{3.80}$$

and the radius of slip is

$$\frac{c^2}{a_0^2} = 1 + \frac{\delta u_0 + (\frac{2B+C}{2B})\, f\delta w_0}{u_0 + (\frac{2B+C}{2B})\, fw_0}. \tag{3.81}$$

At the end of this phase, when the unloading is complete, the radius of slip has reached its minimum value of

$$\frac{c_{-*}^2}{a_0^2} = 1 - \frac{\delta u_0^* + (\frac{2B+C}{2B})\, f\delta w_0^*}{u_0 + (\frac{2B+C}{2B})\, fw_0} \tag{3.82}$$

and the final displacements on $c_* \le r \le a$ are

$$\begin{aligned} u_r^{-*}(x,y) &= u_0 + \delta u_0^{-*} + \frac{\pi^2}{4}(2B+C)K_1 a_{-*}^2 \\ &\quad - \frac{\pi^2}{16}K_1\left\{(4B+C)x^2 + (4B+3C)y^2\right\} \\ &\quad + \frac{\pi}{8}K_2\left\{4(2B+C)c_*^2 - (4B+C)x^2 - (4B+3C)y^2\right\}\, \sin^{-1}(c_*/r) \\ &\quad + \frac{\pi}{8}K_2 c_*(r^2-c_*^2)^{1/2}\left\{4B + \frac{C}{r^2}\left[x^2 + 3y^2 + 2c_*^2\left(\frac{x^2-y^2}{r^2}\right)\right]\right\} \\ v_r^{-*}(x,y) &= \frac{\pi^2}{8}K_1 Cxy + K_2\frac{Cxy}{r^4}\left\{r^4\, \sin^{-1}(c_*/r) + c_*(2c_*^2 - r^2)(r^2-c_*^2)^{1/2}\right\}. \end{aligned} \tag{3.83}$$

Phases 4 and 5 : Reloading with counterslip

Phases 4 and 5 cover the displacement from $\delta u_0 = \delta u_0^{-*}$ to $\delta u_0 = \delta u_0^*$ and may be

considered together. Figure 3-12 shows the cross-section of the contact area during these phases. A radius of counterslip b starts at $r = a_{-*}$ and progresses to $r = b_*$ at the end of loading. The tangential force is of the form

$$P + \delta P = \begin{cases} K_1(a^2 - r^2)^{1/2} + K_2(c_{-*}^2 - r^2)^{1/2} + K_3(b^2 - r^2)^{1/2} & , \ 0 \le r \le c_{-*} \\ K_1(a^2 - r^2)^{1/2} + K_3(b^2 - r^2)^{1/2} & , \ c_{-*} \le r \le b \\ K_1(a^2 - r^2)^{1/2} & , \ b \le r \le a. \end{cases} \tag{3.84}$$

Slip is occurring on the annulus $b \le r \le a$ and the value of K_1 satisfying the slip condition (1.53) and opposing the direction of slip is

$$K_1 = -\frac{2f}{\pi^2 RB}. \tag{3.85}$$

The displacements on the annulus $c_{-*} \le r \le b$ are given by

$$\begin{aligned} u_r(x,y) &= u_0 + \delta u_0 + \frac{\pi^2}{4}(2B + C)\{K_1 a^2 + K_3 b^2\} \\ &\quad - \frac{\pi^2}{16}(K_1 + K_3)\{(4B + C)x^2 + (4B + 3C)y^2\} \\ &\quad + \frac{\pi}{8}K_2\{4(2B + C)c_{-*}^2 - (4B + C)x^2 - (4B + 3C)y^2\} \sin^{-1}(c_{-*}/r) \\ &\quad + \frac{\pi}{8}K_2 c_{-*}(r^2 - c_{-*}^2)^{1/2}\left\{4B + \frac{C}{r^2}\left[x^2 + 3y^2 + 2c_{-*}^2\left(\frac{x^2 - y^2}{r^2}\right)\right]\right\} \\ v_r(x,y) &= \frac{\pi^2}{8}(K_1 + K_3)Cxy \\ &\quad + \frac{\pi}{4}K_2\frac{Cxy}{r^4}\left\{r^4 \sin^{-1}(c_{-*}/r) + c_{-*}(2c_{-*}^2 - r^2)(r^2 - c_{-*}^2)^{1/2}\right\}. \end{aligned} \tag{3.86}$$

Matching the displacements due to the above distribution with those at the end of phase 3, we obtain the equations

$$\begin{aligned} K_2 &= K_2' \\ K_1 + K_3 &= K_1' \\ u_0 + \delta u_0 + \frac{\pi^2}{4}\{K_1 a^2 + K_3 b^2\} &= u_0 + \delta u_0^{-*} + \frac{\pi^2}{4}(2B + C)K_1' a_{-*}^2. \end{aligned} \tag{3.87}$$

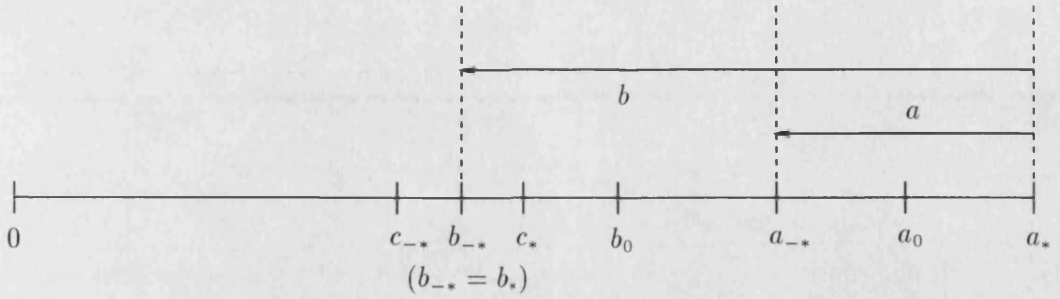

Figure 3-13: *Phases 6 and 7 : Re-loading with counterslip*

Solving the above system we obtain the solution

$$\begin{aligned} K_1 &= -\frac{2f}{\pi^2 RB} \\ K_2 &= -\frac{2f}{\pi^2 RB} - \frac{4u_0}{\pi^2 R(2B+C)w_0} \\ K_3 &= \frac{4f}{\pi^2 RB} \end{aligned} \tag{3.88}$$

and the radius of counterslip is

$$\frac{b^2}{a_0^2} = 1 + \frac{\delta w_0 - \delta w_0^*}{2w_0} - \frac{B}{(2B+C)fw_0}(\delta u_0 + \delta u_0^*). \tag{3.89}$$

At the end of phase 5, the final radius of counterslip is given by

$$\frac{b_*^2}{a_0^2} = 1 - \frac{2B\delta u_0^*}{(2B+C)fw_0} \tag{3.90}$$

which we note lies between c_{-*} and c_*.

Phases 6 and 7 : Unloading with counterslip

During phases 6 and 7 the displacement is unloaded from $\delta u_0 = \delta u_0^*$ to $\delta u_0 = \delta u_0^{-*}$ and the contact radius progresses from a_* to a_{-*}. A radius of slip b progresses from a_* to b_{-*} at the end of the loading as shown in figure 3-13. The tangential distribution is of the form

$$P+\delta P=\begin{cases} K_1(a^2-r^2)^{1/2}+K_2(c_{-*}^2-r^2)^{1/2} & \\ \qquad +K_3(b_*^2-r^2)^{1/2}+K_4(b^2-r^2)^{1/2} & , 0\le r\le c_{-*} \\ K_1(a^2-r^2)^{1/2}+K_3(b_*^2-r^2)^{1/2}+K_4(b^2-r^2)^{1/2} & , c_{-*}\le r\le b \\ K_1(a^2-r^2)^{1/2}+K_4(b^2-r^2)^{1/2} & , b_*\le r\le a \\ K_1(a^2-r^2)^{1/2} & , b\le r\le a. \end{cases} \tag{3.91}$$

The slip condition on $b \le r \le a$ requires that we have

$$K_1=\frac{2f}{\pi^2 RB}. \tag{3.92}$$

The displacements caused by this distribution on $c_{-*} \le r \le b_*$ are

$$\begin{aligned} u_r(x,y) &= u_0+\delta u_0+\frac{\pi^2}{4}(2B+C)\left\{K_1a^2+K_3b_*^2+K_4b^2\right\} \\ &\quad -\frac{\pi^2}{16}(K_1+K_3+K_4)\left\{(4B+C)x^2+(4B+3C)y^2\right\} \\ &\quad +\frac{\pi}{8}K_2\left\{4(2B+C)c_{-*}^2-(4B+C)x^2-(4B+3C)y^2\right\}\sin^{-1}(c_{-*}/r) \\ &\quad +\frac{\pi}{8}K_2c_{-*}(r^2-c_{-*}^2)^{1/2}\left\{4B+\frac{C}{r^2}\left[x^2+3y^2+2c_{-*}^2\left(\frac{x^2-y^2}{r^2}\right)\right]\right\} \\ v_r(x,y) &= \frac{\pi^2}{8}(K_1+K_3)Cxy \\ &\quad +\frac{\pi}{4}K_2\frac{Cxy}{r^4}\left\{r^4\sin^{-1}(c_{-*}/r)+c_{-*}(2c_{-*}^2-r^2)(r^2-c_{-*}^2)^{1/2}\right\}. \end{aligned} \tag{3.93}$$

Matching terms of the above displacements with the displacements at the end of phase 5, we obtain the solution as

$$\begin{aligned} K_1 &= \frac{2f}{\pi^2 RB} \\ K_2 &= -\frac{2f}{\pi^2 RB}-\frac{4u_0}{\pi^2 R(2B+C)w_0} \\ K_3 &= \frac{4f}{\pi^2 RB} \end{aligned}$$

$$K_4 = -\frac{4f}{\pi^2 RB} \tag{3.94}$$

and the radius of slip is

$$\frac{b^2}{a_0^2} = 1 + \frac{\delta w_0 + \delta w_0^*}{2w_0} + \frac{B}{(2B+C)fw_0}(\delta u_0 - \delta u_0^*). \tag{3.95}$$

At the end of the loading, the radius of counterslip is at its minimum value of

$$\frac{b_{-*}^2}{a_0^2} = 1 - \frac{2B\delta u_0^*}{(2B+C)fw_0} \tag{3.96}$$

which we note is equal to the radius of slip b_* at the end of phase 5.

Thus all of the slip which occurred in phases 4 and 5 has been relieved in phases 6 and 7. Consequently, the spheres are under the same conditions as they were at the end of phase 4. Phases 4/5 and 6/7 may now be repeated, thereby establishing the stable cycle.

3.4.3 Sliding Originally, Further Slip - $\theta_0 > \theta_c$ and $\theta > \theta_c$

We now turn attention to consider the incremental problem imposed on the initial state in which there was sliding originally. Here we examine the conditions under which further slip may occur for the case in which there was sliding in the initial deformation. At the end of the initial deformation, the surface displacements were

$$\begin{aligned} u_r(x,y) &= u_0 + \frac{\pi^2}{4}(2B+C)K_0 a_0^2 - \frac{\pi^2}{16}K_0\{(4B+C)x^2 + (4B+3C)y^2\} \\ v_r(x,y) &= \frac{\pi^2}{8}K_0 Cxy. \end{aligned} \tag{3.97}$$

Phase 1 : Sliding continues

The slip condition (3.35) shows that during phase 1, when the radius of contact increases from a_0 to a_* (see figure 3-14), sliding must continue with force distribution

$$P + \delta P = K_1(a^2 - r^2)^{1/2}. \tag{3.98}$$

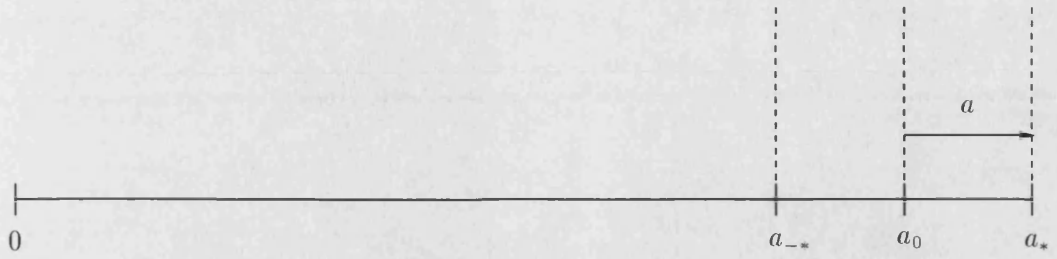

Figure 3-14: *Phase 1 : Loading, sliding continues*

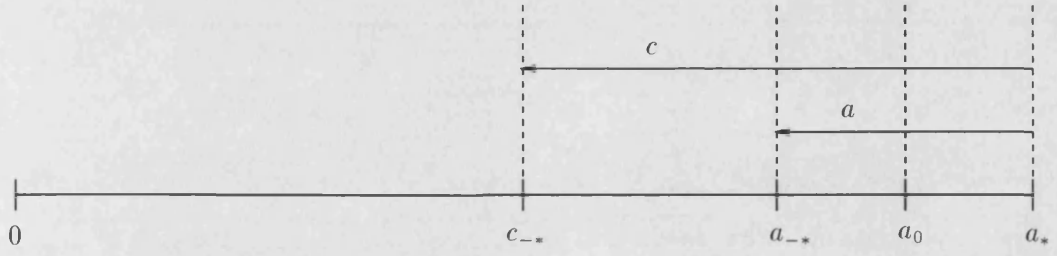

Figure 3-15: *Phases 2 and 3 : Unloading with slip*

To satisfy the slip condition, the force constant must be

$$K_1 = -\frac{2f}{\pi^2 RB}. \tag{3.99}$$

The displacements in $0 \leq r \leq a^*$ at the end of phase 1 are

$$\begin{aligned} u_r^*(x,y) &= u_0 + \delta u_0^* + \frac{\pi^2}{4}(2B+C)K_1 a_*^2 - \frac{\pi^2}{16}K_1\{(4B+C)x^2 + (4B+3C)y^2\} \\ v_r^*(x,y) &= \frac{\pi^2}{8}K_1 Cxy. \end{aligned} \tag{3.100}$$

Phases 2 and 3 : Unloading with slip

Phases 2 and 3 consist of an unloading from $\delta u_0 = \delta u_0^*$ to $\delta u_0 = \delta u_0^{-*}$. A radius of slip c is assumed to progress from $r = a_*$ to $r = c_{-*}$ as shown in figure 3-15. The force distribution is

$$P+\delta P=\begin{cases} K_1(a^2-r^2)^{1/2}+K_2(c^2-r^2)^{1/2} & ,\ 0\le r\le c \\ K_1(a^2-r^2)^{1/2} & ,\ c\le r\le a. \end{cases} \tag{3.101}$$

Applying the slip condition (1.53) on the annulus $c \le r \le a$, we obtain the value of K_1 as

$$K_1=\frac{2f}{\pi^2 RB}. \tag{3.102}$$

The displacements on the stick region $0 \le r \le c$ are

$$\begin{aligned} u_r(x,y) &= u_0+\delta u_0+\frac{\pi^2}{4}(2B+C)\left\{K_1a^2+K_2c^2\right\} \\ &\quad -\frac{\pi^2}{16}K_1\left\{(4B+C)x^2+(4B+3C)y^2\right\} \\ v_r(x,y) &= \frac{\pi^2}{8}(K_1+K_2)Cxy \end{aligned} \tag{3.103}$$

and matching the displacements in the usual way we obtain

$$K_2=-\frac{4f}{\pi^2 RB} \tag{3.104}$$

and the radius of slip as

$$\frac{c^2}{a_0^2}=1+\frac{\delta w_0+\delta w_0^*}{2w_0}+\frac{B}{(2B+C)fw_0}(\delta u_0-\delta u_0^*). \tag{3.105}$$

The minimum value of the radius of slip is

$$\frac{c_{-*}^2}{a_0^2}=1-\frac{2B}{(2B+C)fw_0}\delta u_0^*. \tag{3.106}$$

Phases 4 and 5 : Reloading with counterslip

Phases 4 and 5 cover the displacement from $\delta u_0 = \delta u_0^{-*}$ to $\delta u_0 = \delta u_0^*$. A radius of counterslip progresses from $r = a_{-*}$ to $r = b_*$ as shown in figure 3-16. The appropriate force distribution is

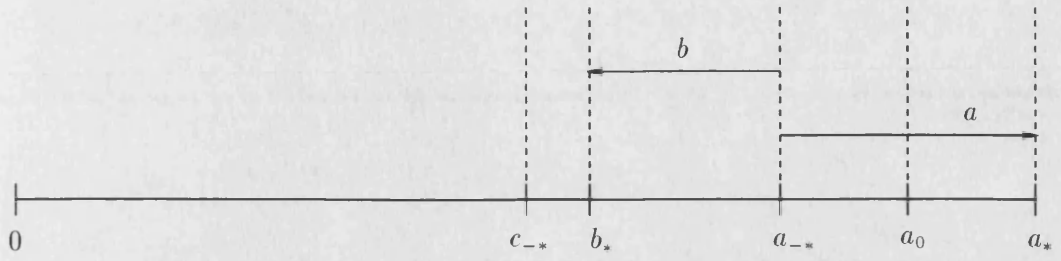

Figure 3-16: *Phases 4 and 5 : Reloading with counterslip*

$$P+\delta P=\begin{cases} K_1(a^2-r^2)^{1/2}+K_2(c_{-*}^2-r^2)^{1/2}+K_3(b^2-r^2)^{1/2} & ,\ 0\le r\le c_{-*} \\ K_1(a^2-r^2)^{1/2}+K_3(b^2-r^2)^{1/2} & ,\ c_{-*}\le r\le b \\ K_1(a^2-r^2)^{1/2} & ,\ b\le r\le a. \end{cases} \tag{3.107}$$

The value of K_1 satisfying the slip condition is

$$K_1=-\frac{2f}{\pi^2 RB} \tag{3.108}$$

and the displacements due to the distribution on the central region $0\le r\le c_{-*}$ are

$$\begin{aligned} u_r(x,y) &= u_0+\delta u_0^{-*}+\frac{\pi^2}{4}(2B+C)\left\{K_1a^2+K_2c_{-*}^2+K_3b^2\right\} \\ &\quad -\frac{\pi^2}{16}(K_1+K_2+K_3)\left\{(4B+C)x^2+(4B+3C)y^2\right\}. \end{aligned} \tag{3.109}$$

Matching with those at the end of phase 3 we obtain

$$\begin{aligned} K_1+K_3 &= K_1' \\ u_0+\delta u_0+\frac{\pi^2}{4}(2B+C)\left\{K_1a^2+K_3b^2\right\} &= u_0+\delta u_0^{-*}+\frac{\pi^2}{4}(2B+C)K_1'a_{-*}^2. \end{aligned} \tag{3.110}$$

Solving the above we obtain the solution as

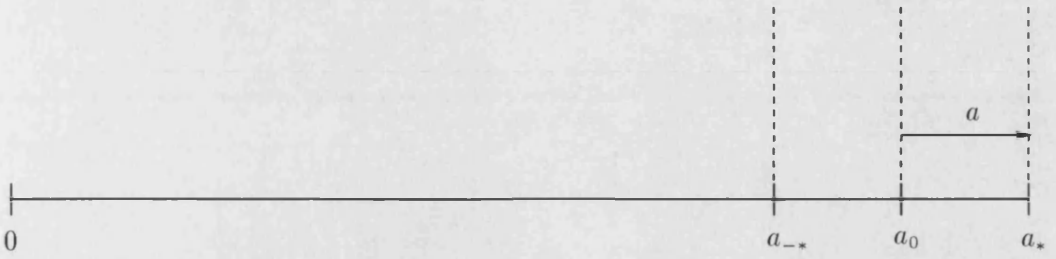

Figure 3-17: *Phase 1 : Loading without slip*

$$\begin{aligned} K_1 &= -\frac{2f}{\pi^2 RB} \\ K_2 &= -\frac{4f}{\pi^2 RB} \\ K_3 &= \frac{4f}{\pi^2 RB} \end{aligned} \tag{3.111}$$

with radius of counterslip given by

$$\frac{b^2}{a_0^2} = 1 + \frac{\delta w_0 - \delta w_0^*}{2w_0} - \frac{B}{(2B+C)fw_0}(\delta u_0 + \delta u_0^*). \tag{3.112}$$

The final value of the radius of counterslip is given by

$$\frac{b_*^2}{a_0^2} = 1 - \frac{2B\delta u_0^*}{(2B+C)fw_0} \tag{3.113}$$

which is equal to c_{-*} at the end of phases 2 and 3 thereby establishing the stable cycle.

3.4.4 Sliding Originally, No Further Slip - $\theta_0 > \theta_c$ and $\theta \leq \theta_c$

The final case which we have to consider is that in which there was sliding originally followed by no further slip. The normal force distribution remains as (3.11) and the displacement at the end of the initial stage is given by (3.14).

Phase 1 : Loading without slip

The contact radius is shown in figure 3-17 progressing from $r = a_0$ to $r = a_*$. The no-slip solution is of the same form as that used in section (3.4.2)

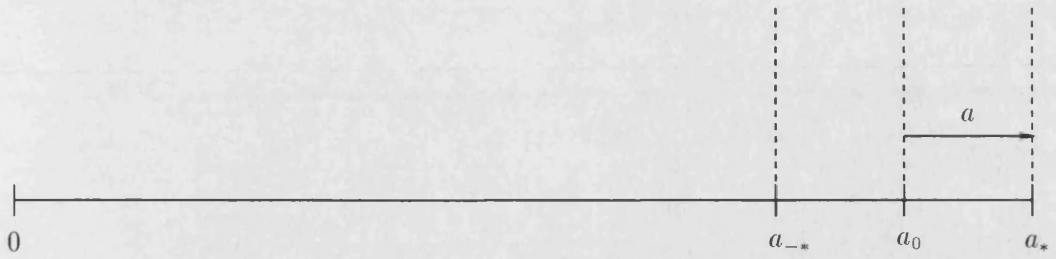

Figure 3-18: *Phase 2 : Unloading, reversal of phase 1*

$$P+\delta P=\begin{cases} K_1(a^2-r^2)^{1/2}+K_2(a_0^2-r^2)^{1/2} & ,\ 0\le r\le a_0 \\ K_1(a^2-r^2)^{1/2} & ,\ a_0\le r\le a. \end{cases} \tag{3.114}$$

The displacements caused by the above distribution on the region $0 \le r \le a_0$ are

$$\begin{aligned} u_r(x,y) &= u_0+\delta u_0+\frac{\pi^2}{4}(2B+C)\left\{K_1a^2+K_2a_0^2\right\} \\ &\quad -\frac{\pi^2}{16}(K_1+K_2)\left\{(4B+C)x^2+(4B+3C)y^2\right\} \\ v_r(x,y) &= \frac{\pi^2}{8}(K_1+K_2)Cxy \end{aligned} \tag{3.115}$$

and matching terms of the above with the displacements at the end of the initial sliding phase (3.26) we obtain the constants

$$\begin{aligned} K_1 &= -\frac{4}{\pi^2R(2B+C)}\frac{\delta u_0}{\delta w_0} \\ K_2 &= \frac{4}{\pi^2R(2B+C)}\frac{\delta u_0}{\delta w_0}-\frac{2f}{\pi^2RB}. \end{aligned} \tag{3.116}$$

Phase 2 : Unloading, reversal of phase 1

Since no slip occurred during phase 1, the unloading of phase 2 is simply reversed along the path of loading, exactly as was seen in section (3.4.1).

Phase 3 : Unloading with sliding

During phase 3, the condition (3.35) requires that sliding occurs on the entire contact

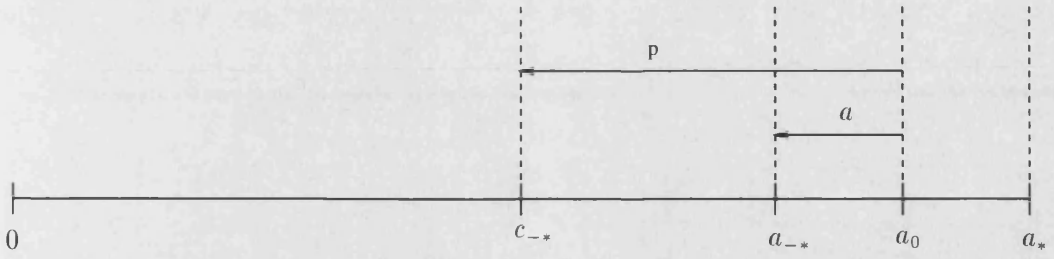

Figure 3-19: *Phase 3 : unloading with sliding*

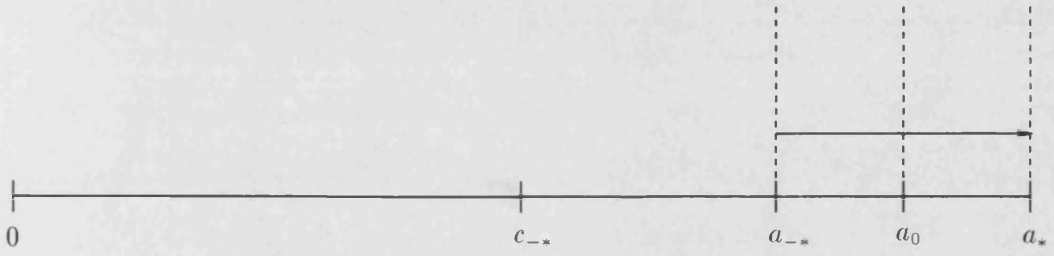

Figure 3-20: *Phases 4 and 5 : Reloading without slip*

area. As was the case in section (3.4.3), sliding must continue giving a solution of the form

$$P + \delta P = K_1(a^2 - r^2)^{1/2}. \tag{3.117}$$

Note that sliding only occurs at this stage in attaining the stable cycle. Once the cycle is established, there will be no further sliding.

Phases 4 and 5 : Reloading without slip

Reloading occurs during phase 4 and 5, shown in figure 3-20, with a force distribution of the form

$$P + \delta P = \begin{cases} K_1(a^2 - r^2)^{1/2} + K_2(a_{-*}^2 - r^2)^{1/2} & , 0 \le r \le a_{-*} \\ K_1(a^2 - r^2)^{1/2} & , a_{-*} \le r \le a. \end{cases} \tag{3.118}$$

Matching the displacement terms in the usual way, we obtain the force constants K_1 and K_2 as

$$\begin{aligned} K_1 &= \frac{4}{\pi^2 R(2B+C)}\left(\frac{\delta u_0 + \delta u_0^*}{\delta w_0 + \delta w_0^*}\right) \\ K_2 &= -\frac{4}{\pi^2 R(2B+C)}\left(\frac{\delta u_0 + \delta u_0^*}{\delta w_0 + \delta w_0^*}\right) - \frac{2f}{\pi^2 RB}. \end{aligned} \tag{3.119}$$

Noting that any subsequent loading may be reversed along this path back to the beginning of phase 4, we conclude that this establishes the stable cycle.

3.5 Total Forces on the Contact Area

Now that the actual force distributions have been established for each stable cycle, we calculate the resultant total forces at each stage of the cycles. The total force due to a distribution $P(x,y)$ acting over a region $\mathcal{R}$ is given by the integral of $P(x,y)$ over $\mathcal{R}$, written as

$$\overline{P} = \int_{\mathcal{R}} P(x,y)\, \mathrm{d}\mathcal{R}. \tag{3.120}$$

When the force distribution is of the general Hertzian form

$$P(x,y) = K(a^2 - r^2)^{1/2}, \tag{3.121}$$

K being the usual force constant, then the region $\mathcal{R}$ is the circular contact region of radius a and the above integral may be written in plane-polar coordinates (r,θ) as

$$\overline{P} = \int_{r=0}^{a} (a^2 - r^2)^{1/2} r\, \mathrm{d}r\, \mathrm{d}\theta. \tag{3.122}$$

This is easily evaluated to give the total force in terms of a and K as

$$\overline{P} = \frac{2}{3}\pi K a^3. \tag{3.123}$$

Consider now some of the force distributions arising from the previous sections. The total force due to the initial loading in which sliding did not originally occur may be calculated by substituting a_0 and K_0 from equation (3.16) into equation (3.123) to obtain

$$\overline{P_0} = \frac{2}{3}\pi K_0 a_0^3 = -\frac{8u_0}{3\pi R(2B+C)w_0}a_0^3 \tag{3.124}$$

as the total tangential force in the x-direction. Similarly, the total force due to the initial loading during which sliding did occur is

$$\overline{P_0} = \frac{2}{3}\pi K_0 a_0^3 = -\frac{4f}{3\pi RB}a_0^3. \tag{3.125}$$

In each of the above cases the total normal force is the same and may be found from the distribution (3.11) as

$$\overline{N_0} = \frac{4a_0^3}{3\pi RB}. \tag{3.126}$$

The total forces in the incremental problem may be calculated by summing equation (3.123) for each of the component force distributions associated with the constants K_1, K_2, K_3, etc. Here we list the total forces during the four stable cycles:

3.5.1 No Sliding Originally

Stick Cycle, $\theta < \theta_c$

The stick cycle is described by phases 4 and 5 in section (3.4.2). The force distribution during these phases is given by equation (3.42) with constants of equation (3.47). The total force may be calculated using equation (3.123) and the force increment found by subtracting the total initial force (3.124). Thus the total tangential force in the x-direction at any point of the cycle is given by

$$\begin{aligned}\overline{\delta P} \;=\; & \frac{2\pi}{3}a_0^3\left\{-\frac{4}{\pi^2 R(2B+C)}\left(\frac{\delta u_0+\delta u_0^*}{\delta w_0+\delta w_0^*}\right)\frac{a^3}{a_0^3}\right. \\ & -\left(\frac{2f}{\pi^2 RB}+\frac{4u_0}{\pi^2 R(2B+C)w_0}\right)\frac{c_{-*}^3}{a_0^3} \\ & \left.+\left[\frac{4}{\pi^2 R(2B+C)}\left(\frac{\delta u_0+\delta u_0^*}{\delta w_0+\delta w_0^*}\right)+\frac{2f}{\pi^2 RB}\right]\frac{a_{-*}}{a_0^3}+\frac{4u_0}{\pi^2 R(2B+C)w_0}a_0^3\right\}.\end{aligned} \tag{3.127}$$

Slip Cycle, $\theta \geq \theta_c$

The slip cycle in this case is described by phases 4, 5, 6 and 7 of section (3.4.2). Using the force distributions (3.84) and (3.91) and the constants given by equations (3.88) and (3.94) we obtain the total incremental force during phases 4 and 5 as

$$\overline{\delta P} = \frac{2\pi}{3}a_0^3\left\{-\frac{2f}{\pi^2 RB}\frac{a^3}{a_0^3} - \left(\frac{2f}{\pi^2 RB} + \frac{4u_0}{\pi^2 R(2B+C)}\right)\frac{c_{-*}^3}{a_0^3} + \frac{4f}{\pi^2 RB}\frac{b^3}{a_0^3} + \frac{4u_0}{\pi^2 R(2B+C)w_0}\right\} \tag{3.128}$$

and during phases 6 and 7 the total incremental force is

$$\overline{\delta P} = \frac{2\pi}{3}a_0^3\left\{\frac{2f}{\pi^2 RB}\frac{a^3}{a_0^3} - \left(\frac{2f}{\pi^2 RB} + \frac{4u_0}{\pi^2 R(2B+C)}\right)\frac{c_{-*}^3}{a_0^3} + \frac{4f}{\pi^2 RB}\frac{b_*^3}{a_0^3} - \frac{4f}{\pi^2 RB}\frac{b^3}{a_0^3} + \frac{4u_0}{\pi^2 R(2B+C)w_0}\right\}. \tag{3.129}$$

3.5.2 Sliding Originally

Stick Cycle, $\theta < \theta_c$

The stick cycle after initial sliding is described in section (3.4.4) and the total incremental force during the stable cycle phases 4 and 5 may be calculated as

$$\overline{\delta P} = \frac{2\pi}{3}a_0^3\left\{\frac{4}{\pi^2 R(2B+C)}\left(\frac{\delta u_0 + \delta u_0^*}{\delta w_0 + \delta w_0^*}\right)\frac{a^3}{a_0^3} - \left[\frac{4}{\pi^2 R(2B+C)}\left(\frac{\delta u_0 + \delta u_0^*}{\delta w_0 + \delta w_0^*}\right) + \frac{2f}{\pi^2 RB}\right]\frac{a_{-*}^3}{a_0^3} + \frac{2f}{\pi^2 RB}\right\}. \tag{3.130}$$

Slip Cycle, $\theta \geq \theta_c$

Phases 2 and 3 of section (3.4.3) have a total incremental force of

$$\overline{\delta P} = \frac{2\pi}{3}a_0^3\left\{\frac{2f}{\pi^2 RB}\frac{a^3}{a_0^3} - \frac{4f}{\pi^2 RB}\frac{c^3}{a_0^3} + \frac{2f}{\pi^2 RB}\right\}. \tag{3.131}$$

During phases 4 and 5 of the stable cycle, the total incremental force is given by

$$\overline{\delta P} = \frac{2\pi}{3}a_0^3\left\{-\frac{2f}{\pi^2 RB}\frac{a^3}{a_0^3} - \frac{4f}{\pi^2 RB}\frac{c_{-*}^3}{a_0^3} + \frac{4f}{\pi^2 RB}\frac{b^3}{a_0^3} + \frac{2f}{\pi^2 RB}\right\}. \tag{3.132}$$

3.5.3 Normal Forces

Throughout all the above cases the incremental normal force has the form given by equation (3.28). Therefore, the total normal force may be calculated as

$$\overline{N+\delta N} = \frac{4a^3}{3\pi RB}. \tag{3.133}$$

Subtracting the initial normal force (3.11) and making use of equations (3.12) and (3.29) we obtain the total incremental force as

$$\overline{\delta N} = \frac{4R^{1/2}}{3\pi B}\left\{(w_0+\delta w_0)^{3/2} - w_0^{3/2}\right\}. \tag{3.134}$$

3.6 Linearisation of Total Forces

Since the incremental deformation is assumed to be infinitesimal in the sense that it is much smaller than the initial loading, it is sufficient to consider the linearised cycles. In this section, the total forces will be expanded to first order in the incremental quantities δu_0 and δw_0.

3.6.1 Normal Forces

The total normal force increment during all the incremental deformations is given by equation (3.133). The incremental Hertz radius is given by equation (3.29) and we may write

$$\frac{a^3}{a_0^3} = \left(\frac{a^2}{a_0^2}\right)^{3/2} = \left(1+\frac{\delta w_0}{w_0}\right)^{3/2}. \tag{3.135}$$

Expanding to first order in the infinitesimal quantity δw_0 we obtain

$$\frac{a^3}{a_0^3} = 1 + \frac{3\delta w_0}{2w_0} + \cdots \tag{3.136}$$

where the dots $(\cdots)$ denote terms of higher order. Substituting the above into equation (3.133) and subtracting the initial total normal force N_0 (3.126), we obtain the

linearised normal force-displacement relationship as

$$\overline{\delta N} = \frac{2(Rw_0)^{1/2}}{\pi B}\delta w_0. \tag{3.137}$$

3.6.2 Tangential Forces

The tangential incremental forces may be linearised as follows. As an example we consider the stable cycle of slip arising from section (3.4.2) in which no sliding occurred originally followed by further slip. The radii a, b, c_{-*} etc. are given by equations (3.29), (3.95) and (3.82) in terms of the increments δu_0 and δw_0 as

$$\frac{a^3}{a_0^3} = 1 + \frac{\delta w_0}{w_0} \tag{3.138}$$

$$\frac{c_{-*}^2}{a_0^2} = 1 - \frac{\delta u_0^* + (\frac{2B+C}{2B})\, f\delta w_0^*}{u_0 + (\frac{2B+C}{2B})\, fw_0} \tag{3.139}$$

$$\frac{b^2}{a_0^2} = 1 + \frac{\delta w_0 - \delta w_0^*}{2w_0} - \frac{B}{(2B+C)fw_0}(\delta u_0 + \delta u_0^*). \tag{3.140}$$

We write the cubed radii in terms of the known squared values and expand the above expressions to first order in δw_0 or δu_0 to obtain

$$\frac{a^3}{a_0^3} = \left(\frac{a^2}{a_0^2}\right)^{3/2} = 1 + \frac{3\delta w_0}{2w_0} + \cdots \tag{3.141}$$

$$\frac{c_{-*}^3}{a_0^3} = \left(\frac{c_{-*}^2}{a_0^2}\right)^{3/2} = 1 - \frac{3\delta u_0^* + 3\,(\frac{2B+C}{2B})\, f\delta w_0^*}{2u_0 + 2\,(\frac{2B+C}{2B})\, fw_0} + \cdots \tag{3.142}$$

$$\frac{b^3}{a_0^3} = \left(\frac{b^2}{a_0^2}\right)^{3/2} = 1 + \frac{3(\delta w_0 - \delta w_0^*)}{4w_0} - \frac{3B}{2(2B+C)fw_0}(\delta u_0 + \delta u_0^*) + \cdots \tag{3.143}$$

where the dots $(\cdots)$ denote higher order terms. Substituting the above linearised values into the total force expression (3.128), and making use of the relationships (3.48), we obtain the linearised incremental force as

$$\begin{aligned}\overline{\delta P} = \frac{2\pi a_0^3}{3}\Bigg\{ & -\frac{6}{\pi^2 R(2B+C)w_0}(\delta u_0 + \delta u_0^*) - \frac{3f\delta w_0^*}{\pi^2 RBw_0} \\ & + \left(\frac{2f}{\pi^2 RB} + \frac{4u_0}{\pi^2 R(2B+C)w_0}\right)\left(\frac{3\delta u_0^* + 3\,(\frac{2B+C}{2B})\, f\delta w_0^*}{2u_0 + 2\,(\frac{2B+C}{2B})\, fw_0}\right)\Bigg\}.\end{aligned} \tag{3.144}$$

This same result may be obtained for phase 6 and 7 of the same cycle and also from the results of section (3.4.1) in which no further slip occurred.

Now consider the cases in which sliding occurred originally. Sections (3.4.3) and (3.4.4) give the stable cycles for no further slip and further slip respectively and the total force is given by equation (3.132). Expanding the radii to first order gives the linearised force, in both cases of further slip or no further slip, as

$$\overline{\delta P} = \frac{2\pi a_0^3}{3}\left\{-\frac{6}{\pi^2 R(2B+C)w_0}(\delta u_0 + \delta u_0^*) - \frac{3f}{\pi^2 RB}\frac{\delta w_0^*}{w_0}\right\}. \tag{3.145}$$

Examining the above equations it can be seen that the coefficients of δu_0 are the same in each case, the other terms being constant. Therefore we may regard the above equations as equivalent force-displacement relationships, each displaced from the others by a constant amount. The incremental tangential force may be written in terms of the tangential displacement as

$$\overline{\delta P} = -\frac{4(Rw_0)^{1/2}}{\pi(2B+C)}\delta u_0 \tag{3.146}$$

and the incremental normal force we recall is given by

$$\overline{\delta N} = \frac{2(Rw_0)^{1/2}}{\pi B}\delta w_0. \tag{3.147}$$

It is sufficient to consider the increments (3.146) and (3.147) regardless of whether or not sliding originally took place, and therefore the eventual linearised stable cycles may be regarded as independent of the initial state.

We also note that, to first order, there is no frictional energy loss during a cycle and consequently the incremental motion dissipates no energy.

3.7 Extension to Three-Dimensions

For the two-dimensional problems considered so far, the incremental displacement of the lower sphere of amount $(\delta u_0, 0, -\delta w_0)$ is always in the same plane as the initial displace-

ment $(u_0, 0, -w_0)$. The general three-dimensional problem would have an initial displacement of $(u_0, v_0, -w_0)$ followed by an incremental displacement of $(\delta u_0, \delta v_0, -\delta w_0)$. However, without loss of generality, we may take the increment to be $(\delta u_0, 0, -\delta w_0)$, the y-component being zero.

Following the method used to find the initial force constant (3.15), we find the initial force distributions in the x- and y-directions respectively as

$$\begin{aligned} P_0(r) &= -\frac{4u_0}{\pi^2 R(2B+C)w_0}(a_0^2 - r^2)^{1/2} \\ Q_0(r) &= -\frac{4v_0}{\pi^2 R(2B+C)w_0}(a_0^2 - r^2)^{1/2}. \end{aligned} \tag{3.148}$$

The normal force remains as N_0 in equation (3.11). The magnitude of the tangential force is $\sqrt{P_0^2 + Q_0^2}$ and the condition for no slip may be written as

$$\sqrt{P_0^2 + Q_0^2} \leq fN_0 \tag{3.149}$$

which is satisfied when

$$\sqrt{\frac{u_0^2}{w_0^2} + \frac{v_0^2}{w_0^2}} \leq \left(\frac{2B+C}{2B}\right) f. \tag{3.150}$$

As was seen in the two-dimensional case, this condition is independent of position on the contact area meaning that if slip does occur it will be in the form of sliding. Therefore, when the condition (3.149) is violated, the sliding solution may be calculated as

$$\begin{aligned} P_0(r) &= -\frac{2f}{\pi^2 RB}\frac{u_0}{\sqrt{u_0^2 + v_0^2}}(a_0^2 - r^2)^{1/2} \\ Q_0(r) &= -\frac{2f}{\pi^2 RB}\frac{v_0}{\sqrt{u_0^2 + v_0^2}}(a_0^2 - r^2)^{1/2}. \end{aligned} \tag{3.151}$$

with the normal force distribution remaining as in equation (3.11).

Consider now the incremental deformation $(\delta u_0, 0, -\delta w_0)$ which is purely in the x-direction. If slip were to occur at any point on the contact area, Admontons' Law would require

$$(P+\delta P)^2+(Q+\delta Q)^2=f^2(N+\delta N)^2 \tag{3.152}$$

at that point. However, it is not possible to obtain analytic solutions of the analogous form to those for the two-dimensional case by matching displacement terms in the slip and stick regions because any solution obtained in this way will violate the condition that slip opposes the direction of the force causing it.

In the two-dimensional case, we saw that the eventual linearised cycles were independent of the initial state and therefore it is reasonable to assume that in the three-dimensional case we will eventually reach a stable cycle of slip or stick similar to those we have already seen. Therefore, if we assume that the stable cycle has been established we must represent the force distributions on the contact area as a combination of unknown fixed forces $\tilde{P}(r)$ in the tangential x-direction and $\tilde{Q}(r)$ in the tangential y-direction, together with oscillating forces.

3.7.1 A 3D Stick Cycle

When the stable cycle established is a stick cycle, such as those seen in sections (3.4.1) and (3.4.4), the form of force distribution during both loading and unloading phases is

$$\begin{aligned} P+\delta P &= \begin{cases} \tilde{P}(r)+K_1(a^2-r^2)^{1/2}+K_2(a_{-*}^2-r^2)^{1/2} & ,\ 0\le r\le a_{-*} \\ K_1(a^2-r^2)^{1/2} & ,\ a_{-*}\le r\le a. \end{cases} \\ Q+\delta Q &= \tilde{Q}. \end{aligned} \tag{3.153}$$

This gives rise to displacements on $0\le r\le a_{-*}$ of

$$\begin{aligned} u_r(x,y) &= \tilde{u}_r(x,y)+\delta u_0^*+\delta u_0+\frac{\pi^2}{4}(2B+C)\left\{K_1a^2+K_2a_{-*}^2\right\} \\ &\quad +\frac{\pi^2}{16}(K_1+K_2)\left\{(4B+C)x^2+(4B+3C)y^2\right\} \\ v_r(x,y) &= \tilde{v}_r(x,y)+\frac{\pi^2}{8}(K_1+K_2)Cxy \end{aligned} \tag{3.154}$$

where $\tilde{u}_r(x,y)$ and $\tilde{v}_r(x,y)$ are the displacements due to the unknown force distributions $\tilde{P}(r)$ and $\tilde{Q}(r)$. Stick occurs everywhere on the contact area and so the displacements

u_r and v_r must be constant. Equating the displacements at the beginning, the end and an intermediate point on this unloading cycle and solving for K_1 and K_2, we obtain the same values as in equations (3.47) and (3.119). Since no slip has taken place, this loading is reversible thus establishing a stable stick cycle.

3.7.2 A 3D Slip Cycle

During a stable slip cycle, such as those seen in sections (3.4.2) and (3.4.3) a radius of slip c oscillates between a fixed value and the contact area radius a. The force distribution during the unloading phases of the cycle will be

$$\begin{aligned} P+\delta P &= \begin{cases} \tilde{P}(r)+K_1'(a^2-r^2)^{1/2}+K_2'(c^2-r^2)^{1/2} & , 0\le r\le c \\ K_1'(a^2-r^2)^{1/2} & , c\le r\le a. \end{cases} \\ Q+\delta Q &= \tilde{Q} \end{aligned} \tag{3.155}$$

giving displacements on $0 \le r \le c$ of

$$\begin{aligned} u_r(x,y) &= \tilde{u}_r(x,y)+\delta u_0+\frac{\pi^2}{4}(2B+C)\left\{K_1'a^2+K_2'c^2\right\} \\ &\quad +\frac{\pi^2}{16}(K_1'+K_2')\left\{(4B+C)x^2+(4B+3C)y^2\right\} \\ v_r(x,y) &= \tilde{v}_r(x,y)+\frac{\pi^2}{8}(K_1'+K_2')Cxy. \end{aligned} \tag{3.156}$$

The slip condition on $c \le r \le a$ requires a value for K_1' of

$$K_1' = \frac{2f}{\pi^2 RB} \tag{3.157}$$

giving K_2' as

$$K_2' = -\frac{2f}{\pi^2 RB}. \tag{3.158}$$

During the reloading phase the force distribution will be of the form

$$P+\delta P = \begin{cases} \tilde{P}(r)+K_1(a^2-r^2)^{1/2}+K_2(c_{-*}^2-r^2)^{1/2}+K_3(b^2-r^2)^{1/2} & , 0 \le r \le c_{-*} \\ K_1(a^2-r^2)^{1/2}+K_3(b^2-r^2)^{1/2} & , c_{-*} \le r \le b \\ K_1(a^2-r^2)^{1/2} & , b \le r \le a \end{cases}$$

$$Q+\delta Q = \tilde{Q} \tag{3.159}$$

with displacements

$$\begin{aligned} u_r(x,y) &= \tilde{u}_r(x,y)+\delta u_0+\frac{\pi^2}{4}(2B+C)\left\{K_1a^2+K_2c_{-*}^2+K_3b^2\right\} \\ &\quad +\frac{\pi^2}{16}(K_1+K_2+K_3)\left\{(4B+C)x^2+(4B+3C)y^2\right\} \\ v_r(x,y) &= \tilde{v}_r(x,y)+\frac{\pi^2}{8}(K_1+K_2+K_3)Cxy. \end{aligned} \tag{3.160}$$

The slip condition on $b \le r \le a$ gives

$$K_1 = -\frac{2f}{\pi^2 RB}. \tag{3.161}$$

Equating these displacements at each end of these loading cycles with the displacements at an intermediate point gives values for K_1, K_2 and K_3 the same as those in section (3.4.3). Similary, we obtain the force constants for the varying terms of the stable cycle established in section (3.4.2).

An identical linearisation process as seen in section (3.6) for the two-dimensional cases may be applied to the above cycles to obtain the incremental tangential forces generalised to three-dimensions as

$$\begin{aligned} \overline{\delta P} &= -\frac{4(Rw_0)^{1/2}}{\pi(2B+C)}\delta u_0 \\ \overline{\delta Q} &= -\frac{4(Rw_0)^{1/2}}{\pi(2B+C)}\delta v_0 \end{aligned} \tag{3.162}$$

and the incremental normal force we recall is given by

$$\overline{\delta N} = \frac{2(Rw_0)^{1/2}}{\pi B}\delta w_0. \tag{3.163}$$

Chapter 4

Wave Propagation in Cubic Packings

4.1 Introduction

This chapter considers wave propagation within a cubic packing of identical elastic spheres. A cubic packing is one of the simplest types of regular packings; each sphere may be thought of as being contained within a cube of side $2R$ where R is the sphere radius. The spheres are packed in an array such that each cube is face to face with its six nearest neighbours to form a cubic lattice, therefore each sphere has six point contacts. A small section of a cubic packing is shown in figure 4-1.

Obviously, any regular packing is a rather idealised model of a real granular media such as an ocean sediment, but there are several good reasons why such a model should be considered. The geometry of regular packings is easier to work with than the complex structure of a random packing and regular packings also exhibit many of the qualitative properties of random packings. For example, Kendall [38] considers the elastic properties of a variety of regular sphere packings, each of different packing densities. The required elastic modulus of a random packing is then estimated by interpolation of a plot of elastic modulus against packing density. Walton [64] and [65] considered a fluid saturated cubic packing as a simple model of an ocean sediment and discussed some of the qualitative properties of such a model. Duffy [25] examined the stress-strain relationships for a regular hexagonal close-packed array of elastic spheres.

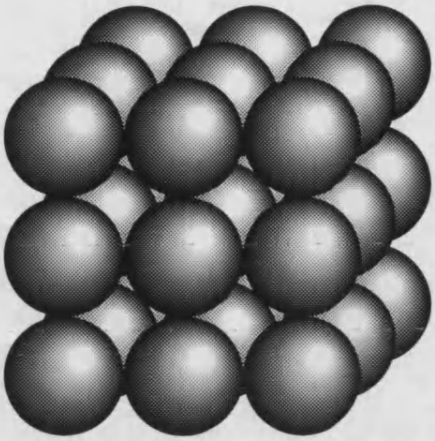

Figure 4-1: *A section from a cubic packing*

The work presented here considers elastic wave speeds within the cubic packing and derives conditions for propagation on the wave frequency. As usual, the sphere material is homogeneous, elastically isotropic and all deformations are taken to be small enough for linear elasticity and Hertz theory to apply. A finite and non-zero coefficient of friction exists between any two spheres and the results of chapter 3 will be used to describe the interaction of individual spheres within the packing.

For simplicity, we will be considering only deformations in which the displacement of the spheres' centres are in the xz-plane. The packing deformation proceeds in two stages: an initial confining strain followed by an incremental deformation. The initial deformation is a uniaxial compression, as already seen in section (1.3.1) equation (1.92), which confines the packing and forms contact areas between spheres initially in point contact. A hydrostatic compression, such as that described by equation (1.90), could also be considered but as will be seen, no frictional effects would be observed. A uniaxial compression inclined at an angle to the coordinate axes ensures that the line of compression between two arbitrary spheres is not generally along their lines of centres, thereby ensuring that slip may occur between them. As was discussed in section (3.3), two possible cases of stick or sliding arise during such a compression and each needs to be considered separately. The average stresses for both sliding and stick combinations are calculated. The results of section (3.3) are essentially valid for quasi-static deformations and therefore the displacements and rotations in the initial state are treated as having

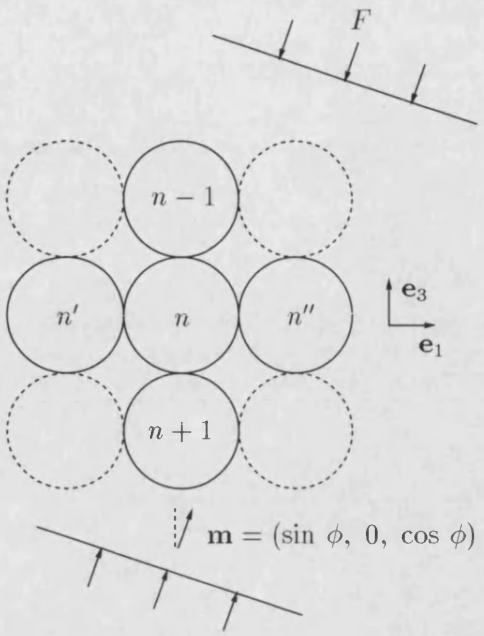

Figure 4-2: *Sphere n with four contacting neighbours*

no time dependencies. Therefore, the results obtained are appropriate for low frequency wave propagation.

The incremental problem consists of an infinitesimal deformation imposed on the initial state. This is the dynamic part of the problem, the time-dependency being the oscillatory nature of the incremental displacements and rotations. The dynamic equations of motion are analysed and the discrete nature of the packing gives rise to a system of difference equations which are solved to determine the required propagation conditions on the wave frequency.

4.2 The Initial State

Figure 4-2 shows sphere n of the packing surrounded by its four contacting neighbours in the xz-plane. The axis of strain $\mathbf{m}$ is in the xz-plane and therefore all displacements of the sphere centres are in the xz-plane. Also, the axes of any rotations must be in the y-direction. It is sufficient to consider only the plane of spheres shown in figure 4-2, and the two out of plane contacts of sphere n will suffer no relative motion between them. The spheres above and below sphere n are labelled $n-1$ and $n+1$ respectively. To the left is sphere n' and to the right is sphere n''.

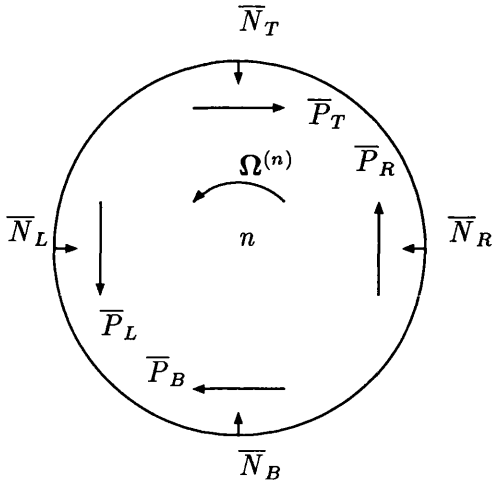

Figure 4-3: *Sphere n showing contact forces*

In the usual notation, as used in section (1.3.1), the centre of sphere n is initially at position vector $\mathbf{X}^{(n)}$ and undergoes a displacement $\mathbf{u}^{(n)}$ in the xz-plane only. The sphere also undergoes a rotation $\boldsymbol{\Omega}^{(n)}$ about the axis $\mathbf{e}_2$ passing through the centre $\mathbf{X}^{(n)}$. The unit vectors $\mathbf{I}^{(nm)}$ joining the centres of two contacting spheres are defined in the usual way by

$$\mathbf{I}^{(nm)} = \frac{\mathbf{X}^{(n)} - \mathbf{X}^{(m)}}{2R} \tag{4.1}$$

where m takes values $n-1$, $n+1$, n' and n''. Because of the regular nature of the packing, $\mathbf{I}^{(nm)}$ can take one of four possible values: $\pm\mathbf{e}_1$ or $\pm\mathbf{e}_3$.

The force exerted on sphere n by sphere m across the contact area is denoted by $\mathbf{F}^{(nm)}$. Each sphere has four contact areas with corresponding forces $\mathbf{F}^{(n,n+1)}$, $\mathbf{F}^{(n,n-1)}$, $\mathbf{F}^{(nn')}$ and $\mathbf{F}^{(nn'')}$.

The problem described has certain symmetries which may be made use of. Rotating figure 4-2 through 180° results in an identical problem to the one we are considering, and therefore the magnitudes of the top and bottom normal and tangential forces must be equal and in opposite directions. The same applies to the two side forces resulting in the relationships

$$\overline{N}_T = \overline{N}_B,\ \overline{P}_T = \overline{P}_B \quad \text{and} \quad \overline{N}_L = \overline{N}_R,\ \overline{P}_L = \overline{P}_R \tag{4.2}$$

where $\overline{N}$ denotes the total normal force, $\overline{P}$ the total tangential force and the subscripts L, R and T, B refer to the left, right and top, bottom contacts respectively. In vector notation this is

$$\mathbf{F}^{(n,n+1)} = -\mathbf{F}^{(n,n-1)} \quad \text{and} \quad \mathbf{F}^{(nn')} = -\mathbf{F}^{(nn'')}. \tag{4.3}$$

By the same symmetries, the top and bottom contacts will either both stick or both slide. The same applies to the two side contacts. We also note that the rotation of each sphere must be equal, that is

$$\mathbf{\Omega}^{(n)} = \mathbf{\Omega}^{(m)} = \Omega \mathbf{e}_2 \tag{4.4}$$

for all values of n and m.

The normal and tangential contact forces are shown in figure 4-3. Since the sphere must be in linear and rotational equilibrium and considering the relationships (4.2), we deduce that

$$\overline{N}_T = \overline{N}_B,\ \overline{N}_L = \overline{N}_R \quad \text{and} \quad \overline{P}_T = \overline{P}_B = \overline{P}_L = \overline{P}_R. \tag{4.5}$$

The values of the above forces will be calculated in terms of the confining strain in sections (4.2.1) and (4.2.2).

The confining uniaxial strain, indicated by the arrows in the direction of the axis of strain $\mathbf{m}$, is inclined to the vertical at an angle ϕ. The strain tensor for this type of deformation is represented as

$$e_{ij} = e m_i m_j \tag{4.6}$$

where the axis of symmetry for this uniaxial strain is given by

$$\mathbf{m} = (\sin\phi,\ 0,\ \cos\phi). \tag{4.7}$$

The displacement of the centre of each sphere is consistent with the applied uniform strain (1.86), that is

$$u_i^{(n)} = e m_i m_j X_j^{(n)}. \tag{4.8}$$

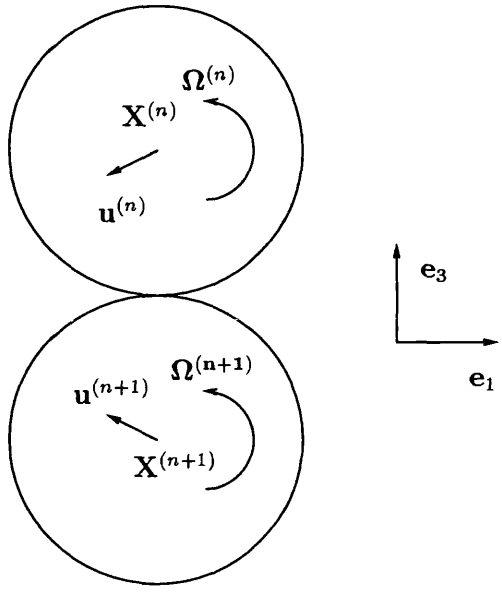

Figure 4-4: *The vertical contact problem*

The displacement of sphere n relative to sphere m may now be written, using equation (4.1), in terms of the unit vector $\mathbf{I}^{(nm)}$ as

$$\begin{aligned} u_i^{(m)} - u_i^{(n)} &= em_i m_j (X_j^{(m)} - X_j^{(n)}) \\ &= -2eRm_i m_j I_j^{(nm)}. \end{aligned} \tag{4.9}$$

When the confining strain is applied, spheres initially in point contact will be pressed together to form a contact area. As described in chapter 3, the spheres will either stick together during this deformation or sliding will occur over the entire contact area, depending on the angle of compression. Four contact problems may be identified from figure 4-2 when considering the central sphere n. Because of the symmetries previously mentioned, it is sufficient to consider only the lower and left contacts. We will refer to the problem of sphere n in contact with the left sphere n' as the horizontal problem and similarly, the contact between sphere n and the lower sphere $n+1$ will be referred to as the vertical problem. For each of these problems, we must also consider the two cases of the contact area sticking or sliding.

4.2.1 The Vertical Problem

Here we consider the problem of the n-th sphere in contact with the lower or $(n+1)$-th

sphere as shown in figure 4-4. The unit vector in the direction of the line joining the two centres is given by

$$\mathbf{I}^{(n,n+1)} = \mathbf{e}_3 \tag{4.10}$$

and the rotation of each sphere is of the form

$$\mathbf{\Omega}^{(n)} = \Omega^{(n)}\mathbf{e}_2. \tag{4.11}$$

The relative displacement of the two spheres becomes

$$u_i^{(n+1)} - u_i^{(n)} = -2Rem_i m_3 \tag{4.12}$$

and the compression in the normal direction is

$$w_0^{(n,n+1)} = -eRm_3^2. \tag{4.13}$$

We now derive the expressions for the force vector between the spheres in the two cases of sliding or sticking on the contact area.

Stick on Contact Area: $u_0/w_0 \leq (2B+C)f/2B$

Recall from section (3.5) that, during a deformation in which the contact areas stick together, the total normal and tangential forces acting on the lower contact are, respectively,

$$\overline{N}_B = \frac{4(Rw_0^3)^{1/2}}{3\pi B} \quad \text{and} \quad \overline{P}_B = \frac{8u_0(Rw_0)^{1/2}}{3\pi(2B+C)} \tag{4.14}$$

where B and C are elastic moduli given in terms of the Lamé moduli by equation (1.7), and $(u_0, 0, w_0)$ is the displacement of the sphere centres relative to the point of first contact O. For ease of notation we have written w_0 and u_0 instead of $w_0^{(n,n+1)}$ and $u_0^{(n,n+1)}$ but it is important to note that these compressions depend on which contact problem we are considering. The force vector is derived by combining the above forces and the displacement of the contact area, as seen in section (1.3.1), to obtain

$$\mathbf{F}^{(n,n+1)} = \frac{4(Rw_0^3)^{1/2}}{3\pi B}\mathbf{I}^{(n,n+1)} + \frac{8(Rw_0)^{1/2}}{3\pi(2B+C)}\left\{\frac{1}{2}(\mathbf{u}^{(n+1)} - \mathbf{u}^{(n)})\right.$$

$$+\frac{1}{2}(\boldsymbol{\Omega}^{(n+1)}+\boldsymbol{\Omega}^{(n)})\wedge R\mathbf{I}^{(n,n+1)}-w_0\mathbf{I}^{(n,n+1)}\Big\}. \qquad (4.15)$$

Substituting equations (4.10), (4.11), (4.12) and (4.13) into the above, we obtain the i-th component of the force vector as

$$F_i^{(n,n+1)} = \frac{4R^2m_3^3}{3\pi B}(-e)^{3/2}\delta_{i3}+\frac{8R^2m_3}{3\pi(2B+C)}(-e)^{1/2}\left\{-em_im_3+\Omega\delta_{i1}+em_3^2\delta_{i3}\right\}. \qquad (4.16)$$

Sliding on Contact Area: $u_0/w_0 \geq (2B+C)f/2B$

In chapter 3, we saw that if the calculated tangential force exceeds the coefficient of friction times the normal force, then sliding occurs over the entire contact area and the tangential component of the force (4.14) no longer holds. Instead, the tangential force is equal to the coefficient of friction times the normal force, in this case $\overline{P}_B = f\overline{N}_B$. By considering the forces (4.14) we see that $P_B \geq fN_B$ whenever

$$\frac{u_0^{(n,n+1)}}{w_0^{(n,n+1)}} \geq \left(\frac{2B+C}{2B}\right)f \qquad (4.17)$$

and when this is satisfied, the normal and tangential forces are, respectively,

$$\overline{N}_B = \frac{4(Rw_0^3)^{1/2}}{3\pi B} \quad \text{and} \quad \overline{P}_B = f\overline{N}_B = \frac{4f(Rw_0^3)^{1/2}}{3\pi B}. \qquad (4.18)$$

In the same way as before we construct the force vector between the two sliding spheres as

$$\mathbf{F}^{(n,n+1)} = \frac{4(Rw_0^3)^{1/2}}{3\pi B}\left\{\mathbf{I}^{(n,n+1)} + f\left[\frac{\frac{1}{2}(\mathbf{u}^{(n+1)}-\mathbf{u}^{(n)})+\frac{1}{2}(\boldsymbol{\Omega}^{(n+1)}+\boldsymbol{\Omega}^{(n)})\wedge\mathbf{I}^{(n,n+1)}-w_0\mathbf{I}^{(n,n+1)}}{\left|\frac{1}{2}(\mathbf{u}^{(n+1)}-\mathbf{u}^{(n)})+\frac{1}{2}(\boldsymbol{\Omega}^{(n+1)}+\boldsymbol{\Omega}^{(n)})\wedge\mathbf{I}^{(n,n+1)}-w_0\mathbf{I}^{(n,n+1)}\right|}\right]\right\}. \qquad (4.19)$$

Substituting equations (4.10), (4.11), (4.12) and (4.13) into the above, we obtain

$$F_i^{(n,n+1)} = \frac{4R^2m_3^3}{3\pi B}(-e)^{3/2}\left\{\delta_{i3}+f\left[\frac{-em_im_3+\Omega\delta_{i1}+em_3^2\delta_{i3}}{\Omega-em_1m_3}\right]\right\}. \qquad (4.20)$$

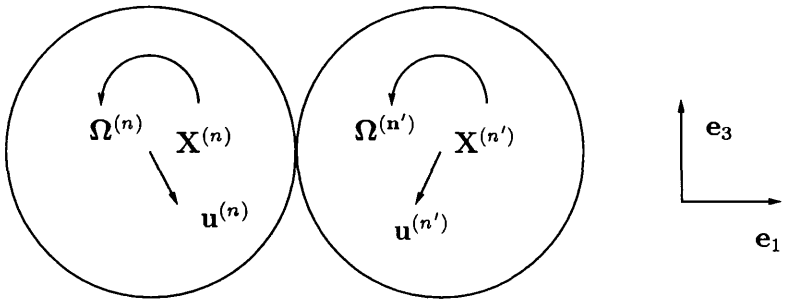

Figure 4-5: *The horizontal contact problem*

4.2.2 The Horizontal Problem

The next problem to be considered is the contact between the n-th sphere and the left or n'-th sphere as shown in figure 4-5. Again we have rotations of the form

$$\mathbf{\Omega}^{(n)} = \Omega^{(n)}\mathbf{e}_2 \tag{4.21}$$

and the vector joining the two centres is

$$\mathbf{I}^{(nn')} = \mathbf{e}_1. \tag{4.22}$$

The relative displacement of the two centres is

$$u_i^{(n')} - u_i^{(n)} = -2Rem_i m_1 \tag{4.23}$$

and the normal compression is given by

$$w_0^{(nn')} = -eRm_1^2. \tag{4.24}$$

Stick on Contact Area: $u_0/w_0 \leq (2B+C)f/2B$

The total normal and tangential forces on the left-most contact area are, respectively,

$$\overline{N}_L = \frac{4(Rw_0^3)^{1/2}}{3\pi B} \quad \text{and} \quad \overline{P}_L = \frac{8u_0(Rw_0)^{1/2}}{3\pi(2B+C)} \tag{4.25}$$

which are the same as the forces (4.14) except that u_0 and w_0 now refer to $u_0^{(nn')}$ and $w_0^{(nn')}$ respectively. Similarly we calculate the force vector between the two spheres as

$$\mathbf{F}^{(nn')} = \frac{4(Rw_0^3)^{1/2}}{3\pi B}\mathbf{I}^{(nn')} + \frac{8(Rw_0)^{1/2}}{3\pi(2B+C)}\left\{\frac{1}{2}(\mathbf{u}^{(n')} - \mathbf{u}^{(n)}) + \frac{1}{2}(\mathbf{\Omega}^{(n')} + \mathbf{\Omega}^{(n)}) \wedge R\mathbf{I}^{(nn')} - w_0\mathbf{I}^{(nn')}\right\} \tag{4.26}$$

which, in index notation, may be written

$$F_i^{(nn')} = \frac{4R^2m_1^3}{3\pi B}(-e)^{3/2}\delta_{i1} + \frac{8R^2m_1}{3\pi(2B+C)}(-e)^{1/2}\left\{-em_im_1 - \Omega\delta_{i3} + em_1^2\delta_{i1}\right\}. \tag{4.27}$$

Sliding on Contact Area: $u_0/w_0 \geq (2B+C)f/2B$

Sliding will occur on the left contact when

$$\frac{u_0^{(nn')}}{w_0^{(nn')}} \geq \left(\frac{2B+C}{2B}\right)f \tag{4.28}$$

and the total normal and tangential forces are, respectively,

$$\overline{N}_L = \frac{4(Ru_0^3)^{1/2}}{3\pi B} \quad \text{and} \quad \overline{P}_L = f\overline{N}_L = \frac{4f(Ru_0^3)^{1/2}}{3\pi B}. \tag{4.29}$$

The force vector on the left contact is

$$\mathbf{F}^{(nn')} = \frac{4(Rw_0^3)^{1/2}}{3\pi B}\left\{\mathbf{I}^{(nn')} + f\left[\frac{\frac{1}{2}(\mathbf{u}^{(n')} - \mathbf{u}^{(n)}) + \frac{1}{2}(\mathbf{\Omega}^{(n')} + \mathbf{\Omega}^{(n)}) \wedge \mathbf{I}^{(nn')} - w_0\mathbf{I}^{(nn')}}{\left|\frac{1}{2}(\mathbf{u}^{(n')} - \mathbf{u}^{(n)}) + \frac{1}{2}(\mathbf{\Omega}^{(n')} + \mathbf{\Omega}^{(n)}) \wedge \mathbf{I}^{(nn')} - w_0\mathbf{I}^{(nn')}\right|}\right]\right\} \tag{4.30}$$

which may be written in index notation as

$$F_i^{(nn')} = \frac{4R^2m_1^3}{3\pi B}(-e)^{3/2}\left\{\delta_{i1} + f\left[\frac{-em_im_1 - \Omega\delta_{i3} + em_1^2\delta_{i1}}{\Omega + em_1m_3}\right]\right\}. \tag{4.31}$$

4.2.3 Sphere Equilibrium

Now that we have derived the required force vectors for all necessary sphere configurations and cases of stick or sliding, we require that they are of a form which guarantees

equilibrium of individual spheres. To achieve this, the following conditions of linear and rotational equilibrium must be satisfied

$$\mathbf{F}^{(n,n+1)} + \mathbf{F}^{(n,n-1)} + \mathbf{F}^{(nn')} + \mathbf{F}^{(nn'')} = \mathbf{0} \tag{4.32}$$

$$\mathbf{F}^{(n,n+1)} \wedge \mathbf{I}^{(n,n+1)} + \mathbf{F}^{(nn')} \wedge \mathbf{I}^{(nn')} = \mathbf{0}. \tag{4.33}$$

Condition (4.32) is clearly satisfied since we have already deduced that

$$\mathbf{F}^{(n,n+1)} = -\mathbf{F}^{(n,n-1)} \quad \text{and} \quad \mathbf{F}^{(nn')} = -\mathbf{F}^{(nn'')}. \tag{4.34}$$

In writing the condition (4.33) we have also made use of these relationships in the form

$$\mathbf{F}^{(n,n+1)} \wedge \mathbf{I}^{(n,n+1)} = \mathbf{F}^{(n+1,n)} \wedge \mathbf{I}^{(n+1,n)} \quad \text{and} \quad \mathbf{F}^{(nn')} \wedge \mathbf{I}^{(nn')} = \mathbf{F}^{(n'n)} \wedge \mathbf{I}^{(n'n)}. \tag{4.35}$$

For rotational equilibrium, we must choose an appropriate value for Ω such that condition (4.33) is satisfied. Obviously the forces will depend on whether stick or sliding occurs on the contacts and this in turn will affect the value of Ω. Therefore, we must determine Ω in each of the following three cases.

Stick on Bottom, Stick on Sides

At first we will assume that stick occurs on all contacts and subsequently derive conditions for this assumption to break down. The moments of each force about the centre of sphere n are

$$\left[\mathbf{F}^{(n,n+1)} \wedge R\mathbf{I}^{(n,n+1)}\right]_i = \frac{8R^3 m_3}{3\pi(2B+C)}(-e)^{1/2}\{e m_1 m_3 \delta_{i2} - \Omega\delta_{i2}\} \tag{4.36}$$

on the bottom, and

$$\left[\mathbf{F}^{(nn')} \wedge R\mathbf{I}^{(nn')}\right]_i = \frac{8R^3 m_1}{3\pi(2B+C)}(-e)^{1/2}\{-e m_1 m_3 \delta_{i2} - \Omega\delta_{i2}\} \tag{4.37}$$

on the side. Substituting these moments into the condition (4.33) and rearranging, we

find that the required value of Ω is

$$\Omega = \left(\frac{m_3 - m_1}{m_3 + m_1}\right) m_1 m_3 e. \tag{4.38}$$

Substituting back into the force vectors (4.16) and (4.20), we find that the components of the force vector are

$$\begin{aligned} F_1^{(n,n+1)} = F_3^{(nn')} &= \frac{16R^2 m_1^2 m_3^2 (-e)^{3/2}}{3\pi(2B+C)(m_1+m_3)} = \overline{P}_L = \overline{P}_T \\ F_3^{(n,n+1)} &= \frac{4R^2 m_3^2 (-e)^{3/2}}{3\pi B} = \overline{N}_T \\ F_1^{(nn')} &= \frac{4R^2 m_1^3 (-e)^{3/2}}{3\pi B} = \overline{N}_L. \end{aligned} \tag{4.39}$$

We now examine how this state in which all the contacts stick may give rise to contact sliding. The condition for the side contact to slide is

$$\left|\frac{\overline{P}_L}{\overline{N}_L}\right| = \left|\frac{F_3^{(nn')}}{F_1^{(nn')}}\right| \geq f \tag{4.40}$$

or in terms of the components of **m** the condition becomes

$$\frac{2m_3^2}{m_1(m_1+m_3)} \geq \left(\frac{2B+C}{2B}\right) f \tag{4.41}$$

and when sliding does occur, the tangential force is

$$\overline{P}_B = f\overline{N}_B. \tag{4.42}$$

Similarly, the condition for the bottom contact to slide is

$$\left|\frac{\overline{P}_B}{\overline{N}_B}\right| = \left|\frac{F_3^{(n,n+1)}}{F_1^{(n,n+1)}}\right| \geq f \tag{4.43}$$

which is equivalent to

$$\frac{2m_1^2}{m_3(m_1+m_3)} \geq \left(\frac{2B+C}{2B}\right) f \tag{4.44}$$

with tangential force

$$\overline{P}_L = f\overline{N}_L \tag{4.45}$$

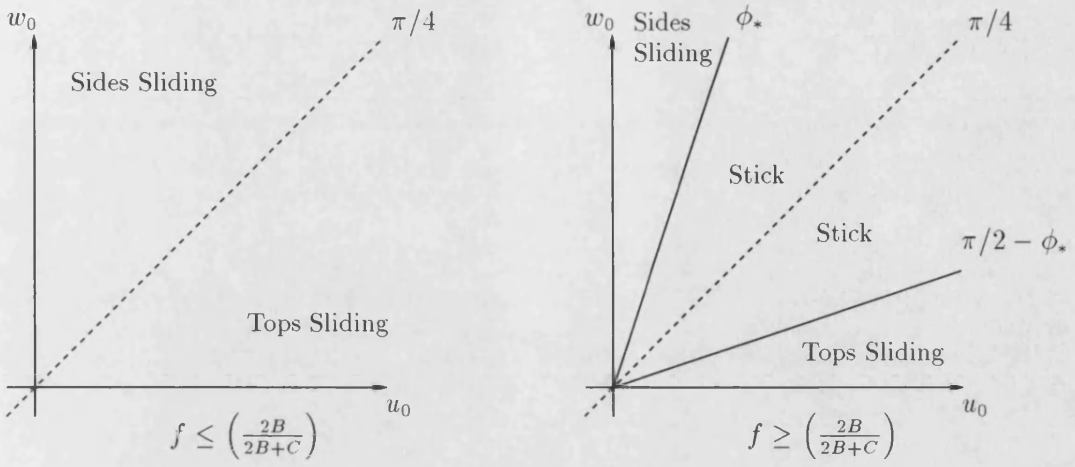

Figure 4-6: *Possible stick/slide combinations between two spheres*

when sliding occurs.

Suppose now that $m_3 > m_1$. Then $|\overline{P}_L/\overline{N}_L| > |\overline{P}_B/\overline{N}_B|$ and therefore the left contact must slide before the bottom contact giving $\overline{P}_L = f\overline{N}_L$. Then noting that $\overline{P}_B = \overline{P}_L$, we write

$$\frac{\overline{P}_B}{\overline{N}_B} = \frac{\overline{P}_L}{\overline{N}_L} \times \frac{\overline{N}_L}{\overline{N}_B} = f\frac{m_1^3}{m_3^3} < f \tag{4.46}$$

showing that sliding will not occur on the upper or lower contacts. A similar argument when $m_1 > m_3$ shows that sliding will never occur on the bottom and side contacts simultaneously.

Consider now the conditions for sliding when $m_3 > m_1$, that is $\tan\phi < 1$ or $\phi < \pi/4$. Then sliding will occur on the side contacts if

$$\frac{2m_3^2}{m_1(m_1+m_3)} \geq \left(\frac{2B+C}{2B}\right) = \tan\phi_c \tag{4.47}$$

that is

$$\frac{2}{\tan\phi\,(1+\tan\phi)} \geq \tan\phi_c. \tag{4.48}$$

As the angle ϕ varies from 0 to $\pi/4$, the value of $\tan\phi$ varies from 0 to 1 and so the left-hand side of the above expression varies from infinity to 1 monotonically. Therefore, if $\phi_c > \pi/4$ there exists a unique value of $\phi = \phi_*$ for which

$$\frac{2}{\tan\phi_* \ (1+\tan\phi_*)} = \tan\phi_c \tag{4.49}$$

and sliding will occur if $\phi < \phi_*$.

When $\phi_c < \pi/4$, then sliding occurs for all values of ϕ as shown in figure 4-6 by the left-hand diagram.

The corresponding condition when $m_1 > m_3$ is

$$\frac{2\tan^2\phi}{1+\tan\phi} \geq \tan\phi_c \tag{4.50}$$

or by defining $\psi = \pi/2 - \phi$ this becomes

$$\frac{2}{\tan\psi \ (1+\tan\psi)} \geq \tan\phi_c \tag{4.51}$$

and a similar argument shows that sliding occurs if $\psi < \phi_*$, that is $\phi > \pi/2 - \phi_*$, and if $\phi_c < \pi/4$ sliding occurs for all values of ϕ.

Stick on Bottom, Sliding on Sides: $2m_3^2/[m_1(m_1+m_3)] \geq (2B+C)f/2B$

When sliding occurs on the left contact and stick on the lower contact, the moment of the sticking force is given by equation (4.36) and the moment of the sliding force (4.31) may be calculated as

$$\left[\mathbf{F}^{(nn')} \wedge R\mathbf{I}^{(nn')}\right]_i = -\frac{4R^3m_1^3}{3\pi B}(-e)^{3/2}f\delta_{i2}. \tag{4.52}$$

Substituting into the rotational equilibrium condition (4.33) yields a value for the rotation of

$$\Omega = em_1m_3 + e\frac{m_1^3}{m_3}\left(\frac{2B+C}{2B}\right)f. \tag{4.53}$$

Substituting back into the force vectors (4.16) and (4.31), we find that

$$F_1^{(n,n+1)} = F_3^{(nn')} = -\frac{4R^3m_1^3(-e)^{3/2}}{3\pi B}f = \overline{P}_L = \overline{P}_B$$

$$\begin{aligned} F_3^{(n,n+1)} &= \frac{4R^3 m_3^3(-e)^{3/2}}{3\pi B} = \overline{N}_B \\ F_1^{(nn')} &= \frac{4R^2 m_1^3(-e)^{3/2}}{3\pi B} = \overline{N}_L. \end{aligned} \tag{4.54}$$

Sliding on Bottom, Stick on Sides: $2m_1^2/[m_3(m_1+m_3)] \geq (2B+C)f/2B$

When the bottom and top contacts slide and the side contacts stick, the required forces are equations (4.20) and (4.27). The same calculations as carried out in the previous section yield a value for Ω of

$$\Omega = -em_1 m_3 + e\frac{m_3^3}{m_1}\left(\frac{2B+C}{2B}\right) f. \tag{4.55}$$

Substituting back into the force vectors (4.16) and (4.31), we find that

$$\begin{aligned} F_1^{(n,n+1)} = F_3^{(nn')} &= \frac{4R^3 m_3^3(-e)^{3/2}}{3\pi B} f = \overline{P}_L = \overline{P}_B \\ F_3^{(n,n+1)} &= \frac{4R^3 m_3^3(-e)^{3/2}}{3\pi B} = \overline{N}_B \\ F_1^{(nn')} &= \frac{4R^2 m_1^3(-e)^{3/2}}{3\pi B} = \overline{N}_L. \end{aligned} \tag{4.56}$$

4.2.4 The Initial Stress

In section (1.3.1), we derived the average stress within a sphere packing as

$$\langle \sigma_{ij} \rangle = -\frac{2R}{V} \sum_{\text{contacts}} I_i^{(nm)} F_j^{(nm)} \tag{4.57}$$

where V is the volume of the medium and the summation is taken over all contacts within V. This formula is equally valid for a cubic packing but the regular geometry makes the form of the resulting stresses much simpler. The volume of the medium is $V = NV_n$ where N is the total number of spheres in the packing and $V_n = 8R^3$ is the volume of an individual cube of side $2R$ exactly enclosing a sphere. Since each contact is identical to the corresponding contact on any other sphere, the sum in (4.57) may be written as N times the contribution of that contact from one sphere, that is

$$\begin{aligned} \langle \sigma_{ij} \rangle = -\frac{2R}{NV_n} \times N \Big\{ & I_i^{(n,n+1)} F_j^{(n,n+1)} + I_i^{(n,n-1)} F_j^{(n,n-1)} \\ & + I_i^{(nn')} F_j^{(nn')} + I_i^{(nn'')} F_j^{(nn'')} \Big\}. \end{aligned} \tag{4.58}$$

Cancelling the N's and making use of the relationships

$$\begin{aligned} \mathbf{F}^{(n,n+1)} &= -\mathbf{F}^{(n,n-1)} \quad \text{and} \quad \mathbf{F}^{(nn')} = -\mathbf{F}^{(nn'')}, \\ \mathbf{I}^{(n,n+1)} &= -\mathbf{I}^{(n,n-1)} \quad \text{and} \quad \mathbf{I}^{(nn')} = -\mathbf{I}^{(nn'')} \end{aligned} \tag{4.59}$$

we obtain

$$\langle \sigma_{ij} \rangle = -\frac{4R}{V_n} \left\{ I_i^{(n,n+1)} F_j^{(n,n+1)} + I_i^{(nn')} F_j^{(nn')} \right\}. \tag{4.60}$$

There are two stick or sliding combinations to consider, as below.

Stick on Bottom, Stick on Sides

When all the contacts stick, the relevant forces are (4.16) and (4.27). Substituting into equation (4.57) gives the average stress components as

$$\begin{aligned} \langle \sigma_{11} \rangle &= -\frac{2m_1^3(-e)^{3/2}}{3\pi B} \\ \langle \sigma_{22} \rangle &= 0 \\ \langle \sigma_{33} \rangle &= -\frac{2m_3^3(-e)^{3/2}}{3\pi B} \\ \langle \sigma_{12} \rangle = \langle \sigma_{21} \rangle = \langle \sigma_{23} \rangle = \langle \sigma_{32} \rangle &= 0 \\ \langle \sigma_{13} \rangle = \langle \sigma_{31} \rangle &= -\frac{8m_1^2 m_3^2(-e)^{3/2}}{3\pi(2B+C)(m_1+m_3)}. \end{aligned} \tag{4.61}$$

The component of the force per unit area acting in the direction of $\mathbf{m}$ on a plane perpendicular to $\mathbf{m}$ may be calculated in terms of the average stress as

$$F = \langle \sigma_{ij} \rangle \, m_i m_j \tag{4.62}$$

which evaluates to

$$F = -\frac{2(-e)^{3/2}}{3\pi B} \left[(2B+C)m_1^5 + 8B\frac{m_1^3 m_3^3}{m_1+m_3} + (2B+C)m_3^5 \right]. \tag{4.63}$$

This force, shown in figure 4-2, is the applied confining force. The lateral force acting perpendicular to $\mathbf{m}$ may be interpreted as the restraining force.

Sliding on Bottom, Stick on Sides: $2m_1^2/[m_3(m_1+m_3)] \geq (2B+C)f/2B$

Similarly, the forces (4.20) and (4.31) substituted into (4.57) yields stress components

$$\begin{aligned} \langle\sigma_{11}\rangle &= -\frac{2m_1^3(-e)^{3/2}}{3\pi B} \\ \langle\sigma_{22}\rangle &= 0 \\ \langle\sigma_{33}\rangle &= -\frac{2m_3^3(-e)^{3/2}}{3\pi B} \\ \langle\sigma_{12}\rangle = \langle\sigma_{21}\rangle = \langle\sigma_{23}\rangle = \langle\sigma_{32}\rangle &= 0 \\ \langle\sigma_{13}\rangle = \langle\sigma_{31}\rangle &= -\frac{2m_3^3(-e)^{3/2}f}{3\pi B}. \end{aligned} \tag{4.64}$$

The force (4.62) is given by

$$F = -\frac{2(-e)^{3/2}}{3\pi B}\left[m_1^5 + 2fm_1m_3^4 + m_3^5\right]. \tag{4.65}$$

Stick on Bottom, Sliding on Sides: $2m_3^2/[m_1(m_1+m_3)] \geq (2B+C)f/2B$

When sliding occurs on the side contacts, the average stress is calculated as

$$\begin{aligned} \langle\sigma_{11}\rangle &= -\frac{2m_1^3(-e)^{3/2}}{3\pi B} \\ \langle\sigma_{22}\rangle &= 0 \\ \langle\sigma_{33}\rangle &= -\frac{2m_3^3(-e)^{3/2}}{3\pi B} \\ \langle\sigma_{12}\rangle = \langle\sigma_{21}\rangle = \langle\sigma_{23}\rangle = \langle\sigma_{32}\rangle &= 0 \\ \langle\sigma_{13}\rangle = \langle\sigma_{31}\rangle &= \frac{2m_3^3(-e)^{3/2}f}{3\pi B} \end{aligned} \tag{4.66}$$

with confining force

$$F = -\frac{2(-e)^{3/2}}{3\pi B}\left[m_3^5 - 2fm_3m_1^4 + m_1^5\right]. \tag{4.67}$$

4.3 The Incremental Problem

The incremental problem is imposed on the initial state and takes the form of an extra displacement $\delta\mathbf{u}^{(n)}$ of the centre of each sphere. As was the case in the initial state, for simplicity all displacements are taken to be in the xz-plane and the incremental rotation

is of the form

$$\delta\boldsymbol{\omega}^{(n)} = \delta\omega^{(n)}\mathbf{e}_2. \tag{4.68}$$

The incremental displacement and rotation are assumed to depend on time t purely through the factor $e^{-i\omega t}$. Because of this time-dependence, the symmetry of the initial state is lost. However, because we will be seeking only waves travelling vertically down the packing, we may make the simplification that each sphere in the same row suffers the same displacement and undergoes the same rotation; that is

$$\delta\mathbf{u}^{(n)} = \delta\mathbf{u}^{(n')} \quad \text{and} \quad \delta\boldsymbol{\omega}^{(n)} = \delta\boldsymbol{\omega}^{(n')}. \tag{4.69}$$

As was shown in chapter 3, the total incremental forces are

$$\overline{\delta N} = \frac{2(Rw_0)^{1/2}}{\pi B}\delta w_0 \quad \text{and} \quad \overline{\delta P} = \frac{4(Rw_0)^{1/2}}{\pi(2B+C)}\delta u_0 \tag{4.70}$$

where $(\delta u_0, 0, \delta w_0)$ is the relative displacement of the centres of the two spheres. The above incremental forces are to first order and are valid for infinitesimal values of δu_0 and δw_0. As considered in section (3.6), partial slip and counterslip occurs in the incremental problem but friction, being a higher order effect, does not appear in the incremental forces. Hence we do not need to distinguish between the cases of slip or stick in the following two problems.

4.3.1 The Incremental Vertical Problem

The incremental force vector may be derived in the same fashion as the force vector in the initial state. Combining the above incremental forces with the contact area displacements yields the force vector on the lower contact as

$$\begin{aligned}\delta\mathbf{F}^{(n,n+1)} = \frac{(Rw_0)^{1/2}}{\pi B(2B+C)}\Big\{&2B\left[\delta\mathbf{u}^{(n+1)} - \delta\mathbf{u}^{(n)} + (\delta\boldsymbol{\omega}^{(n+1)} + \delta\boldsymbol{\omega}^{(n)}) \wedge R\mathbf{I}^{(n,n+1)}\right] \\ &+ C\left[(\delta\mathbf{u}^{(n+1)} - \delta\mathbf{u}^{(n)}) \cdot \mathbf{I}^{(n,n+1)}\right]\mathbf{I}^{(n,n+1)}\Big\}.\end{aligned} \tag{4.71}$$

Substituting the unit vector for the vertical problem (4.10) and the initial compression (4.13) into the above, we obtain

$$\delta F_i^{(n,n+1)} = \frac{Rm_3(-e)^{1/2}}{\pi B(2B+C)}\left\{2B\left[\delta u_i^{(n+1)} - \delta u_i^{(n)} + R(\delta\omega^{(n+1)} + \delta\omega^{(n)})\delta_{i1}\right] + C\left[\delta u_3^{(n+1)} - \delta u_3^{(n)}\right]\delta_{i3}\right\}. \quad (4.72)$$

Because of the dynamic nature of the incremental problem $\delta\omega^{(n)}$ varies with position within the packing. Therefore, the incremental force vector on the upper contact is

$$\delta\mathbf{F}^{(n,n-1)} = \frac{(Rw_0)^{1/2}}{\pi B(2B+C)}\left\{2B\left[\delta\mathbf{u}^{(n-1)} - \delta\mathbf{u}^{(n)} + (\delta\boldsymbol{\omega}^{(n-1)} + \delta\boldsymbol{\omega}^{(n)}) \wedge R\mathbf{I}^{(n,n-1)}\right] + C\left[(\delta\mathbf{u}^{(n-1)} - \delta\mathbf{u}^{(n)}) \cdot \mathbf{I}^{(n,n-1)}\right]\mathbf{I}^{(n,n-1)}\right\}. \quad (4.73)$$

In index notation, with the appropriate unit vector and compression, this becomes

$$\delta F_i^{(n,n-1)} = \frac{Rm_3(-e)^{1/2}}{\pi B(2B+C)}\left\{2B\left[\delta u_i^{(n-1)} - \delta u_i^{(n)} - R(\delta\omega^{(n-1)} + \delta\omega^{(n)})\delta_{i1}\right] + C\left[\delta u_3^{(n-1)} - \delta u_3^{(n)}\right]\delta_{i3}\right\}. \quad (4.74)$$

4.3.2 The Incremental Horizontal Problem

The incremental force vector on the left hand contact is

$$\delta\mathbf{F}^{(nn')} = \frac{(Rw_0)^{1/2}}{\pi B(2B+C)}\left\{2B\left[\delta\mathbf{u}^{(n')} - \delta\mathbf{u}^{(n)} + (\delta\boldsymbol{\omega}^{(n')} + \delta\boldsymbol{\omega}^{(n)}) \wedge R\mathbf{I}^{(nn')}\right] + C\left[(\delta\mathbf{u}^{(n')} - \delta\mathbf{u}^{(n)}) \cdot \mathbf{I}^{(nn')}\right]\mathbf{I}^{(nn')}\right\}. \quad (4.75)$$

The unit vector $\mathbf{I}^{(nn')}$ is given by (4.22), the compression w_0 is given by (4.24) and the above force becomes

$$\delta F_i^{(nn')} = -\frac{4R^2m_1(-e)^{1/2}}{\pi(2B+C)}\delta\omega^{(n)}\delta_{i3} \quad (4.76)$$

and similarly, the force on the right-hand contact is

$$\delta F_i^{(nn'')} = \frac{4R^2m_1(-e)^{1/2}}{\pi(2B+C)}\delta\omega^{(n)}\delta_{i3}. \quad (4.77)$$

4.3.3 Linear Motion

Having now found all the required forces acting on the central sphere, we now consider the equations of motion satisfied by the time dependent $\delta\mathbf{u}^{(n)}$ and $\delta\boldsymbol{\omega}^{(n)}$. Newton's second law requires that

$$\delta\mathbf{F}^{(n,n+1)} + \delta\mathbf{F}^{(n,n-1)} + \delta\mathbf{F}^{(nn')} + \delta\mathbf{F}^{(nn'')} = \frac{4}{3}\pi R^3\rho\delta\ddot{\mathbf{u}}^{(n)} \tag{4.78}$$

where ρ is the density of the sphere material. The side forces $\delta\mathbf{F}^{(nn')}$ and $\delta\mathbf{F}^{(nn'')}$ cancel since equations (4.76) and (4.77) show that one is minus the other.

The displacements $\delta\mathbf{u}^{(n)}$ and the rotations $\delta\boldsymbol{\omega}^{(n)}$ depend on time t purely through the factor $e^{-i\omega t}$ where ω is a wave frequency. Thus second derivatives of these quantities are of the forms

$$\delta\ddot{\mathbf{u}}^{(n)} = -\omega^2\delta\mathbf{u}^{(n)} \quad \text{and} \quad \delta\ddot{\boldsymbol{\omega}}^{(n)} = -\omega^2\delta\boldsymbol{\omega}^{(n)}. \tag{4.79}$$

Then the equation resulting from (4.78) is

$$\frac{R(-e)^{1/2}m_3}{\pi B(2B+C)}\left\{2B\left[\delta u_i^{(n+1)} - 2\delta u_i^{(n)} + \delta u_i^{(n+1)} + R(\delta\omega^{(n+1)} - \delta\omega^{(n-1)})\delta_{i1}\right]\right.$$
$$\left. + C\left[\delta u_3^{(n+1)} - 2\delta u_3^{(n)} + \delta u_3^{(n-1)}\right]\delta_{i3}\right\} = -\frac{4}{3}\pi R^3\rho\omega^2\delta u_i^{(n)}. \tag{4.80}$$

Taking $i = 1$ we obtain

$$3(-e)^{1/2}m_3(\delta u_1^{(n+1)} + \delta u_1^{(n-1)}) + 2\left[\pi^2(2B+C)R^2\rho\omega^2 - 3(-e)^{1/2}m_3\right]\delta u_1^{(n)}$$
$$+ 3R(-e)^{1/2}m_3(\delta\omega^{(n+1)} - \delta\omega^{(n-1)}) = 0. \tag{4.81}$$

Taking $i = 2$ yields no useful information and taking $i = 3$ results in the equation

$$3(-e)^{1/2}m_3\delta u_3^{(n+1)} + 2\left[2\pi^2BR^2\rho\omega^2 - 3m_3(-e)^{1/2}\right]\delta u_3^{(n)}$$
$$+ 3(-e)^{1/2}m_3\delta u_3^{(n-1)} = 0. \tag{4.82}$$

Equations (4.81) and (4.82) are difference equations involving unknowns δu_1, δu_3 and $\delta\omega$.

Note that equation (4.82) for δu_3 may be solved alone without the need for further equations. This is due to the decoupling of the problem into normal and tangential systems. To obtain the extra tangential equation necessary to solve (4.81) for δu_1 and $\delta\omega$, we now consider the equations of rotational motion.

4.3.4 Rotational Motion

The angular acceleration satisfies

$$\delta\mathbf{F}^{(n,n+1)} \wedge R\mathbf{I}^{(n,n+1)} + \delta\mathbf{F}^{(n,n-1)} \wedge R\mathbf{I}^{(n,n-1)} + \delta\mathbf{F}^{(nn')} \wedge R\mathbf{I}^{(nn')} + \delta\mathbf{F}^{(nn'')} \wedge R\mathbf{I}^{(nn'')} = I\delta\ddot{\omega} \tag{4.83}$$

where $I = 8\pi\rho R^5/15$ is the moment of inertia of a solid sphere about its centre.

The moments of the incremental forces are, on the upper and lower contacts,

$$\begin{aligned}\left[\delta\mathbf{F}^{(n,n+1)} \wedge R\mathbf{I}^{(n,n+1)}\right]_i &= \frac{2R^2m_3(-e)^{1/2}}{\pi(2B+C)}\left\{\epsilon_{ij3}(\delta u_j^{(n+1)} - \delta u_j^{(n)}) - R\delta_{i2}(\delta\omega^{(n+1)} + \delta\omega^{(n)})\right\}\\ \left[\delta\mathbf{F}^{(n,n-1)} \wedge R\mathbf{I}^{(n,n-1)}\right]_i &= -\frac{2R^2m_3(-e)^{1/2}}{\pi(2B+C)}\left\{\epsilon_{ij3}(\delta u_j^{(n-1)} - \delta u_j^{(n)}) + R\delta_{i2}(\delta\omega^{(n-1)} + \delta\omega^{(n)})\right\}\end{aligned} \tag{4.84}$$

and on the side contacts

$$\left[\delta\mathbf{F}^{(nn')} \wedge R\mathbf{I}^{(nn')}\right]_i = \left[\delta\mathbf{F}^{(nn'')} \wedge R\mathbf{I}^{(nn'')}\right]_i = -\frac{4R^3m_1(-e)^{1/2}}{\pi(2B+C)}\delta\omega^{(n)}\delta_{i2}. \tag{4.85}$$

Substituting into equation (4.83) yields the required difference equation

$$\begin{aligned}15(-e)^{1/2}m_3\left\{\epsilon_{ij3}(\delta u_j^{(n+1)} - \delta u_j^{(n-1)}) - R(\delta\omega^{(n+1)} + 2\delta\omega^{(n)} + \delta\omega^{(n-1)})\delta_{i2}\right\}\\ -60R(-e)^{1/2}m_1\delta\omega^{(n)}\delta_{i2} = -4\pi^2(2B+C)R^3\rho\omega^2\delta\omega^{(n)}\delta_{i2}.\end{aligned} \tag{4.86}$$

4.3.5 The Wave Solution

We now have a complete system of difference equations: (4.81), (4.82) and (4.86). To solve them, we make the following trial solutions

$$\delta\omega^{(n)} = \delta\omega\, x^n e^{-i\omega t} \tag{4.87}$$

$$\delta u_1^{(n)} = \delta u_1\, x^n e^{-i\omega t} \tag{4.88}$$

$$\delta u_3^{(n)} = \delta u_3\, x^n e^{-i\omega t} \tag{4.89}$$

where x is a complex number of the form

$$x = e^{i\theta} = \cos\theta + i\sin\theta. \tag{4.90}$$

Substituting the trial solutions into the difference equations results in the following system of equations

$$\begin{aligned}
-15Rm_3(-e)^{1/2}(x+x^{-1})\delta\omega & \\
+2\left[2\pi^2(2B+C)R^3\rho\omega^2 - 15R(m_3+2m_1)(-e)^{1/2}\right]\delta\omega & \\
-15m_3(-e)^{1/2}(x-x^{-1})\delta u_1 &= 0 \\
3m_3(-e)^{1/2}(x+x^{-1})\delta u_1 + 2\left[\pi^2(2B+C)R^2\rho\omega^2 - 3m_3(-e)^{1/2}\right]\delta u_1 & \\
+3Rm_3(-e)^{1/2}(x-x^{-1})\delta\omega &= 0 \\
3m_3(-e)^{1/2}(x+x^{-1}) + 2\left[2\pi^2BR^2\rho\omega^2 - 3m_3(-e)^{1/2}\right] &= 0.
\end{aligned} \tag{4.91}$$

The third equation of this system may be solved alone: noting that

$$\begin{aligned}
x + x^{-1} &= 2\cos\theta \\
x - x^{-1} &= 2i\sin\theta
\end{aligned} \tag{4.92}$$

we obtain

$$\cos\theta = 1 - \frac{2\pi^2 BR^2\rho\omega^2}{3m_3(-e)^{1/2}}. \tag{4.93}$$

This determines the required value of x giving the solution as

$$\delta u_3^{(n)} = \delta u_3 \exp\left[-i(\omega t - n\theta)\right]. \tag{4.94}$$

For wave-type solutions of this form we require that

$$-1 \leq \cos\theta \leq 1. \tag{4.95}$$

Values of $\cos\theta$ outside this range would result in real values of x and exponential type solutions for the difference equation. Physically, this corresponds to total reflection of the wave. Considering $\cos\theta \leq 1$ gives the trivial condition $\omega^2 \geq 0$. Considering $\cos\theta \geq -1$ gives the condition

$$\omega^2 \leq \frac{3m_3(-e)^{1/2}}{\pi^2 R^2\rho B} = \omega_0^2. \tag{4.96}$$

We can compare this solution with a plane-wave of the form

$$\exp\left[ik(z - ct)\right] \tag{4.97}$$

where k is the wave-number, c is the wave speed and z is the spatial coordinate in the direction of propagation. For a cubic packing with a wave propagating in the vertical direction the vertical distance z is given in terms of the central column sphere number n as $z = 2Rn$. Matching terms in the above two waves (4.94) and (4.97), we identify the wave speed as

$$c = \frac{2R\omega}{\theta}. \tag{4.98}$$

Equation (4.93) may now be re-written to relate the wave speed c to the frequency ω, as the dispersion relation

$$\sin^2\left(\frac{R\omega}{c}\right) = \frac{\pi^2 BR^2\rho\omega^2}{3m_3(-e)^{1/2}}. \tag{4.99}$$

Figures 4-7, 4-8, 4-9 and 4-10 show plots of this relationship with dimensionless frequency against dimensionless wave speed where

$$V^2 = \frac{\pi^2 B R^2 \rho}{(-e)^{1/2}}. \tag{4.100}$$

The range of θ plotted in each figure is from $\theta = 0$ to $\theta = 3\pi$, giving the three loops shown. Extending the range of θ would result in more of these loops, each smaller than and below the previous one. Thus an infinite number of wave speeds may be found for any value of ω satisfying the condition (4.96).

The values of ω_1 can be picked out from the plots as the point at which each loop of the graph turns back on itself. Beyond this point, there are no real values of the wave speed c corresponding to each ω.

The same method applied to the remaining two equations of the system (4.91) yields

$$\cos\theta = \frac{\alpha\beta + 180 m_3^2 Re}{6(-e)^{1/2} m_3 (5\alpha R - \beta)} \tag{4.101}$$

where α and β depend on ω through the relationships

$$\alpha = 2\left[\pi^2(2B+C)R^2\rho\omega^2 - 3m_3(-e)^{1/2}\right] \tag{4.102}$$

$$\beta = 2\left[2\pi^2(2B+C)R^3\rho\omega^2 - 15(-e)^{1/2}R(m_3+2m_1)\right]. \tag{4.103}$$

The dispersion relation obtained from (4.101) is

$$\sin^2\left(\frac{R\omega}{c}\right) = \frac{-\pi^4(2B+C)^2R^4\rho^2\omega^4 + 15(-e)^{1/2}(m_1+m_3)\pi^2(2B+C)R^2\rho\omega^2}{9(-e)^{1/2}m_3\pi^2(2B+C)R^2\rho\omega^2 + 90(-e)m_1m_3} \tag{4.104}$$

which may also be written as

$$\sin^2\left(\frac{R\omega}{c}\right) = \frac{-W^4\omega^4 + 15W^2(m_1+m_3)\omega^2}{9m_3(W^2\omega^2 + 10m_1)} \tag{4.105}$$

where

$$W^2 = \frac{\pi^2(2B+C)R^2\rho}{(-e)^{1/2}}. \tag{4.106}$$

Solving $\cos\theta = 1$ for ω^2 gives

$$\omega_1^2 = \frac{15(-e)^{1/2}(m_1 + m_3)}{\pi^2(2B + C)R^2\rho}. \tag{4.107}$$

Therefore the condition $\cos\theta \leq 1$ requires that

$$\omega^2 \leq \frac{15(-e)^{1/2}(m_1 + m_3)}{\pi^2(2B + C)R^2\rho} = \omega_1^2. \tag{4.108}$$

When considering $\cos\theta \geq -1$, two roots for ω^2 occur

$$\omega_\pm^2 = \frac{3(-e)^{1/2}}{2\pi^2(2B + C)R^2\rho}\{2m_3 + 5m_1 \pm (2m_3 - 5m_1)\} \tag{4.109}$$

which gives

$$\omega_+^2 = \frac{6(-e)^{1/2}m_3}{\pi^2(2B + C)R^2\rho} \quad \text{and} \quad \omega_-^2 = \frac{15(-e)^{1/2}m_1}{\pi^2(2B + C)R^2\rho}. \tag{4.110}$$

These two roots coincide when $2m_3 = 5m_1$, and therefore $\omega_+ > \omega_-$ when $2m_3 > 5m_1$. Similarly, $w_+ < w_-$ when $2m_3 < 5m_1$. Comparing with ω_1^2 as calculated above, we may write

$$\omega_1^2 = \frac{5}{2}\omega_+^2 + \omega_-^2 \tag{4.111}$$

from which we may deduce that $\omega_1 > \omega_-$ and $\omega_1 > \omega_+$. Considering the above conditions and inequalities we arrive at the following conditions on ω:

(1) When $\omega_+ > \omega_-$ $(2m_3 > 5m_1)$

$$0 \leq \omega^2 \leq \frac{15(-e)^{1/2}m_1}{\pi^2(2B + C)R^2\rho} \quad \text{or} \quad \frac{6m_3(-e)^{1/2}}{\pi^2(2B + C)R^2\rho} \leq \omega^2 \leq \frac{15(-e)^{1/2}(m_1 + m_3)}{\pi^2(2B + C)R^2\rho};$$

(2) When $\omega_+ < \omega_-$ $(2m_3 < 5m_1)$

$$0 \leq \omega^2 \leq \frac{6m_3(-e)^{1/2}}{\pi^2(2B + C)R^2\rho} \quad \text{or} \quad \frac{15(-e)^{1/2}m_1}{\pi^2(2B + C)R^2\rho} \leq \omega^2 \leq \frac{15(-e)^{1/2}(m_1 + m_3)}{\pi^2(2B + C)R^2\rho};$$

(3) When $\omega_+ = \omega_-$ $(2m_3 = 5m_1)$

$$0 \leq \omega^2 \leq \frac{15(-e)^{1/2}(m_1 + m_3)}{\pi^2(2B + C)R^2\rho}.$$

These conditions give the ranges of ω for which waves may propagate through the packing. Values of ω outside these ranges mean that the solutions obtained are of the exponential type associated with real roots; these solutions decay rapidly with depth and physically represent total reflection of the wave. The first two conditions relate to the displacement δu_1 and the rotation $\delta\omega$ representing a shear wave. A compressional wave having displacements of amplitude δu_3 propagates when the third condition is satisfied.

Figures 4-11 and 4-12 plot the shear wave dispersion relation (4.105) when ϕ is 0 or $\pi/12$ respectively. The roots ω_+ and ω_- coincide when $\phi = \tan^{-1}(2/5)$ and this case is plotted in figure 4-13. Further plots are shown in figures 4-14, 4-15 and 4-16 for values of ϕ being $\pi/6$, $\pi/3$ and $9\pi/20$ respectively.

In each plot, the range of θ is from $\theta = 0$ to $\theta = 3\pi$. Again, there are an infinite number of wave speeds for each ω within the valid frequency ranges.

The effect of friction may be examined by rearranging equation (4.65) to obtain

$$(-e)^{1/2} = \left(\frac{-3\pi BF}{2}\right)^{1/3} \left[m_1^5 + 2fm_1m_3^4 + m_3^5\right]^{-1/3}. \tag{4.112}$$

As previously mentioned, friction is a higher order effect and does not appear in the force equations (4.70) for the incremental state. However, friction does appear in the dispersion relations (4.99) and (4.105) through the initial confining strain e: equation (4.65) may be substituted into the dispersion relations to give the wave speeds in terms of the frequency and the coefficient of friction. Equation (4.112) is for the case of sliding occurring on the top and bottom contacts with stick on the sides. Similar equations may be obtained for stick on the top and bottom contacts with sliding on the sides, or stick on all contacts. When all contacts stick, the coefficient of friction will not appear in the equations.

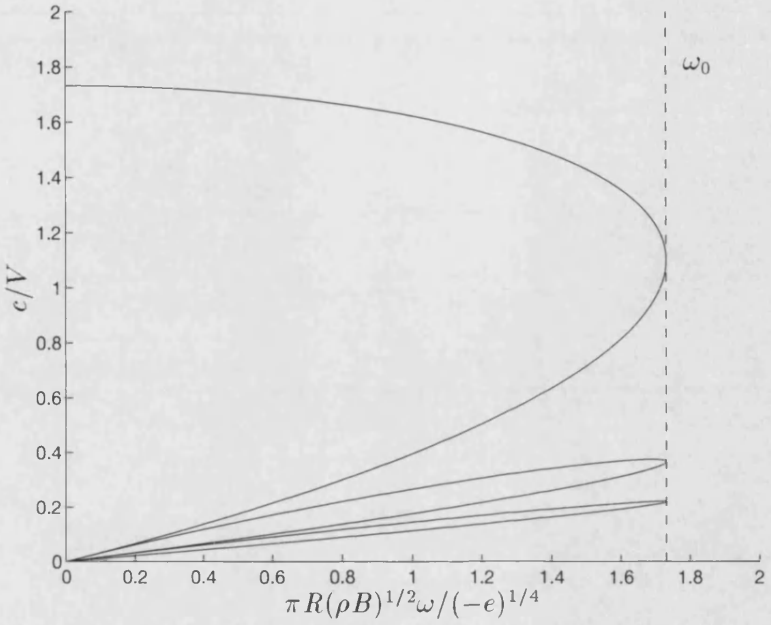

Figure 4-7: *A plot of dimensionless frequency against wave speed, $\phi = 0$*

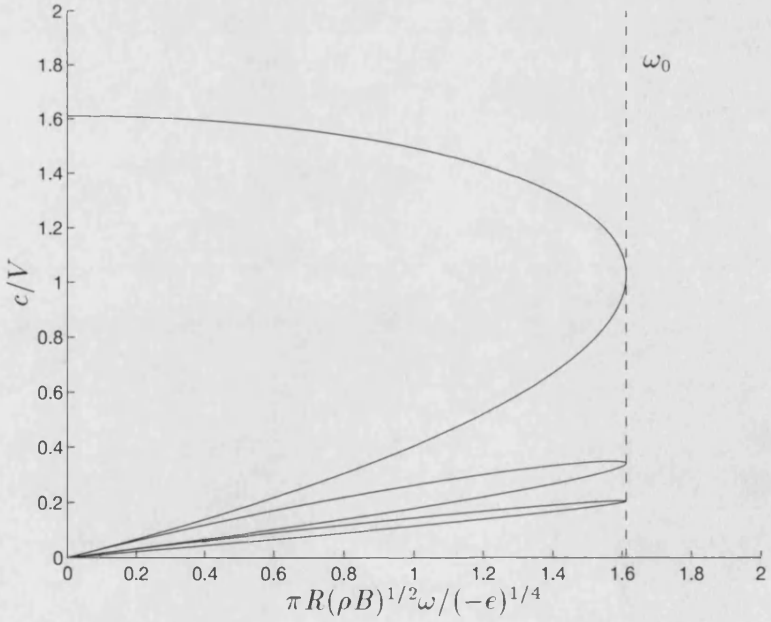

Figure 4-8: *A plot of dimensionless frequency against wave speed, $\phi = \pi/6$*

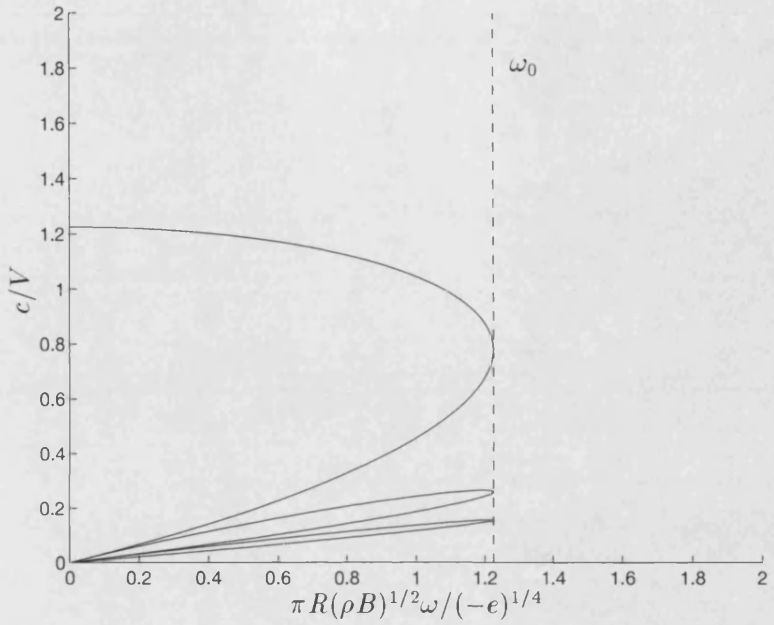

Figure 4-9: *A plot of dimensionless frequency against wave speed, $\phi = \pi/3$*

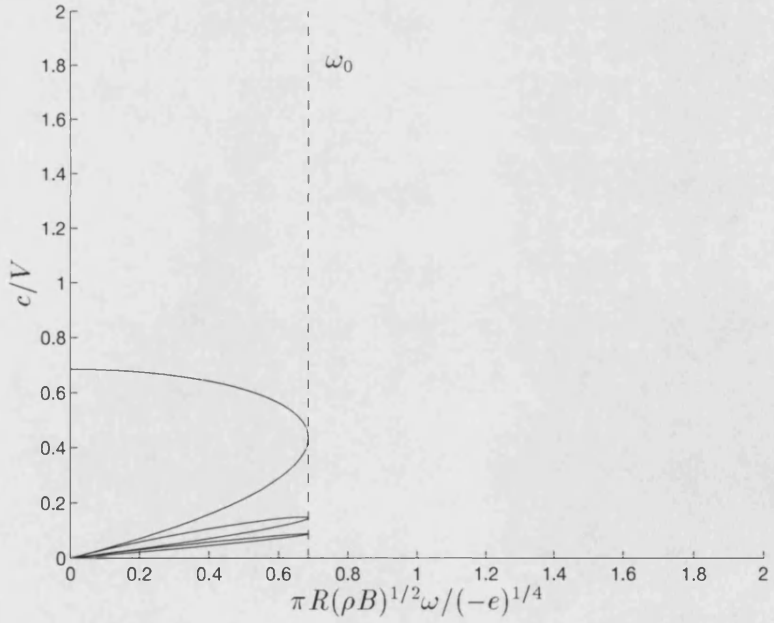

Figure 4-10: *A plot of dimensionless frequency against wave speed, $\phi = 9\pi/20$*

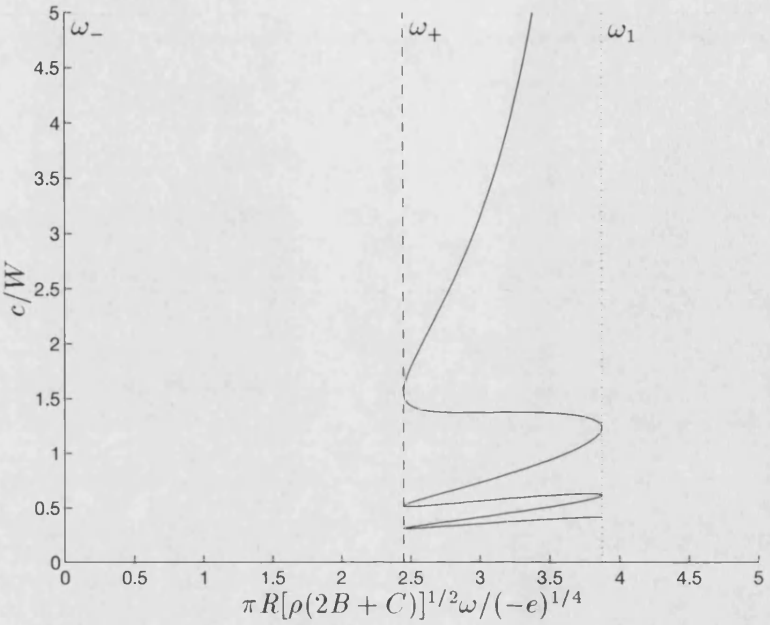

Figure 4-11: *A plot of dimensionless frequency against wave speed, $\phi = 0$*

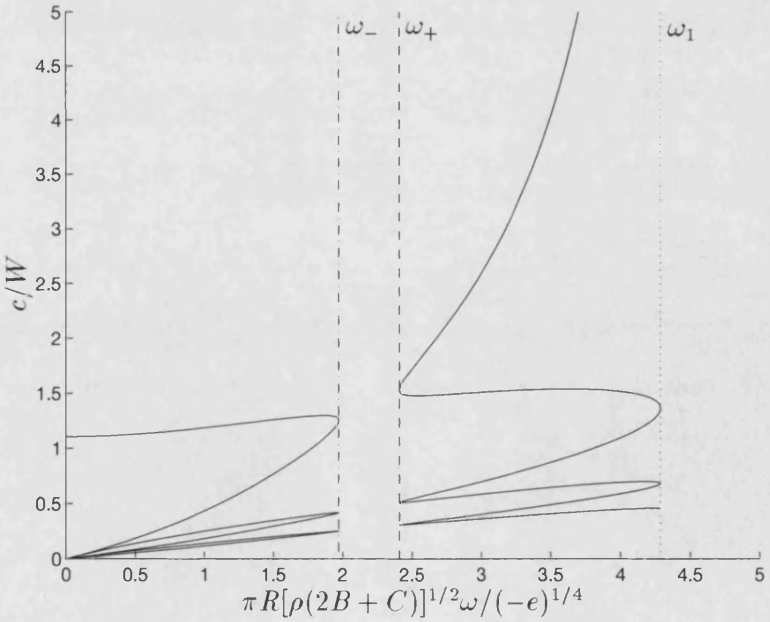

Figure 4-12: *A plot of dimensionless frequency against wave speed, $\phi = \pi/12$*

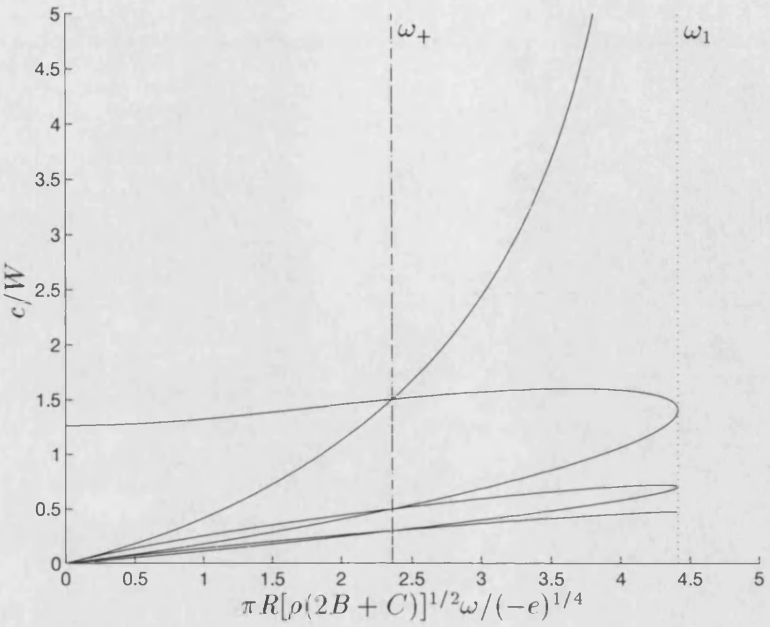

Figure 4-13: *A plot of dimensionless frequency against wave speed,* $\phi = \tan^{-1}(2/5)$

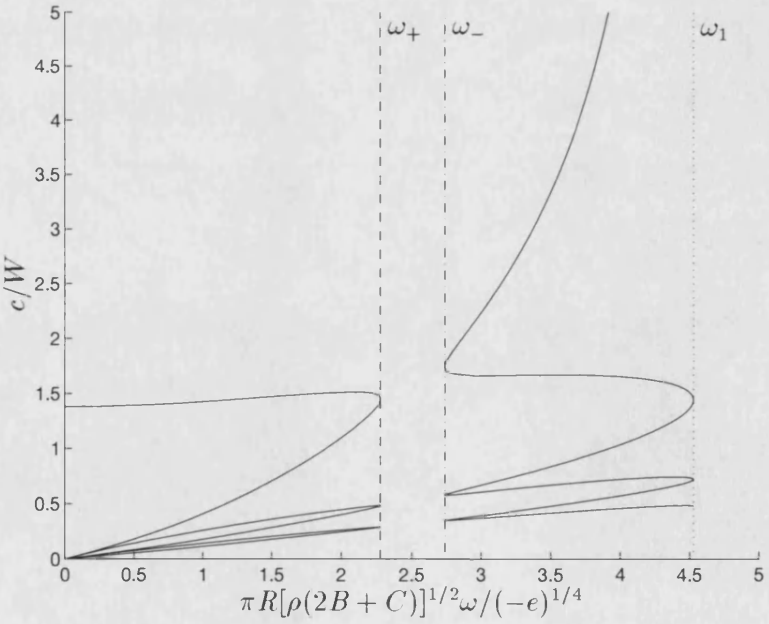

Figure 4-14: *A plot of dimensionless frequency against wave speed,* $\phi = \pi/6$

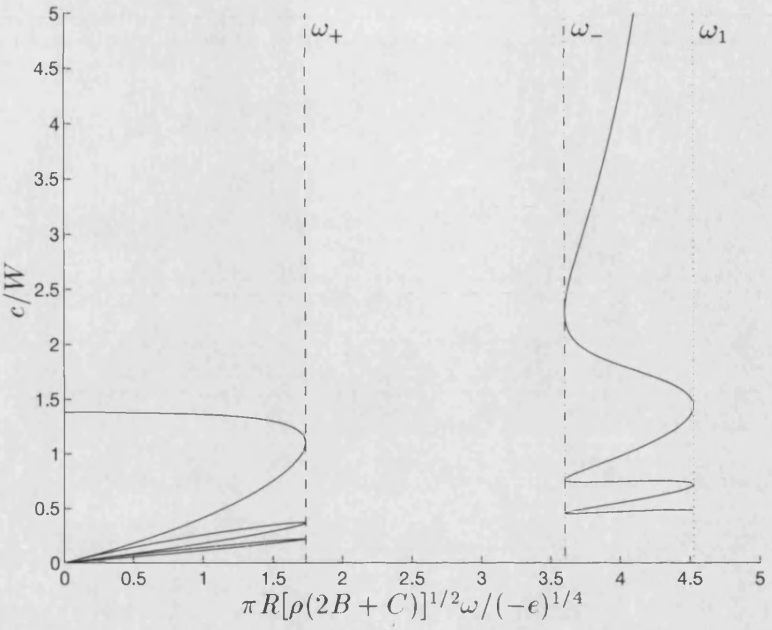

Figure 4-15: *A plot of dimensionless frequency against wave speed,* $\phi = \pi/3$

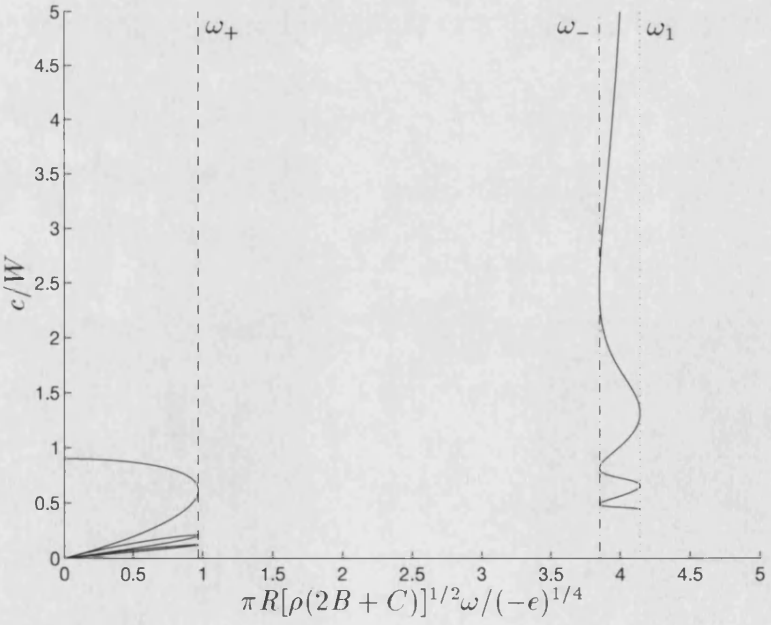

Figure 4-16: *A plot of dimensionless frequency against wave speed,* $\phi = 9\pi/20$

Chapter 5

A Random Packing of Spheres with Frictional Contacts

5.1 Introduction

We now turn attention to the effects of inter-granular friction within random packings of spheres. The motivation behind studying the oblique contact of two spheres with a finite value of the coefficient of friction, seen in chapter 3, was to provide the contact laws required in this chapter. Our aim is to predict the effective elastic moduli of the packing and in doing so, the oblique contact problem and the study of the inter-granular contact play important roles in determining the overall properties.

The spheres or grains within the packing are made of a homogeneous and elastically isotropic material. Each sphere is identical to the others having equal radius and elastic moduli. The random packing is formed from a large number of such spheres, each initially in point contact with several of its neighbours, the position vectors of the centres being randomly and uniformly distributed over the volume occupied by the packing. Because of the random nature of the packing geometry, it is not possible to make many of the simplifications for the regular geometry of the cubic packing seen in chapter 4. Instead, we make use of statistical information such as the average number of contacts per sphere and the probability distribution of these contacts over the sphere surfaces. An averaging scheme is defined which allows us to determine average macroscopic quantities such as stress in terms of known statistical properties and other microstructural information.

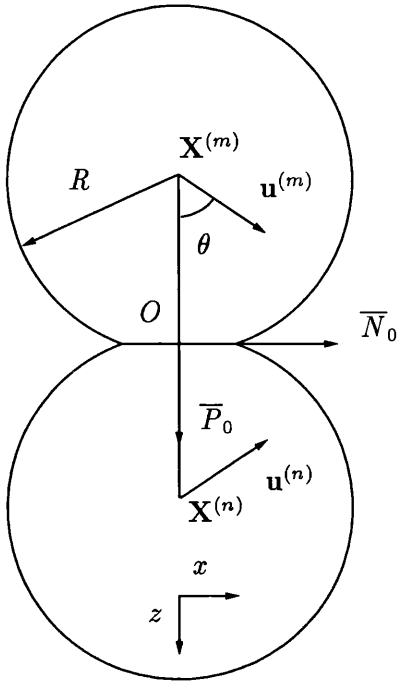

Figure 5-1: *The compression of two elastic spheres*

The effective elastic moduli are determined, in two stages, by considering an initial state followed by an incremental problem. To ensure that no inter-granular separation occurs in the packing, the boundary of the medium is first subjected to an initial confining strain. The spheres are compressed together, in general obliquely, and finite contact areas are formed. For simplicity, we assume that no new contacts occur. As discussed in section (3.3), two cases of stick or sliding are possible depending on the angle of compression. The averaging scheme is constructed by examining the range of angles for which sliding may or may not take place and performing the averaging integrals or summations over the required ranges. The average stress of the initial state is then determined in terms of the average strain.

A further incremental strain is imposed on the initial state and is infinitesimal in the sense that it is much smaller than the initial strain and small enough to permit use of the linearised force equations (3.162) and (3.163). The average incremental stress is determined in terms of this average incremental strain, and from this the effective elastic moduli are obtained.

5.2 The Initial State

We start with the familiar description of the packing geometry, the centre of each sphere being at position vector $\mathbf{X}^{(n)}$ relative to some fixed origin, and each centre undergoing displacement $\mathbf{u}^{(n)}$ under the confining strain. The unit vector joining the centre of sphere m to the centre of sphere n is defined as

$$\mathbf{I}^{(nm)} = \frac{\mathbf{X}^{(n)} - \mathbf{X}^{(m)}}{2R} \tag{5.1}$$

where R is the sphere radius and the initial contact point is located at position vector $(\mathbf{X}^{(n)} + \mathbf{X}^{(m)})/2$. Figure 5-1 shows the oblique compression of sphere n and sphere m. The axes $Oxyz$ are defined as the origin O being the point of first contact, the xy-plane being the common tangent plane of the two spheres, as shown in figure 3-1, and the z-axis being directed into the lower sphere. The centre of the upper sphere is displaced by an amount $(-u_0, -v_0, w_0)$ relative to the initial contact point, while the lower sphere undergoes an equal and opposite displacement of $(u_0, v_0, -w_0)$.

In chapter 2 it was shown that on average rotations will not occur in the initial state when the confining strain is either a hydrostatic or uniaxial compression. As discussed in chapter 4, when the initial compression is hydrostatic, described by equation (1.90), the spheres are compressed normally and therefore no frictional effects occur. Therefore, we will only be considering a uniaxial compression and rotations will be neglected here. For a uniaxial compression as given by equation (1.92), the spheres are compressed obliquely and sliding between them may occur. Then the displacement of the upper sphere relative to the lower sphere is

$$\mathbf{u}^{(m)} - \mathbf{u}^{(n)} \tag{5.2}$$

and the compression of the top sphere, relative to O, is given by

$$w_0 = \frac{1}{2}(\mathbf{u}^{(m)} - \mathbf{u}^{(n)}) \cdot \mathbf{I}^{(nm)}. \tag{5.3}$$

The confining strain e_{ij} takes the form of a displacement imposed on the boundary of the medium, described by equation (1.72). We make the assumption used by Walton [67], which was also discussed in section (1.3.1), that the displacement of the centre of each sphere is consistent with the applied uniform strain, meaning that we may write

$$u_i^{(n)} = e_{ij} X_j^{(n)}. \tag{5.4}$$

Substituting the above into (5.2) and (5.3), we obtain the relative displacement as

$$u_i^{(m)} - u_i^{(n)} = -2Re_{ij} I_j^{(nm)} \tag{5.5}$$

and the normal displacement of the centre of each sphere is

$$w_0 = -Re_{pq} I_p^{(nm)} I_q^{(nm)}. \tag{5.6}$$

The form of strain for a hydrostatic compression is

$$e_{ij} = e\delta_{ij} \tag{5.7}$$

where $e < 0$ for compression. When equation (5.7) is substituted into equation (5.5) we obtain the relative displacement as

$$u_i^{(m)} - u_i^{(n)} = -2ReI_i^{(nm)} \tag{5.8}$$

which is along the line of centres of the two spheres. Consequently, all the spheres within the packing are compressed together normally along the vectors $\mathbf{I}^{(nm)}$ meaning that no sliding will occur during a hydrostatic deformation. For this reason we will be considering just the uniaxial compression which may be written as

$$e_{ij} = e_3 \delta_{i3} \delta_{j3} \tag{5.9}$$

giving the relative displacement as

$$u_i^{(m)} - u_i^{(n)} = -2Re_3 \delta_{i3} I_3^{(nm)} \tag{5.10}$$

and the normal compression

$$w_0 = -Re_3 I_3^{(nm)2}. \tag{5.11}$$

To calculate the average stress in the initial state we will need to know the forces acting on each sphere across the contact areas. There are two possible forms of contact forces:

that in which the contact surfaces remain stuck together throughout the deformation in the initial or original state; and that in which sliding will occur over the entire contact area. We will refer to these two possibilities as cases A and B respectively.

5.2.1 Case A: No Sliding Originally

In chapter 3 we saw that the total contact area normal and tangential forces are given by

$$\overline{N}_0 = \frac{4(Rw_0^3)^{1/2}}{3\pi B} \quad \text{and} \quad \overline{P}_0 = \frac{8u_0(Rw_0)^{1/2}}{3\pi(2B+C)} \tag{5.12}$$

where B and C are elastic moduli given in terms of the Lamé moduli λ and μ by equation (1.7). The two contact areas remain stuck together as long as the calculated tangential force is less than the coefficient of friction f times the normal force, that is $\overline{P}_0 \leq f\overline{N}_0$. This condition is true for u_0 and w_0 satisfying

$$\frac{u_0}{w_0} < \left(\frac{2B+C}{2B}\right) f. \tag{5.13}$$

The force vector is constructed in the way it was in section (1.3.1) by resolving the displacement of the contact area into normal and tangential components and combining with the above forces to obtain

$$\mathbf{F}^{(nm)} = \frac{4(Rw_0^3)^{1/2}}{3\pi B}\mathbf{I}^{(nm)} + \frac{8(Rw_0)^{1/2}}{3\pi(2B+C)}\left\{\frac{1}{2}(\mathbf{u}^{(m)} - \mathbf{u}^{(n)}) - w_0\mathbf{I}^{(nm)}\right\}. \tag{5.14}$$

Making the assumption (5.4) and using equations (5.5) and (5.6) we obtain the components of the force vector as

$$\begin{aligned} F_i^{(nm)} &= \frac{4R^2(-e_{pq}I_p^{(nm)}I_q^{(nm)})^{3/2}}{3\pi B} I_i^{(nm)} \\ &\quad + \frac{8R^2(-e_{pq}I_p^{(nm)}I_q^{(nm)})^{1/2}}{3\pi(2B+C)}\left\{-e_{ij}I_j^{(nm)} + e_{pq}I_p^{(nm)}I_q^{(nm)}I_i^{(nm)}\right\}. \end{aligned} \tag{5.15}$$

Substituting the uniaxial compression (5.9) into the above, we obtain the force vector components as

$$F_i^{(nm)} = \frac{4R^2(-e_3)^{3/2}}{3\pi B(2B+C)}\left\{C|I_3^{(nm)}|^3 I_i^{(nm)} + 2BI_3^{(nm)}|I_3^{(nm)}|\delta_{i3}\right\}. \tag{5.16}$$

5.2.2 Case B: Sliding Originally

When condition (5.13) is not true, that is u_0 and w_0 satisfy

$$\frac{u_0}{w_0} \geq \left(\frac{2B+C}{2B}\right) f, \tag{5.17}$$

sliding will occur over the entire contact area and, as shown in section (3.5), the normal and tangential forces are respectively

$$\overline{N}_0 = \frac{4(Rw_0^3)^{1/2}}{3\pi B} \quad \text{and} \quad \overline{P}_0 = f\overline{N}_0 = \frac{4f(Rw_0^3)^{1/2}}{3\pi B}. \tag{5.18}$$

By the same method described in the previous section, we obtain the force vector for sliding contacts as

$$\mathbf{F}^{(nm)} = \frac{4(Rw_0^3)^{1/2}}{3\pi B}\left\{\mathbf{I}^{(nm)} + f\left[\frac{\frac{1}{2}(\mathbf{u}^{(m)} - \mathbf{u}^{(n)}) - w_0\mathbf{I}^{(nm)}}{|\frac{1}{2}(\mathbf{u}^{(m)} - \mathbf{u}^{(n)}) - w_0\mathbf{I}^{(nm)}|}\right]\right\}. \tag{5.19}$$

Making the substitutions (5.10) and (5.11), we find the force components under a uniaxial compression as

$$F_i^{(nm)} = \frac{4R^2(-e_3)^{3/2}|I_3^{(nm)}|^3}{3\pi B}\left\{I_i^{(nm)} + f\left[\frac{\delta_{i3} - |I_3^{(nm)}|I_i^{(nm)}}{(1 - I_3^{(nm)2})^{1/2}}\right]\right\} \tag{5.20}$$

which we note is equal to equation (5.16) when $\theta = \theta_c$ where θ is the angle of compression defined by

$$\tan\theta = \frac{u_0}{w_0} \tag{5.21}$$

and θ_c is the critical angle of friction for which equality occurs in the condition (5.17), that is

$$\tan\theta_c = \left(\frac{2B+C}{2B}\right) f. \tag{5.22}$$

5.2.3 A Modified Averaging Scheme

We consider the averaging scheme used in section (1.3.1) which gives the average stress as

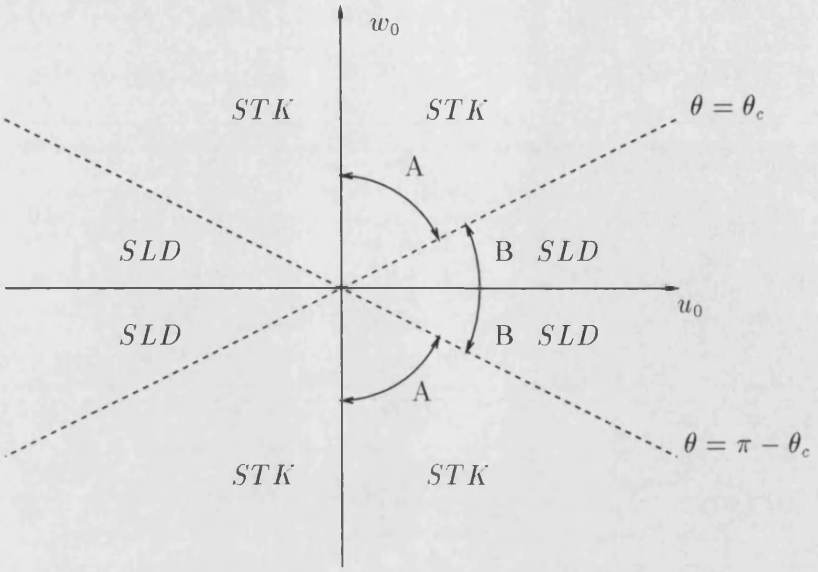

Figure 5-2: *Ranges of integration over sliding and stick regions*

$$\langle \sigma_{ij} \rangle = -\frac{R}{V} \sum_{\text{contacts}} \left\{ I_i^{(nm)} F_j^{(nm)} + I_j^{(nm)} F_i^{(nm)} \right\} \tag{5.23}$$

where V is the total volume of the medium and the summation is over all contacts m and n. An extra consideration is that each contact may now either slide or stick depending on the angle of compression and the summation must be written in a form which distinguishes between these two possible cases. By summing over the sliding and sticking contacts separately, it is possible to write the average stress in the form

$$\langle \sigma_{ij} \rangle = -\frac{R}{V} \left[\sum_A \left\{ I_i^{(nm)} F_{j(A)}^{(nm)} + I_j^{(nm)} F_{i(A)}^{(nm)} \right\} + \sum_B \left\{ I_i^{(nm)} F_{j(B)}^{(nm)} + I_j^{(nm)} F_{i(B)}^{(nm)} \right\} \right] \tag{5.24}$$

where the first summation is over sticking contacts (case A) only and the second is over sliding contacts (case B) only. The forces subscripted (A) and (B) represent the sticking and sliding forces (5.16) and (5.20) respectively.

Following the same argument as used in section (1.3.1), we now write the summations in terms of averaged quantities. By assuming that the unit vectors $\mathbf{I}^{(nm)}$ are uniformly distributed (that is the contact points are distributed with uniform probability over the surface of each sphere) and since there are many spheres contained within the volume V, we may write the above summation as

$$\langle \sigma_{ij} \rangle = -\frac{RnN}{2V} \left[\langle I_i F_j \rangle_A + \langle I_j F_i \rangle_A + \langle I_i F_j \rangle_B + \langle I_i F_j \rangle_B \right] \tag{5.25}$$

where n is the average number of contacts per sphere and N is the total number of spheres in the volume V. The angled brackets $\langle \cdot \rangle_A$ denote that the average is taken only over those values satisfying the no-sliding condition (5.13). Similarly, $\langle \cdot \rangle_B$ denotes that the average is taken only over those values for which sliding occurs satisfying (5.17).

In Walton [67], the definition of the averaging scheme was given in terms of the integrals

$$\langle \cdot \rangle = \frac{1}{4\pi} \int_0^{2\pi} \mathrm{d}\phi \int_0^{\pi} \mathrm{d}\theta \; (\cdot) \sin\theta \tag{5.26}$$

in which the extra $\sin\theta$ is necessary since the surface element required when integrating over the surface of a unit sphere is $\mathrm{d}S = \sin\theta \; \mathrm{d}\theta \; \mathrm{d}\phi$. Figure 5-2 shows the θ range of integration from 0 to π split into regions A and B satisfying conditions (5.13) and (5.17) respectively. The above integral is split as follows:

$$\langle \cdot \rangle_A = \frac{1}{4\pi} \int_0^{2\pi} \mathrm{d}\phi \left(\int_0^{\theta_c} + \int_{\pi-\theta_c}^{\pi} \right) (\cdot) \sin\theta \; \mathrm{d}\theta \tag{5.27}$$

$$\langle \cdot \rangle_B = \frac{1}{4\pi} \int_0^{2\pi} \mathrm{d}\phi \int_{\theta_c}^{\pi-\theta_c} (\cdot) \sin\theta \; \mathrm{d}\theta. \tag{5.28}$$

This definition is repeated in appendix B together with the explicit vector averages required later in this chapter.

5.2.4 The Initial Stress

Using equation (5.25) and the force components (5.16) and (5.20), we calculate the initial stress as

$$\begin{aligned} \langle \sigma_{ij} \rangle = & -\frac{n\phi(-e_3)^{3/2}}{\pi^2} \left\{ \frac{1}{B} \langle |I_3|^3 I_i I_j \rangle \right. \\ & + \frac{1}{2B+C} \langle I_3 |I_3| I_i \delta_{j3} + I_3 |I_3| I_j \delta_{i3} - 2|I_3|^3 I_i I_j \rangle_A \\ & \left. + \frac{f}{2B} \left\langle \frac{I_3^2}{(1-I_3^2)^{1/2}} (I_i \delta_{j3} + I_j \delta_{i3} - 2 I_3 I_i I_j) \right\rangle_B \right\} \end{aligned} \tag{5.29}$$

where ϕ is the sphere material volume concentration, not to be confused with the polar

angle ϕ in the averaging scheme integral. The first term within the braces does not have an A or B subscript since it is required to average this quantity over the entire range of θ. The quantities N and V in the above have been replaced by ϕ through the relationships

$$\phi = \frac{NV_n}{V} = \frac{4\pi R^3 N}{3V} \quad \text{or} \quad \frac{N}{V} = \frac{3\phi}{4\pi R^3} \tag{5.30}$$

where V_n denotes the volume of a single sphere.

Considering first the normal stresses we find that $\langle\sigma_{11}\rangle = \langle\sigma_{22}\rangle$ and that

$$\begin{aligned}
\langle\sigma_{11}\rangle &= -\frac{n\phi(-e_3)^{3/2}}{\pi^2}\left\{\frac{1}{B}\langle I_1^2|I_3|^3\rangle - \frac{2}{2B+C}\langle I_1^2|I_3|^3\rangle_A - \frac{f}{B}\left\langle\frac{I_1^2 I_3^4}{(1-I_3^2)^{1/2}}\right\rangle_B\right\} \\
\langle\sigma_{33}\rangle &= -\frac{n\phi(-e_3)^{3/2}}{\pi^2}\left\{\frac{1}{B}\langle|I_3|^5\rangle + \frac{2}{2B+C}\langle|I_3|^3 - |I_3|^5\rangle_A\right. \\
&\qquad \left. + \frac{f}{B}\left\langle\frac{I_3^3}{(1-I_3^2)^{1/2}}(I_3 - I_3^3)\right\rangle_B\right\}.
\end{aligned} \tag{5.31}$$

The trace of the stress tensor may be found by summing over $i = j = 1$, $i = j = 2$ and $i = j = 3$ to give

$$\langle\sigma_{kk}\rangle = 2\langle\sigma_{11}\rangle + \langle\sigma_{33}\rangle = -\frac{n\phi(-e_3)^{3/2}}{4\pi^2}. \tag{5.32}$$

The shear stresses are all zero due to the symmetries of the averaging scheme as discussed in section (2.4.1). Then by rearranging equation (5.32) to obtain $\langle\sigma_{11}\rangle$ and substituting the averaged values from appendix B into equation (5.31) we find that

$$\begin{aligned}
\langle\sigma_{ij}\rangle &= 0 \quad \text{for} \quad i \neq j \\
\langle\sigma_{11}\rangle &= \langle\sigma_{22}\rangle = -\frac{n\phi(-e_3)^{3/2}}{8\pi^2} - \frac{1}{2}\langle\sigma_{33}\rangle \\
\langle\sigma_{33}\rangle &= -\frac{n\phi(-e_3)^{3/2}}{\pi^2}\left\{\frac{1}{6B} + \left(\frac{\pi - 2\theta_c}{32B}\right)f + \frac{\sin^2\theta_c\,(3 - 2\sin^2\theta_c)}{24(2B+C)}\right\}.
\end{aligned} \tag{5.33}$$

The uniaxial displacement considered here may be interpreted as arising from the application of a vertical compressive force of magnitude F, where

$$F = \langle \sigma_{33} \rangle = \frac{n\phi(-e_3)^{3/2}}{\pi^2} \left\{ \frac{1}{6B} + \left(\frac{\pi - 2\theta_c}{32B} \right) f + \frac{\sin^2 \theta_c \, (3 - 2\sin^2 \theta_c)}{24(2B + C)} \right\}. \tag{5.34}$$

5.3 The Incremental State

Recall from section (3.6) that the incremental forces due to the incremental displacement $(\delta u_0, \delta v_0, \delta w_0)$ are given, in the normal direction, by

$$\overline{\delta N} = \frac{2(Rw_0)^{1/2}}{\pi B} \delta w_0 \tag{5.35}$$

and, in the tangential directions, by

$$\overline{\delta P} = \frac{4(Rw_0)^{1/2}}{\pi(2B + C)} \delta u_0 \quad \text{and} \quad \overline{\delta Q} = \frac{4(Rw_0)^{1/2}}{\pi(2B + C)} \delta v_0. \tag{5.36}$$

In chapter 2 we showed that, for equilibrium of the packing, it is necessary to consider the rotations of each sphere, denoted $\delta\boldsymbol{\omega}$, in the incremental problem. Equation (2.22) gives the incremental force exerted by sphere m on sphere n as

$$\begin{aligned} \delta \mathbf{F}^{(nm)} = \frac{(Rw_0)^{1/2}}{\pi B(2B + C)} \Big\{ & 2B \left[\delta \mathbf{u}^{(m)} - \delta \mathbf{u}^{(n)} + (\delta\boldsymbol{\omega}^{(m)} + \delta\boldsymbol{\omega}^{(n)}) \wedge R\mathbf{I}^{(nm)} \right] \\ & + C \left[(\delta \mathbf{u}^{(m)} - \delta \mathbf{u}^{(n)}) \cdot \mathbf{I}^{(nm)} \right] \mathbf{I}^{(nm)} \Big\}. \end{aligned} \tag{5.37}$$

We make the same assumptions about the form of the displacements and rotations as for the initial state that they are consistent with the applied uniform strain:

$$\delta u_i^{(n)} = \delta e_{ij} X_j^{(n)} \quad \text{and} \quad \delta\boldsymbol{\omega}^{(n)} = \delta\boldsymbol{\omega}^{(m)} = \delta\boldsymbol{\omega}. \tag{5.38}$$

Substituting these and the compression for the uniaxial strain $e_{ij} = e_3 \delta_{i3} \delta_{j3}$, given by equation (5.9), into the force vector (5.37) we obtain the components of the incremental force as

$$\begin{aligned} \delta F_i^{(nm)} = \frac{-R^2(-e_3)^{1/2} |I_3^{(nm)}|}{\pi B(2B + C)} \Big\{ & 4B \delta e_{ip} I_p^{(nm)} \\ & + 2C \delta e_{pq} I_p^{(nm)} I_q^{(nm)} I_i^{(nm)} - 4B \epsilon_{ipq} \delta\omega_p I_q^{(nm)} \Big\}. \end{aligned} \tag{5.39}$$

Recall from section (2.2) that in order to ensure rotational equilibrium we imposed the condition

$$\sum_m \mathbf{I}^{(nm)} \wedge \delta\mathbf{F}^{(nm)} = \mathbf{0} \tag{5.40}$$

from which the required value of $\delta\boldsymbol{\omega}$ was determined. Section (2.4) considered the case of an initial uniaxial compression which gave the incremental rotation vector as

$$\delta\omega_1 = -\frac{1}{3}\delta e_{23}, \quad \delta\omega_2 = \frac{1}{3}\delta e_{13}, \quad \delta\omega_3 = 0. \tag{5.41}$$

5.3.1 The Incremental Stress

The average incremental stress is given by the analogue of equation (5.23) which is

$$\langle \delta\sigma_{ij} \rangle = -\frac{R}{V} \sum_{\text{contacts}} \left\{ I_i^{(nm)} \delta F_j^{(nm)} + I_j^{(nm)} \delta F_i^{(nm)} \right\}. \tag{5.42}$$

Here there need be no distinction between sliding and sticking since, as already mentioned in section (3.6), friction is a higher order effect and does not appear in the force equations (5.35) and (5.36). Following the same procedure as for the initial stress of writing the summation as an average and substituting the force (5.37) into equation (5.42), we obtain

$$\begin{aligned} \langle \delta\sigma_{ij} \rangle \;=\; & \frac{3n\phi(-e_3)^{1/2}}{2\pi^2 B(2B+C)} \{ [2B \langle I_i I_l |I_3| \rangle \delta_{jk} + C \langle I_i I_j I_k I_l |I_3| \rangle] \langle \delta e_{kl} \rangle \\ & - 2B \langle \epsilon_{jpq} \delta\omega_p I_q I_i |I_3| \rangle \}. \end{aligned} \tag{5.43}$$

The rotations are given by equation (5.41) and so the above equation relates the average incremental stress to the average incremental strain.

5.3.2 The Effective Elastic Moduli

The stress given in equation (5.43) may also be written as

$$\langle \delta\sigma_{ij} \rangle = C^*_{ijkl} \langle \delta e_{kl} \rangle \tag{5.44}$$

where C^*_{ijkl} are the effective elastic moduli. In chapter 2 we showed that five independent elastic moduli are required to describe this transversely isotropic medium. By taking

the appropriate values for i and j in equation (5.43) and using the calculated rotation vector (5.41), we obtain the elastic moduli as:

$$\begin{aligned} C^*_{11} = C^*_{1111} &= 3(\alpha + 2\beta) \\ C^*_{12} = C^*_{1122} &= \alpha - 2\beta \\ C^*_{13} = C^*_{1133} = C^*_{2233} &= 2(\alpha - 2\beta) \\ C^*_{33} = C^*_{3333} &= 8(\alpha + \beta) \\ C^*_{44} = C^*_{1313} = C^*_{2323} &= 2(\alpha + 2\beta) \end{aligned} \tag{5.45}$$

in which α and β are defined, as in Walton [67], by

$$\alpha = \frac{\phi n(-e_3)^{1/2}}{32\pi^2 B} \quad \text{and} \quad \beta = \frac{\phi n(-e_3)^{1/2}}{32\pi^2(2B+C)} \tag{5.46}$$

which in terms of the confining force F (5.34) may be written as

$$\alpha = \frac{n\phi}{32\pi^2 B}\left(\frac{\pi^2 F}{n\phi}\right)^{1/3}\left\{\frac{1}{6B} + \left(\frac{\pi - 2\theta_c}{32B}\right)f + \frac{\sin^2\theta_c\,(3 - 2\sin^2\theta_c)}{24(2B+C)}\right\}^{-1/3} \tag{5.47}$$

and

$$\beta = \frac{n\phi}{32\pi^2(2B+C)B}\left(\frac{\pi^2 F}{n\phi}\right)^{1/3}\left\{\frac{1}{6B} + \left(\frac{\pi - 2\theta_c}{32B}\right)f + \frac{\sin^2\theta_c\,(3 - 2\sin^2\theta_c)}{24(2B+C)}\right\}^{-1/3}. \tag{5.48}$$

5.3.3 Wave Speeds

We now consider a plane wave propagating in the direction of a unit vector $\mathbf{m}$. The stresses are related to the displacement $\mathbf{u}$ through the relationship

$$\sigma_{ij} = C^*_{ijkl} u_{k,l} \tag{5.49}$$

where the moduli C^*_{ijkl} are given by equation (5.45) and $u_{k,l}$ denotes differentiation of u_k with respect to the coordinate x_l. The equation of motion is

$$\sigma_{ij,j} = \rho \ddot{u}_i \tag{5.50}$$

where $\ddot{u}_i$ denotes the second time derivative of u_i and ρ is the effective density of the medium, that is $\rho = \phi\rho_s$ where ρ_s is the density of the sphere material. Consider a plane-wave solution of the form

$$u_i = d_i \exp\{i(k\mathbf{m}\cdot\mathbf{x} - \omega t)\} \tag{5.51}$$

where $\mathbf{d}$ is the particle polarisation, k is the wave number and ω the frequency. Substituting this solution into the equations (5.49) and (5.50) we obtain

$$-C^*_{ijkl} d_k k^2 m_l m_j = -\rho\omega^2 d_i \tag{5.52}$$

and

$$\rho c^2 d_i = (C^*_{ijkl} m_j m_l) d_k \tag{5.53}$$

where $c = \omega/k$ is the wave speed. Then combining the above two equations, we may write

$$(C^*_{ijkl} m_j m_l - \rho c^2 \delta_{ik}) d_k = 0 \tag{5.54}$$

showing that ρc^2 must be an eigenvalue of $C^*_{ijkl} m_j m_l$ with corresponding eigenvector $\mathbf{d}$. By defining the matrix

$$D_{ik} = C^*_{ijkl} m_j m_l \tag{5.55}$$

we may write the components as

$$\begin{aligned}
D_{11} &= C^*_{1111} m_1^2 + C^*_{1212} m_2^2 + C^*_{1313} m_3^2 \\
D_{22} &= C^*_{2121} m_1^2 + C^*_{2222} m_2^2 + C^*_{2323} m_3^2 \\
D_{33} &= C^*_{3131} m_1^2 + C^*_{3232} m_2^2 + C^*_{3333} m_3^2 \\
D_{12} &= C^*_{1122} m_1 m_2 + C^*_{1221} m_1 m_2 \\
D_{21} &= C^*_{2112} m_1 m_2 + C^*_{2211} m_1 m_2
\end{aligned}$$

$$\begin{aligned} D_{13} &= C^*_{1133}m_1m_3 + C^*_{1331}m_1m_3 \\ D_{31} &= C^*_{3113}m_1m_3 + C^*_{3311}m_1m_3 \\ D_{23} &= C^*_{2233}m_2m_3 + C^*_{2332}m_2m_3 \\ D_{32} &= C^*_{3223}m_2m_3 + C^*_{3322}m_2m_3. \end{aligned} \tag{5.56}$$

Because of the symmetry of the transversely isotropic state, it is sufficient to consider a propagation direction of the form

$$\mathbf{m} = (\sin\psi,\ 0,\ \cos\psi) \tag{5.57}$$

where ψ is the angle measured from the xy-plane. Then the matrix (5.56) simplifies to

$$\begin{aligned} D_{11} &= C_{1111}m_1^2 + C_{1313}m_3^2 \\ D_{22} &= C_{2121}m_1^2 + C_{1313}m_3^2 \\ D_{33} &= C_{3131}m_1^2 + C_{3333}m_3^2 \\ D_{12} &= D_{21} = 0 \\ D_{13} &= D_{31} = (C_{1133} + C_{1331})m_1m_3 \\ D_{23} &= D_{32} = 0 \end{aligned} \tag{5.58}$$

and the eigenvalue problem (5.54) may be written in matrix form as

$$\begin{vmatrix} D_{11} - \rho c^2 & 0 & D_{13} \\ 0 & D_{22} - \rho c^2 & 0 \\ D_{13} & 0 & D_{33} - \rho c^2 \end{vmatrix} = 0 \tag{5.59}$$

and as a system of equations for the eigenvectors $\mathbf{d}$:

$$\begin{aligned} (D_{11} - \rho c^2)d_1 + D_{13}d_3 &= 0 \\ (D_{22} - \rho c^2)d_2 &= 0 \\ D_{13}d_1 + (D_{33} - \rho c^2)d_3 &= 0. \end{aligned} \tag{5.60}$$

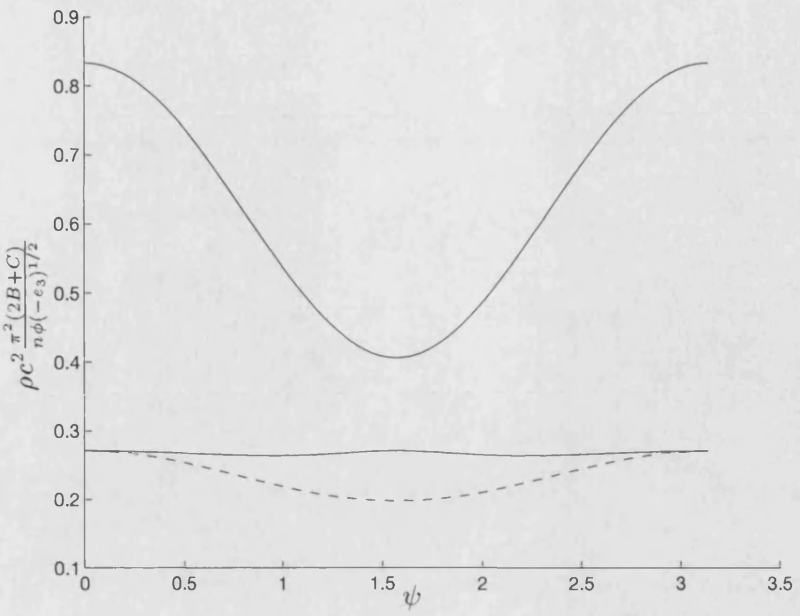

Figure 5-3: *A plot of dimensionless wave speed against angle*

There are three solutions to consider, the first of which is an S-wave:

The S-Wave Solution

From the middle equation of the above system we have that

$$D_{22} = \rho c^2 \quad \text{and} \quad d_1 = d_3 = 0. \tag{5.61}$$

or writing in terms of the confining force F (5.34)

$$c^2 = \frac{1}{32\rho_s B(2B+C)} \left(\frac{n^2 F}{\pi^4 \phi}\right)^{1/3} \{2B(6m_1^2 + 8m_3^2) + C(m_1^2 + 2m_3^2)\} \times \left\{\frac{1}{6B} + \left(\frac{\pi - 2\theta_c}{32B}\right) f + \frac{\sin^2\theta_c\,(3 - 2\sin^2\theta_c)}{24(2B+C)}\right\}^{-1/3}. \tag{5.62}$$

The particle displacement is in the direction of $\mathbf{e}_2$ which is perpendicular to the direction of propagation, the resulting wave being recognised as an S-wave.

The Remaining Solutions

To determine the remaining two solutions, it is necessary to solve the quadratic obtained from the first and third equations of the system (5.60) as

$$(D_{11}D_{33} - D_{13}^2) - (D_{11} + D_{33})\rho c^2 + \rho^2 c^4 = 0. \tag{5.63}$$

In general, the two waves arising from this quadratic will be neither purely longitudinal nor purely shear. We solve numerically for selected values of ϕ and plot non-dimensional wave speed against angle of compression, as shown in figure 5-3. The dashed line represents the shear wave (5.61) and the two solid lines are obtained from the solution of equation (5.63). A value of $B/C = 1/3$ was chosen.

Special Cases

Two special cases for which explicit expressions may be derived for wave speeds and polarisations are considered here. The first is a uniaxial compression in the x-direction with axis of strain described by

$$\mathbf{m} = (1, 0, 0) \tag{5.64}$$

for which $\psi = \pi/2$. The solutions obtained are an S-wave with wave speed given by

$$\rho c^2 = \frac{1}{2}(C_{11} - C_{22}) \tag{5.65}$$

which may be written in terms of the confining force F (5.34) as

$$c^2 = \frac{6B + C}{32\rho_s B(2B + C)} \left(\frac{n^2 F}{\pi^4 \phi}\right)^{1/3} \left\{ \frac{1}{6B} + \left(\frac{\pi - 2\theta_c}{32B}\right) f + \frac{\sin^2\theta_c\,(3 - 2\sin^2\theta_c)}{24(2B + C)} \right\}^{-1/3}. \tag{5.66}$$

Two other waves are obtained from equation (5.63), with speeds

$$\rho c^2 = C_{1111} \quad \text{and} \quad \rho c^2 = C_{1313}. \tag{5.67}$$

The first of these is a P-wave with speed

$$c^2 = \frac{3(4B + C)}{32\rho_s B(2B + C)} \left(\frac{n^2 F}{\pi^4 \phi}\right)^{1/3} \left\{ \frac{1}{6B} + \left(\frac{\pi - 2\theta_c}{32B}\right) f + \frac{\sin^2\theta_c\,(3 - 2\sin^2\theta_c)}{24(2B + C)} \right\}^{-1/3} \tag{5.68}$$

and the second is an S-wave with speed

$$c^2 = \frac{4B+C}{16\rho_s B(2B+C)}\left(\frac{n^2F}{\pi^4\phi}\right)^{1/3}\left\{\frac{1}{6B}+\left(\frac{\pi-2\theta_c}{32B}\right)f+\frac{\sin^2\theta_c\,(3-2\sin^2\theta_c)}{24(2B+C)}\right\}^{-1/3}. \tag{5.69}$$

The second special case we consider is that seen in Slade and Walton [55], the axis of strain being in the z-direction as follows:

$$\mathbf{m} = (0,0,1) \tag{5.70}$$

for which $\psi = 0$. The solutions obtained are an S-wave with speed

$$\rho c^2 = C^*_{2323} = C^*_{1313} \tag{5.71}$$

which may also be written in terms of F as equation (5.69), and two other waves with speeds

$$\rho c^2 = C_{1313} \quad \text{and} \quad \rho c^2 = C_{3333}. \tag{5.72}$$

The first of these is an S-wave with speed given in terms of F by equation (5.69) and the second is the P-wave seen in Slade and Walton [55] which examined an initial uniaxial compression followed by the incremental uniaxial compression $\delta e_{ij} = \delta e\ \delta_{i3}\delta_{j3}$. The wave speed obtained from the C_{3333} modulus is

$$c^2 = \frac{3B+C}{4\rho_s B(2B+C)}\left(\frac{n^2F}{\pi^4\phi}\right)^{1/3}\left\{\frac{1}{6B}+\left(\frac{\pi-2\theta_c}{32B}\right)f+\frac{\sin^2\theta_c\,(3-2\sin^2\theta_c)}{24(2B+C)}\right\}^{-1/3} \tag{5.73}$$

which is in agreement with the corrected equation (34) of Slade and Walton [55] given in appendix A as equation (A.5).

Figures 5-4 and 5-5 plot the dimensionless wave speed against the coefficient of friction varying from 0 to 1. In figure 5-5 the value of ψ is $\pi/2$ with the P-wave and S-wave speeds from equation (5.67) plotted by the dashed and dot-dashed lines respectively. The solid line is the P-wave speed from equation (5.65). The value of ψ in figure 5-4 is 0 and shows the P-wave as a dot-dashed line and the two S-waves of equations (5.71)

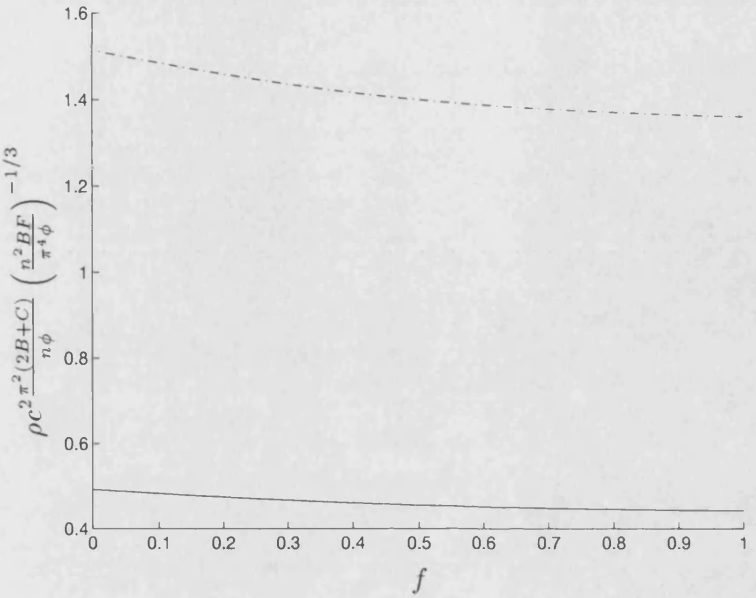

Figure 5-4: *A plot of dimensionless wave speed against coefficient of friction,* $\psi = 0$

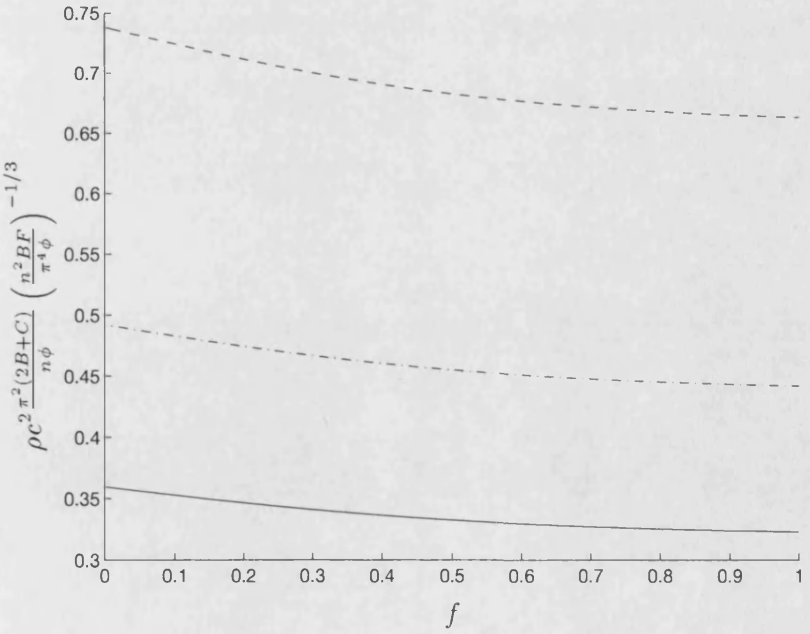

Figure 5-5: *A plot of dimensionless wave speed against coefficient of friction,* $\psi = \pi/2$

and (5.72) as a solid line.

All of the results in this chapter are for the dry sphere packing only. The presence of fluid would create an additional hydrostatic pressure causing the spheres to be compressed normally. The Biot theory of porous media (see references [5] and [6]) provides one method of allowing for fluid effects by examining the relative motion between the solid and fluid phases, which in turn requires parameters coupling solid and fluid properties. Walton [64] and [63] and Digby and Walton [23] have considered a fluid-saturated cubic packing by solving the linearised equations of solid and fluid motion within a single (cubic) cell of the packing.

A fluid-saturated random packing is examined in Walton and Digby [69]. A low frequency expansion technique is used to obtain the linearised equations of solid and fluid motion, and an averaging scheme is defined to homogenise the medium. The effect of the hydrostatic fluid pressure is an additional displacement to that which would be experienced by the equivalent dry-frame problem. Thus the fluid effect may be added once the dry-frame moduli are known. Comparisons are also made with the equations of Biot [5] showing that either approach would be suitable for the addition of a fluid component in the frictional random packing model.

Chapter 6

The Oblique Contact of Two Oblate Spheroidal Bodies

6.1 Introduction

The normal Hertzian contact of non-spherical elastic bodies has been extensively studied and is reviewed by Sackfield and Hills [49]. The problem in which tangential forces are transmitted between the two bodies has been studied by Deresiewicz [20], Vermeulen and Johnson [61] and again is reviewed by Sackfield and Hills [50]. Rough contact between elastically and geometrically identical bodies are considered by Raoof and Hobbs [47] and Bryant and Keer [12].

The purpose of this chapter is to derive the oblique contact laws between two contacting spheroidal bodies which are aligned in the sense that their principal axes in the three coordinate directions are parallel. The geometry of this problem is treated as a special case of the general Hertz geometries seen in the above references, which was also presented in section (1.2.4). Here we will assume that the bodies are infinitely rough so that there is no relative slip between them. First, the oblique Hertz problem is solved for bodies of a general profile by extending the results of Walton [66] for spheres, in which the normal and tangential displacements are occurring simultaneously. Next, the incremental oblique displacement is imposed on this initial compression, as described in Walton [67] and section (1.3.1).

6.2 Surface Displacements

Before considering the Hertzian contact of bodies of a general profile, it is necessary to calculate the displacements on a half-space due to distributions of the form

$$N(x,y) = N_0 \left(1 - \frac{x^2}{a^2} - \frac{y^2}{b^2}\right)^{1/2} \tag{6.1}$$

acting normally, with a similar Hertzian pressure distribution

$$P(x,y) = K \left(1 - \frac{x^2}{a^2} - \frac{y^2}{b^2}\right)^{1/2} \tag{6.2}$$

acting in a general tangential direction and the elliptical punch pressure distribution

$$P(x,y) = K \left(1 - \frac{x^2}{a^2} - \frac{y^2}{b^2}\right)^{-1/2} \tag{6.3}$$

also acting tangentially, where K and N are force constants. The half-space is defined as $z < 0$ and the xy-plane forms the boundary of the half-space as seen in section (1.2.1). These distributions act in the plane-elliptical region

$$\frac{x^2}{a^2} + \frac{y^2}{b^2} \leq 1 \tag{6.4}$$

where $2a$ and $2b$ are the lengths of the principal axes of the ellipse and $a > b$. The load is zero outside this elliptical region. The eccentricity, e, of the ellipse is defined by

$$e^2 = 1 - \frac{b^2}{a^2}. \tag{6.5}$$

In section (1.2.1) we saw that for force distributions satisfying the symmetries required in the contact problem, the surface displacement integrals (1.8) may be decoupled into normal and tangential systems by defining the relative and absolute normal displacements as

$$\begin{aligned} w_r(x,y) &= \frac{1}{2}\{w_+(x,y) - w_-(x,y)\} \\ w_a(x,y) &= \frac{1}{2}\{w_+(x,y) + w_-(x,y)\} \end{aligned} \tag{6.6}$$

where $w_+(x,y)$ is the displacement in the z-direction on the surface of the half-space

$z < 0$ due to the distribution (P, Q, N) and $w_-(x, y)$ is the displacement on the surface of the half-space $z > 0$ due to the distribution $(-P, -Q, -N)$. Similar definitions may be made for the functions $u_r(x, y)$, $u_a(x, y)$, $v_r(x, y)$ and $v_a(x, y)$ where $u(x, y)$ and $v(x, y)$ are the tangential displacements in the x- and $y-$ directions respectively.

The surface displacements are given by the integrals (1.8) which were derived in section (1.2.1) from the results of the Boussinesq and Cerutti problems. The decoupled displacements required in this chapter are:

$$\begin{aligned} u_r(x,y) &= \int_{\mathcal{R}} \left\{ \frac{BP(x',y')}{S} + \frac{C\,[X^2 P(x',y') + XYQ(x',y')]}{S^3} \right\} \mathrm{d}x'\,\mathrm{d}y' \\ w_r(x,y) &= \int_{\mathcal{R}} \frac{BN(x',y')}{S}\,\mathrm{d}x'\,\mathrm{d}y'. \end{aligned} \tag{6.7}$$

Details of the method of calculation of these integrals for the pressure distributions of the forms (6.1), (6.2) and (6.3) over the region (6.4), are given in appendix C. For the Hertz distributions (6.1) and (6.2), the required displacements are:

$$\begin{aligned} u_r(x,y) &= u_0 + \frac{\pi b}{e^2} K \left\{ (Be^2 + C)\mathbf{K}(e) - C\mathbf{E}(e) \right\} \\ &\quad - \frac{x^2}{a^2}\frac{\pi b}{e^4} K \left\{ \left[2C + e^2(B - C)\right]\mathbf{K}(e) - (Be^2 + 2C)\mathbf{E}(e) \right\} \\ &\quad - \frac{y^2}{b^2}\frac{\pi b}{e^4} K \left\{ \left[2C + e^2(B - C)\right]\mathbf{E}(e) - (1 - e^2)(Be^2 + 2C)\mathbf{E}(e) \right\} \\ &\quad + \frac{2\pi b}{a^2 e^4} LC \left\{ (2 - e^2)\mathbf{K}(e) - 2\mathbf{E}(e) \right\} xy \end{aligned} \tag{6.8}$$

$$\begin{aligned} v_r(x,y) &= v_0 + \frac{\pi b}{e^2} L \left\{ [Be^2 - (1 - e^2)C]\mathbf{K}(e) + C\mathbf{E}(e) \right\} \\ &\quad - \frac{x^2}{a^2}\frac{\pi b}{e^4} L \left\{ [Be^2 - 2(1 - e^2 - 2(1 - e^2)C]\mathbf{K}(e) + [(2 - e^2)C - Be^2]\mathbf{E}(e) \right\} \\ &\quad - \frac{y^2}{b^2}\frac{\pi b}{e^4} L \left\{ [C(1 - e^2)(2 - e^2) - Be^2(1 - e^2)]\mathbf{K}(e) + [Be^2 - 2(1 - e^2)]\mathbf{E}(e) \right\} \\ &\quad + \frac{2\pi b}{a^2 e^4} KC \left\{ (2 - e^2)\mathbf{K}(e) - 2\mathbf{E}(e) \right\} xy \end{aligned} \tag{6.9}$$

$$w_r(x,y) = w_0 + \pi b B N_0 \left\{ \mathbf{K}(e) - \frac{x^2}{a^2}\frac{\mathbf{K}(e) - \mathbf{E}(e)}{e^2} - \frac{y^2}{b^2}\frac{\mathbf{E}(e) - (1 - e^2)\mathbf{K}(e)}{e^2} \right\} \tag{6.10}$$

where $\mathbf{K}(e)$ and $\mathbf{E}(e)$ are complete elliptic integrals of the first and second kinds respec-

tively, as defined in appendix C, and L is the force constant for the distribution of the form (6.2) in the y-direction. For the tangential punch-type pressure (6.3), the required displacements are:

$$u_r(x,y) = u_0 + \frac{2\pi b}{e^2} K \left\{ (Be^2 + C)\mathbf{K}(e) - C\mathbf{E}(e) \right\} \tag{6.11}$$

$$v_r(x,y) = v_0 + \frac{2\pi b}{e^2} L \left\{ [Be^2 - C(1-e^2)]\mathbf{K}(e) + C\mathbf{E}(e) \right\} \tag{6.12}$$

which are uniform across the region on which the distribution acts.

6.2.1 The Normal Hertz Problem

In section (1.2.3) the geometry of two bodies of general profiles was analysed; the point of first contact defined an origin O of a rectangular system of Cartesian coordinates $Oxyz$ with the xy-plane being the tangent plane common to the two bodies, and the z-axis being directed into the lower body. Recall that when the bodies are compressed normally to form a finite contact area, the conditions of contact on the contact area are

$$2w_r(x,y) = \delta - \alpha x^2 - \beta y^2 \tag{6.13}$$

and outside the contact area we must have

$$2w_r(x,y) < \delta - \alpha x^2 - \beta y^2 \tag{6.14}$$

where α and β may be obtained in terms of the principle radii of curvature for the two bodies from the system (1.24), and δ is the approach of distant points in the two bodies. The usual Hertz assumptions of section (1.2.4) apply.

The shape of the contact area cannot be determined with certainty in advance. However, comparisons of the problem in elasticity may be made with an analogous problem in electrostatics. Hertz [30] recognised that a charge occupying an elliptical region on the surface of a conductor, the intensity of which varies as the ordinate of a semi-ellipsoid, gives rise to a potential throughout that surface which is parabolic. With this in mind, Hertz proposed that the contact area be an ellipse of the form

$$\frac{x^2}{a_0^2} + \frac{y^2}{b_0^2} \leq 1 \tag{6.15}$$

where a_0 and b_0 are the lengths of the principle axes and $a_0 > b_0$. The eccentricity of the ellipse is defined as $e^2 = 1 - b_0^2/a_0^2$. The corresponding normal pressure distribution is of the form (6.1):

$$N_0(x,y) = N_0\left(1 - \frac{x^2}{a_0^2} - \frac{y^2}{b_0^2}\right)^{1/2} \tag{6.16}$$

where N_0 is a force constant. The displacements on the ellipse (6.4) due to the above distribution are

$$w_r(x,y) = w_0 + BN_0\pi b_0\left\{\mathbf{K}(e) - \frac{x^2}{a_0^2}\frac{\mathbf{K}(e) - \mathbf{E}(e)}{e^2} - \frac{y^2}{b_0^2}\frac{\mathbf{E}(e) - (1-e^2)\mathbf{K}(e)}{e^2}\right\}. \tag{6.17}$$

Applying the condition of contact (6.13), we require that

$$\begin{aligned}\delta - \alpha x^2 - \beta y^2 \;&=\\ 2w_0 \;&+\; 2BN_0\pi b_0\left\{\mathbf{K}(e) - \frac{x^2}{a_0^2}\frac{\mathbf{K}(e) - \mathbf{E}(e)}{e^2} - \frac{y^2}{b_0^2}\frac{\mathbf{E}(e) - (1-e^2)\mathbf{K}(e)}{e^2}\right\}.\end{aligned} \tag{6.18}$$

By equating the constant terms and the coefficients of x^2 and y^2 we obtain values for the constants δ, α and β as

$$\begin{aligned}\delta &= 2w_0 = 2\pi BN_0b_0\mathbf{K}(e)\\ \alpha &= 2\pi BN_0b_0\left[\frac{\mathbf{K}(e) - \mathbf{E}(e)}{a_0^2e^2}\right]\\ \beta &= 2\pi BN_0b_0\left[\frac{\mathbf{E}(e) - (1-e^2)\mathbf{K}(e)}{b_0^2e^2}\right].\end{aligned} \tag{6.19}$$

The constant N_0 may be determined from the first equation of the above as

$$N_0 = \frac{w_0}{\pi Bb_0\mathbf{K}(e)} \tag{6.20}$$

giving a normal distribution of

$$N_0(x,y) = \frac{w_0}{\pi B b_0 \mathbf{K}(e)} \left(1 - \frac{x^2}{a_0^2} - \frac{y^2}{b_0^2}\right)^{1/2}. \tag{6.21}$$

To find the eccentricity e of the ellipse of contact, we write

$$\frac{\beta}{\alpha} = \frac{\mathbf{E}(e) - (1-e^2)\mathbf{K}(e)}{(1-e^2)\left[\mathbf{K}(e) - \mathbf{E}(e)\right]} \tag{6.22}$$

from which e can be found if α and β are known. Note that this equation is inverted compared to the equivalent equation (2.26) of reference [54]. Equation (2.26) of [54] is incorrect although the subsequent equations derived from it are believed to be correct. A similar expression to equation (6.22) may be found as equation (6) in Bryant and Keer [12].

To find the values of a_0 and b_0 in terms of the compression w_0 we write

$$(\alpha\beta)^{1/2} = \frac{1}{2R_e} = \frac{2B\pi N_0}{e^2 a_0} \left[\mathbf{K}(e) - \mathbf{E}(e)\right]^{1/2} \left[\mathbf{E}(e) - (1-e^2)\mathbf{K}(e)\right]^{1/2} \tag{6.23}$$

and so substituting for N_0 and writing in terms of R_e, we obtain

$$a_0^2 = \frac{4R_e w_0}{e^2 \mathbf{K}(e)} \left[\frac{\mathbf{K}(e) - \mathbf{E}(e)}{1-e^2}\right]^{1/2} \left[\mathbf{E}(e) - (1-e^2)\mathbf{K}(e)\right]^{1/2} \tag{6.24}$$

where the geometrical parameter R_e is defined in section (1.2.3) as

$$R_e = \frac{1}{2}(\alpha\beta)^{-1/2}. \tag{6.25}$$

The value of b_0 may be found using the eccentricity $e^2 = 1 - b_0^2/a_0^2$.

6.2.2 The Tangential Problem

The addition of tangential displacements to the normal problem follows the same method used for the spherical contact problem as seen in section (1.2.5). The relevant tangential force distributions are of the forms:

$$P_0(x,y) = K_0 \left(1 - \frac{x^2}{a_0^2} - \frac{y^2}{b_0^2}\right)^{1/2} \tag{6.26}$$

$$Q_0(x,y) = L_0 \left(1 - \frac{x^2}{a_0^2} - \frac{y^2}{b_0^2}\right)^{1/2} \tag{6.27}$$

in the tangential x- and y-directions respectively, K_0 and L_0 being force constants. Relative to the point of first contact, the displacement of the centre of the upper body is $(u_0, v_0, -w_0)$. The values of the two constants K_0 and L_0 can be calculated by applying the condition that there is no relative displacement of the two surfaces on the contact area. The required tangential displacements are

$$\begin{aligned} u_r(x,y) &= u_0 + \frac{\pi b_0}{e^2} K_0 \left\{ (Be^2 + C)\mathbf{K}(e) - C\mathbf{E}(e) \right\} \\ &\quad - \frac{x^2}{a_0^2} \frac{\pi b_0}{e^4} K_0 \left\{ \left[2C + e^2(B - C)\right] \mathbf{K}(e) - (Be^2 + 2C)\mathbf{E}(e) \right\} \\ &\quad - \frac{y^2}{b_0^2} \frac{\pi b_0}{e^4} K_0 \left\{ \left[2C + e^2(B - C)\right] \mathbf{E}(e) - (1 - e^2)(Be^2 + 2C)\mathbf{K}(e) \right\} \\ &\quad + \frac{2\pi b_0}{a_0^2 e^4} L_0 C \left\{ (2 - e^2)\mathbf{K}(e) - 2\mathbf{E}(e) \right\} xy \end{aligned} \tag{6.28}$$

with a similar expression for the displacements $v_r(x,y)$, derived from equation (6.9), and the no-slip condition gives values of K_0 and L_0 of:

$$\begin{aligned} K_0 &= \frac{-e^2 u_0}{\pi b_0 \{(Be^2 + C)\mathbf{K}(e) - C\mathbf{E}(e)\}} \\ L_0 &= \frac{-e^2 v_0}{\pi b_0 \{[Be^2 - C(1 - e^2)]\mathbf{K}(e) + C\mathbf{E}(e)\}} \end{aligned} \tag{6.29}$$

which determines the force tangential force distributions (6.26) and (6.27) during the initial state.

6.3 The Incremental Deformation

An incremental displacement is now imposed on the initial state of the previous section. The increment is of amount $(\delta u_0, \delta v_0, -\delta w_0)$ and is assumed to be small enough that contact is maintained between the two bodies. Following the Hertz distribution (6.21), the normal force becomes

$$N + \delta N = \frac{(w_0 + \delta w_0)}{\pi B b \mathbf{K}(e)} \left(1 - \frac{x^2}{a^2} - \frac{y^2}{b^2}\right)^{1/2} \tag{6.30}$$

where the lengths of the principal axes of the contact ellipse are now $2a$ and $2b$, replacing the initial lengths $2a_0$ and $2b_0$. It is assumed that the eccentricity of the contact ellipse is independent of the applied load and depends only on the local geometry of the contact ellipse and therefore we may write $a/b = a_0/b_0$. The semi-axis length for the incremental problem is

$$a^2 = \frac{4R_e(w_0 + \delta w_0)}{e^2\mathbf{K}(e)}\left[\frac{\mathbf{K}(e) - \mathbf{E}(e)}{1-e^2}\right]^{1/2}\left[\mathbf{E}(e) - (1-e^2)\mathbf{K}(e)\right]^{1/2}. \tag{6.31}$$

Analogous to the sphere problem of section (1.3.1), the incremental tangential force depends on the sign of δw_0. When $\delta w_0 < 0$ the tangential force distributions are of the forms

$$P + \delta P = K_1\left(1 - \frac{x^2}{a^2} - \frac{y^2}{b^2}\right)^{1/2} + K_2\left(1 - \frac{x^2}{a^2} - \frac{y^2}{b^2}\right)^{-1/2} \tag{6.32}$$

$$Q + \delta Q = L_1\left(1 - \frac{x^2}{a^2} - \frac{y^2}{b^2}\right)^{1/2} + L_2\left(1 - \frac{x^2}{a^2} - \frac{y^2}{b^2}\right)^{-1/2} \tag{6.33}$$

which we note is the sum of a Hertz-type pressure (6.2) and a punch pressure (6.3). To find the tangential displacements we make use of equations (6.8) and (6.11) to obtain

$$\begin{aligned} u_r(x,y) = {} & u_0 + \delta u_0 + \frac{\pi b}{e^2}(K_1 + 2K_2)\left\{(Be^2 + C)\mathbf{K}(e) - C\mathbf{E}(e)\right\} \\ & - \frac{x^2}{a^2}\frac{\pi b}{e^4}K_1\left\{\left[2C + e^2(B-C)\right]\mathbf{K}(e) - (Be^2 + 2C)\mathbf{E}(e)\right\} \\ & - \frac{y^2}{b^2}\frac{\pi b}{e^4}K_1\left\{\left[2C + e^2(B-C)\right]\mathbf{E}(e) - (1-e^2)(Be^2 + 2C)\mathbf{E}(e)\right\} \\ & + \frac{2\pi b_0}{a_0^2 e^4}L_1 C\left\{(2-e^2)\mathbf{K}(e) - 2\mathbf{E}(e)\right\}xy \end{aligned} \tag{6.34}$$

$$\begin{aligned} v_r(x,y) = {} & v_0 + \delta v_0 + \frac{\pi b}{e^2}(L_1 + 2L_2)\left\{[Be^2 - C(1-e^2)]\mathbf{K}(e) + C\mathbf{E}(e)\right\} \\ & - \frac{x^2}{a^2}\frac{\pi b}{e^4}L_1\left\{[Be^2 - 2C(1-e^2)]\mathbf{K}(e) + [C(2-e^2) - Be^2]\mathbf{E}(e)\right\} \\ & - \frac{y^2}{b^2}\frac{\pi b}{e^4}L_1\left\{(1-e^2)[C(2-e^2) - Be^2]\mathbf{K}(e) + [Be^2 - 2C(1-e^2)]\mathbf{E}(e)\right\} \\ & + \frac{2\pi b}{a^2 e^4}K_1 C\left\{(2-e^2)\mathbf{K}(e) - 2\mathbf{E}(e)\right\}xy. \end{aligned} \tag{6.35}$$

The no-slip condition applied over the contact area requires force constants

$$\begin{aligned} K_1 &= \frac{-a^2e^2u_0}{\pi a_0^2 b\left\{(Be^2+C)\mathbf{K}(e)-C\mathbf{E}(e)\right\}} \\ K_2 &= \frac{e^2\left[u_0(a^2-a_0^2)-a_0^2\delta u_0\right]}{2\pi a_0^2 b\left\{(Be^2+C)\mathbf{K}(e)-C\mathbf{E}(e)\right\}} \end{aligned} \tag{6.36}$$

and

$$\begin{aligned} L_1 &= \frac{-a^2e^2v_0}{\pi a_0^2 b\left\{[Be^2-C(1-e^2)]\mathbf{K}(e)+C\mathbf{E}(e)\right\}} \\ L_2 &= \frac{e^2\left[v_0(a^2-a_0^2)-a_0^2\delta v_0\right]}{2\pi a_0^2 b\left\{[Be^2-C(1-e^2)]\mathbf{K}(e)+C\mathbf{E}(e)\right\}}. \end{aligned} \tag{6.37}$$

When $\delta w_0 > 0$, new contact area is formed and the tangential force distributions are, in the x-direction,

$$P+\delta P = \begin{cases} K_1\left(1-\frac{x^2}{a_0^2}-\frac{y^2}{b_0^2}\right)^{1/2}+K_2\left(1-\frac{x^2}{a^2}-\frac{y^2}{b^2}\right)^{1/2} & , \quad (x,y)\in E^0 \\ K_2\left(1-\frac{x^2}{a^2}-\frac{y^2}{b^2}\right)^{1/2} & , \quad (x,y)\in E\setminus E^0 \end{cases} \tag{6.38}$$

and in the y-direction

$$Q+\delta Q = \begin{cases} L_1\left(1-\frac{x^2}{a_0^2}-\frac{y^2}{b_0^2}\right)^{1/2}+L_2\left(1-\frac{x^2}{a^2}-\frac{y^2}{b^2}\right)^{1/2} & , \quad (x,y)\in E^0 \\ L_2\left(1-\frac{x^2}{a^2}-\frac{y^2}{b^2}\right)^{1/2} & , \quad (x,y)\in E\setminus E^0 \end{cases} \tag{6.39}$$

where the regions E^0 and E are defined as the sets

$$E^0=\left\{(x,y):\frac{x^2}{a_0^2}+\frac{y^2}{b_0^2}\le 1\right\} \quad \text{and} \quad E=\left\{(x,y):\frac{x^2}{a^2}+\frac{y^2}{b^2}\le 1\right\}. \tag{6.40}$$

The displacements on the inner region E^0 are found by summing the displacements (6.8) due to the K_1 and K_2 terms of (6.38) to obtain

$$
\begin{aligned}
u_r(x,y) &= u_0 + \delta u_0 + \frac{\pi}{e^2}(b_0K_1 + bK_2)\left\{ (Be^2+C)\mathbf{K}(e) - C\mathbf{E}(e)\right\} \\
&- \frac{\pi x^2}{e^4}\left(\frac{b_0}{a_0^2}K_1 + \frac{b}{a^2}K_2\right)\left\{ \left[2C - e^2(B-C)\right]\mathbf{K}(e) - (Be^2+2C)\mathbf{E}(e) \right\} \\
&- \frac{\pi y^2}{e^4}\left(\frac{b_0}{b_0^2}K_1 + \frac{b}{b^2}K_2\right)\left\{ \left[2C + e^2(B-C)\right]\mathbf{E}(e) - (1-e^2)(Be^2+2C)\mathbf{E}(e) \right\} \\
&+ \frac{2\pi}{e^4}\left(\frac{b_0}{a_0^2}L_1 + \frac{b}{a^2}L_2\right)C\left\{ (2-e^2)\mathbf{K}(e) - 2\mathbf{E}(e) \right\} xy \qquad (6.41)
\end{aligned}
$$

$$
\begin{aligned}
v_r(x,y) &= v_0 + \delta v_0 + \frac{\pi}{e^2}(b_0L_1 + bL_2)\left\{ [Be^2 - C(1-e^2)]\mathbf{K}(e) + C\mathbf{E}(e)\right\} \\
&- \frac{\pi x^2}{e^4}\left(\frac{b_0}{a_0^2}L_1 + \frac{b}{a^2}L_2\right)\left\{ [Be^2 - 2C(1-e^2)]\mathbf{K}(e) + C\mathbf{E}(e) \right\} \\
&- \frac{\pi y^2}{e^4}\left(\frac{b_0}{b_0^2}L_1 + \frac{b}{b^2}L_2\right)\left\{ (1-e^2)[C(2-e^2) - Be^2]\mathbf{K}(e) + [Be^2 - 2(1-e^2)]\mathbf{E}(e) \right\} \\
&+ \frac{2\pi}{e^4}\left(\frac{b_0}{a_0^2}K_1 + \frac{b}{a^2}K_2\right)C\left\{ (2-e^2)\mathbf{K}(e) - 2\mathbf{E}(e) \right\} xy. \qquad (6.42)
\end{aligned}
$$

Applying the same no-slip condition over the original and newly created contact area, the force constants obtained are

$$
\begin{aligned}
K_1 &= \frac{e^2\left\{(a^2-a_0^2)u_0 - a_0^2\delta u_0\right\}}{\pi b_0(a_0^2-a^2)\left\{(Be^2+C)\mathbf{K}(e) - C\mathbf{E}(e)\right\}} \\
K_2 &= \frac{a^2e^2\delta u_0}{\pi b(a_0^2-a^2)\left\{(Be^2+C)\mathbf{K}(e) - C\mathbf{E}(e)\right\}} \qquad (6.43)
\end{aligned}
$$

and

$$
\begin{aligned}
L_1 &= \frac{e^2\left\{(a^2-a_0^2)v_0 - a_0^2\delta v_0\right\}}{\pi b_0(a_0^2-a^2)\left\{[Be^2 - C(1-e^2)]\mathbf{K}(e) + C\mathbf{E}(e)\right\}} \\
L_2 &= \frac{a^2e^2\delta v_0}{\pi b(a_0^2-a^2)\left\{[Be^2 - C(1-e^2)]\mathbf{K}(e) + C\mathbf{E}(e)\right\}} \qquad (6.44)
\end{aligned}
$$

which determines the tangential force distributions (6.38) and (6.39).

6.4 Calculation of the Total Forces

In section (3.5) the total forces acting between two contacting spheres were calculated by integrating the force distributions over the circular contact area. To calculate the total forces between two contacting bodies of arbitrary profiles, it is necessary to integrate the force distributions $P(x,y)$ over the contact area $\mathcal{R}$ as

$$\overline{P} = \int_{\mathcal{R}} P(x,y)\, \mathrm{d}\mathcal{R}. \tag{6.45}$$

For force distributions of the form

$$P(x,y) = K\left(1 - \frac{x^2}{a^2} - \frac{y^2}{b^2}\right)^{1/2} \tag{6.46}$$

the contact area is an ellipse given by equation (6.4) and may be represented in plane polar coordinates (r,θ) as

$$r = f(\theta) = (a^2 \sin^2\theta + b^2 \cos^2\theta)^{-1/2} ab. \tag{6.47}$$

Then the integral (6.45) may be transformed to

$$\overline{P} = K \int_{\theta=0}^{2\pi} \int_{r=0}^{f(\theta)} \left(1 - \frac{x^2}{a^2} - \frac{y^2}{b^2}\right)^{1/2} r\, \mathrm{d}r\, \mathrm{d}\theta \tag{6.48}$$

and using the results of appendix C, the integral is evaluated as

$$\overline{P} = \frac{2\pi ab}{3} K. \tag{6.49}$$

For the punch-type pressure

$$P(x,y) = K\left(1 - \frac{x^2}{a^2} - \frac{y^2}{b^2}\right)^{-1/2} \tag{6.50}$$

the total force may be obtained by substituting $P(x,y)$ into the integral (6.45) and evaluated in the same way as before to obtain

$$\overline{P} = 2\pi ab K. \tag{6.51}$$

6.4.1 Total Initial Forces

In the initial state, the normal force distribution is given by equation (6.16) and by using equation (6.49) the total normal force $\overline{N}_0$ may be calculated as

$$\overline{N}_0 = \frac{2w_0 a_0}{3B\mathbf{K}(e)}. \tag{6.52}$$

The total tangential forces $\overline{P}_0$ and $\overline{Q}_0$ may be calculated from equations (6.26) and (6.27) as

$$\begin{aligned} \overline{P}_0 &= \frac{-2e^2 u_0 a_0}{3\left\{(Be^2+C)\mathbf{K}(e) - C\mathbf{E}(e)\right\}} \\ \overline{Q}_0 &= \frac{-2e^2 v_0 a_0}{3\left\{[Be^2 - C(1-e^2)]\mathbf{K}(e) + C\mathbf{E}(e)\right\}}. \end{aligned} \tag{6.53}$$

6.4.2 Total Incremental Forces

Throughout the incremental deformation the normal force is given by equation (6.30) and the corresponding total force is

$$\overline{N_0 + \delta N} = \frac{2(w_0 + \delta w_0)a}{3B\mathbf{K}(e)}. \tag{6.54}$$

By subtracting the total initial force (6.52) from the above, we obtain the actual force increment $\overline{\delta N}$ as

$$\overline{\delta N} = \frac{2}{3B\mathbf{K}(e)}\left\{a(w_0 + \delta w_0) - a_0 w_0\right\}. \tag{6.55}$$

The tangential force distributions depend on the sign of the displacement increment δw_0. When $\delta w_0 < 0$, the total forces may be obtained from equations (6.32) and (6.33) as:

$$\overline{P + \delta P} = \frac{ae^2(u_0 a^2 - 3u_0 a_0^2 - 3a_0^2 \delta u_0)}{3a_0^2\left\{(Be^2+C)\mathbf{K}(e) - C\mathbf{E}(e)\right\}} \tag{6.56}$$

$$\overline{Q + \delta Q} = \frac{ae^2(v_0 a^2 - 3v_0 a_0^2 - 3a_0^2 \delta v_0)}{3a_0^2\left\{[Be^2 - C(1-e^2)]\mathbf{K}(e) + C\mathbf{E}(e)\right\}} \tag{6.57}$$

with force increments of:

$$\overline{\delta P} = \frac{e^2\{3aa_0^2 - u_0(a_0-a)^2(a+2a_0)\delta u_0\}}{3a_0^2\{(Be^2+C)\mathbf{K}(e) - C\mathbf{E}(e)\}} \tag{6.58}$$

$$\overline{\delta Q} = \frac{e^2\{3aa_0^2 - v_0(a_0-a)^2(a+2a_0)\delta v_0\}}{3a_0^2\{[Be^2 - C(1-e^2)]\mathbf{K}(e) + C\mathbf{E}(e)\}}. \tag{6.59}$$

For $\delta w_0 > 0$, the total forces are obtained from equations (6.38) and (6.39) as

$$\overline{P+\delta P} = \frac{2e^2\{(a^2+aa_0+a_0^2)\delta u_0 + a_0(a_0+a)u_0\}}{3(a+a_0)\{(Be^2+C)\mathbf{K}(e) - \mathbf{E}(e)\}} \tag{6.60}$$

$$\overline{Q+\delta Q} = \frac{2e^2\{(a^2+aa_0+a_0^2)\delta v_0 + a_0(a_0+a)v_0\}}{3(a+a_0)\{[Be^2 - C(1-e^2)]\mathbf{K}(e) + C\mathbf{E}(e)\}} \tag{6.61}$$

with force increments of:

$$\overline{\delta P} = \frac{2e^2(a^2+aa_0+a_0^2)\delta u_0}{3(a+a_0)\{(Be^2+C)\mathbf{K}(e) - \mathbf{E}(e)\}} \tag{6.62}$$

$$\overline{\delta Q} = \frac{2e^2(a^2+aa_0+a_0^2)\delta v_0}{3(a+a_0)\{[Be^2 - C(1-e^2)]\mathbf{K}(e) + C\mathbf{E}(e)\}}. \tag{6.63}$$

6.5 The Linearised Increments

When the incremental displacement is much smaller than the initial displacement, the increments δu_0, δv_0 and δw_0 may be regarded as infinitesimals. As such, the force increments (6.58), (6.59), (6.62) and (6.63) may be expanded in powers of δu_0, δv_0 and δw_0 in a similar way as was seen for spheres in section (3.6). Recall that the incremental radius a is given by equation (6.31) and may be written as

$$a = (R_* w_0)^{1/2}\left(1 + \frac{\delta w_0}{w_0}\right)^{1/2} \tag{6.64}$$

where we have defined

$$R_* = \frac{4R_e}{e^2\mathbf{K}(e)}\left[\frac{\mathbf{K}(e) - \mathbf{E}(e)}{1-e^2}\right]^{1/2}[\mathbf{E}(e) - (1-e^2)\mathbf{K}(e)]^{1/2}. \tag{6.65}$$

Equation (6.64) may be expanded in powers of $\delta w_0/w_0$. For the normal increment $\overline{\delta N}$,

we wish to expand the expression

$$\overline{\delta N} = \frac{2}{3B\mathbf{K}(e)} \{a(w_0 + \delta w_0) - a_0 w_0\}. \tag{6.66}$$

By replacing the radii a_0 and a in the above, we obtain

$$\overline{\delta N} = \frac{2R_*^{1/2}}{3B\mathbf{K}(e)} w_0^{3/2} \left\{ \left(1 + \frac{\delta w_0}{w_0}\right)^{3/2} - 1 \right\} \tag{6.67}$$

which may be expanded to first order to give

$$\overline{\delta N} = \frac{(R_* w_0)^{1/2} \delta w_0}{B\mathbf{K}(e)}. \tag{6.68}$$

Considering the tangential increment $\overline{\delta P}$ when $\delta w_0 > 0$, it is necessary to expand the expression

$$\frac{a_0^2 + a a_0 + a^2}{a + a_0}. \tag{6.69}$$

The δw_0 dependencies of the above may be expanded as

$$\frac{2w_0 + \delta w_0 + w_0^{1/2}(w_0 + \delta w_0)^{1/2}}{(w_0 + \delta w_0)^{1/2} + w_0^{1/2}} = \frac{3w_0^{1/2}}{2} + \frac{3}{8w_0^{1/2}} \delta w_0 + O(\delta w_0^2) \tag{6.70}$$

from which the force increments (6.62) and (6.63) become

$$\begin{aligned} \overline{\delta P} &= \frac{e^2 (R_* w_0)^{1/2} \delta u_0}{(Be^2 + C)\mathbf{K}(e) - C\mathbf{E}(e)} \\ \overline{\delta Q} &= \frac{e^2 (R_* w_0)^{1/2} \delta v_0}{[Be^2 - C(1 - e^2)]\mathbf{K}(e) + C\mathbf{E}(e)}. \end{aligned} \tag{6.71}$$

The same expansion technique, when applied to the increments $\overline{\delta P}$ and $\overline{\delta Q}$ in the case $\delta w_0 < 0$, yields the same equations as above. Thus, when the incremental displacements are infinitesimal, equations (6.58), (6.59), (6.62) and (6.63) reduce to the same forms (6.71) regardless of the conditions $\delta w_0 > 0$ or $\delta w_0 < 0$. It may also be checked, using appendix D, that the above expressions reduce to the sphere force increments (3.162) and (3.163) as the eccentricity e tends to zero.

6.6 The Geometry of Spheroidal Bodies

6.6.1 Oblate Spheroidal Coordinates

Having examined the contact problem for solids of a general profile, we apply the results obtained to oblate spheroidal bodies. Gladwell [27] page 498, defines a system of oblate spheroidal coordinates (ξ, η, θ) which are related to cylindrical polar coordinates (r, z, θ) by the equations

$$\begin{aligned} r &= a' \left[(1+\xi^2)(1-\eta^2)\right]^{1/2} \\ z &= a'\xi\eta \end{aligned} \tag{6.72}$$

where $-1 \leq \eta \leq 1$ and $\xi \geq 0$. The surfaces $\xi = 0$ and $\eta = 0$ are respectively the interior and exterior of the circle $r = a'$, where a' is a constant, in the plane $z = 0$. The surfaces on which ξ is constant are given by the concentric ellipsoids

$$\frac{r^2}{a'^2(1+\xi^2)} + \frac{z^2}{a'^2\xi^2} = 1 \tag{6.73}$$

from which the principal axes may be identified to be of length $2A$ in the r-direction and of length $2C$ is the z-direction, where

$$\xi = \frac{C}{\sqrt{A^2 - C^2}} \quad \text{and} \quad a' = \sqrt{A^2 - C^2}. \tag{6.74}$$

In terms of rectangular Cartesian coordinates, the system may be written as

$$\begin{aligned} x &= a' \left[(1+\xi^2)(1-\eta^2)\right]^{1/2} \cos\theta \\ y &= a' \left[(1+\xi^2)(1-\eta^2)\right]^{1/2} \sin\theta \\ z &= a'\xi\eta \end{aligned} \tag{6.75}$$

and the scale factors of this transformation from (x, y, z) to (ξ, η, θ) are given by

$$h_1 = \left|\frac{\partial \mathbf{r}}{\partial \xi}\right| = a' \left(\frac{\xi^2 + \eta^2}{1+\xi^2}\right)^{1/2}$$

$$
\begin{aligned}
h_2 &= \left|\frac{\partial \mathbf{r}}{\partial \eta}\right| = a'\left(\frac{\xi^2+\eta^2}{1-\eta^2}\right)^{1/2} \\
h_3 &= \left|\frac{\partial \mathbf{r}}{\partial \theta}\right| = a'\left[(1+\xi^2)(1-\eta^2)\right]^{1/2}
\end{aligned} \tag{6.76}
$$

where $\mathbf{r} = (x, y, z)$. The unit tangent vectors to the ξ-, η- and θ-coordinate lines are, respectively,

$$
\begin{aligned}
\mathbf{e}_\xi &= \frac{1}{h_1}\frac{\partial \mathbf{r}}{\partial \xi} = \left(\frac{1-\eta^2}{\xi^2+\eta^2}\right)^{1/2}\left[\xi\cos\theta,\ \xi\sin\theta,\ \eta\left(\frac{1+\xi^2}{1-\eta^2}\right)^{1/2}\right] \\
\mathbf{e}_\eta &= \frac{1}{h_2}\frac{\partial \mathbf{r}}{\partial \eta} = \left(\frac{1+\xi^2}{\xi^2+\eta^2}\right)^{1/2}\left[-\eta\cos\theta,\ -\eta\sin\theta,\ \xi\left(\frac{1-\eta^2}{1+\xi^2}\right)^{1/2}\right] \\
\mathbf{e}_\theta &= \frac{1}{h_3}\frac{\partial \mathbf{r}}{\partial \theta} = [-\sin\theta,\ \cos\theta,\ 0]
\end{aligned} \tag{6.77}
$$

which are mutually perpendicular and form a right-handed orthonormal triad. On the surfaces of constant ξ, the vectors $\mathbf{e}_\eta$ and $\mathbf{e}_\theta$ are tangent to the surface and define the tangent plane at a point, and the vector $\mathbf{e}_\xi$ is always normal to the surface as shown in figure 6-1.

6.6.2 Curvature of a Spheroidal Surface

Let $\mathbf{r} = \mathbf{r}(s,t)$, where s and t are scalars, be a parameterisation of a smooth surface expressed in rectangular Cartesian coordinates relative to some origin O. The principal curvatures, λ_1 and λ_2, at a general point P on the surface are the solutions of the generalised eigenvalue problem

$$
\lambda\begin{bmatrix} \frac{\partial \mathbf{r}}{\partial s}\cdot\frac{\partial \mathbf{r}}{\partial s} & \frac{\partial \mathbf{r}}{\partial t}\cdot\frac{\partial \mathbf{r}}{\partial s} \\ \frac{\partial \mathbf{r}}{\partial t}\cdot\frac{\partial \mathbf{r}}{\partial s} & \frac{\partial \mathbf{r}}{\partial t}\cdot\frac{\partial \mathbf{r}}{\partial t} \end{bmatrix}\mathbf{v} = \begin{bmatrix} \frac{\partial^2 \mathbf{r}}{\partial s^2}\cdot\mathbf{n} & \frac{\partial^2 \mathbf{r}}{\partial s\partial t}\cdot\mathbf{n} \\ \frac{\partial^2 \mathbf{r}}{\partial s\partial t}\cdot\mathbf{n} & \frac{\partial^2 \mathbf{r}}{\partial t^2}\cdot\mathbf{n} \end{bmatrix}\mathbf{v} \tag{6.78}
$$

where $\mathbf{v}$ is a principal direction and $\mathbf{n}$ is the outward normal to the surface at P. The partial derivatives are also evaluated at the surface point P. The radii of curvature, denoted ρ_1 and ρ_2, are defined to be the reciprocal of the curvatures, that is

$$
\rho_1 = \frac{1}{\lambda_1} \quad \text{and} \quad \rho_2 = \frac{1}{\lambda_2}. \tag{6.79}
$$

We now wish to find the curvatures of the spheroidal surfaces defined by equations (6.74) and (6.73). The surface is parameterised by η and θ with ξ held constant. Solving the

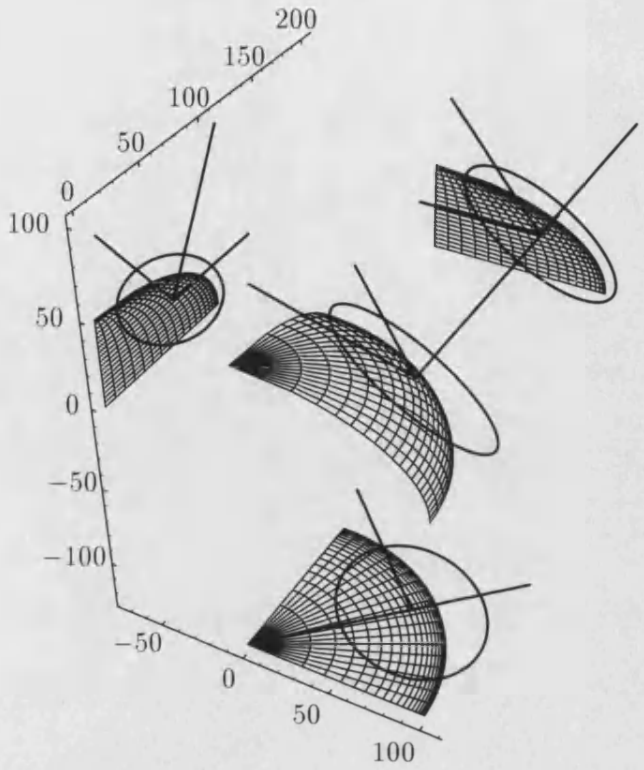

Figure 6-1: *Unit tangent vectors on spheroidal surface*

eigenvalue problem (6.78) with $\mathbf{r} = (x, y, z)$ as defined by equation (6.75) and identifying the unit normal $\mathbf{n}$ as being $\mathbf{e}_\xi$ from equation (6.77), we obtain the curvatures

$$\begin{aligned} \lambda_1 &= \frac{-\xi(1+\xi^2)^{1/2}}{a'(\xi^2+\eta^2)^{3/2}} \\ \lambda_2 &= \frac{-\xi}{a'\left[(1+\xi^2)(\xi^2+\eta^2)\right]^{1/2}}. \end{aligned} \tag{6.80}$$

The radii of curvature may now be obtained from equations (6.79) and (6.80) and are negative since the surface curves away from the point P at which they are evaluated. Also, there is no θ-dependence due to the rotational symmetry of the surface about the z-axis.

6.7 Contact of Aligned Spheroidal Bodies

Figure 6-2 shows two identical spheroidal bodies with aligned axes in contact. The point of first contact, relative to the centre of the upper spheroid, can be expressed in terms

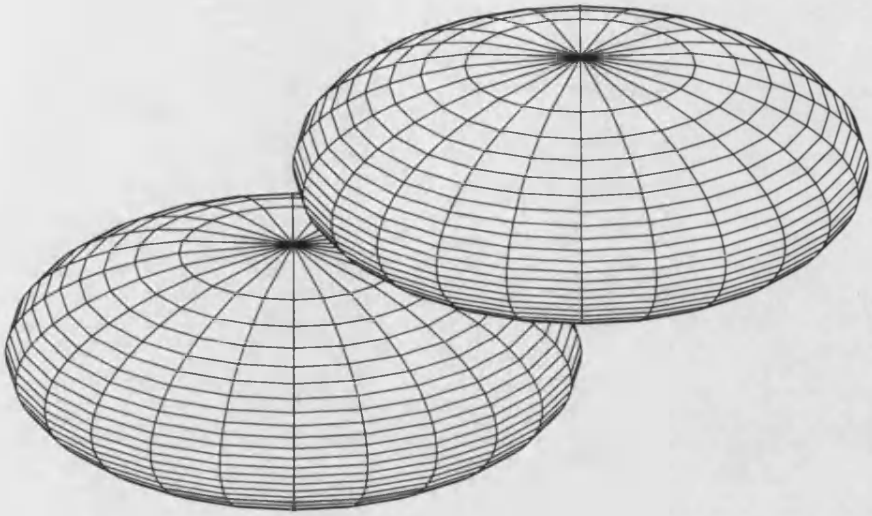

Figure 6-2: *Two aligned oblate spheroidal bodies in contact*

of the two varying parameters η and θ and is taken as the origin in a rectangular system of cartesian coordinates in which the tangent lines $\mathbf{e}_\theta$, $\mathbf{e}_\eta$ and $\mathbf{e}_\xi$ correspond to the x-, y- and z-axes respectively. By symmetry, the radii of curvature at the contact point are the same for both bodies, that is

$$R_1' = R_2' \quad \text{and} \quad R_1'' = R_2''. \tag{6.81}$$

Recall the constants α and β which appear in the conditions of contact (6.13) and (6.14), the values of which were found in section (1.2.3) for bodies of arbitrary profile. In the case of spheroids, α and β may be found in terms of the radii R_1' and R_1'' by solving the equations (1.24). The angle between the two sets of axes of principal curvature for each body is 180° and so taking $\theta = \pi$ in the equations (1.24) we obtain

$$\alpha + \beta = \frac{1}{R_1'} + \frac{1}{R_1''} \quad \text{and} \quad |\alpha - \beta| = \frac{1}{R_1'} - \frac{1}{R_1''} \tag{6.82}$$

which gives the values of α and β as

$$\alpha = \frac{1}{R_1'} \quad \text{and} \quad \beta = \frac{1}{R_1''}. \tag{6.83}$$

The principal radii of curvature are found from equations (6.79) and (6.80) as:

$$\begin{aligned} R_1' &= \frac{a'}{\xi}\left[(1+\xi^2)(\xi^2+\eta^2)\right]^{1/2} \\ R_1'' &= \frac{a'(\xi^2+\eta^2)^{3/2}}{\xi(1+\xi^2)^{1/2}}. \end{aligned} \tag{6.84}$$

The spheroid has planes of symmetry on which θ is constant. The curvature R_1'' lies in one of these planes of symmetry (determined by the value of θ) and the curvature R_1' lies in the perpendicular plane. The effective radius of curvature is defined as

$$R_e = \frac{1}{2}(\alpha\beta)^{-1/2} = \frac{a'(\xi^2+\eta^2)}{2\xi}. \tag{6.85}$$

Applying these values to the results of sections (6.2.1) and (6.2.2), equation (6.22) reduces to

$$\frac{\xi^2+\eta^2}{1+\xi^2} = \frac{(1-e^2)\left[\mathbf{K}(e)-\mathbf{E}(e)\right]}{\mathbf{E}(e)-(1-e^2)\mathbf{K}(e)} \tag{6.86}$$

from which the eccentricity of the contact ellipse may be found in terms of the parameter η which is the scaled distance of the contact point from the plane $z = 0$. Equation (6.24) becomes

$$a_0^2 = \frac{2w_0}{e^2\mathbf{K}(e)}\frac{a'(\xi^2+\eta^2)^{3/2}}{\xi(1+\xi^2)^{1/2}}\left[\mathbf{K}(e)-\mathbf{E}(e)\right] \tag{6.87}$$

which gives a_0 (and hence b_0) in terms of η and the compression w_0. Using the above equations (6.84), (6.22) and (6.87) the initial force distributions (6.26) and (6.27) may be determined.

The equivalent expression for the incremental radius a is

$$a^2 = \frac{2(w_0+\delta w_0)}{e^2\mathbf{K}(e)}\frac{a'(\xi^2+\eta^2)^{3/2}}{\xi(1+\xi^2)^{1/2}}\left[\mathbf{K}(e)-\mathbf{E}(e)\right] \tag{6.88}$$

from which, together with the equations (6.84) and (6.22) the linearised incremental forces (6.68) and (6.71) may be determined.

Chapter 7

A Random Packing of Oblate Spheroidal Particles

7.1 Introduction

In chapter 6, we derived contact laws for the compression of two aligned spheroidal bodies subjected to an initial oblique compression followed by a smaller incremental deformation. The results obtained are used in this chapter to model a random packing of these spheroidal particles, the motivation being to apply the results to the study of shale-like rocks.

Scanning electron microphotographs of shale samples, such as that shown in figure 7-1, reveal a complex microstructure consisting of connected solid and fluid phases. The solid phase is comprised of several mineral components, mostly clay in the form of flat plate-like particles which make up the load bearing skeleton of the shale. Other minerals are present as isolated inclusions which are not connected and so are not load bearing and therefore have less effect than the clay platelets on the overall elastic properties of the shale. The platelets are seen to have a preferred direction of orientation which is horizontal with local misalignment in the vicinity of larger silt particles. The platelets tend to wrap around any inclusion causing only local disorder in particle alignment.

Shales make up 75 per cent of sedimentary basins and overlie most hydrocarbon bearing reservoirs. Successful seismic imaging of such reservoirs relies on a knowledge of the elastic properties of the overlying strata. At present, most models of hydrocarbon

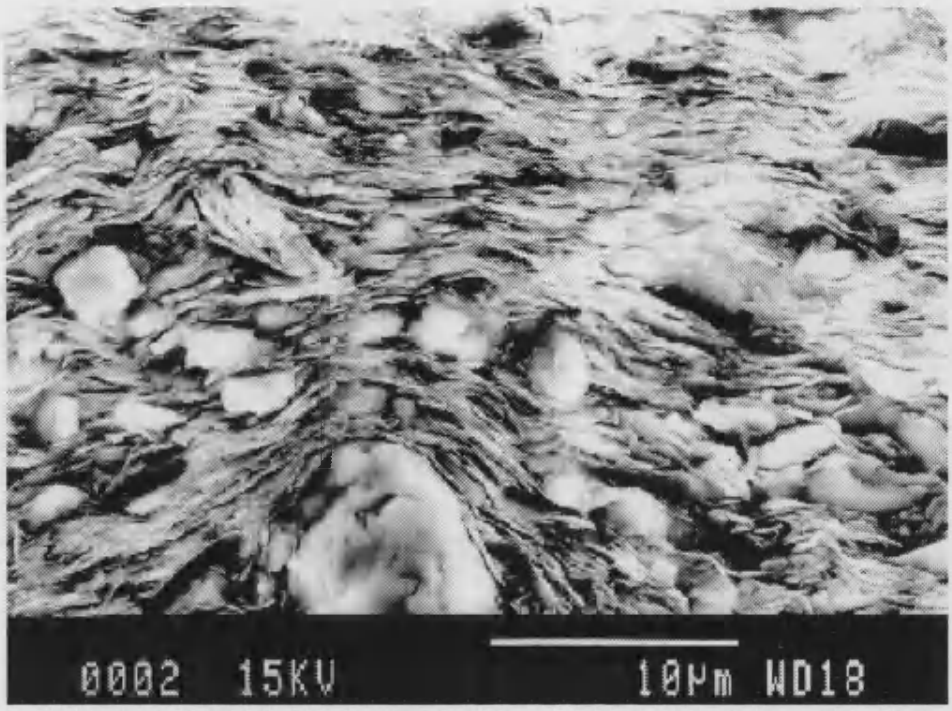

Figure 7-1: *Scanning electron-micrograph of shale sample*

reservoirs treat the shale as an isotropic fluid layer. However, shales are known to be elastically anisotropic and this anisotropy must be taken into account when using more advanced techniques of seismic imaging. Ideally, any proposed model of anisotropic shale behaviour would predict macro-seismic properties from micro-structural information such as the elastic moduli of the matrix material and the shale porosity. Due to the complex microstructure of shales, analysis of scanning electron microphotographs must be used to propose simplified models of shale structure. One such model is used by Hornby, Schwartz and Hudson [32] in which the clay platelets are treated as spheroids of high cross sectional aspect ratio and the elastic properties are determined using a combination of the self-consistent approximation (see Hill [31]) and differential effective medium theory. The work in this chapter models the platelets again as spheroids, but they are treated as interacting solid bodies rather than a collection of inclusions as in the self-consistent method. Hence the effects of inter-platelet contact will play an important role in determining the elastic properties of the medium. Similar work, with sphere packings, has already successfully modelled certain types of porous rocks and this work adapts the averaging scheme of Walton [67] which was described in section (1.3.1).

The problem that we will be considering here is the determination of the effective elastic moduli of a random packing of oblate spheroidal bodies. The spheroids are taken to be identical in every way, the matrix material is taken to be homogeneous and elastically isotropic and all spheroids are assumed to lie flat and be aligned in the same direction. The packing may be considered as a random sphere packing scaled down by a certain factor in the z-direction. For most shales the scale factor is about 20, see Hornby, Schwartz and Hudson [32]. In such a model the effect of inter-granular contact will play an important role and, in particular, the coefficient of friction between the platelets is assumed to be infinite in analogy with section (1.3.1).

Using the results of the previous chapter, the packing is subjected to an initial confining strain which is small enough that the equations of linear elasticity still apply in the spheroid material. The resulting stress is then determined in terms of this strain. An incremental strain is then imposed on this initial state and is assumed to be infinitesimal in the sense that it is much smaller than the confining strain. The resulting incremental stress is determined in terms of the incremental strain and from this relationship the effective elastic moduli can be determined.

The spheroidal contact problem was seen to be much more complex than the sphere contact problem considered in Walton [66] and consequently, the averaging procedure is harder to implement. The analogous integrals treated in section (3.2) cannot be evaluated analytically, but we are still able to write down the effective elastic moduli in terms of an averaging integral suitable for numerical integration.

7.2 The Random Packing

7.2.1 Packing Geometry

The packing consists of a large number of oblate spheroids randomly packed together and initially in point contact. The axis of symmetry of each spheroid is taken to be aligned parallel to the z-axis as seen in chapter 6.

In the undeformed configuration, the centre of the n-th spheroid is at position vector $\mathbf{X}^{(n)}$ relative to some fixed origin. Under the imposed deformation, the centre of the spheroid suffers a rigid body displacement $\mathbf{u}^{(n)}$. The rotation of each spheroid about its centre is denoted $\boldsymbol{\omega}^{(n)}$. Figure 7-2 shows the n-th and m-th spheroids, starting from

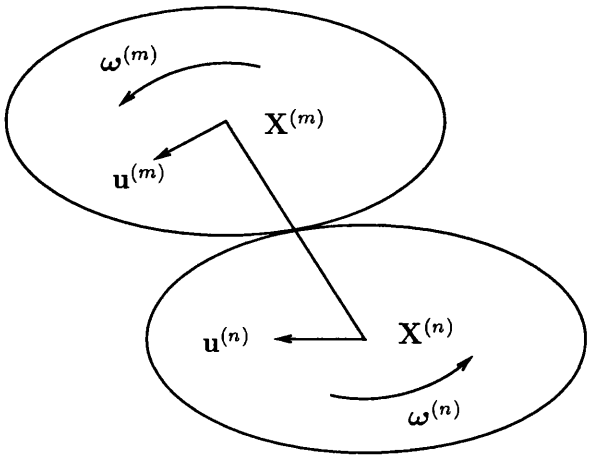

Figure 7-2: *Initial deformation with rotations*

point contact, undergoing the initial deformation. The unit vector joining the centres of two touching spheroids is given by

$$\mathbf{I}^{(nm)} = \frac{\mathbf{X}^{(n)} - \mathbf{X}^{(m)}}{2D^{(nm)}} \tag{7.1}$$

and is directed from $\mathbf{X}^{(m)}$ towards $\mathbf{X}^{(n)}$. The scalar $D^{(nm)}$ is the distance from the centre of the spheroid to a point on its surface (in this case the contact point). The superscript (nm) will be omitted from now on for brevity. By symmetry, we see that the initial position of the contact point is

$$\frac{\mathbf{X}^{(n)} + \mathbf{X}^{(m)}}{2} \tag{7.2}$$

and relative to $\mathbf{X}^{(m)}$ the contact point is located at

$$\mathbf{x}_c^{(nm)} = \frac{\mathbf{X}^{(n)} - \mathbf{X}^{(m)}}{2}. \tag{7.3}$$

We make use of the system of oblate spheroidal coordinates described in section (6.6.1). The surfaces are parameterised by η and θ with the third coordinate ξ fixed and dependent only on the geometry of the spheroids. The value of ξ and the constant a' are given in terms of the lengths of the principal axes of the spheroids by equation (6.74). Each point on the surface has a unique coordinate pair (η, θ) and therefore at the contact point there exist η and θ such that

$$\mathbf{x}_c^{(nm)} = (a'\left[(1+\xi^2)(1-\eta^2)\right]^{1/2}\cos\theta,\ a'\left[(1+\xi^2)(1-\eta^2)\right]^{1/2}\sin\theta,\ a'\xi\eta) \tag{7.4}$$

which is also relative to the centre of the m-th spheroid. At this point the unit normal is, from equation (6.77),

$$\mathbf{e}_\xi^{(nm)} = \left(\frac{1-\eta^2}{\xi^2+\eta^2}\right)^{1/2}\left[\xi\cos\theta,\ \xi\sin\theta,\ \eta\left(\frac{1+\xi^2}{1-\eta^2}\right)^{1/2}\right]. \tag{7.5}$$

Combining equations (7.1), (7.3) and (7.5) we obtain a relationship between the unit normal $\mathbf{e}_\xi^{(nm)}$ and the position vectors $\mathbf{X}^{(n)}$ and $\mathbf{X}^{(m)}$:

$$\mathbf{e}_\xi^{(nm)} = \frac{\xi}{a'\sqrt{(1+\xi^2)(\xi^2+\eta^2)}}\begin{bmatrix} 1 & 0 & 0 \\ 0 & 1 & 0 \\ 0 & 0 & \dfrac{1+\xi^2}{\xi^2} \end{bmatrix}\frac{\mathbf{X}^{(n)}-\mathbf{X}^{(m)}}{2}. \tag{7.6}$$

Inverting the matrix we obtain

$$\frac{\mathbf{X}^{(n)}-\mathbf{X}^{(m)}}{2} = M\mathbf{e}_\xi^{(nm)} \tag{7.7}$$

where

$$M = \frac{a'}{\xi}\sqrt{(1+\xi^2)(\xi^2+\eta^2)}\begin{bmatrix} 1 & 0 & 0 \\ 0 & 1 & 0 \\ 0 & 0 & \dfrac{\xi^2}{1+\xi^2} \end{bmatrix}. \tag{7.8}$$

The left-hand side of equation (7.7) is equal to $D\mathbf{I}^{(nm)}$ giving a relationship between the unit normal at the contact point and the unit vector between the two centres as

$$D\mathbf{I}^{(nm)} = M\mathbf{e}_\xi^{(nm)}. \tag{7.9}$$

Finally, it is easily shown that the scalar D is given by

$$D = a'\sqrt{1+\xi^2-\eta^2}. \tag{7.10}$$

7.3 The Averaging Scheme

The averaging scheme used here is similar to that used in section (1.3.1) when considering a random packing of spheres. Quantities such as the average Cauchy stress are defined as

$$\langle \sigma_{ij} \rangle = \frac{1}{V} \int \sigma_{ij} \, \mathrm{d}V = \frac{1}{V} \sum_n \int_{V_n} \sigma_{ij}^{(n)} \, \mathrm{d}V \tag{7.11}$$

in which V denotes the total volume of the medium and V_n denotes the volume of the n-th spheroid. As was the case when considering spheres, it can be shown that, for a single spheroid, we may write

$$\int_{V_n} \sigma_{ij}^{(n)} \, \mathrm{d}V = \frac{1}{2} \int_{S_n} (x_i' t_j^{(n)} + x_j' t_i^{(n)}) \, \mathrm{d}S \tag{7.12}$$

where $\mathbf{x}' = \mathbf{x} - \mathbf{X}^{(n)}$ denotes the position vector of a material point of the spheroid relative to its centre $\mathbf{X}^{(n)}$. The traction across the spheroidal surface S_n is denoted by $\mathbf{t}^{(n)}$ and will be zero at all points on the surface except for where the spheroid is in contact with other spheroids. Furthermore, the dimensions of the contact area are assumed to be small when compared with the dimensions of the spheroids and so, when spheroid n is in contact with spheroid m, we may approximate the material point $\mathbf{x}'$ by

$$\mathbf{x}' = \frac{1}{2}(\mathbf{X}^{(m)} - \mathbf{X}^{(n)}). \tag{7.13}$$

The integral of the traction of the contact area is now given by the force between the two bodies. The force exerted by spheroid m on spheroid n is denoted by $\mathbf{F}^{(nm)}$ and so equation (7.12) now reduces to

$$\int_{V_n} \sigma_{ij}^{(n)} \, \mathrm{d}V = \frac{1}{2} \sum_m \left\{ \frac{1}{2}(X_i^{(m)} - X_i^{(n)}) F_j^{(nm)} + \frac{1}{2}(X_j^{(m)} - X_j^{(n)}) F_i^{(nm)} \right\}, \tag{7.14}$$

the summation being over all spheroids in contact with the n-th spheroid. Substituting this into equation (7.11), and making use of equation (7.7), we obtain the average initial stress as

$$\langle \sigma_{ij} \rangle = -\frac{1}{V} \sum_{\text{contacts}} \left\{ M_{ik} e_{\xi k}^{(nm)} F_j^{(nm)} + M_{jk} e_{\xi k}^{(nm)} F_i^{(nm)} \right\} \tag{7.15}$$

in which the summation is now taken over all contacts between all spheroids. Since

each contact appears twice in the summation over both n and m, the factor $1/2$ in equation (7.14) does not appear. Assuming a packing dense enough, we may also write the above equation in terms of averaged quantities

$$\langle \sigma_{ij} \rangle = -\frac{nN}{2V} \{ \langle M_{ik} e_{\xi k} F_j \rangle + \langle M_{jk} e_{\xi k} F_i \rangle \} \tag{7.16}$$

where n is the average number of contacts per spheroid and N is the total number of spheroids within the volume V.

The volume concentration of spheroids is given by

$$\phi = \frac{NV_n}{V} \tag{7.17}$$

where the volume of the n-th spheroid is

$$V_n = \frac{4}{3}\pi a'^3 \xi(\xi^2 + 1) \tag{7.18}$$

and so substituting these into (7.16), we obtain the average initial stress as

$$\langle \sigma_{ij} \rangle = \frac{-3n\phi}{8\pi a'^3 \xi(\xi^2 + 1)} \{ \langle M_{ik} e_{\xi k} F_j \rangle + \langle M_{jk} e_{\xi k} F_i \rangle \} . \tag{7.19}$$

It now remains to determine the form of the force $\mathbf{F}^{(nm)}$ acting between the two spheroids.

7.3.1 The Symmetry Properties of the Averaging Scheme

First we discuss the symmetry properties of the averaging scheme as defined in section (7.3) by equation (7.11). The ranges of integration are η from -1 to 1 and θ from $-\pi$ to π. Therefore, for a non-zero result, the function which is integrated can be odd in neither η nor θ.

Typical expressions to be averaged involve the components of the matrix M_{ij} (7.8), which are even in η, and products of the components of the unit normal vector $\mathbf{e}_\xi$ defined by

$$\mathbf{e}_\xi = \left(\frac{1-\eta^2}{\xi^2+\eta^2} \right)^{1/2} \left[\xi \cos\theta,\ \xi \sin\theta,\ \eta \left(\frac{1+\xi^2}{1-\eta^2} \right)^{1/2} \right] . \tag{7.20}$$

We construct the following table for the components of $\mathbf{e}_\xi$:

Variable	$e_{\xi 1}$	$e_{\xi 2}$	$e_{\xi 3}$
η	even	even	odd
θ	even	odd	even.

It can be deduced from the above table that for a product of components $e_{\xi i}e_{\xi j}$ to be even in both η and θ, we must have $i = j$. Thus for a non-zero result when products of this type are averaged, the components must appear in equal pairs.

7.4 The Initial Deformed State

The initial deformation takes the form of an applied strain which compresses the spheroids together to form contact areas between spheroids initially in point contact, as described for spheres in chapter 1.

To determine the form of the vector force between two spheroids, we consider the displacement of the spheroids under the imposed deformation. The displacement of the contact area, relative to the centre of spheroid m, is

$$\frac{1}{2}(\mathbf{u}^{(m)} - \mathbf{u}^{(n)}) + \frac{1}{2}(\boldsymbol{\omega}^{(n)} + \boldsymbol{\omega}^{(m)}) \wedge D\mathbf{I}^{(nm)}. \tag{7.21}$$

Resolving into components normal and tangential to the surface at the contact point we find that the displacement along $\mathbf{e}_{\xi}^{(nm)}$, denoted w_0, is

$$w_0 = \left\{\frac{1}{2}(\mathbf{u}^{(m)} - \mathbf{u}^{(n)}) + \frac{1}{2}(\boldsymbol{\omega}^{(n)} + \boldsymbol{\omega}^{(m)}) \wedge D\mathbf{I}^{(nm)}\right\} \cdot \mathbf{e}_{\xi}^{(nm)}. \tag{7.22}$$

The tangential or shear displacement, being the remainder of the contact area displacement (7.21), is

$$\frac{1}{2}(\mathbf{u}^{(m)} - \mathbf{u}^{(n)}) + \frac{1}{2}(\boldsymbol{\omega}^{(n)} + \boldsymbol{\omega}^{(m)}) \wedge D\mathbf{I}^{(nm)} - w_0\mathbf{e}_{\xi}^{(nm)}. \tag{7.23}$$

Each spheroid will initially be in contact with more than one other spheroid and the forces acting across any contact area will cause displacements which will affect other contacts. However, in using contact theory, we have made the Hertzian assumptions that the contact area is small in relation to the size of the body and that each body may be replaced by an elastic half space when considering the forces and displacements on the contact area. Consequently, it is a good approximation to assume that the effects of one contact area on the others are negligible.

The total normal and tangential forces have previously been found in section (6.4) and so when combined with equations (7.21) and (7.23) we obtain

$$\begin{aligned}\mathbf{F}^{(nm)} &= \frac{2a_0w_0}{3B\mathbf{K}(e)}\mathbf{e}_\xi^{(nm)} + \sqrt{\frac{S_x^2(u_0/v_0)^2+S_y^2}{1+(u_0/v_0)^2}}\ \times \\ &\left\{\frac{1}{2}(\mathbf{u}^{(m)}-\mathbf{u}^{(n)}) + \frac{1}{2}(\boldsymbol{\omega}^{(n)}+\boldsymbol{\omega}^{(m)})\wedge D\mathbf{I}^{(nm)} - w_0\mathbf{e}_\xi^{(nm)}\right\} \qquad (7.24)\end{aligned}$$

where B and C are the elastic moduli given by equation (1.7), a_0 is the initial contact area radius described by equation (6.87), e is the contact area eccentricity (6.5) and $\mathbf{K}(e)$ and $\mathbf{E}(e)$ are the elliptic integrals given in appendix C. The stiffnesses in the x- and y-directions, S_x and S_y, are respectively defined as

$$\begin{aligned}S_x &= \frac{\overline{P_0}}{u_0} = \frac{2e^2a_0}{3\{(Be^2+C)\mathbf{K}(e)-C\mathbf{E}(e)\}} \\ S_y &= \frac{\overline{Q_0}}{v_0} = \frac{2e^2a_0}{3\{[Be^2-C(1-e^2)]\mathbf{K}(e)+C\mathbf{E}(e)\}}. \qquad (7.25)\end{aligned}$$

In index notation the above force may be written as

$$\begin{aligned}F_i^{(nm)} &= \frac{2a_0w_0}{3B\mathbf{K}(e)}e_{\xi i}^{(nm)} + \sqrt{\frac{S_x^2(u_0/v_0)^2+S_y^2}{1+(u_0/v_0)^2}}\ \times \\ &\left\{\frac{1}{2}(u_i^{(m)}-u_i^{(n)}) + \frac{1}{2}\epsilon_{ipq}(\omega_p^{(n)}+\omega_p^{(m)})DI_q^{(nm)} - w_0e_{\xi i}^{(nm)}\right\}. \qquad (7.26)\end{aligned}$$

We now make some assumptions about the form of the relative displacement $(\mathbf{u}^{(m)}-\mathbf{u}^{(n)})$ and the rotations $\boldsymbol{\omega}^{(n)}$ and $\boldsymbol{\omega}^{(m)}$. We assume that the displacement of each spheroid centre is consistent with the applied uniform strain, as discussed in section (1.3.1), that is

$$u_i^{(n)} = E_{ij}X_j^{(n)}. \qquad (7.27)$$

Clearly this is not exactly correct for each spheroid but will be true in some average sense and is a reasonable approximation to make. We make a similar assumption about the form of the rotations: we assume that on average the rotations of the spheroids are equal, that is

$$\boldsymbol{\omega}^{(n)} = \boldsymbol{\omega}^{(m)} = \boldsymbol{\omega}. \tag{7.28}$$

Then in terms of the applied strain we find that the relative displacement becomes

$$u_i^{(m)} - u_i^{(n)} = -2E_{ip}M_{pq}e_{\xi q}^{(nm)} \tag{7.29}$$

and substituting this into equation (7.26) the force is given by

$$\begin{aligned} F_i^{(nm)} &= \frac{2a_0w_0}{3B\mathbf{K}(e)}e_{\xi i}^{(nm)} + \sqrt{\frac{S_x^2(u_0/v_0)^2 + S_y^2}{1+(u_0/v_0)^2}} \times \\ &\quad \left\{-E_{ip}M_{pq}e_{\xi q}^{(nm)} + \epsilon_{ipq}\omega_p DI_q^{(nm)} - w_0 e_{\xi i}^{(nm)}\right\}. \end{aligned} \tag{7.30}$$

The normal displacement (7.22) becomes

$$\begin{aligned} w_0 &= -E_{pr}M_{rq}e_{\xi q}^{(nm)}e_{\xi p}^{(nm)} + \epsilon_{pqr}M_{rs}e_{\xi s}^{(nm)}e_{\xi p}^{(nm)}\omega_q \\ &= -\Lambda_{kp}E_{kp} + \epsilon_{kpq}\Lambda_{kq}\omega_p \end{aligned} \tag{7.31}$$

where, for later ease of notation, we have defined the tensors

$$\beta_{ij} = M_{ip}e_{\xi p}^{(nm)}M_{jq}e_{\xi q}^{(nm)} \quad \text{and} \quad \Lambda_{ij} = M_{jp}e_{\xi p}^{(nm)}e_{\xi i}^{(nm)}. \tag{7.32}$$

Note that β_{ij} is symmetric in i and j but that Λ_{ij} is not.

7.4.1 Conditions of Equilibrium

For equilibrium of the n-th spheroid, we require that the sum of all the forces $\mathbf{F}^{(nm)}$ be zero, and also that the sum of their moments be zero; that is

$$\sum_m \mathbf{F}^{(nm)} = \mathbf{0} \tag{7.33}$$

$$\sum_m \mathbf{F}^{(nm)} \wedge D\mathbf{I}^{(nm)} = \mathbf{0}. \tag{7.34}$$

In index notation, the condition (7.34) is equivalent to

$$\sum_m \epsilon_{irs} F_r^{(nm)} DI_s^{(nm)} = 0. \tag{7.35}$$

Substituting the force (7.30) and the normal displacement (7.31) into equation (7.35) we obtain the condition for equilibrium of moments as

$$\begin{aligned}\sum_m \Bigg\{ \frac{2a_0}{3B\mathbf{K}(e)} \epsilon_{irs}\Lambda_{rs}\epsilon_{kpq}\Lambda_{kp} + \sqrt{\frac{S_x^2(u_0/v_0)^2 + S_y^2}{1+(u_0/v_0)^2}} \times \\ (-\beta_{kk}\delta_{ip} + \beta_{pi} - \epsilon_{irs}\Lambda_{rs}\epsilon_{kpq}\Lambda_{kp}) \Bigg\} \omega_p \quad = \\ \sum_m \Bigg\{ \frac{2a_0}{3B\mathbf{K}(e)} \epsilon_{irs}\Lambda_{rs}\Lambda_{kp} + \sqrt{\frac{S_x^2(u_0/v_0)^2 + S_y^2}{1+(u_0/v_0)^2}} \times \\ (\epsilon_{iks}\beta_{sp} - \epsilon_{irs}\Lambda_{rs}\Lambda_{kp}) \Bigg\} E_{kp}. \end{aligned} \tag{7.36}$$

By summing over all spheroids n and assuming a packing dense enough that the summation over m and n may be written in terms of averages, this condition becomes

$$\begin{aligned}\Bigg\langle \frac{2a_0}{3B\mathbf{K}(e)} \epsilon_{irs}\Lambda_{rs}\epsilon_{kpq}\Lambda_{kp} + \sqrt{\frac{S_x^2(u_0/v_0)^2 + S_y^2}{1+(u_0/v_0)^2}} \times \\ (-\beta_{kk}\delta_{ip} + \beta_{pi} - \epsilon_{irs}\Lambda_{rs}\epsilon_{kpq}\Lambda_{kp}) \Bigg\rangle \langle\omega_p\rangle \quad = \\ \Bigg\langle \frac{2a_0}{3B\mathbf{K}(e)} \epsilon_{irs}\Lambda_{rs}\Lambda_{kp} + \sqrt{\frac{S_x^2(u_0/v_0)^2 + S_y^2}{1+(u_0/v_0)^2}} \times \\ (\epsilon_{iks}\beta_{sp} - \epsilon_{irs}\Lambda_{rs}\Lambda_{kp}) \Bigg\rangle \langle E_{kp}\rangle . \end{aligned} \tag{7.37}$$

It is important to note that, although the above condition has been written with the rotation and strain terms separated, the contact area major axis length a_0, as defined by equation (6.87), depends on w_0 and hence on ω and E_{ij}. Despite this, the following argument remains valid because we show that the right-hand side of (7.37) is zero using arguments of symmetry and since a_0 is an even function of the scaled z-coordinate η and is independent of the polar angle θ, the required symmetries remain.

The case of practical interest was that of a hydrostatic compression which may be written as

$$E_{ij} = E\delta_{ij} \tag{7.38}$$

where $E < 0$ for compression. Substituting the above into the condition (7.37), the right-hand side becomes

$$\left\langle \frac{2a_0}{3B\mathbf{K}(e)}\epsilon_{irs}\Lambda_{rs}\Lambda_{kk} + \sqrt{\frac{S_x^2(u_0/v_0)^2 + S_y^2}{1+(u_0/v_0)^2}}(\epsilon_{iks}\beta_{sk} - \epsilon_{irs}\Lambda_{rs}\Lambda_{kk}) \right\rangle E. \tag{7.39}$$

The term $\epsilon_{iks}\beta_{sk}$ is the sum over the indices k and s of a symmetric tensor multiplied by an anti-symmetric tensor and so must be zero. In section (7.3.1) we will show that the terms involving $\epsilon_{irs}\Lambda_{rs}\Lambda_{kk}$, when averaged are also zero due to the symmetry properties of the averaging scheme. Then we must have, from equation (7.39),

$$\langle \boldsymbol{\omega} \rangle = \mathbf{0} \tag{7.40}$$

showing that, for an initial hydrostatic compression, the spheroid rotations have no effect and therefore the confining stress is symmetric. This result is to be expected since, by symmetry, the forces attempting to rotate a given spheroid clockwise about a horizontal direction will on average be balanced by those attempting to turn it anti-clockwise.

Finally, we consider the condition of linear equilibrium given by equation (7.33). Substituting the force (7.30), summing over n and writing in terms of averages, we obtain

$$\left\langle \frac{2a_0 w_0}{2B\mathbf{K}(e)}e_{\xi i} + \sqrt{\frac{S_x^2(u_0/v_0)^2 + S_y^2}{1+(u_0/v_0)^2}}(-M_{ip}e_{\xi q} + \epsilon_{iqp}M_{pq}e_{\xi p}\omega_q) \right\rangle = 0. \tag{7.41}$$

The symmetry properties of the averaging scheme, discussed in section (7.3.1), show that each term in the left-hand side of the above is zero and hence the condition is satisfied.

7.4.2 The Average Initial Stress

Substituting the force (7.30) into equation (7.16) gives the initial average stress as

$$\langle \sigma_{ij} \rangle = -\frac{nN}{V}\left\langle -\frac{2a_0}{3B\mathbf{K}(e)}E\Lambda_{kk}\Lambda_{ji} + \sqrt{\frac{S_x^2(u_0/v_0)^2 + S_y^2}{1+(u_0/v_0)^2}}\left[-E\beta_{ij} + E\Lambda_{kk}\Lambda_{ji}\right]\right\rangle \tag{7.42}$$

This equation relates the average stress to the average strain during the initial deformation and is valid for an initial hydrostatic compression only.

7.5 The Incremental Problem

We now consider the incremental problem and show that the rotations of the spheroids are significant, but that only one of the five non-zero elastic moduli necessary to describe a transversely isotropic medium is affected. In analogy with equation (7.21), the incremental displacement of the contact area, relative to spheroid m, is

$$\frac{1}{2}(\delta\mathbf{u}^{(m)} - \delta\mathbf{u}^{(n)}) + \frac{1}{2}(\delta\boldsymbol{\omega}^{(n)} + \delta\boldsymbol{\omega}^{(m)}) \wedge D\mathbf{I}^{(nm)}. \tag{7.43}$$

Then the incremental normal displacement is given by

$$\delta w_0 = \left\{\frac{1}{2}(\delta\mathbf{u}^{(m)} - \delta\mathbf{u}^{(n)}) + \frac{1}{2}(\delta\boldsymbol{\omega}^{(n)} + \delta\boldsymbol{\omega}^{(m)}) \wedge D\mathbf{I}^{(nm)}\right\} \cdot \mathbf{e}_\xi^{(nm)} \tag{7.44}$$

and the remainder of the displacement is the tangential component given by

$$\frac{1}{2}(\delta\mathbf{u}^{(m)} - \delta\mathbf{u}^{(n)}) + \frac{1}{2}(\delta\boldsymbol{\omega}^{(n)} + \delta\boldsymbol{\omega}^{(m)}) \wedge D\mathbf{I}^{(nm)} - \delta w_0 \mathbf{e}_\xi^{(nm)}. \tag{7.45}$$

The incremental force is found by combining equations (7.43) and (7.45) with the total infinitesimal forces (6.68) and (6.71) to yield

$$\begin{aligned}\delta\mathbf{F}^{(nm)} = {} & \frac{(R_* w_0)^{1/2}\delta w_0}{B\mathbf{K}(e)}\mathbf{e}_\xi^{(nm)} + \sqrt{\frac{s_x^2(\delta u_0/\delta v_0)^2 + s_y^2}{1+(\delta u_0/\delta v_0)^2}} \times \\ & \left[\frac{1}{2}(\delta\mathbf{u}^{(m)} - \delta\mathbf{u}^{(n)}) + \frac{1}{2}(\delta\boldsymbol{\omega}^{(n)} + \delta\boldsymbol{\omega}^{(m)}) \wedge D\mathbf{I}^{(nm)} - \delta w_0 \mathbf{e}_\xi^{(nm)}\right]\end{aligned} \tag{7.46}$$

The incremental stiffnesses in the x- and y-directions, s_x and s_y, are respectively defined as

$$s_x = \frac{\overline{\delta P}}{\delta u_0} = \frac{e^2(R_* w_0)^{1/2}}{(Be^2 + C)\mathbf{K}(e) - C\mathbf{E}(e)}$$

$$s_y = \frac{\overline{\delta Q}}{\delta v_0} = \frac{e^2(R_* w_0)^{1/2}}{[Be^2 - C(1-e^2)]\mathbf{K}(e) + C\mathbf{E}(e)}. \tag{7.47}$$

The radius-like quantity R_* is defined by

$$R_* = \frac{4R_e}{e^2\mathbf{K}(e)}\left[\frac{\mathbf{K}(e) - \mathbf{E}(e)}{1-e^2}\right]^{1/2}\left[\mathbf{E}(e) - (1-e^2)\mathbf{K}(e)\right]^{1/2} \tag{7.48}$$

and varies with position on the spheroidal surface. The effective radius R_e was defined in chapter 6, equation (6.85), as

$$R_e = \frac{a'(\xi^2 + \eta^2)}{2\xi}. \tag{7.49}$$

In index notation, equation (7.44) may be written

$$\delta w_0 = \left\{\frac{1}{2}(\delta u_p^{(m)} - \delta u_p^{(n)}) + \frac{1}{2}\epsilon_{pqr}(\delta\omega_q^{(n)} + \delta\omega_q^{(m)})DI_r^{(nm)}\right\} e_{\xi p}^{(nm)} \tag{7.50}$$

and equation (7.46) becomes

$$\delta F_i^{(nm)} = \frac{(R_* w_0)^{1/2}\delta w_0}{B\mathbf{K}(e)} e_{\xi i}^{(nm)} + \sqrt{\frac{s_x^2(\delta u_0/\delta v_0)^2 + s_y^2}{1 + (\delta u_0/\delta v_0)^2}} \times \left[\frac{1}{2}(\delta u_i^{(m)} - \delta u_i^{(n)}) + \frac{1}{2}\epsilon_{ipq}(\delta\omega_p^{(n)} + \delta\omega_p^{(m)})DI_q^{(nm)} - \delta w_0 e_{\xi i}^{(nm)}\right]. \tag{7.51}$$

Making the same assumptions about the forms of the incremental displacement and the rotations, as seen in the initial state, we may write

$$\delta u_i^{(n)} = \delta E_{ij} X_j^{(n)} \quad \text{and} \quad \delta\boldsymbol{\omega}^{(n)} = \delta\boldsymbol{\omega}^{(m)} = \delta\boldsymbol{\omega}. \tag{7.52}$$

Substituting the above into the incremental force (7.51) we obtain

$$\delta F_i^{(nm)} = \frac{(R_* w_0)^{1/2}\delta w_0}{B\mathbf{K}(e)} e_{\xi i}^{(nm)} + \sqrt{\frac{s_x^2(\delta u_0/\delta v_0)^2 + s_y^2}{1 + (\delta u_0/\delta v_0)^2}} \times \left[-\delta E_{ip} M_{pq} e_{\xi q}^{(nm)} + \epsilon_{ipq}\delta\omega_p M_{qr} e_{\xi r}^{(nm)} - \delta w_0 e_{\xi i}^{(nm)}\right] \tag{7.53}$$

and the incremental normal displacement is given by

$$\delta w_0 = -\delta E_{kp}\Lambda_{kp} + \epsilon_{pqr}\Lambda_{pr}\delta\omega_q. \tag{7.54}$$

7.5.1 Conditions of Equilibrium

For equilibrium of each spheroid in the incremental problem, we require conditions analogous to (7.33) and (7.34) for the incremental force, that is

$$\sum_m \delta\mathbf{F}^{(nm)} = \mathbf{0} \tag{7.55}$$

$$\sum_m \delta\mathbf{F}^{(nm)} \wedge D\mathbf{I}^{(nm)} = \mathbf{0} \tag{7.56}$$

or, in index notation, the condition (7.56) becomes

$$\sum_m \epsilon_{ipq}\delta F_p^{(nm)} M_{qr} e_{\xi r}^{(nm)} = 0. \tag{7.57}$$

Substituting the incremental force (7.53) and the incremental compression (7.54) into the condition (7.57), we obtain the condition for the equilibrium of moments as

$$\sum_m \left\{ \frac{-(R_* w_0)^{1/2}\epsilon_{ipt}\Lambda_{pt}\epsilon_{qsr}\Lambda_{sr}}{B\mathbf{K}(e)} + \sqrt{\frac{s_x^2(\delta u_0/\delta v_0)^2 + s_y^2}{1+(\delta u_0/\delta v_0)^2}} \times \right.$$
$$\left. (\beta_{iq} - \beta_{kk}\delta_{iq} + \epsilon_{ipt}\Lambda_{pt}\epsilon_{qsr}\Lambda_{sr}) \right\} \delta\omega_q =$$
$$\sum_m \left\{ \frac{(R_* w_0)^{1/2}\epsilon_{isr}\Lambda_{sr}\Lambda_{pq}}{B\mathbf{K}(e)} + \sqrt{\frac{s_x^2(\delta u_0/\delta v_0)^2 + s_y^2}{1+(\delta u_0/\delta v_0)^2}}(\epsilon_{ips}\beta_{qs} - \epsilon_{isr}\Lambda_{sr}\Lambda_{pq}) \right\} \delta E_{pq}. \tag{7.58}$$

Summing over all spheroids n and writing the summations as averages, we obtain

$$\Phi_{iq}\delta\omega_q = \chi_{ipq}\delta E_{pq} \tag{7.59}$$

where the tensors Φ_{iq} and χ_{ipq} are defined as

$$\Phi_{iq} = \left\langle \frac{-(R_* w_0)^{1/2}\epsilon_{ipt}\Lambda_{pt}\epsilon_{qsr}\Lambda_{sr}}{B\mathbf{K}(e)} + \sqrt{\frac{s_x^2(\delta u_0/\delta v_0)^2 + s_y^2}{1+(\delta u_0/\delta v_0)^2}} \times \right.$$

$$(\beta_{iq} - \beta_{kk}\delta_{iq} + \epsilon_{ipt}\Lambda_{pt}\epsilon_{qsr}\Lambda_{sr}) \Big\rangle \quad (7.60)$$

$$\chi_{ipq} = \left\langle \frac{(R_* w_0)^{1/2}\epsilon_{isr}\Lambda_{sr}\Lambda_{pq}}{B\mathbf{K}(e)} + \sqrt{\frac{s_x^2(\delta u_0/\delta v_0)^2 + s_y^2}{1+(\delta u_0/\delta v_0)^2}} \times \right.$$

$$\left. (\epsilon_{ips}\beta_{qs} - \epsilon_{isr}\Lambda_{sr}\Lambda_{pq}) \right\rangle . \quad (7.61)$$

From this condition, the required rotations may, in principle, be determined by writing $\delta\omega_i$ in terms of the applied strain as

$$\delta\omega_i = \Psi_{ipq}\delta E_{pq} \quad (7.62)$$

where $\Psi = \Phi^{-1}\chi$.

The condition (7.55) for linear equilibrium of the incremental forces can be shown to be satisfied in the same way as condition (7.33) was shown to be satisfied in the incremental state.

7.5.2 The Effect of the Rotation Term

As we will see later, the equation for the effective elastic moduli will depend on the rotations through the term

$$\epsilon_{ipq}\Psi_{pkl}\beta_{qj}. \quad (7.63)$$

Recall that the definition of the tensor Ψ was

$$\Psi = \Phi^{-1}\chi \quad (7.64)$$

where χ and Φ are defined by equations (7.60) and (7.61). Here we will use the symmetry properties of the averaging scheme to simplify the tensors Φ_{ij} and χ_{ijk}. In particular, we will show that χ_{ijk} has only six non-zero components occurring when i, j and k are distinct and that Φ_{ij} is diagonal.

7.5.3 The Tensor χ_{ijk}

Consider just the term $\epsilon_{isr}\langle\Lambda_{sr}\Lambda_{jk}\rangle$ from χ_{ijk}. Strictly speaking, we should consider the averages

$$\left\langle \frac{-(R_* w_0)^{1/2} \epsilon_{isr} \Lambda_{sr} \Lambda_{jk}}{B\mathbf{K}(e)} \right\rangle \quad \text{and} \quad \left\langle \Lambda_{sr}\Lambda_{jk} \sqrt{\frac{s_x^2(\delta u_0/\delta v_0)^2 + s_y^2}{1+(\delta u_0/\delta v_0)^2}} \right\rangle \tag{7.65}$$

but since the expressions

$$\frac{-(R_* w_0)^{1/2}}{B\mathbf{K}(e)} \quad \text{and} \quad \sqrt{\frac{s_x^2(\delta u_0/\delta v_0)^2 + s_y^2}{1+(\delta u_0/\delta v_0)^2}} \tag{7.66}$$

are even functions of both η and θ, they have no effect on whether the averaged quantity is zero or not. The same applies to all terms considered here.

Expanding, using the definition of Λ_{ij}, we obtain

$$\epsilon_{isr} \langle \Lambda_{sr}\Lambda_{jk} \rangle = \epsilon_{isr} \langle M_{rp} e_{\xi p} e_{\xi s} M_{kq} e_{\xi q} e_{\xi j} \rangle . \tag{7.67}$$

We now determine the conditions required on the indices i, s, r, j, k in the above expression to give a non-zero result:

Matrix M is diagonal	:	$r = p\ , k = q$	(i)
The alternating tensor ϵ_{isr}	:	$i \neq s \neq r \neq i$	(ii)
Properties of $\langle \cdot \rangle$	:	p, s, q, j must be in equal pairs.	(iii)

Possible pairs satisfying (iii) are: $p = q$ and $s = j$ or $p = j$ and $s = q$. The remaining pairs, $p = s$ and $q = j$, will give a zero result since (i) states $r = p$ — meaning the first pair becomes $s = r$ which contradicts (ii). We may construct the following table for both non-zero cases:

$$\begin{aligned} & p = q,\ s = j \ \Rightarrow\ r = k,\ s = j \ \Rightarrow\ k \neq j \\ \text{or}\quad & p = j,\ s = q \ \Rightarrow\ r = j,\ s = k \ \Rightarrow\ k \neq j. \end{aligned}$$

The first implication follows from (i), the second from (ii). In both cases we conclude that $j \neq k$. Condition (ii) ensures that we must also have $i \neq j$ and $i \neq k$ which shows that, for a non-zero result, the free indices i, j and k of equation (7.67) must be distinct. A similar argument will show that, for the remaining term of $\epsilon_{ijs} \langle \beta_{ks} \rangle$ in χ, the indices i, j and k must again be distinct.

An alternative method of determining this restriction on the indices is to express the diagonal matrix M in index notation as

$$M_{ij} = M_1(\delta_{i1}\delta_{j1} + \delta_{i2}\delta_{j2}) + M_3\delta_{i3}\delta_{j3} \tag{7.68}$$

where $M_1 = M_{11} = M_{22}$ and $M_3 = M_{33}$. Substituting M_{ij} and expanding, we obtain

$$\begin{aligned}
\epsilon_{isr}\langle\Lambda_{sr}\Lambda_{jk}\rangle &= \Big\langle M_1^2(\epsilon_{is1}\delta_{k1}e_{\xi1}^2e_{\xi s}e_{\xi j} + \epsilon_{is1}\delta_{k2}e_{\xi1}e_{\xi2}e_{\xi s}e_{\xi j} \\
&\quad + \epsilon_{is2}\delta_{k1}e_{\xi2}e_{\xi1}e_{\xi s}e_{\xi j} + \epsilon_{is2}\delta_{k2}e_{\xi2}^2e_{\xi s}e_{\xi j}) \\
&\quad + M_1M_3(\epsilon_{is1}\delta_{k3}e_{\xi1}e_{\xi3}e_{\xi s}e_{\xi j} + \epsilon_{is2}\delta_{k3}e_{\xi2}e_{\xi3}e_{\xi s}e_{\xi j} \\
&\quad + \epsilon_{is3}\delta_{k1}e_{\xi3}e_{\xi1}e_{\xi s}e_{\xi j} + \epsilon_{is3}\delta_{k2}e_{\xi2}e_{\xi3}e_{\xi s}e_{\xi j}) \\
&\quad + M_3^2(\epsilon_{is3}\delta_{k3}e_{\xi3}^2e_{\xi s}e_{\xi j})\Big\rangle .
\end{aligned} \tag{7.69}$$

By examining each term separately we may determine the required values of s and j. For example, the first term contains the alternating tensor ϵ_{is1} meaning that s can only take values of 2 and 3. Also, we require that $s = j$ to ensure the pairs $e_{\xi1}^2e_{\xi2}^2$ and $e_{\xi1}^2e_{\xi3}^2$ when the sum is taken over s. The second term is similar except that s may only take the value 2. This is because if s were 3 then it would not be possible for $e_{\xi1}e_{\xi2}e_{\xi3}e_{\xi j}$ to be written as pairs of components whatever the value of j. Similar arguments may be applied to the other terms, resulting in the expression

$$\begin{aligned}
\epsilon_{isr}\langle\Lambda_{sr}\Lambda_{jk}\rangle &= \delta_{i1}\delta_{j2}\delta_{k3}\left\langle(M_3^2 - M_1M_3)e_{\xi2}^2e_{\xi3}^2\right\rangle \\
&\quad + \delta_{i1}\delta_{j3}\delta_{k2}\left\langle(M_1M_3 - M_1^2)e_{\xi2}^2e_{\xi3}^2\right\rangle \\
&\quad + \delta_{i2}\delta_{j1}\delta_{k3}\left\langle(M_1M_3 - M_3^2)e_{\xi1}^2e_{\xi3}^2\right\rangle \\
&\quad + \delta_{i2}\delta_{j3}\delta_{k1}\left\langle(M_1^2 - M_1M_3)e_{\xi1}^2e_{\xi3}^2\right\rangle .
\end{aligned} \tag{7.70}$$

Applying the same argument to the second part of χ_{ijk}, we find that

$$\epsilon_{ijs}\langle\beta_{ks}\rangle = \left\langle M_1^2(\epsilon_{ij1}\delta_{k1}e_{\xi1}^2 + \epsilon_{ij2}\delta_{k2}e_{\xi2}^2)\right\rangle + \left\langle M_3^2(\epsilon_{ij3}\delta_{k3}e_{\xi3}^2)\right\rangle \tag{7.71}$$

showing that the indices must be distinct for a non-zero value of χ_{ijk}. This also proves the result required in section (7.4.1) that $\epsilon_{irs}\langle\Lambda_{rs}\Lambda_{kk}\rangle = 0$ by taking $j = k$ in equation (7.70).

7.5.4 The Tensor Φ_{ij}

We now examine the tensor Φ_{ij} and, using the methods seen above, show that it is diagonal. The first term of Φ_{ij} we consider is $\epsilon_{ipt}\Lambda_{pt}\epsilon_{jsr}\Lambda_{sr}$. Substituting the matrix M_{ij}, as given by equation (7.8), and expanding, we obtain

$$\begin{aligned}\langle\epsilon_{ipt}\Lambda_{pt}\epsilon_{jsr}\Lambda_{sr}\rangle &= \Big\langle M_1^2(\epsilon_{ip1}\epsilon_{js1}e_{\xi1}^2e_{\xi p}e_{\xi s} + \epsilon_{ip1}\epsilon_{js2}e_{\xi1}e_{\xi2}e_{\xi p}e_{\xi s} \\ &\quad + \epsilon_{ip2}\epsilon_{js1}e_{\xi2}e_{\xi1}e_{\xi p}e_{\xi s} + \epsilon_{ip2}\epsilon_{js2}e_{\xi2}^2e_{\xi p}e_{\xi s}) \\ &\quad + M_1M_3(\epsilon_{ip1}\epsilon_{js3}e_{\xi1}e_{\xi3}e_{\xi p}e_{\xi s} + \epsilon_{ip2}\epsilon_{js3}e_{\xi2}e_{\xi3}e_{\xi p}e_{\xi s} \\ &\quad + \epsilon_{ip3}\epsilon_{js1}e_{\xi3}e_{\xi1}e_{\xi p}e_{\xi s} + \epsilon_{ip3}\epsilon_{js2}e_{\xi3}e_{\xi2}e_{\xi p}e_{\xi s}) \\ &\quad + M_3^2(\epsilon_{ip3}\epsilon_{js3}e_{\xi3}^2e_{\xi p}e_{\xi s})\Big\rangle. \end{aligned} \tag{7.72}$$

Examining each term in turn, we choose the required values for p and s to obtain

$$\begin{aligned}\langle\epsilon_{ipt}\Lambda_{pt}\epsilon_{jsr}\Lambda_{sr}\rangle &= \Big\langle M_1^2(\delta_{i2}\delta_{j2}e_{\xi1}^2e_{\xi3}^2 - \delta_{i1}\delta_{j2}e_{\xi2}^2e_{\xi3}^2)\Big\rangle \\ &\quad - 2\Big\langle M_1M_3(\delta_{i1}\delta_{j1}e_{\xi2}^2e_{\xi3}^2 + \delta_{i2}\delta_{j2}e_{\xi1}^2e_{\xi3}^2)\Big\rangle \\ &\quad + \Big\langle M_3^2(\delta_{i1}\delta_{j1}e_{\xi2}^2e_{\xi3}^2 + \delta_{i2}\delta_{j2}e_{\xi1}^2e_{\xi3}^2)\Big\rangle. \end{aligned} \tag{7.73}$$

The remaining part of Φ_{ij} can similarly be shown to be

$$\begin{aligned}\langle\beta_{ij}\rangle - \langle\beta_{kk}\rangle\,\delta_{ij} &= \Big\langle M_1^2\left\{\delta_{i1}\delta_{j1}e_{\xi1}^2 + \delta_{i2}\delta_{j2}e_{\xi2}^2 - (e_{\xi1}^2 + e_{\xi2}^2)\delta_{ij}\right\}\Big\rangle \\ &\quad + \Big\langle M_3^2\left\{\delta_{i3}\delta_{j3}e_{\xi3}^2 - e_{\xi3}^2\delta_{ij}\right\}\Big\rangle \end{aligned} \tag{7.74}$$

and we deduce that Φ_{ij} is diagonal.

7.5.5 The Incremental Stress

We now consider how the results of the previous section may be used to predict the average stress. The equation for the average incremental stress is, in analogy with equation (7.11) for the initial stress,

$$\langle \delta\sigma_{ij} \rangle = -\frac{1}{V} \sum_{\text{contacts}} \left\{ M_{ik} e_{\xi k}^{(nm)} \delta F_j^{(nm)} + M_{jk} e_{\xi k}^{(nm)} \delta F_i^{(nm)} \right\} \tag{7.75}$$

which may also be written as

$$\langle \delta\sigma_{ij} \rangle = -\frac{2}{V} \sum_{\text{contacts}} M_{ik} e_{\xi k}^{(nm)} \delta F_j^{(nm)}. \tag{7.76}$$

Substituting the incremental force (7.53) into equation (7.75) and writing the resulting expression as an averaged quantity, we obtain

$$\begin{aligned} \langle \delta\sigma_{ij} \rangle \;=\; -\frac{nN}{V} \Bigg\langle & \frac{-(-R_* E \Lambda_{pp})^{1/2} \delta E_{kl} \Lambda_{kl} \Lambda_{ij}}{B\mathbf{K}(e)} + \sqrt{\frac{s_x^2 (\delta u_0/\delta v_0)^2 + s_y^2}{1 + (\delta u_0/\delta v_0)^2}} \times \\ & (-\delta E_{kl} \beta_{lj} \delta_{ik} + \epsilon_{ipq} \beta_{qj} \delta\omega_p + \delta E_{kl} \Lambda_{kl} \Lambda_{ij}) \Bigg\rangle . \end{aligned} \tag{7.77}$$

The above equation may be rewritten, using equation (7.83) to replace $\delta\omega_i$ and equations (7.17) and (7.18) to eliminate N/V, as

$$\begin{aligned} \langle \delta\sigma_{ij} \rangle \;=\; -\frac{3n\phi}{4\pi a'^3 \xi(\xi^2+1)} \Bigg\langle & \frac{-(-R_* E \Lambda_{pp})^{1/2} \Lambda_{kl} \Lambda_{ij}}{B\mathbf{K}(e)} + \sqrt{\frac{s_x^2 (\delta u_0/\delta v_0)^2 + s_y^2}{1 + (\delta u_0/\delta v_0)^2}} \times \\ & (-\beta_{lj} \delta_{ik} + \epsilon_{ipq} \Psi_{pkl} \beta_{qj} + \Lambda_{kl} \Lambda_{ij}) \, \delta E_{kl} \Bigg\rangle . \end{aligned} \tag{7.78}$$

7.5.6 The Effective Elastic Moduli

The incremental stress and incremental strain are related through

$$\langle \delta\sigma_{ij} \rangle = C^*_{ijkl} \langle \delta E_{kl} \rangle \tag{7.79}$$

from which we identify the effective elastic moduli as

$$C^*_{ijkl} = -\frac{3n\phi}{4\pi a'^3\xi(\xi^2+1)}\left[\left\langle \frac{-(-R_*E\Lambda_{pp})^{1/2}\Lambda_{kl}\Lambda_{ij}}{B\mathbf{K}(e)} + \sqrt{\frac{s_x^2(\delta u_0/\delta v_0)^2+s_y^2}{1+(\delta u_0/\delta v_0)^2}}\times \right.\right.$$
$$\left.\left.(-\beta_{lj}\delta_{ik}+\epsilon_{ipq}\Psi_{pkl}\beta_{qj}+\Lambda_{kl}\Lambda_{ij})\right\rangle\right]_{k,l}. \quad (7.80)$$

where the brackets $[\cdot]$ denote the symmetric part with respect to the indices k and l.

The rotation vector may be calculated by taking values for i and j in equation (7.62) and using the relationship

$$\Phi_{ij} = \epsilon_{pjq}\chi_{ipq} \quad (7.81)$$

which is easily proved. Then substituting the above into the relationship between $\delta\omega$ and δE_{pq} (7.62), we obtain

$$\chi_{ipq}(\epsilon_{pjq}\delta\omega_j - \delta E_{pq}) = 0. \quad (7.82)$$

By taking $i = 1,2,3$ in the above and making use of the properties of the tensor χ_{ijk}, as derived in section (7.3.1), we obtain the rotation vector as

$$\begin{aligned}
\delta\omega_1 &= \left(\frac{\chi_{123}+\chi_{132}}{\chi_{132}-\chi_{123}}\right)\delta E_{23} \\
\delta\omega_2 &= \left(\frac{\chi_{213}+\chi_{231}}{\chi_{213}-\chi_{231}}\right)\delta E_{13} \\
\delta\omega_3 &= \left(\frac{\chi_{312}+\chi_{321}}{\chi_{321}-\chi_{312}}\right)\delta E_{12}
\end{aligned} \quad (7.83)$$

and we are now able to calculate specific moduli using the above values. Taking $i = j = 1$ in equation (7.78), we obtain

$$\langle\delta\sigma_{11}\rangle = -\frac{nN}{V}\left\langle -\frac{(-R_*E\Lambda_{pp})^{1/2}\delta E_{kl}\Lambda_{kl}\Lambda_{11}}{B\mathbf{K}(e)} + \sqrt{\frac{S_x^2(u_0/v_0)^2+S_y^2}{1+(u_0/v_0)^2}}\times \right.$$
$$\left.[-\delta E_{kl}\beta_{l1}\delta_{1k}+\epsilon_{1pq}\beta_{q1}\delta\omega_p+\delta E_{kl}\Lambda_{kl}\Lambda_{11}]\right\rangle \quad (7.84)$$

the rotation term being zero. Summing over the indices k and l and using the symmetry properties of the averaging scheme as discussed in section (7.3.1), we obtain the following

moduli:

$$
\begin{aligned}
C^*_{1111} &= -\frac{nN}{V}\left\langle -\frac{(-R_*E\Lambda_{pp})^{1/2}\Lambda_{11}^2}{B\mathbf{K}(e)} + \sqrt{\frac{s_x^2(\delta u_0/\delta v_0)^2 + s_y^2}{1+(\delta u_0/\delta v_0)^2}}\,[-\beta_{11}+\Lambda_{11}^2]\right\rangle \\
C^*_{1122} &= -\frac{nN}{V}\left\langle -\frac{(-R_*E\Lambda_{pp})^{1/2}\Lambda_{11}\Lambda_{22}}{B\mathbf{K}(e)} + \sqrt{\frac{s_x^2(\delta u_0/\delta v_0)^2 + s_y^2}{1+(\delta u_0/\delta v_0)^2}}\,\Lambda_{11}\Lambda_{22}\right\rangle \\
C^*_{1133} &= -\frac{nN}{V}\left\langle -\frac{(-R_*E\Lambda_{pp})^{1/2}\Lambda_{11}\Lambda_{33}}{B\mathbf{K}(e)} + \sqrt{\frac{s_x^2(\delta u_0/\delta v_0)^2 + s_y^2}{1+(\delta u_0/\delta v_0)^2}}\,\Lambda_{11}\Lambda_{33}\right\rangle . \qquad (7.85)
\end{aligned}
$$

When $i = j = 3$, we obtain, from equation (7.78),

$$
\begin{aligned}
\langle \delta\sigma_{33}\rangle &= -\frac{nN}{V}\left\langle -\frac{(-R_*E\Lambda_{pp})^{1/2}\delta E_{kl}\Lambda_{kl}\Lambda_{33}}{B\mathbf{K}(e)} + \sqrt{\frac{s_x^2(\delta u_0/\delta v_0)^2 + s_y^2}{1+(\delta u_0/\delta v_0)^2}}\,\times \right. \\
&\qquad \left. [-\delta E_{kl}\beta_{l3}\delta_{3k} + \epsilon_{3pq}\beta_{q1}\delta\omega_p + \delta E_{kl}\Lambda_{kl}\Lambda_{33}]\right\rangle \qquad (7.86)
\end{aligned}
$$

and again summing over the indices k and l we obtain

$$
\begin{aligned}
C^*_{3311} &= -\frac{nN}{V}\left\langle -\frac{(-R_*E\Lambda_{pp})^{1/2}\Lambda_{11}\Lambda_{33}}{\mathbf{K}(e)} + \sqrt{\frac{s_x^2(\delta u_0/\delta v_0)^2 + s_y^2}{1+(\delta u_0/\delta v_0)^2}}\,\Lambda_{11}\Lambda_{33}\right\rangle \\
C^*_{3333} &= -\frac{nN}{V}\left\langle -\frac{(-R_*E\Lambda_{pp})^{1/2}\Lambda_{33}^2}{\mathbf{K}(e)} + \sqrt{\frac{s_x^2(\delta u_0/\delta v_0)^2 + s_y^2}{1+(\delta u_0/\delta v_0)^2}}\,[-\beta_{33}+\Lambda_{33}^2]\right\rangle .
\end{aligned} \qquad (7.87)
$$

Finally, when $i = 1$ and $j = 3$, the rotation term is non-zero and the average incremental stress is given by

$$
\begin{aligned}
\langle \delta\sigma_{13}\rangle &= -\frac{nN}{V}\left\langle -\frac{(-R_*E\Lambda_{pp})^{1/2}\delta E_{kl}\Lambda_{kl}\Lambda_{13}}{B\mathbf{K}(e)} + \sqrt{\frac{s_x^2(\delta u_0/\delta v_0)^2 + s_y^2}{1+(\delta u_0/\delta v_0)^2}}\,\times \right. \\
&\qquad \left. [-\delta E_{kl}\beta_{l3}\delta_{1k} + \epsilon_{1pq}\beta_{q3}\delta\omega_p + \delta E_{kl}\Lambda_{kl}\Lambda_{13}]\right\rangle .
\end{aligned} \qquad (7.88)
$$

The rotation term may be expanded by summing over the indices p and q and substituting the components $\delta\omega_p$ from equation (7.83). The modulus C^*_{1313} is obtained from the above as

$$C^*_{1313} = -\frac{nN}{2V}\left\langle -\frac{(-R_*E\Lambda_{pp})^{1/2}(\Lambda_{13}^2+\Lambda_{13}\Lambda_{31})}{B\mathbf{K}(e)} + \sqrt{\frac{s_x^2(\delta u_0/\delta v_0)^2+s_y^2}{1+(\delta u_0/\delta v_0)^2}}\times \left[-\beta_{33}+\beta_{33}\left(\frac{\chi_{213}+\chi_{231}}{\chi_{213}-\chi_{231}}\right)+\Lambda_{13}^2+\Lambda_{13}\Lambda_{31}\right]\right\rangle. \tag{7.89}$$

Equations (7.85), (7.87) and (7.89) give the five effective elastic moduli required to describe a transversely isotropic medium such as shale. It may also be shown that all other independent moduli are zero. Because of the complexity of the expressions for the moduli, given in terms of averages of the tensor Λ_{ij}, β_{ij} and other terms depending on e, any further progress will have to involve numerical integration of the averaging integrals. The averaging scheme (7.11) may be written as

$$\langle f(e)\rangle = \frac{1}{S}\int_{\theta=-\pi}^{\pi}\int_{\eta=-1}^{1} f(e)\; h_2h_3\; \mathrm{d}\eta\; \mathrm{d}\theta \tag{7.90}$$

where $f(e)$ is the function to be averaged, h_3 and h_3 are the scale factors (6.76) and S is the surface area of a spheroid given by

$$S = 2\pi a^2\xi^2(1+\xi^2)\left[\sinh^{-1}\left(\frac{1}{\xi}\right)+\frac{\sqrt{1+\xi^2}}{\xi^2}\right]. \tag{7.91}$$

However, the eccentricity e depends on η through the relationship (6.86):

$$\frac{\xi^2+\eta^2}{1+\xi^2} = \frac{(1-e^2)\,[\mathbf{K}(e)-\mathbf{E}(e)]}{\mathbf{E}(e)-(1-e^2)\mathbf{K}(e)} \tag{7.92}$$

which may be solved numerically to find e for any value of η at each stage of the numerical integration. Alternatively, equation (7.92) may be differentiated with respect to e to obtain

$$\frac{2\eta}{1+\xi^2}\frac{\mathrm{d}\eta}{\mathrm{d}e} = \frac{3e\mathbf{E}^2(e)-2e(2-e^2)\mathbf{K}(e)\mathbf{E}(e)+e(e^2-1)\mathbf{K}^2(e)}{[\mathbf{E}(e)-(1-e^2)\mathbf{K}(e)]^2} \tag{7.93}$$

where we have used the results

$$\begin{aligned}\mathbf{K}'(e) &= \frac{\mathbf{E}(e)-(1-e^2)\mathbf{K}(e)}{e(1-e^2)}\\ \mathbf{E}'(e) &= \frac{\mathbf{E}(e)-\mathbf{K}(e)}{e}.\end{aligned} \tag{7.94}$$

The averaging integral (7.90) is transformed to

$$\langle f(e)\rangle = \frac{1}{S}\int_{\theta=-\pi}^{\pi}\int_{e=0}^{e_{max}} f(e)\; h_2 h_3\; \frac{\mathrm{d}\eta}{\mathrm{d}e}\; \mathrm{d}e\; \mathrm{d}\theta \tag{7.95}$$

which may be evaluated without the need to solve equation (7.92) at each numerical step, the limit e_{max} being the largest value of e obtained from just one solution of equation (7.92) at $\eta = 0$.

Clearly, the results obtained from this random packing of spheroids model cannot possibly account for all of the elastic properties of a rock with such a complex microstructure. The model is very simplified and contains a number of assumptions. As mentioned in section (7.1), the shale contains many isolated silt inclusions and regions in the shale are locally misaligned from the average bedding direction. Ideally, the results of this chapter would be included in a more sophisticated shale model, such as that of Hornby, Schwartz and Hudson [32], which would average the properties of a representative shale element over the experimentally measured platelet alignment distribution, and make considerations for the presence of silt inclusions.

Appendix A

Inter-Granular Friction: Corrections

In Slade and Walton [55] a simplified case of the work covered in chapter 5 was considered. A number of typographical errors and one algebraic error have since been discovered, and so to allow comparison between the results of Slade and Walton [55] and those of chapter 5, the corrections are listed here.

The first term of equation (26), inside the braces, should read

$$\frac{1}{B}\left\langle |I_3|^3 I_i I_j \right\rangle . \tag{A.1}$$

The first line of equation (27) should be

$$\left\langle |I_3|^3 \right\rangle_A = \frac{1}{4\pi}\int_0^{2\pi} \mathrm{d}\phi \left(\int_0^{\theta_c} \sin\theta \, |\cos\theta|^3 \, \mathrm{d}\theta + \int_{\pi-\theta_c}^{\pi} \sin\theta \, |\cos\theta|^3 \, \mathrm{d}\theta \right). \tag{A.2}$$

Equation (28) is incorrect due to an algebraic error during the calculation of the averages. The corrected version is

$$\langle \delta\sigma_{33} \rangle = -\frac{\phi n \alpha^{3/2}}{\pi^2} \left\{ \frac{1}{6B} + \left(\frac{\pi - 2\theta_c}{32B} \right) f + \frac{\sin^2\theta_c \, (3 - 2\sin^2\theta_c)}{24(2B+C)} \right\}. \tag{A.3}$$

The left-hand side of equation (32) should be the incremental stress

$$\langle \delta\sigma_{33} \rangle \tag{A.4}$$

Equation (34) is derived from equation (28) and as such should read

$$c^2 = \frac{3B+C}{4\rho B(2B+C)}\left(\frac{n^2F}{\pi^4\phi}\right)^{1/3}\left\{\frac{1}{6B}+\left(\frac{\pi-2\theta_c}{32B}\right)f+\frac{\sin^2\theta_c\,(3-2\sin^2\theta_c)}{24(2B+C)}\right\}^{-1/3} \tag{A.5}$$

where the modulus D is defined in Slade and Walton [55] as $2D = 2B + C$.

Appendix B

Calculation of the Averages

In chapter 5, we introduced the modified averaging scheme

$$\langle\cdot\rangle_A = \frac{1}{4\pi}\int_0^{2\pi} \mathrm{d}\phi \left(\int_0^{\theta_c} + \int_{\pi-\theta_c}^{\pi}\right)(\cdot)\,\sin\theta\,\mathrm{d}\theta \tag{B.1}$$

$$\langle\cdot\rangle_B = \frac{1}{4\pi}\int_0^{2\pi} \mathrm{d}\phi \int_{\theta_c}^{\pi-\theta_c}(\cdot)\,\sin\theta\,\mathrm{d}\theta \tag{B.2}$$

where $0 \leq \theta_c \leq \pi/2$, and θ_c is the critical angle of friction. The scheme used by Walton [67], denoted $\langle\cdot\rangle$, is defined as

$$\langle\cdot\rangle = \frac{1}{4\pi}\int_0^{2\pi} \mathrm{d}\phi \int_0^{\pi}(\cdot)\,\sin\theta\,\mathrm{d}\theta \tag{B.3}$$

and is equivalent to

$$\langle\cdot\rangle = \langle\cdot\rangle_A + \langle\cdot\rangle_B \tag{B.4}$$

Figure (5-2) shows the interval $[0,\pi]$ split into the ranges A and B.

The unit vector $\mathbf{I}^{(nm)}$ joining the centres of two spheres may be written in polar coordinates as

$$\mathbf{I}^{(nm)} = (\,\sin\theta\cos\phi,\ \sin\theta\sin\phi,\ \cos\theta\,). \tag{B.5}$$

The components of this vector then appear in the quantities to be averaged, for example

$$\langle I_1^2 |I_3| \rangle = \langle \sin^2 \theta \cos^2 \phi \, |\cos \theta| \rangle . \tag{B.6}$$

This appendix lists the values for the averaging integrals required to calculate the initial stresses (5.33) from equation (5.31). Firstly, there are two averages over the entire range:

$$\begin{aligned} \langle I_1^2 |I_3|^3 \rangle &= \frac{1}{24} \\ \langle |I_3|^5 \rangle &= \frac{1}{6}. \end{aligned} \tag{B.7}$$

Over the range A we calculate:

$$\begin{aligned} \langle I_1^2 |I_3|^3 \rangle_A &= \frac{1}{24} \sin^4 \theta_c \, (3 - 2 \sin^2 \theta_c) \\ \langle |I_3|^5 \rangle_A &= \frac{1}{6} \sin^2 \theta_c \, (3 - 3 \sin^2 \theta_c + \sin^4 \theta_c) \\ \langle |I_3|^3 \rangle_A &= \frac{1}{2} \sin^2 \theta_c \, (2 - \sin^2 \theta_c). \end{aligned} \tag{B.8}$$

Finally, the required B ranges are:

$$\begin{aligned} \left\langle \frac{I_3^4}{(1 - I_3^2)^{1/2}} \right\rangle_B &= \frac{1}{8} \left\{ 3 \left(\frac{\pi}{2} - \theta_c \right) - 5 \sin \theta_c \cos \theta_c + 2 \sin^3 \theta_c \cos \theta_c \right\} \\ \left\langle \frac{I_1^2 I_3^4}{(1 - I_3^2)^{1/2}} \right\rangle_B &= \frac{1}{192} \left\{ 12 \left(\frac{\pi}{2} - \theta_c \right) + 10 \sin \theta_c \cos \theta_c \right. \\ &\qquad \left. - 48 \sin^3 \theta_c \cos \theta_c + 24 \sin^5 \theta_c \cos \theta_c \right\} \\ \left\langle \frac{I_3^6}{(1 - I_3^2)^{1/2}} \right\rangle_B &= \frac{1}{92} \left\{ 30 \left(\frac{\pi}{2} - \theta_c \right) - 66 \sin \theta_c \cos \theta_c \right. \\ &\qquad \left. + 52 \sin^3 \theta_c \cos \theta_c - 16 \sin^5 \theta_c \cos \theta_c \right\}. \end{aligned} \tag{B.9}$$

Further averages are calculated by Walton [67] using the scheme (B.3) and are listed here for reference. Equation (4.8) of Walton [67] uses the isotropy of the packing to deduce that

$$\langle I_i I_j \rangle = \frac{1}{3} \delta_{ij} \tag{B.10}$$

and

$$\langle I_i I_j I_k I_l \rangle = \frac{1}{15}(\delta_{ij}\delta_{kl} + \delta_{ik}\delta_{jl} + \delta_{il}\delta_{jk}). \tag{B.11}$$

Further averages are calculated explicitly in equations (3.23) of Walton [67]:

$$\begin{aligned} \langle |I_3|^3 I_1^2 \rangle &= \frac{1}{24} \\ \langle |I_3| I_3^2 \rangle &= \frac{1}{4} \\ \langle |I_3| I_3^4 \rangle &= \frac{1}{6} \end{aligned} \tag{B.12}$$

and from equation (4.13) of Walton [67]:

$$\begin{aligned} \langle |I_3| I_1^2 \rangle &= \frac{1}{8} \\ \langle |I_3| I_1^4 \rangle &= \frac{1}{16} \\ \langle |I_3| I_1^2 I_2^2 \rangle &= \frac{1}{48}. \end{aligned} \tag{B.13}$$

Appendix C

Details of the Calculation of Surface Displacements

C.1 Definitions of Elliptic Integrals

Many of the integrals involved in the calculation of the surface displacements cannot be evaluated analytically and so are expressed in terms of elliptic integrals. Tables of elliptic integrals may be used to find numerical values as required. The definitions of the elliptic integrals used throughout this report are reproduced here for reference.

The complete elliptic integral of the first kind is defined as

$$\mathbf{K}(e) = \int_0^{\pi/2} (1 - e^2 \sin^2 \theta)^{-1/2} \, \mathrm{d}\theta \tag{C.1}$$

and the complete elliptic integral of the second kind is defined as

$$\mathbf{E}(e) = \int_0^{\pi/2} (1 - e^2 \sin^2 \theta)^{1/2} \, \mathrm{d}\theta. \tag{C.2}$$

Tabulated values of these functions may be found in Adams and Hippisley [1], together with useful results concerning elliptic functions and derivatives of $\mathbf{K}(e)$ and $\mathbf{E}(e)$.

C.2 Surface Displacement Integrals

The calculation of the surface displacements due to normal and tangential force distributions involves the calculation of the integrals from equations (1.10) and (1.11). For a

force distribution of the form

$$P(x,y) = K\left(1 - \frac{x^2}{a^2} - \frac{y^2}{b^2}\right)^{1/2} \tag{C.3}$$

the integrals arising are of the form

$$I_1 = \int_{\mathcal{R}} \frac{(1 - x'^2/a^2 - y'^2/b^2)^{1/2}}{[(x'-x)^2 + (y'-y)^2]^{1/2}}\, \mathrm{d}x'\, \mathrm{d}y' \tag{C.4}$$

$$I_3 = \int_{\mathcal{R}} \frac{(x'-x)(y'-y)(1 - x'^2/a^2 - y'^2/b^2)^{1/2}}{[(x'-x)^2 + (y'-y)^2]^{3/2}}\, \mathrm{d}x'\, \mathrm{d}y' \tag{C.5}$$

$$I_4 = \int_{\mathcal{R}} \frac{(x'-x)^2(1 - x'^2/a^2 - y'^2/b^2)^{1/2}}{[(x'-x)^2 + (y'-y)^2]^{3/2}}\, \mathrm{d}x'\, \mathrm{d}y' \tag{C.6}$$

and for force distributions of the form

$$P(x,y) = K\left(1 - \frac{x^2}{a^2} - \frac{y^2}{b^2}\right)^{-1/2} \tag{C.7}$$

the integrals are

$$I_1 = \int_{\mathcal{R}} \frac{(1 - x'^2/a^2 - y'^2/b^2)^{-1/2}}{[(x'-x)^2 + (y'-y)^2]^{1/2}}\, \mathrm{d}x'\, \mathrm{d}y' \tag{C.8}$$

$$I_3 = \int_{\mathcal{R}} \frac{(x'-x)(y'-y)(1 - x'^2/a^2 - y'^2/b^2)^{-1/2}}{[(x'-x)^2 + (y'-y)^2]^{3/2}}\, \mathrm{d}x'\, \mathrm{d}y' \tag{C.9}$$

$$I_4 = \int_{\mathcal{R}} \frac{(x'-x)^2(1 - x'^2/a^2 - y'^2/b^2)^{-1/2}}{[(x'-x)^2 + (y'-y)^2]^{3/2}}\, \mathrm{d}x'\, \mathrm{d}y'. \tag{C.10}$$

To illustrate the method of integration we consider I_1 in the case of Hertzian pressure. We change to the (s, ψ) system of polar coordinates with the substitution

$$\begin{aligned} x' &= r\cos\theta + s\cos(\psi + \theta) \\ y' &= r\sin\theta + s\sin(\psi + \theta). \end{aligned} \tag{C.11}$$

The Jacobian for this transformation is

$$J = \begin{vmatrix} \partial x'/\partial s & \partial x'/\partial \psi \\ \partial y'/\partial s & \partial y'/\partial \psi \end{vmatrix} = s \tag{C.12}$$

and the integral transforms to

$$I_1 = \int_{\mathcal{R}} \left\{1 - [r\cos\theta + s\cos(\psi+\theta)]^2/a^2 - [r\sin\theta + s\sin(\psi+\theta)]^2/b^2\right\}^{1/2} \mathrm{d}s\,\mathrm{d}\psi. \tag{C.13}$$

The squared terms in the above expression are expanded to give a quadratic expression in s. After some algebraic manipulation we obtain

$$I_1 = -\int_{\mathcal{R}} \left(\frac{a^2\sin^2(\psi+\theta) + b^2\cos^2(\psi+\theta)}{a^2b^2}\right) \times \left[\left(s + r\,\frac{a^2\sin\theta\sin(\psi+\theta) + b^2\cos\theta\cos(\psi+\theta)}{a^2\sin^2(\psi+\theta) + b^2\cos^2(\psi+\theta)}\right)^2 - \frac{a^2b^2\{a^2\sin^2(\psi+\theta) + b^2\cos^2(\psi+\theta) - r^2\sin^2\psi\}}{[a^2\sin^2(\psi+\theta) + b^2\cos^2(\psi+\theta)]^2}\right]^{1/2} \mathrm{d}s\,\mathrm{d}\psi \tag{C.14}$$

in which the square has been completed (variable s) in the integrand. The integration with respect to s can now be performed by way of the substitution

$$s + r\,\frac{a^2\sin\theta\sin(\psi+\theta) + b^2\cos\theta\cos(\psi+\theta)}{a^2\sin^2(\psi+\theta) + b^2\cos^2(\psi+\theta)} = \frac{ab\{a^2\sin^2(\psi+\theta) + b^2\cos^2(\psi+\theta) - r^2\sin^2\psi\}^{1/2}}{a^2\sin^2(\psi+\theta) + b^2\cos^2(\psi+\theta)}\sin\chi \tag{C.15}$$

and the integral simplifies to

$$I_1 = ab\int_{-\pi/2}^{\pi/2}\int_0^{\pi} \frac{a^2\sin^2(\psi+\theta) + b^2\cos^2(\psi+\theta) - r^2\sin^2\psi}{[a^2\sin^2(\psi+\theta) + b^2\cos^2(\psi+\theta)]^{3/2}}\cos^2\chi\,\mathrm{d}\chi\,\mathrm{d}\psi$$

$$= \frac{\pi ab}{2}\int_{\psi=0}^{\pi} \frac{a^2\sin^2(\psi+\theta) + b^2\cos^2(\psi+\theta) - r^2\sin^2\psi}{[a^2\sin^2(\psi+\theta) + b^2\cos^2(\psi+\theta)]^{3/2}}\,\mathrm{d}\psi$$

$$= \frac{\pi ab}{2} \int_{\phi=\theta}^{\pi+\theta} \frac{a^2 \sin^2\phi + b^2 \cos^2\phi - r^2 \sin^2(\phi-\theta)}{\left[a^2 \sin^2\phi + b^2 \cos^2\phi\right]^{3/2}} \, \mathrm{d}\phi \tag{C.16}$$

where $\phi = \psi + \theta$. Note that, since the integrand is periodic, the limits may be changed to be between 0 and $\pi/2$ and the integral multiplied by an appropriate factor. The cross term obtained in the expansion of $\sin^2(\phi - \theta)$ is an odd function in ϕ and so integrates to zero over a period. Thus we obtain

$$\begin{aligned} I_1 = \pi ab \Bigg\{ & \int_0^{\pi/2} \frac{\mathrm{d}\phi}{\left[a^2 \sin^2\phi + b^2 \cos^2\phi\right]^{1/2}} \\ & - x^2 \int_0^{\pi/2} \frac{\sin^2\phi \, \mathrm{d}\phi}{\left[a^2 \sin^2\phi + b^2 \cos^2\phi\right]^{3/2}} - y^2 \int_0^{\pi/2} \frac{\cos^2\phi \, \mathrm{d}\phi}{\left[a^2 \cos^2\phi + b^2 \cos^2\phi\right]^{3/2}} \Bigg\} \end{aligned} \tag{C.17}$$

and using the results from appendix C.3 we obtain

$$I_1 = \pi a \left\{ \mathbf{K}(e) - \frac{x^2}{a^2} \frac{\mathbf{E}(e) - (1-e^2)\mathbf{K}(e)}{e^2} - \frac{y^2}{b^2} \frac{\mathbf{K}(e) - \mathbf{E}(e)}{e^2} \right\} \tag{C.18}$$

where $\mathbf{K}(e)$ and $\mathbf{E}(e)$ are the complete elliptic integrals of the first and second kinds respectively, as defined in appendix C.1, and $e^2 = 1 - a^2/b^2$. Note that e has real values only when $a < b$. If we wish to consider the case when $a > b$ then we redefine e as $e^2 = 1 - b^2/a^2$, and so we have

$$e^2 = \begin{cases} 1 - b^2/a^2 & , \; a > b \\ 0 & , \; a = b \\ 1 - a^2/b^2 & , \; a < b. \end{cases} \tag{C.19}$$

In the case $a > b$, the integral form for I_1 may be re-written using the transformation $\phi \mapsto \pi/2 - \phi$ to give

$$\begin{aligned} I_1 = \pi ab \Bigg\{ & \int_0^{\pi/2} \frac{\mathrm{d}\phi}{\left[a^2 \cos^2\phi + b^2 \sin^2\phi\right]^{1/2}} \\ & - x^2 \int_0^{\pi/2} \frac{\cos^2\phi \, \mathrm{d}\phi}{\left[a^2 \cos^2\phi + b^2 \sin^2\phi\right]^{3/2}} - y^2 \int_0^{\pi/2} \frac{\cos^2\phi \, \mathrm{d}\phi}{\left[a^2 \cos^2\phi + b^2 \cos^2\phi\right]^{3/2}} \Bigg\} \end{aligned}$$

$$= \pi b \left\{ \mathbf{K}(e) - \frac{x^2}{a^2} \frac{\mathbf{K}(e) - \mathbf{E}(e)}{e^2} - \frac{y^2}{b^2} \frac{\mathbf{E}(e) - (1-e^2)\mathbf{K}(e)}{e^2} \right\}. \tag{C.20}$$

C.3 Integral Identities

$$e^2 = 1 - \frac{b^2}{a^2} \quad \text{where} \quad a > b$$

$$\int_0^{\pi/2} \frac{\mathrm{d}\phi}{[a^2 \sin^2\phi + b^2 \cos^2\phi]^{1/2}} = \frac{\mathbf{K}(e)}{a}$$

$$\int_0^{\pi/2} \frac{\sin^2\phi \, \mathrm{d}\phi}{[a^2 \sin^2\phi + b^2 \cos^2\phi]^{1/2}} = \frac{\mathbf{E}(e) - (1-e^2)\mathbf{K}(e)}{ae^2}$$

$$\int_0^{\pi/2} \frac{\cos^2\phi \, \mathrm{d}\phi}{[a^2 \sin^2\phi + b^2 \cos^2\phi]^{1/2}} = \frac{\mathbf{K}(e) - \mathbf{E}(e)}{ae^2}$$

$$\int_0^{\pi/2} \frac{\mathrm{d}\phi}{[a^2 \sin^2\phi + b^2 \cos^2\phi]^{3/2}} = \frac{\mathbf{E}(e)}{a^3(1-e^2)}$$

$$\int_0^{\pi/2} \frac{\sin^2\phi \, \mathrm{d}\phi}{[a^2 \sin^2\phi + b^2 \cos^2\phi]^{3/2}} = \frac{\mathbf{K}(e) - \mathbf{E}(e)}{a^3e^2}$$

$$\int_0^{\pi/2} \frac{\cos^2\phi \, \mathrm{d}\phi}{[a^2 \sin^2\phi + b^2 \cos^2\phi]^{3/2}} = \frac{\mathbf{E}(e) - (1-e^2)\mathbf{K}(e)}{a^3e^2(1-e^2)}$$

$$\int_0^{\pi/2} \frac{\sin^4\phi \, \mathrm{d}\phi}{[a^2 \sin^2\phi + b^2 \cos^2\phi]^{3/2}} = \frac{(2-e^2)\mathbf{E}(e) - 2(1-e^2)\mathbf{K}(e)}{a^3e^4}$$

$$\int_0^{\pi/2} \frac{\cos^4\phi \, \mathrm{d}\phi}{[a^2 \sin^2\phi + b^2 \cos^2\phi]^{3/2}} = \frac{(2-e^2)\mathbf{E}(e) - 2(1-e^2)\mathbf{K}(e)}{a^3e^4(1-e^2)}$$

$$\int_0^{\pi/2} \frac{\cos^2\phi \sin^2\phi \, \mathrm{d}\phi}{[a^2 \sin^2\phi + b^2 \cos^2\phi]^{3/2}} = \frac{(2-e^2)\mathbf{K}(e) - 2\mathbf{E}(e)}{a^3e^4}$$

C.4 Hertzian Pressure Distribution ($a > b$)

$$P(x,y) = K\left(1 - \frac{x^2}{a^2} - \frac{y^2}{b^2}\right)^{1/2} \tag{C.21}$$

$$\begin{aligned} I_1 &= \int_{\mathcal{R}} \frac{(1 - x'^2/a^2 - y'^2/b^2)^{1/2}}{[(x'-x)^2 + (y'-y)^2]^{1/2}}\, \mathrm{d}x'\, \mathrm{d}y' \\ &= \pi ab \int_0^{\pi/2} \left\{ \frac{1}{[a^2\cos^2\phi + b^2\sin^2\phi]^{1/2}} \right. \\ &\qquad \left. - \frac{x^2\cos^2\phi}{[a^2\cos^2\phi + b^2\sin^2\phi]^{3/2}} - \frac{y^2\sin^2\phi}{[a^2\cos^2\phi + b^2\sin^2\phi]^{3/2}} \right\} \mathrm{d}\phi \\ &= \pi b \left\{ \mathbf{K}(e) - \frac{x^2}{a^2}\frac{\mathbf{K}(e) - \mathbf{E}(e)}{e^2} - \frac{y^2}{b^2}\frac{\mathbf{E}(e) - (1-e^2)\mathbf{K}(e)}{e^2} \right\} \end{aligned}$$

$$\begin{aligned} I_3 &= \int_{\mathcal{R}} \frac{(x'-x)(y'-y)(1 - x'^2/a^2 - y'^2/b^2)^{1/2}}{[(x'-x)^2 + (y'-y)^2]^{3/2}}\, \mathrm{d}x'\, \mathrm{d}y' \\ &= 2\pi ab\, xy \int_0^{\pi/2} \frac{\cos^2\phi \sin^2\phi\, \mathrm{d}\phi}{[a^2\cos^2\phi + b^2\sin^2\phi]^{3/2}} \\ &= \frac{2\pi b}{a^2 e^4}\{(2-e^2)\mathbf{K}(e) - 2\mathbf{E}(e)\}\, xy \end{aligned}$$

$$\begin{aligned} I_4 &= \int_{\mathcal{R}} \frac{(x'-x)^2(1 - x'^2/a^2 - y'^2/b^2)^{1/2}}{[(x'-x)^2 + (y'-y)^2]^{3/2}}\, \mathrm{d}x'\, \mathrm{d}y' \\ &= \pi ab \int_0^{\pi/2} \frac{a^2\cos^2\phi\sin^2\phi + b^2\sin^4\phi - x^2\cos^2\phi\sin^2\phi - y^2\sin^4\phi}{[a^2\cos^2\phi + b^2\sin^2\phi]^{3/2}}\, \mathrm{d}\phi \\ &= \frac{\pi b}{e^4}\left\{ e^2[\mathbf{K}(e) - \mathbf{E}(e)] \right. \\ &\qquad - \frac{x^2}{a^2}[(2-e^2)\mathbf{K}(e) - 2\mathbf{E}(e)] \\ &\qquad \left. - \frac{y^2}{b^2}[(2-e^2)\mathbf{E}(e) - 2(1-e^2)\mathbf{K}(e)] \right\} \end{aligned}$$

C.5 Punch Type Pressure ($a > b$)

$$P(x,y) = K\left(1 - \frac{x^2}{a^2} - \frac{y^2}{b^2}\right)^{-1/2} \tag{C.22}$$

$$\begin{aligned} I_1 &= \int_{\mathcal{R}} \frac{(1 - x'^2/a^2 - y'^2/b^2)^{-1/2}}{[(x'-x)^2 + (y'-y)^2]^{1/2}}\, \mathrm{d}x'\, \mathrm{d}y' \\ &= 2\pi ab \int_0^{\pi/2} \frac{\mathrm{d}\phi}{[a^2\cos^2\phi + b^2\sin^2\phi]^{1/2}} \\ &= 2\pi b \mathbf{K}(e) \end{aligned}$$

$$\begin{aligned} I_3 &= \int_{\mathcal{R}} \frac{(x'-x)(y'-y)(1 - x'^2/a^2 - y'^2/b^2)^{-1/2}}{[(x'-x)^2 + (y'-y)^2]^{3/2}}\, \mathrm{d}x'\, \mathrm{d}y' \\ &= \pi ab \int_0^{\pi} \frac{\sin\phi\cos\phi\,\mathrm{d}\phi}{[a^2\cos^2\phi + b^2\sin^2\phi]^{1/2}} \\ &= 0 \end{aligned}$$

$$\begin{aligned} I_4 &= \int_{\mathcal{R}} \frac{(x'-x)^2(1 - x'^2/a^2 - y'^2/b^2)^{-1/2}}{[(x'-x)^2 + (y'-y)^2]^{3/2}}\, \mathrm{d}x'\, \mathrm{d}y' \\ &= 2\pi ab \int_0^{\pi/2} \frac{\cos^2\phi\,\mathrm{d}\phi}{[a^2\cos^2\phi + b^2\sin^2\phi]^{1/2}} \\ &= \frac{2\pi b}{e^2}[\mathbf{K}(e) - \mathbf{E}(e)] \end{aligned}$$

Appendix D

Some Useful Limits Involving Elliptic Integrals

Since the spheroid packing model of chapter 7 uses an averaging scheme similar to that seen in Walton [67] and section (1.3.1), it is instructive to consider the case in which the spheroids tend, in the limit, to spheres. Some useful results to enable us to take this limit are considered here. Firstly, from the definitions of the elliptic integrals given in appendix C.1 we may evaluate

$$\mathbf{K}(0) = \mathbf{E}(0) = \frac{\pi}{2}. \tag{D.1}$$

By writing the integrands over a common denominator, we consider the limit

$$\lim_{e\to 0} \frac{1}{e^2}\left[\mathbf{K}(e) - \mathbf{E}(e)\right] = \lim_{e\to 0} \int_0^{\pi/2} \frac{\sin^2\theta}{(1-e^2\sin^2\theta)^{1/2}} \mathrm{d}\theta = \frac{\pi}{4}. \tag{D.2}$$

Similarly, we may obtain the limit

$$\lim_{e\to 0} \frac{1}{e^2}\left[(Be^2 + C)\mathbf{K}(e) - C\mathbf{E}(e)\right] = \frac{\pi}{4}(2B + C). \tag{D.3}$$

Other frequently occurring limits are:

$$\lim_{e\to 0} \frac{1}{e^2}\left[\mathbf{E}(e) - (1-e^2)\mathbf{K}(e)\right] \quad = \quad \frac{\pi}{4} \tag{D.4}$$

$$\lim_{e\to 0} \frac{\mathbf{E}(e) - (1-e^2)\mathbf{K}(e)}{(1-e^2)\left[\mathbf{K}(e) - \mathbf{E}(e)\right]} = 1 \tag{D.5}$$

$$\lim_{e\to 0} \frac{\mathbf{K}(e) - \mathbf{E}(e)}{e^2\mathbf{K}(e)} = \frac{1}{2}. \tag{D.6}$$

As an example, consider the infinitesimal force increments arising from the contact of two oblate spheroidal bodies given by equations (6.68) and (6.71). By taking the limit as e tends to zero and using the results listed above, it is easily shown that these forces tend to those given as equation (1.69) for spheres.

Appendix E

Table of Isotropic Elastic Constants

	E, ν	E, μ	λ, μ	B, C
λ	$\frac{E\nu}{(1+\nu)(1-2\nu)}$	$\frac{\mu(E-2\mu)}{3\mu-E}$	λ	$\frac{C}{\pi(B^2-C^2)}$
μ	$\frac{E}{2(1+\nu)}$	μ	μ	$\frac{1}{2\pi(B+C)}$
E	E	E	$\frac{\mu(3\lambda+2\mu)}{\lambda+\mu}$	$\frac{B+2C}{\pi(B+C)}$
ν	ν	$\frac{E-2\mu}{2\mu}$	$\frac{\lambda}{2(\lambda+\mu)}$	$\frac{C}{B+C}$
κ	$\frac{E}{3(1-2\nu)}$	$\frac{\mu E}{3(3\mu-E)}$	$\lambda+\frac{2}{3}\mu$	$\frac{2B+C}{3\pi(B^2-C^2)}$
B	$\frac{1-\nu}{\pi E}$	$\frac{4\mu-E}{4\pi\mu^2}$	$\frac{1}{4\pi}\left(\frac{1}{\mu}+\frac{1}{\lambda+\mu}\right)$	B
C	$\frac{\nu(1+\nu)}{\pi E}$	$\frac{E-2\mu}{4\pi\mu^2}$	$\frac{1}{4\pi}\left(\frac{1}{\mu}-\frac{1}{\lambda+\mu}\right)$	C
E^*	$\frac{E}{2(1-\nu^2)}$	$\frac{2\mu^2}{E-4\mu}$	$\frac{2\mu(\lambda+\mu)}{\lambda+2\mu}$	$\frac{1}{2\pi B}$

Bibliography

[1] E. P. ADAMS AND R. L. HIPPISLEY, *Smithsonian Mathematical Formulae and Tables of Elliptic Functions*, Smithsonian Institution, 1938.

[2] G. K. BATCHELOR AND R. W. O'BRIEN, *Thermal or electrical conduction through a granular material*, Proc. R. Soc. Lond. A, 355 (1977), pp. 313–333.

[3] J. D. BERNAL AND J. MASON, *Co-ordination of randomly packed spheres*, Nature, 188 (1960), p. 910.

[4] J. BIAREZ AND R. GOURVÉS, eds., *Powders and Grains, Proceedings of the International Conference on Micromechics of Granular Media*, Balkema, 1989.

[5] M. A. BIOT, *Theory of elastic waves in a fluid-saturated porous solid. I — Low-frequency range*, J. Acoustical Soc. Am., 28 (1956), pp. 168–178.

[6] ——, *Theory of elastic waves in a fluid-saturated porous solid. II — Higher-frequency range*, J. Acoustical Soc. Am., 28 (1956), pp. 179–191.

[7] J. BOUSSINESQ, *Application des potentials à l'étude de l'équilibre et du mouvement des solides élastiques*, Paris: Gauthier-Villars, (1885).

[8] F. P. BOWDEN AND D. TABOR, *Friction and Lubrication of Solids Pts I and II*, Clarendon, Oxford, 1964.

[9] ——, *Friction: An Introduction to Tribology*, Heinemann, London, 1974.

[10] H. BRANDT, *A study of the speed of sound in porous granular media*, J. Appl. Mech., 22 (1955), pp. 479–486.

[11] B. J. BRISCOE, L. POPE, AND M. J. ADAMS, *Interfacial friction of powders on concave counterfaces*, Powder Technology, 37 (1984), pp. 169–181.

[12] M. D. BRYANT AND L. M. KEER, *Rough contact between elastically and geometrically identical curved bodies*, Journal of Applied Mechanics, 49 (1982), pp. 345–352.

[13] B. CAMBOU, *From global to local variables in granular materials*, Proceedings of the first international conference on micromechanics of granular media, (1993), pp. 73–86.

[14] C. CATTANEO, *Sul contatto di due corpi elastici: distribuzione locale degli sforzi*, Rendiconti dell' Accademia nazionale dei Lincei, 27 (1938).

[15] V. CERUTTI, *Roma acc. lincei*, Mem. fis. mat., (1882).

[16] C. S. CHING AND C. L. LIAO, *Constitutive relation for a particulate medium with the effect of particle rotation*, Int. J. Solids Structures, 26 (1990), pp. 437–453.

[17] J. CHRISTOFFERSEN, M. M. MEHRABADI, AND S. NEMAT-NASSER, *A micromechanical description of granular material behavior*, J. Appl. Mech., 48 (1981), pp. 339–344.

[18] C. A. COULOMB, *Mém acad. sci. savants étrangers*, Mém Acad. Sci. Savants Étrangers, 7 (1773), pp. 343–382.

[19] G. R. DARBRE AND J. P. WOLF, *Nonlinear elastic constitutive law for granular materials applicable to pebble-bed core*, Nuclear Engineering and Design, 88 (1985), pp. 161–168.

[20] H. DERESIEWICZ, *Oblique contact of nonspherical elastic bodies*, Journal of Applied Mechanics, (1957), pp. 623–624.

[21] ——, *Stress-strain relationships for a simple model of a granular media*, J. Appl. Mech., 25 (1958), pp. 402–406.

[22] P. DIGBY, *The effective elastic moduli of porous granular rocks*, J. Appl. Mechanics, 48 (1981), pp. 803–808.

[23] P. J. DIGBY AND K. WALTON, *Wave propagation through elastically-anisotropic fluid-saturated porous rocks*, Journal of Applied Mechanics, 111 (1989), p. 744.

[24] R. DOBRY, T.-T. NG, E. PETRAKIS, AND A. SERIDI, *General model for contact law between two rough spheres*, Journal of Engineering Mechanics, 117 (1991), pp. 1365–1381.

[25] J. DUFFY, *A differential stress-strain relation for the hexagonal close-packed array of elastic spheres*, J. Appl. Mech., 26 (1959), pp. 88–94.

[26] A. L. ENDRES, *The effect of contact generation on the elastic properties of a granular medium*, J. Appl. Mech. Trans. ASME, 57 (1990), pp. 330–336.

[27] G. M. L. GLADWELL, *The Contact of Deformable Bodies*, Sijthoff and Noordhoff, 1980.

[28] M. T. HANSON AND T. JOHNSON, *The elastic field for spherical Hertzian contact of isotropic bodies revisited: Some alternative expressions*, Journal of Tribology, 115 (1993), pp. 327–332.

[29] Z. HASHIN AND S. SHTRIKMAN, *A variational approach to the theory of the elastic behavior of multiphase materials*, J. Mech. Phys. Solids, 11 (1963), pp. 127–140.

[30] H. HERTZ, *Über die berührung fester elastische körper*, J. reine und angewandte Mathematik, 92 (1882), pp. 156–171.

[31] R. HILL, *A self-consistent mechanics of composite materials*, Journal of Mechanics and Physics of Solids, 13 (1965), pp. 213–222.

[32] B. E. HORNBY, L. M. SCHWARTZ, AND J. A. HUDSON, *Anisotropic effective-medium modeling of the elastic properties of shales*, Geophysics, 59 (1994).

[33] J. JÄGER, *Elastic contact of equal spheres under oblique forces*, Archive of Applied Mechanics, 63 (1993), pp. 402–412.

[34] K. L. JOHNSON, *Energy dissipation at spherical surfaces in contact transmitting oscillating forces*, Journal Mechanical Engineering Science, 3 (1961).

[35] ——, *Contact Mechanics*, Cambridge University Press, 1985.

[36] K. L. JOHNSON, K. KENDALL, AND A. D. ROBERTS, *Surface energy and the contact of elastic solids*, Proc. R. Soc. Lond., 324 (1971), pp. 301–313.

[37] K. KENDALL, *Inadequacy of Coulomb's friction law for particle assemblies*, Letters to Nature, 319 (1986), pp. 203–205.

[38] ——, *Solid surface energy measured electrically*, J. Phys. D : Appl. Phys., 23 (1990), pp. 1329–1331.

[39] ——, *Surface energy of solids from ultrasonic studies of particle assemblies*, Powder Technology, 66 (1991), pp. 101–104.

[40] K. KENDALL, N. M. ALFORD, AND J.D.BIRCHALL, *Elasticity of particle assemblies as a measure of the surface energy of solids*, Proc. R. Soc. Lond., 412 (1986), pp. 269–283.

[41] ——, *A new method for measuring the surface energy of solids*, Nature, 325 (1987), pp. 794–796.

[42] A. E. H. LOVE, *A Treatise on the Mathematical Theory of Elasticity*, Dover, New York, 1944.

[43] A. K. MAL AND S. J. SINGH, *Deformation of Elastic Solids*, Prentice Hall, 1991.

[44] R. D. MINDLIN, *Compliance of elastic bodies in contact*, J. Appl. Mech., 16 (1949), pp. 259–268.

[45] R. D. MINDLIN AND H. DERESIEWICZ, *Elastic spheres in contact under varying oblique forces.*, Trans. ASME E, Journal of Applied Mechanics, 20 (1953), pp. 237–344.

[46] H. PORITSKY AND N. Y. SCHENECTADY, *Stresses and deflections of cylindrical bodies in contact with application to contact of gears and of locomotive wheels*, Journal of Applied Mechanics, 17 (1950), pp. 191–201.

[47] M. RAOOF AND R. E. HOBBS, *Tangential compliance of rough elastic bodies in contact*, Journal of Tribology, 111 (1989), pp. 726–729.

[48] A. REUSS, *Berechnung der fliessgrense von miscкristallen auf grund der plastizitatbedingun fur einkristalle*, Zeitschrift fur Angewandte Mathematik aus Mechanik, 9 (1929), pp. 49–58.

[49] A. SACKFIELD AND D. A. HILLS, *Some useful results in the classical Hertz contact problem*, Journal of Strain Analysis, 18 (1983), pp. 101–105.

[50] ——, *Some useful results in the tangentially loaded Hertzian contact problem*, Journal of Strain Analysis, 18 (1983), pp. 107–110.

[51] L. M. SCHWARTZ, *Acoustic properties of porous systems: II Microscopic description*, American Institute of Physics, 107 (1984), pp. 105–118.

[52] L. M. SCHWARTZ, WILLIAM F. MURPHY III, AND J. G. BERRYMAN, *Stress-induced transverse isotropy in rocks*, Private Communication, (1994).

[53] G. D. SCOTT, *Packing of equal spheres*, Nature, 188 (1960), p. 908.

[54] R. E. SLADE, *Predicting the effective anisotropic elastic properties of a random packing of spheroidally shaped particles*, Schulumberger Cambridge Research internal report, (1993).

[55] R. E. SLADE AND K. WALTON, *Inter-granular friction and the mechanical and acoustical properties of granular media*, Proceedings of the second international conference on micromechanics of granular media, (1993), pp. 93–98.

[56] R. D. STOLL, *Stress-induced anisotropy in sediment acoustics*, Journal Acoustical Society of America, 85 (1989), pp. 702–708.

[57] C. THORNTON, ed., *Powders and Grains, Proceedings of the International Conference on Micromechics of Granular Media*, Balkema, 1993.

[58] C. THORNTON AND K. K. YIN, *Impact of elastic spheres, with and without adhesion*, Powder Technology, 65 (1991), pp. 153–166.

[59] U. TÜZÜN, M. J. ADAMS, AND B. J. BRISCOE, *An interface dilation model for the prediction of wall friction in a particulate bed*, Chemical engineering science, 43 (1988), pp. 1083–1098.

[60] U. TÜZÜN AND O. R. WALTON, *Micromechanical modelling of load-dependent friction in contacts of elastic spheres*, J. Phys. D: Appl. Phys., 25 (1992), pp. A44–A52.

[61] P. J. VERMEULEN AND K. L. JOHNSON, *Contact of nonspherical elastic bodies transmitting tangential forces*, Journal of Applied Mechanics, (1964), pp. 338–340.

[62] W. VOIGT, *Lehrbuch der kirstallphysik*, Teubner, Leipzig, (1928).

[63] K. WALTON, *The effective elastic moduli of model sediments*, Geophys. J. R. Astr. Soc., 43 (1975), pp. 293–306.

[64] ——, *Elastic wave propagation in model sediments — I*, Geophys. J. R. Astr. Soc., 48 (1977), pp. 461–478.

[65] ——, *Elastic wave propagation in model sediments — II*, Geophys. J. R. Astr. Soc., 50 (1977), pp. 473–486.

[66] ——, *The oblique compression of two elastic spheres*, J. Mech. Phys. Solids, 26 (1978), pp. 139–150.

[67] ——, *The effective elastic moduli of a random packing of spheres*, J. Mech. Phys. Solids, 35 (1987), pp. 213–226.

[68] ——, *Wave propagation within random packings of spheres*, Geophysical Journal, 92 (1987), pp. 89–97.

[69] K. WALTON AND P. J. DIGBY, *Wave propagation through fluid saturated porous rocks*, Journal of Applied Mechanics, 54 (1987), pp. 788–793.

[70] Z. WANG AND A. NUR, *Seismic and Acoustic Velocities in Reservoir Rocks*, Society of Exploration Geophysicists, 1992.

[71] H. M. WESTERGAARD, *Theory of Elasticity and Plasticity*, Dover, New York, 1952.

[72] J. R. WILLIS, *Hertzian contact of anisotropic bodies*, Journal of the Mechanics and Physics of Solids, 14 (1966), p. 163.

[73] K. W. WINKLER, *Frequency dependent ultrasonic properties of high-porosity sandstones*, Journal of Geophysical Research, 88 (1983), pp. 9493–9499.

[74] K. W. WINKLER AND WILLIAM F. MURPHY III, *Scattering in glass beads: Effects of frame and pore fluid compressibilities*, J. Acoust. Soc. Am., 76 (1984), pp. 820–825.

[75] A. B. WOOD, *A Textbook of Sound*, G. Bell and Sons, London, 1930.